Homogeneous and Heterogeneous Photocatalytic Degradation of Short Chain Polychlorinated *n*-Alkanes in Natural Water

By

Taha El-Morsi

A Thesis submitted to the Faculty of Graduate Studies in Partial Fulfillment of the Requirements for the Degree of DOCTOR OF PHILOSOPHY

Chemistry Department

University of Manitoba

Winnipeg, Manitoba, Canada

October 2003

Acknowledgements

The successful completion of this work is due to the efforts of many people. I doubt that I will ever be able to convey my appreciation fully, but I owe them my eternal gratitude. I wish to record publicly my deepest appreciation for my supervisors professor Ken Friesen and professor Alaa Abd-El-Aziz, Chemistry Department at the University of Winnipeg, who have been wonderful mentors of their respective areas of specialty throughout the course of this project. Their rich knowledge and meticulous writing skills, as well as their constant patience, encouragement, support and kindness have contributed greatly to the writing and the research described in this thesis. Also their high standards, continual support, advice and scientific discussions have made this project a wonderful learning experience.

I would like to thank the other members of my committee, Dr. Annemieke Farenhorst, Department of Soil Science and Dr. Feiyue Wang Department of Chemistry at the University of Manitoba for the assistance they provided at all levels of the research project.

I am also grateful to professor Moustafa Emara, professor Hassan Abd El Bary, professor Mohsen El Sabbah and Dr. Moustafa Bakr (my MSc thesis's co-supervisors) and the Chemistry Department at Al-Azhar University, Cairo, Egypt for giving me the opportunity to come and work at the University of Winnipeg. I would also like to thank professor Ahmed Bedair (my undergrad project's supervisor), professor Ahmed Elagrody, Dr. Tarek Afifi, and Rawda Okasha Chemistry Department at Al-Azhar University, Cairo, Egypt for their assistance and advice. I would also like to thank Greg Tomy, Research Scientist at the Freshwater Institute for his valuable discussion about the analysis of PCAs and for providing PCA mixtures. I would especially like to thank professor Athar Ata Chemistry Department at the University of Winnipeg for his support, advice and encouragement in so many ways.

I would also like to thank all the wonderful people I work with in the Department of Chemistry at the University of Winnipeg. In particular, I would like to thank Ed Segstro and Doug Goltz for their support and assistance in so many ways. Also I would like to extend my appreciation to all of the department's professors, instructors, staffs,

technicians and secretaries for their assistance throughout the course of this project. I would like to acknowledge the excellent students who worked on this project during their undergrad projects, Wes Budakowski, Andy Zubrycki and Basil Elmayergi. I thank the Department of Water Analysis Laboratory, Freshwater Institute, for the analysis of water samples. Also I thank the Biology Department, the University of Winnipeg, for their great help and allowing me to use their environmental chamber and other instruments. My special thanks goes out to my best friend Abdel Halim Ellamy and his family for their advice and great assistance.

I would also like to thank my family in particular my parents, brothers and sisters for the support they provided me through my entire life. My great acknowledgement goes to my wife and best kids. Without their love, encouragement and assistance, I would not have finished this thesis.

In conclusion, I recognize that this research would not have been possible without the financial assistance of Canadian Chlorine Coordinating Committee (C4), Chloroparaffin Industry Association (CPIA), Manitoba Hydro Graduate Scholarship fund, the Department of Chemistry at the University of Winnipeg and at the University of Manitoba and express my gratitude to those agencies.

Abstract

Polychlorinated *n*-alkanes (PCAs), containing isomers and congeners with different properties, are used in a wide variety of commercial and industrial applications. PCAs are somewhat toxic and little is known about their environmental reactivity by reactions such as hydrolysis, oxidation, biodegradation and photolysis. In this investigation a series of short chain PCA isomers (di-, tetra- and hexachlorinated decanes, tetrachloroundecane and dichlorododecane) and PCA mixtures (decanes, undecanes, dodecanes and tridecanes each containing Cl_5 to Cl_8 congener groups) were studied. The hydrolysis and photolysis half-lives of the PCAs in both pure and natural water were determined to assess their environmental behavior. Hydrolysis half-lives ranged from 17 to 49 d for the PCA isomers and from 72 to 111 d for the PCA mixtures at 15°C. Aqueous photolysis half-lives of the PCA isomers and mixtures were in the range of 5 to 12 and 20 to 33 d, respectively. Hydrolysis rates tended to increase with increasing temperature and pH and decrease with increasing chlorine number and carbon chain length. Chlorine number and carbon chain length had a similar effect on photolysis rates. The relatively slow rates of hydrolysis and photolysis determined in this study support classification of short chain PCAs as relatively persistent compounds.

Homogeneous photodegradation of PCA isomers in pure water using H_2O_2/UV was quite effective with half-lives ranging from 9 to 24 min. Photolysis rates decreased with increasing dissolved organic carbon with half-lives up to 31 min in lake water (Lake Winnipeg) and 65 min in bog water. Modified photo-Fenton conditions (Fe^{3+}/H_2O_2/UV) were the most effective method for the photodegradation of PCAs in pure and natural

water. For example, 79% disappearance of T_4C_{10} occurred in 20 min in pure water; increasing slightly to 90% disappearance in lake water in the same irradiation period.

Homogeneous photodegradation was also effective for PCA mixtures. For example, in pure water 80% disappearance of a composite mixture was observed in 3 h of irradiation using H_2O_2/UV. Photodegradation was again significantly enhanced using the modified photo-Fenton system (Fe^{3+}/H_2O_2/UV), with 75% disappearance of a composite mixture of PCAs in 1 h of irradiation. In lake water (Lake 375 of the Experimental Lakes Area, northwestern Ontario) the photodegradation of PCA mixtures was slightly enhanced in both H_2O_2/UV and Fe^{3+}/H_2O_2/UV systems. The dissolved organic and inorganic carbon levels in Lake 375 were lower than in Lake Winnipeg, hence the effect of hydroxyl radical scavenging is decreased. The observed increased degradation rates may be due to the presence of natural sensitizers in the lake water.

Using H_2O_2/UV the T_4C_{10} isomer was quantitatively dechlorinated in 80 min of irradiation. However, the results indicate the formation of chlorinated organic intermediates which degrade more slowly than the parent tetrachlorodecane. For the composite PCA mixture 85% TOC degradation and 93% chloride ion release in 3 h of irradiation suggested that degradation was approaching complete mineralization.

Heterogeneous photocatalytic degradation using aqueous suspensions of TiO_2 was also effective in degradation of PCAs. The degradation kinetics followed the Langmuir-Hinshelwood model suggesting that the reaction occurred on the surface of the photocatalyst. Presence of $h^+_{vb}/^{\bullet}OH$ radical scavengers, including methanol and iodide inhibited the degradation of 1,10-dichlorodecane (D_2C_{10}), supporting a photooxidation reaction. The lack of transformation of D_2C_{10} in acetonitrile as solvent indicated that the

major oxidants were $^{\bullet}OH$ radicals. The presence of tetranitromethane, effectively eliminating the formation of free $^{\bullet}OH$ radicals in solution, did not affect the degradation rates significantly. This result, combined with the observed increases in photolysis rates with the degree of adsorption of PCAs onto the surface of the photocatalyst, confirmed that the reaction involved adsorbed PCAs and surface bound $^{\bullet}OH$ radicals. The slower photooxidation of PCAs in natural water compared to pure water may be due to light attenuation by dissolved organic carbon [317-318] and/or scavenging of $^{\bullet}OH$ radicals by carbonate ion in natural water. Overall, the photooxidation of the composite PCA mixture with TiO_2/UV was efficient with 50% disappearance of total PCAs in 1 h of irradiation.

Although all three processes (TiO_2/UV, H_2O_2/UV and Fe^{+3}/H_2O_2/UV) were effective in degrading PCAs, the photo-Fenton system appeared to be the most efficient. In this system 85% of total PCAs degraded in 1 h of irradiation compared to 50 and 33% degradation in TiO_2/UV and H_2O_2/UV, respectively.

Table of Contents

		Page
Acknowledgements		ii
Abstract		iv
Table of Contents		vii
List of Tables		Xiv
List of Figures		xvii
Chapter 1: Introduction: A Literature Review		1
1. 1.	Polychlorinated *n*-Alkanes	1
1. 2.	Industrial Synthesis	2
1. 3.	Physical and Chemical Properties	4
	1.3.1. Physical and Partitioning Properties	4
	1.3.2. Chemical Properties	8
1. 4.	Uses and Applications	9
1. 5.	Environmental Release	12
1. 6.	Environmental Levels	13
1. 7.	Toxicity	21
1. 8.	Analysis of Polychlorinated *n*-Alkanes	23
1. 9.	Primary Transformation Processes of Organic Pollutants	25
	1.9.1. Biodegradation Reactions	28
	1.9.2. Oxidation Reactions.	28
	1.9.3. Hydrolysis	29

Page

1.9.4. Photolysis. 33

1.9.4.1. Direct Photoreaction 34

1.9.4.2. Indirect Photoreaction 37

1. 10. Remediation Techniques 43

1.10.1. Granular Activated Carbon. 44

1.10.2. Packed Tower Aeration. 44

1.10.3. Advanced Oxidation Techniques 45

1.10.3.1. Homogeneous Photodegradation 46

1.10.3.1.1. Ultraviolet Ozone (O_3/UV) System 46

1.10.3.1.2. H_2O_2/UV System 48

1.10.3.1.3. Photo-Fenton Systems (H_2O_2/Fe/UV) 53

1.10.3.2. Heterogeneous Photocatalysis 55

1.10.3.2.1. Theory of Semiconductors 56

1.10.3.2.2. Basic Principles of Semiconductor Photocatalysis... 62

1.10.3.2.3. Excitation of Photocatalyst Particles 63

1.10.3.2.4. Photocatalytic Degradation of Organic Substrates... 63

1.10.3.2.5. Identification of a Degradation Pathway..... 69

1.10.3.2.6. Photooxidation Pathway 70

1.10.3.2.7. TiO_2 Photocatalysis 74

1.10.3.2.8. Photocatalytic Degradation of Various Classes of Pollutants by TiO_2 79

1.11. Objectives of This Study. 82

Page

Chapter 2: Synthesis and Characterization of Polychlorinated *n*-Alkanes (C_{10}-C_{13})...85

2.0. Introduction 85

2.1. Experimental..... 85
...

2.1.1. Chemicals and Reagents 85

2.1.2. Synthesis of Polychlorinated *n*-Alkanes (PCAs) 86

2.1.2.1. Synthesis of PCA Isomers 86
.....

2.1.2.2. Extraction and Purification 86

2.1.2.3. Synthesis of PCA Mixtures 88

2.2. Instrumentation 88

2.3. Characterization of Polychlorinated *n*-Alkanes (PCAs) 89

2.3.1. Characterization of PCA Isomers 89

2.3.2. Characterization of PCA Mixtures 90
.....

2.4. Quantification of Polychlorinated *n*-Alkanes (PCAs)..... 101

2.4.1. Concentration of PCA Isomers..... 101

2.4.2. Concentration of PCA Mixtures..... 110

Chapter 3: Hydrolysis and Photolysis of Polychlorinated *n*-Alkanes (C_{10}-C_{13})..... 113

3.0. Introduction 113

3.1. Experimental 113

3.1.1. Water Sources 113

3.1.2. Chemicals and Reagents 114

3.1.3. Sample Preparation 114

3.1.4. Hydrolysis 116

Page

3.1.5. Photolysis 116

3.1.6. Extraction of PCAs..... 117

3.1.7. Analysis of PCAs..... 118

3.1.8. Kinetic Treatment of Degradation 118

3.2. Results and Discussion 118

3.2.1. Extraction Efficiency 118

3.2.2. Hydrolysis of PCA Isomers..... 120

3.2.3. Hydrolysis of PCA Mixtures 128

3.2.4. Photolysis of PCA Isomers..... 131

3.2.5. Photolysis of PCA Mixtures 131

3.3. Conclusion 136

Chapter 4: Homogeneous Photodegradation of Polychlorinated *n*-Alkanes using H_2O_2/UV and photo-Fenton Reaction 140

4.0. Introduction 140

4.1. Experimental 141

4.1.1. Reagents 141

4.1.2. Sample Irradiation 142

4.1.3. Fenton and Modified Fenton Reactions..... 142

4.1.4. Control Experiments..... 144

4.1.5. Hydroxyl Radical Scavenging 144

4.1.6. Determination of reaction kinetics 144

4.2. Analytical Methods 146

4.2.1.Chemical Actinometry 146

Page

4.2.2. Determination of Hydrogen Peroxide Concentration 149

4.2.3. Determination of Fe^{+2} 150

4.2.4. Determination of Chloride Ion (Cl^-)..... 150

4.2.5. Determination of Dissolved Organic Carbon (DOC) 150

4.3. Results and Discussion 151

4.3.1. Homogeneous Photodegradation of PCA Isomers with H_2O_2/UV ... 151

4.3.1.1. Effect of Hydrogen Peroxide Concentration 151

4.3.1.2. Effect of $^{\bullet}OH$ Scavengers 152

4.3.1.3. Photodegradation of PCA Isomers in Pure Water 155

4.3.1.4. Photodegradation of PCA Isomers in Natural Water 160

4.3.2. Photodegradation of PCA Isomers Using Fenton and Photo-Fenton Systems 171

4.3.2.1. Thermal Fenton Systems in Pure Water 173

4.3.2.2. Photo-Fenton System in Pure Water 173

4.3.2.3. Modified photo-Fenton Conditions in Pure Water 177

4.3.2.4. Photolysis of H_2O_2 182

4.3.2.5. Modified Photo-Fenton Reactions in Natural Water 185

4.3.3. Homogeneous Photodegradation of PCA Mixtures 189

4.3.3.1. H_2O_2/UV in Pure Water 194

4.3.3.1.1. Effect of $^{\bullet}OH$ Scavengers 194

4.3.3.1.2. The Effect of H_2O_2 Depletion 201

4.3.3.2. H_2O_2/UV in Lake Water 201

4.3.3.3. Photo-Fenton Conditions in Pure Water 209

Page

4.3.3.4. Photo-Fenton Conditions in Lake Water 209

4.3.4. By-Products of PCA Photooxidation with H_2O_2/UV 222

4.4. Conclusion 225

Chapter 5: Heterogeneous Photocatalytic Degradation of Polychlorinated *n*-Alkanes Using TiO_2 as a Photocatalyst..... 229

5.0. Introduction 229

5.1. Experimental Methods 229

5.1.1. Chemicals And Reagents 229

5.1.2. Preparation of Stock Solutions 230

5.1.3. Photocatalysis in Pure Water 230

5.1.4. Addition of Modifiers 231
.....
5.1.5. Adsorption 232

5.1.6. Photolysis of Adsorbed PCAs 232

5.1.7. Photolyses in Natural Water 233

5.2. Analyses 233

5.3. Results and Discussion 233

5.3.1. Determination of the Optimal Conditions for D_2C_{10} in Pure Water 233

5.3.1.1. Optimum Photocatalyst Concentration 233

5.3.1.2. Optimum Substrate Concentration 235

5.3.2. Photocatalysis of PCA Isomers..... 235

5.3.3. Identification of The Reactive Species..... 238

5.3.3.1. The Effect of Hole Scavengers..... 242

Page

5.3.3.2. The Effect of Electron Scavengers 244

5.3.4. The Site of The Reaction..... 253

5.3.5. Heterogeneous vs Homogeneous Oxidation..... 255

5.3.5.1. Photolysis with Tetranitromethane 255

5.3.5.2. Adsorption Study..... 257

5.3.6. Photocatalytic Degradation of PCA Isomers in Lake Winnipeg Water 259

5.3.7. Photocatalytic Degradation of PCA Isomers in Bog Water 263

5.3.8. Photocatalytic Degradation of PCA Mixtures in Lake 375 Water ... 269

5.4. Conclusion 278

5.5. Future Studies 279

5.6. Overall Conclusions 279

References..... 282

List of Tables

Table		Page
1.1.	Physical properties of individual PCA congeners.....	5
1.2.	Estimated photolysis half-lives of short-chain PCAs in the atmosphere and in the presence of $^{\bullet}OH$	10
1.3.	Consumption of PCAs (kt/year) in the USA, the Canada and the Western Europe in the 1990s.	11
1.4.	Environmental concentration (μg/L) of PCAs in water.....	14
1.5.	Environmental concentration (μg/kg, dry wt) of PCAs in sediments and sewage sludge.	15
1.6.	Environmental concentration (μg/kg, dry wt) of PCAs in aquatic organism.	17
1.7.	Environmental concentration (μg/kg) of PCAs in birds and terrestrial Mammals.....	18
1.8.	Environmental concentration (μg/kg) of PCAs in humans and in human foodstuffs.	19
1.9.	Environmental concentration of PCAs in other media.....	20
1.10.	Time-averaged summer oxidant concentrations in insolated surface waters.	41
1.11.	Rate constants (M^{-1} s^{-1}) for oxidation of major classes of organic compounds in insolated surface waters.	42
1.12.	Band gap energies[a] (V vs. SCE ± 0.1V) and corresponding wavelengths of light for some common semiconductors	66
1.13.	Oxidation potentials of sample organic compounds.....	67
1.14.	Photooxidation pathways.....	72
1.15.	The zero-point charge of common semiconductor	76
1.16.	Fundamental reactions of an excited TiO_2 particle	77

Table		Page
2.1.	Molecular and fragment ions of individual PCA isomers formed by electron ionization (EI).....	99
2.2.	The two prominent ions in the $[M-HCl]^-$ cluster for each congener groups and the most abundant ion (in boldface) used for SIM.....	106
2.3.	Percentage interference of individual PCA mixtures with chlorinated decanes during their elution time	107
3.1.	Analysis of natural and pure water.....	115
3.2.	Extraction efficiencies of chlorinated decane isomers and mixtures using liquid-solid (C-18 Sep-pak) and liquid-liquid (85:15 hexane:dichloromethane) extraction at pH 7.....	119
3.3.	Extraction efficiencies of D_2C_{10} using liquid-liquid (85:15 hexane:dichloromethane) extraction as a function of pH.....	121
3.4.	Hydrolysis of PCA isomers as percent hydrolyzed in 5-8 days at 50°C....	123
3.5.	Buffer mixtures used to adjust the pH of all solutions.....	124
3.6.	Hydrolysis half-lives of PCA isomers at 15°C.....	125
3.7	Hydrolysis half-lives of PCA isomers at 20°C.....	126
3.8.	Hydrolysis half- lives of PCA isomers at 30°C.....	127
3.9.	Hydrolysis half-lives (d) of the congener groups in the chlorinated decane (C_{10}) mixture as a function of pH at 18°C.....	129
3.10.	Hydrolysis half-lives (d) of PCA mixtures at pH 9 and at 18°C.....	132
3.11.	Photolysis half-lives (d) of PCA isomers in lake water and pure water....	134
3.12.	Aqueous photolysis half-lives (d) of PCA mixtures at pH 9 and at 18°C in Milli-Q water.	135
3.13.	Aqueous photolysis half-lives (d) of PCA mixtures in Lake 375 at 38°C..	139
4.1.	Observed first-order rate constants and half-lives for the photo-degradation of PCA isomers in Milli-Q water using 1.0×10^{-2} M H_2O_2....	157
4.2.	Observed first-order rate constants and half-lives for the photodegradation of PCA isomers in Lake Winnipeg water using H_2O_2...	164

Table Page

4.3. Observed first-order rate constants and half-lives for the photodegradation of PCA isomers in bog water using 1.0×10^{-2} M H_2O_2.. 169

5.1. Photocatalytic degradation rate constants (k) for D_2C_{10} (240 μg/L) with different concentrations of TiO_2 at pH 5.4 using 300 nm UV light..... 234

5.2. Photocatalytic degradation rate constants (k) for different concentrations of D_2C_{10} with 150 mg/L TiO_2 at pH 5.4..... 236

List of Figures

Figure		Page
1.1.	Structures of aromatic pollutants.....	27
1.2.	Proposed hydrolysis pathway for 1,2,3-trichloropropane and its intermediate products.	32
1.3.	The overlap of the UV spectrum of *p*-nitroanisole (PNA) with the solar spectrum at the earth's surface.	39
1.4.	Reaction pathways in the H_2O_2/UV degradation of organic compounds (HRH).	50
1.5.	Formation of continuous bands in a semiconductor where N represents the number of molecular orbitals.	57
1.6.	Velence and conduction bands in a semiconductor particle.	58
1.7.	The difference in the band gap energy in conductors, semiconductors and insulators.	59
1.8.	Position of Fermi level in intrinsic and extrinsic semiconductors.....	61
1.9.	Possible reactions occuring during photoexcitation of a photocatalyst particle.	64
2.1.	Total ion chromatograms of the purified 1,2,9,10-tetrachlorodecane of the starting material 1,9-decadiene (B).....	91
2.2.	Electron ionization positive ion mass spectrum of 1,2,9,10 tetrachlorodecane	92
2.3.	Total ion chromatogram of 1,2,5,6,9,10-hexachlorodecane.	93
2.4.	Total ion chromatogram of 1,2,10,11-tetrachloroundecane.....	94
2.5.	Electron ionization positive ion mass spectrum of 1,10-dichlorodecane..	95
2.6.	Electron ionization positive ion mass spectrum of 1,12-dichlorododecane.....	96
2.7.	Electron ionization positive ion mass spectrum of 1,2,5,6,9,10-hexachlorodecane.....	97

Figure		Page
2.8.	Electron ionization positive ion mass spectrum of 1,2,9,10-tetrachloro-undecane	98
2.9.	Total ion chromatogram of the chlorinated decane mixture (A) and elution profiles of the extracted ions representing the Cl_5, Cl_6, Cl_7 and Cl_8 congener groups (B).....	102
2.10.	Total ion chromatogram of the chlorinated undecane mixture (A) and elution profiles of the extracted ions representing the Cl_5, Cl_6, Cl_7 and Cl_8 congener groups (B).....	103
2.11.	Total ion chromatogram of the chlorinated dodecane mixture (A) and elution profiles of the extracted ions representing the Cl_5, Cl_6, Cl_7 and Cl_8 congener groups (B).	104
2.12.	Total ion chromatogram of the chlorinated tridecane mixture (A) and elution profiles of the extracted ions representing the Cl_5, Cl_6, Cl_7 and Cl_8 congener groups (B).	105
2.13.	Mass chromatograms (GC/NCI-MS) showing the similarity in the elution profiles of octachlorinated decanes ($\Sigma C_{10}Cl_8$) with pentachlorinated tridecanes ($\Sigma C_{13}Cl_5$).	108
2.14.	Negative chemical ionization full scan (*m/z* 50-550) total ion chromatogram of a composite mixture of PCAs ($\Sigma C_{10}Cl_{5-8}$ to $\Sigma C_{13}Cl_{5-8}$)	109
2.15.	NCI mass spectra obtained for (A) $C_{10}Cl_5$, (B) $C_{11}Cl_5$ and (C) $C_{13}Cl_5$.....	112
3.1.	Extraction efficiency of H_6C_{10} using liquid-liquid (85:15 hexane:dichloromethane) extraction at pH 4 as a function of time.....	122
3.2.	Hydrolysis half-lives (d) of the congener groups in the chlorinated decane (C_{10}) mixture at acidic and neutral pH at 18°C.	130
3.3.	Hydrolysis half-lives of the heptachlorodecane (Cl_7) mixtures with different carbon chain lengths (C_{10} to C_{13}) at pH 9 and 18°C.....	133
3.4.	Photolysis half-lives of PCA mixtures as a function of carbon chain length at pH 9 and at 38°C in Milli-Q water.....	138

Figure		Page
4.1.	Spectrum of emission from 300 nm lamps used in the Rayonet RPR Photochemical Reactor.....	143
4.2	Calibration Curve for spectrophotometric determination of Fe^{+2} during the determination of UV light intensity by Ferrioxalate actinometry.....	148
4.3.	Homogeneous photodegradation of 1,2,9,10-tetrachlorodecane in 0.1M $NaClO_4$ and pH 2.8 using 300 nm UV with different concentrations of H_2O_2.....	153
4.4.	Homogeneous photodegradation of 1,2,9,10-tetrachlorodecane with 1.0 x 10^{-2} M H_2O_2 in 0.1M $NaClO_4$ and pH 2.8 using 300 nm UV light (a) without added hydroxyl radical scavengers, (b) in the presence of 0.01 M KI and (c) in the presence of 0.10 M *tert*-butyl alcohol.	154
4.5.	Homogeneous photodegradation of 1,10-dichlorodecane in Milli Q water in 0.1M $NaClO_4$ and pH 2.8 using 300 nm UV in the presence of 0.01M H_2O_2.	156
4.6.	Homogeneous photodegradation of 1,2,10,11-tetrachloroundecane in Milli-Q water in 0.1 M $NaClO_4$ and pH 2.8 using 300 nm UV in the presence of 0.01M H_2O_2.	158
4.7.	Homogeneous photodegradation of 1,12-dichlorododecane in Milli-Q water in 0.1M $NaClO_4$ and pH 2.8 using 300 nm UV in the presence of 0.01M H_2O_2.....	159
4.8.	Effect of increased carbon chain length (from C_{10} to C_{11}) on the photodegradation of PCAs in Milli-Q water in 0.1M $NaClO_4$ and pH 2.8 using 300 nm UV in the presence of 0.01M H_2O_2.....	161
4.9.	Effect of increased carbon chain length (from C_{10} to C_{12}) on the photodegradation of PCAs in Milli-Q water in 0.1M $NaClO_4$ and pH 2.8 using 300 nm UV in the presence of 0.01M H_2O_2.....	162
4.10.	First-order plots for the degradation of chlorinated decanes in Lake Winnipeg water in 0.1M $NaClO_4$ and pH 8.3 using 300 nm UV in the presence of 0.01M H_2O_2.....	163
4.11.	Effect of total organic carbon (TOC) on the homogeneous photodegradation of 1,2,10,11-tetrachloroundecane in the presence of 0.01M H_2O_2 in Lake Winnipeg water in 0.1M $NaClO_4$ and pH 8.3.	166

Figure Page

4.12. Absorption spectra of Lake Winnipeg water and an aqueous solution of a mixtures of PCAs in Milli Q water..... 167

4.13. First-order plots for the degradation of chlorinated decanes in bog water in 0.1M $NaClO_4$ and pH 8.6 in the presence of 0.01M H_2O_2. ... 168

4.14. Photodegradation of PCAs of different chlorine number and carbon chain length in bog water in the presence of 0.01M H_2O_2..... 170

4.15. Effect of dissolved organic carbon (DOC) on the homogeneous photodegradation of 1,2,5,6,910-hexachlorodecane in the presence of 0.01M H_2O_2..... 172

4.16. Thermal (dark) degradation of 1,2,9,10-tetrachlorodecane in Milli-Q water under Fenton (1.0×10^{-3} M $Fe(ClO_4)_2$) and modified Fenton (1.0×10^{-3} M $Fe(ClO_4)_3$) conditions in the presence of 0.01M H_2O_2..... 174

4.17. Photodegradation of 1,2,9,10-tetrachlorodecane in Milli-Q water under Fenton and photo-Fenton conditions 175

4.18. Photodegradation of T_4C_{10} by the photo-Fenton reaction at pH 2.8 and 0.1M $NaClO_4$ using ($2.5 \times 10_{-4}$ M $FeSO_4$ and 1×10^{-3} M $Fe(ClO_4)_2$..... 176

4.19. Photodegradation of 1,2,9,10-tetrachlorodecane in Milli-Q water under photo-Fenton (1.0×10^{-3} M $Fe(ClO_4)_2$) and modified photo-Fenton (1.0×10^{-3} M $Fe(ClO_4)_3$) conditions..... 178

4.20. Photodegradation of 1,10-dichlororordecane and 1,12-dichlorododecane in Milli-Q water under modified photo-Fenton conditions..... 179

4.21. Photodegradation of chlorinated decanes in Milli-Q water under modified photo-Fenton conditions..... 180

4.22. Homogeneous photodegradation of 1,2,9,10-tetrachlorodecane and 1,2,10,11-tetrachloroundecane in Milli-Q water under modified photo-Fenton conditions..... 181

4.23. Effect of (0.1M) *tert*-butyl alcohol on the homogeneous photodegradation of 1,2,9,10-tetrachlorodecane in Milli-Q water under modified photo-Fenton conditions..... 183

Figure Page

4.24. Degradation of H_2O_2 as a function of irradiation time in Milli-Q water under modified Fenton (1.0×10^{-3} M $Fe(ClO_4)_3$/1.0×10^{-2} M H_2O_2/dark) and modified photo-Fenton..... 184

4.25. Photodegradation of 1,2,9,10-tetrachlorodecane in Milli-Q water under modified Fenton (1.0×10^{-3} M $Fe(ClO_4)_3$/1.0×10^{-2} M H_2O_2/dark), modified photo-Fenton..... 186

4.26. Formation of Fe^{+2} from reduction of Fe^{+3} by H_2O_2 during the modified photo-Fenton reaction..... 187

4.27. Homogeneous photodegradation of chlorinated decanes (D_2C_{10}, T_4C_{10} and H_6C_{10}) in lake water under modified photo-Fenton conditions..... 188

4.28. Effect of carbon chain length on the homogeneous photodegradation of 1,10-dichlorodecane and 1,12-dichlorododecane in lake water under modified photo-Fenton conditions..... 190

4.29. Effect of carbon chain length on the homogeneous photodegradation of 1,2,9,10-tetrachlorodecane and 1,2,10,11-tetrachloroundecane in lake water under modified photo-Fenton conditions..... 191

4.30. Effect of dissolved organic carbon on the homogeneous photodegradation of 1,2,10,11-tetrachloroundecane in lake water under modified photo-Fenton conditions..... 192

4.31. Effect of dissolved organic carbon on the homogeneous photodegradation of 1,10-dichlorodecane in bog water under modified photo-Fenton conditions..... 193

4.32. Homogeneous photodegradation of the chlorinated decane ($\Sigma C_{10}Cl_{5\text{-}8}$) mixture in Milli Q water in the presence of 2×10^{-2} M H_2O_2..... 195

4.33. Homogeneous photodegradation of the chlorinated undecane ($\Sigma C_{11}Cl_{5\text{-}8}$) mixture in Milli-Q water in the presence of 2×10^{-2} M H_2O_2..... 196

4.34. Homogeneous photodegradation of the chlorinated dodecane ($\Sigma C_{12}Cl_{5\text{-}8}$) mixture in Milli-Q water in the presence of 2×10^{-2} M H_2O_2..... 197

4.35. Homogeneous photodegradation of the chlorinated tridecane ($\Sigma C_{13}Cl_{5\text{-}8}$) mixture in Milli-Q water in the presence of 2×10^{-2} M H_2O_2..... 198

4.36. Homogeneous photodegradation of individual PCA mixtures ($\Sigma C_{10}Cl_{5\text{-}8}$ to $C_{13}Cl_{5\text{-}8}$) in Milli-Q water in the presence of 2×10^{-2} M H_2O_2..... 199

Figure Page

4.37. Effect of 0.1M *tert*-butyl alcohol on the photodegradation of the chlorinated decane ($\Sigma C_{10}Cl_{5\text{-}8}$) mixture in Milli-Q water in the presence of 2 $x10^{-2}$ M H_2O_2..... 200

4.38. Enhancement of the degradation of the composite PCA mixture ($\Sigma C_{10}Cl_{5\text{-}8}$ to $C_{13}Cl_{5\text{-}8}$) in Milli-Q water with the addition of 0.01 M H_2O_2 after 60 min of irradiation..... 202

4.39. Homogeneous photodegradation of chlorinated congener groups in the chlorinated decane ($\Sigma C_{10}Cl_{5\text{-}8}$) mixture in Lake 375 water using 2 $x10^{-2}$ M H_2O_2,..... 203

4.40. Homogeneous photodegradation of chlorinated congener groups in the chlorinated undecane ($\Sigma C_{11}Cl_{5\text{-}8}$) mixture in Lake 375 water using 2 x 10^{-2} M H_2O_2..... 204

4.41. Homogeneous photodegradation of chlorinated congener groups in the chlorinated dodecane ($\Sigma C_{12}Cl_{5\text{-}8}$) mixture in Lake 375 water using 2 $x10^{-2}$ M H_2O_2..... 205

4.42. Homogeneous photodegradation of chlorinated congener groups in the chlorinated tridecane ($\Sigma C_{13}Cl_{5\text{-}8}$) mixture in Lake 375 water using 2 $x10^{-2}$ M H_2O_2,..... 206

4.43. Homogeneous photodegradation of individual PCA ($\Sigma C_{10}Cl_{5\text{-}8}$ to $\Sigma C_{13}Cl_{5\text{-}8}$) mixtures in Lake 375 water using 2 x 10^{-2} M H_2O_2..... 207

4.44. Homogeneous photodegradation of the chlorinated decane ($\Sigma C_{10}Cl_{5\text{-}8}$) mixture in Lake 375 and Milli-Q water in the presence of 2 x 10^{-2} M H_2O_2..... 208

4.45. Homogeneous photodegradation of the chlorinated decane ($\Sigma C_{10}Cl_{5\text{-}8}$) mixture in Milli Q water under modified photo-Fenton (2 x 10^{-2} M H_2O_2/1x10^{-3} M Fe^{+3}) conditions..... 210

4.46. Homogeneous photodegradation of the chlorinated undecane ($\Sigma C_{11}Cl_{5\text{-}8}$) mixture in Milli-Q water under modified photo-Fenton conditions..... 211

4.47. Homogeneous photodegradation of the chlorinated dodecane ($\Sigma C_{12}Cl_{5\text{-}8}$) mixture in Milli-Q water under modified photo-Fenton..... 212

4.48. Homogeneous photodegradation of the chlorinated tridecane ($\Sigma C_{13}Cl_{5\text{-}8}$) mixture in Milli-Q water under modified photo-Fenton... 213

Figure Page

4.49. Homogeneous photodegradation of individual PCA mixtures ($\Sigma C_{10}Cl_{5-8}$ to $\Sigma C_{13}Cl_{5-8}$) in Milli-Q water under modified photo-Fenton..... 214

4.50. Homogeneous photodegradation of the chlorinated decane ($\Sigma C_{10}Cl_{5-8}$) mixture in Lake 375 water under modified photo-Fenton..... 215

4.51. Homogeneous photodegradation of the chlorinated undecane ($\Sigma C_{11}Cl_{5-8}$) mixture in Lake 375 water under modified photo-Fenton... 216

4.52. Homogeneous photodegradation of the chlorinated dodecane ($\Sigma C_{12}Cl_{5-8}$) mixture in Lake 375 water under modified photo-Fenton.. 217

4.53. Homogeneous photodegradation of the chlorinated tridecane ($\Sigma C_{13}Cl_{5-8}$) mixture in Lake 375 water under modified photo-Fenton.. 218

4.54. Homogeneous photodegradation of individual PCA mixtures ($\Sigma C_{10}Cl_{5-8}$ to $\Sigma C_{13}Cl_{5-8}$) mixture in Lake 375 water under modified photo-Fenton..... 219

4.55. Degradation of the composite PCA ($\Sigma C_{10}Cl_{5-8}$ to $\Sigma C_{13}Cl_{5-8}$) mixture in Milli-Q and Lake 375 water under modified photo-Fenton..... 220

4.56. Homogeneous photodegradation of the composite PCA ($\Sigma C_{10}Cl_{5-8}$ to $\Sigma C_{13}Cl_{5-8}$) mixture in Lake 375 water in (H_2O_2/UV), Fenton and modified photo-Fenton conditions..... 221

4.57. Dechlorination of 1,2,9,10-tetrachlorodecane during photolysis using 300 nm UV light in aqueous H_2O_2 solution..... 223

4.58. Changes in total organic carbon and parent PCA ($\Sigma C_{10}Cl_{5-8}$ to $\Sigma C_{13}Cl_{5-8}$) concentrations during photodegradation of PCA mixtures using H_2O_2 224

4.59. Photodegradation of the composite PCA mixture ($\Sigma C_{10}Cl_{5-8}$ to $\Sigma C_{13}Cl_{5-8}$) in Lake 375 water in the presence of ($2x10^{-2}$ M) H_2O_2..... 226

4.60. Release of chloride ion and disappearance of total organic carbon (TOC) during the photodegradation of the composite PCA mixture ($\Sigma C_{10}Cl_{5-8}$ to $\Sigma C_{13}Cl_{5-8}$) in Lake 375 water in the presence of ($2x10^{-2}$ M) H_2O_2 227

Figure		Page
5.1.	Degradation of 1,10-dichlorodecane in a dark control, in a solution without TiO_2 and in the presence of TiO_2 in Milli-Q water.....	237
5.2.	Degradation of 1,2,9,10-tetrachlorodecane and 1,2,5,6,9,10-hexachlorodecane in Milli-Q water with TiO_2.....	239
5.3.	Degradation of 1,2,9,10-tetrachlorodecane and 1,2,10,11-tetrachloroundecane in Milli-Q water with TiO_2.....	240
5.4.	Degradation of 1,10-dichlorodecane and 1,12-dichlorododecane in Milli-Q water with of TiO_2.....	241
5.5.	Effect of the hole scavenger, methanol, on the photodegradation of 1,10-dichlorodecane in Milli-Q water TiO_2	243
5.6.	Effect of the hole scavenger, iodide ion (I^-), on the photocatalytic degradation of 1,10-dichlorodecane in Milli Q water with TiO_2.....	245
5.7.	Effect of Cu^{+2} on the effect of iodide ion (I^-) in the photocatalytic degradation of 1,10-dichlorodecane in Milli Q water with TiO_2.....	246
5.8.	Effect of molecular oxygen levels on the photocatalytic degradation of 1,10-dichlorodecane in Milli Q water with TiO_2.....	248
5.9.	Effect of the electron scavenger, 1.0 mM Ag^+, on the photocatalytic degradation of 1,10-dichlorodecane in Milli Q water with TiO_2.....	249
5.10.	The effect of electron scavengers (10^{-3} M Cu^{+2}, 10^{-3} M Fe^{+3} and 10^{-3} M Ag^+) on the photocatalytic degradation of D_2C_{10} in Milli-Q water with TiO_2.....	251
5.11.	The effect of 10^{-2} M hydrogen peroxide on the photocatalytic degradation of D_2C_{10} in solutions with 0.045 ± 0.015 mM oxygen by TiO_2.....	252
5.12.	Effect of acetonitrile on the photocatalytic degradation of D_2C_{10} with TiO_2	254
5.13.	Fitting the kinetics of photocatalytic degradation of 1,10-dichlorodecane with TiO_2 to the Langmuir-Hinshelwood model.....	256
5.14.	The effect of 10^{-4} M tetranitromethane on the photocatalytic degradation of 1,10-dichlorodecane in Milli Q water with 150 mg/L of TiO_2.....	258

Figure Page

5.15. The rate of adsorption of 1,10-dichlorodecane to TiO_2, showing the mass of solute sorbed to the photocatalyst as a function of the equilibration time..... 260

5.16. Plots showing the correlation between the degree of adsorption of 1,10-dichlorodecane to TiO_2 and the rate of its photodegradation..... 261

5.17. Effect of chlorine number on the photocatalytic degradation of chlorinated decanes in lake water in the presence of 150 mg/L TiO_2 at pH 8.6..... 262

5.18. Photocatalytic degradation of 1,10-dichlorodecane and 1,12-dichlorododecane in lake water in the presence of 150 mg/L TiO_2..... 264

5.19. Photocatalytic degradation of 1,2,9,10-tetrachlorodecane and 1,2,10,11-tetrachloroundecane in Lake Winnipeg water in the presence of 150 mg/L TiO_2 265

5.20. Effect of dissolved organic matter on photocatalytic degradation of 1,10-dichlorodecane in Lake Winnipeg water in the presence of 150 mg/L TiO_2..... 266

5.21. Effect of pH on the photocatalytic degradation of 1,10-dichlorodecane in Lake Winnipeg water in the presence of 150 mg/L TiO_2..... 267

5.22. Photocatalytic degradation Of 1,10-dichlorodecane in pure, lake and bog water in the presence of 150 mg/L TiO_2..... 268

5.23. Effect of chlorine number on the photocatalytic degradation of chlorinated decanes in bog water in the presence of 150 mg/L TiO_2..... 270

5.24. Photocatalytic degradation of PCA isomers in bog water with TiO_2.... 271

5.25. Photocatalytic degradation of the chlorinated decane ($\Sigma C_{10}Cl_{5\text{-}8}$) mixture in Lake 375 water in the presence of 200 mg/L TiO_2..... 272

5.26. Photocatalytic degradation of the chlorinated undecane ($\Sigma C_{11}Cl_{5\text{-}8}$) mixture in Lake 375 water in the presence of 200 mg/L TiO_2..... 273

5.27. Photocatalytic degradation of the chlorinated dodecane ($\Sigma C_{12}Cl_{5\text{-}8}$) mixture in Lake 375 water in the presence of 200 mg/L TiO_2..... 274

5.28. Photocatalytic degradation of the chlorinated tridecane ($\Sigma C_{13}Cl_{5\text{-}8}$) mixture in Lake 375 water in the presence of 200 mg/L TiO_2..... 275

Figure Page

5.29. Photodegradation of individual PCA mixtures (Σ $C_{10}Cl_{5\text{-}8}$ to Σ $C_{13}Cl_{5\text{-}8}$) in Lake 375 water with 200 mg/L TiO_2..... 276

5.30. Photodegradation of the composite PCA mixture (Σ $C_{10}Cl_{5\text{-}8}$ to Σ $C_{13}Cl_{5\text{-}8}$) in Lake 375 water in the presence of 200 mg/L TiO_2, 1 $x10^{-2}$ M H_2O_2 and photo-Fenton conditions 277

CHAPTER 1

Introduction: A Literature Review

1.1. Polychlorinated *n*-Alkanes

Polychloro-*n*-alkanes (PCAs) are chlorinated derivatives of *n*-alkanes of general formula $C_nH_{2n+2-z}Cl_z$, which have carbon chain lengths from ten to thirty carbons. Commercial mixtures of PCAs, also known industrially as chlorinated paraffins, are chemically produced by free radical chlorination of *n*-alkane feedstock with molecular chlorine [1] under high temperature or in the presence of UV light [2]. The low potential selectivity [3,4] of these free radical reactions produced complex formulations consisting of mixtures of optical isomers and congeners of PCAs with chlorine content ranging from 30 to 70% by weight [5].

PCA mixtures are classified by carbon chain length into short (C_{10}-C_{13}), medium (C_{14}-C_{17}), and long-chain (C_{18}-C_{30}). These are further subcategorized according to chlorine content by weight percent chlorine as follows: 40-50%, 50-60% and 60-70% [6]. Due to their varying carbon chain lengths and chlorine content, PCAs provide a complex mixture consisting of a large number of isomers and congener groups with diverse properties, which are used in different commercial and industrial applications. Determining the environmental fate of polychlorinated alkane mixtures has received less attention due to the difficulty associated with the analysis of such complex mixtures.

Short chain PCAs (C_{10}-C_{13}) has similar molecular weights and physical properties (octanol-water partition coefficient, water solubility, and vapor pressure) to many

persistent organochlorines such as PCBs [7] and toxaphene [8]. Medium chain (C_{14}-C_{17}) and long chain (C_{18}-C_{30}) PCAs are extremely hydrophobic and non-volatile and are likely to be associated with particles in aquatic systems [9]. From a recent review [10] it is evident that short-chain PCAs are widespread environmental contaminants at detectable levels in both surface water and biota. The data to date have shown that PCAs are relatively persistent under most conditions, and are not readily removed from the environment once introduced [11]. However, at the present time environmental measurements are very limited in Canada and the USA and are only slightly more detailed in Western Europe [11].

PCAs have received much less attention in terms of exposure and risk assessment than the persistent organic pollutants (POPs) because of lower mammalian toxicity than most POPs [9] and the lack of environmental measurements for estimating human and animal exposure. Up to the present time, there is limited information on the distribution and fate of polychlorinated alkanes in the environment. Future studies will require better analysis methods and certified reference materials to understand the behaviour of different isomers in that mixture, and to evaluate the release of polychlorinated alkanes into the environment. Monitoring PCA mixtures using different analysis methods will be discussed later in this Chapter.

1.2. Industrial Synthesis

Generally, commercial chloroparaffins (CPs) are manufactured by free radical chlorination of a *n*-paraffinic (derived from petroleum fractions) liquid or solid (wax) using molecular chlorine. The free radical reaction may take place at temperatures between 50°C and 150°C at elevated pressure, or in the presence of a catalyst such as ultra-violet (UV) light [2]. Products are viscous, dense oils that are colorless or

sometimes yellowish, except for PCAs of chain length C_{20}-C_{30} and 70% chlorine content, which form solids [12]. The choice of paraffin feedstock and chlorine content depends on the application. For specialized applications, PCAs are produced by chlorine addition to α-olefins [13]. The reaction mechanism for the substitution of hydrogen atoms in *n*-alkanes by chlorine atoms is a free radical chain reaction [14]. The first reaction is the initiation step (1-1), where molecular chlorine absorbs heat or light energy generating chlorine radicals by homolysis.

$$Cl_2 \longrightarrow 2Cl^{\bullet} \qquad (1\text{-}1)$$

In the propagation steps (1-2 and 1-3), the chlorine radical has sufficient energy to induce reaction with the relatively unreactive *n*-alkane, resulting in the abstraction of a hydrogen atom forming a reactive intermediate radical, $C_nH_{2n+1}^{\bullet}$. These alkyl radicals react with Cl_2 to regenerate $Cl^{\bullet}$ and produce $C_nH_{2n+1}Cl$ which is a substrate for further reactions to produce the PCA.

$$Cl^{\bullet} + C_nH_{2n+2} \longrightarrow HCl + C_nH_{2n+1}^{\bullet} \qquad (1\text{-}2)$$

$$C_nH_{2n+1}^{\bullet} + Cl_2 \longrightarrow C_nH_{2n+1}Cl + Cl^{\bullet} \qquad (1\text{-}3)$$

In chain termination (1-4 to 1-6), reactive species are consumed by union or are captured by the reaction vessel walls.

$$Cl^{\bullet} + Cl^{\bullet} \longrightarrow Cl_2 \qquad (1\text{-}4)$$

$$C_nH_{2n+1}^{\bullet} + C_nH_{2n+1}^{\bullet} \longrightarrow C_{2n}H_{4n+2} \qquad (1\text{-}5)$$

$$Cl^{\bullet} + C_nH_{2n+1}^{\bullet} \longrightarrow C_nH_{2n+2-z}Cl_z \qquad (1\text{-}6)$$

Epoxides and organotin compounds are commonly added (with concentration below 0.05%) as stabilizers to inhibit decomposition of PCAs via HCl loss during the chlorination process [5].

1. 3. Physical and Chemical Properties

Physico-chemical properties such as vapor pressure (VP), Henry's Law constant (HLC) and water solubility (S_W) have been reported in past studies based on measurements of synthesized mixtures where individual congeners have been unavailable [10]. Recently Drouillard et al. [15,16] reported more meaningful physico-chemical properties of individual congeners synthesized by chlorine addition to *n*-alkenes [17] These individual congeners served as useful surrogates for assessing the environmental fate and behavior of commercial PCA mixtures [15].

1.3.1. Physical and Partitioning Properties

A summary of published physical and partitioning properties such as vapor pressure, water solubility, Henry's Law constant, octanol-water partition coefficient (K_{OW}) and the organic carbon normalized sorption coefficient (K_{OC}) for selected PCAs are presented in Table 1.1. Vapor pressure is the partial pressure contributed by a solute when the condensed phase and gas coexist in equilibrium at a specified temperature [18]. Vapor pressure is important in environmental fate modeling, for estimations of evaporation rates during chemical spills in the environment, and for estimating whether the chemicals will release into the air (vapor phase) or be adsorbed to soil [19]. Subcooled liquid vapor pressures of individual C_{10}-C_{12} PCAs [15] have been determined by the vapor pressure gas-liquid chromatography correlation technique. Vapor pressures ranged from 1.40×10^{-4} Pa to 0.51 Pa (Table 1.1) and tended to decrease with increasing carbon chain length and degree of chlorination. PCAs have similar vapor pressures to other chlorinated organics, such as PCBs, of the same molecular weight range. For example the vapor pressure of PCBs decreases from 0.042 for 4,4'-dichlorobiphenyl (PCB-15) to 0.0027 Pa

Table 1.1: Physical properties of individual PCA congeners.

Compound	% Cl	VP (Pa)	S_W ($\mu g\ L^{-1}$)	HLC ($Pa\ m^3/mol$)	Log K_{OW}	Log K_{OC}
$C_{10}H_{20}Cl_2$	33	0.500[1]	257[1]	499[1]	NA	NA
$C_{10}H_{18}Cl_4$	50	0.028[1]	668[1]	17.70[1]	5.93[3]	NA
$C_{10}H_{17}Cl_5$	56	0.066[2]	836[1]	14.67[2]	NA	NA
$C_{10}H_{16}Cl_6$	61	0.001-0.002[1]	NA	NA	NA	NA
$C_{11}H_{20}Cl_4$	48	0.010[1]	NA	6.32[1]	5.93[3]	NA
$C_{11}H_{19}Cl_5$	54	0.001-0.002[1]	NA	0.68-1.46[1]	6.2-6.4[3]	NA
$C_{11}H_{18}Cl_6$	58	0.0002-0.0005[1]	NA	NA	NA	NA
$C_{12}H_{24}Cl_2$	29	0.068[1]	22.4[1]	648[1]	NA	NA
$^{14}C_{12}H_{21}Cl_5$	51	0.0016-0.0019[1]	NA	1.37[1]	NA	NA
$^{14}C_{12}H_{20}Cl_6$	56	NA	NA	NA	6.8	4.81-4.94[4]
$C_{13}H_{23}Cl_5$	49	0.00032[2]	NA	4.18	NA	NA
$C_{13}H_{22}Cl_6$	70	2.8×10^{-7} [2]	NA	NA	NA	NA

[1]Drouillard et al. 1997 [15]

[2]Environment Canada 1993 [12]

[3] Tomy et al. [10]

[4]Tomy et al. [10]

for 2,2′,4,4′,6,6′-hexachlorobiphenyl (PCB-155) [7].

Henry's Law Constant (HLC) is a partition coefficient, which describes the distribution of a neutral organic compound between air and water (K_{AW}) at equilibrium [15,18]. A plot of the concentration of the chemical in the air versus the concentration of the chemical in the water is usually linear with a slope of K_{AW}. The K_{AW} is used to predict the mass transfer of the solute between air and water and its fugacity capacities in water, sediment, water-saturated soils and biota. The gas-sparging technique has been used to determine HLC values of PCAs. Tetra- and pentachloro congeners of short chain *n*-alkanes, have HLC values rainging from 17.7 to 1.37 Pa m^3/mol. Short chain PCAs with a chlorine number of 2, such as dichlorodecane (D_2C_{10}) and dichlorododecane (D_2C_{12}), have HLC values of 499 and 648 Pa m^3/mol, respectively [15,18]. These results indicated that low molecular weight PCAs may volatilize from water to air in temperate and tropical environments similar to the behaviour of PCBs and some organochlorine pesticides [8].

Generally, the environmental mobility of chemicals is related to their aqueous solubilities. Highly water-soluble compounds are distributed in the environment *via* the hydrological cycle, and tend to degrade faster than sparingly soluble compounds [20] which would likely be sorbed to sediment and biological phases. The data in Table 1.1 shows water solubilities of individual PCA congeners from C_{10} to C_{12} measured by the generator column technique [16], ranging from 22.4 to 836 μg/L. These results also indicated an apparent inverse relationship between carbon chain length and water solubility, while increasing the degree of chlorination (up to 5 chlorines) appeared to increase the water solubility. These results suggest that PCAs of shorter carbon chain

length with medium chlorine content may be more environmentaly mobile than those of lower chlorine content.

An important descriptor of chemical behavior in the environment is the octanol-water partition coefficient (K_{OW}), which elucidates the hydrophobicity of a chemical, or its tendency to partition from water to an organic medium. Commercial formulations of PCAs have log K_{OW} determined by the slow-stirring technique [21-22], ranging from 5.93 to 6.8 as shown in Table 1.1. The results shown a linear increase in log K_{OW} with increasing degree of chlorination and carbon chain length for short chain PCAs. The fragment constant method [20] estimated log K_{OW} of PCAs as 5.06–8.12 for C_{10}-C_{13}, 6.83-8.96 for C_{14}-C_{17} and 8.70-12.868 for C_{18}-C_{26}. The log K_{OW} value of synthesized ^{14}C-labeled hexachlorododecane [23] has been estimated by reverse-phase HPLC to be 6.8 [24]. On the basis of K_{OW} values, PCAs seem to be very hydrophobic.

In addition, the organic carbon-water partition coefficient (K_{OC}) describes the equilibrium distribution of neutral hydrophobic chemicals between organic carbon (soil, sediment suspended sediment or dissolved organic matter) and the aqueous phase, which are in contact. Sorption of neutral hydrophobic organics is directly proportional to the quantity of the organic carbon associated with the solid. Normalizing the specific soil or sediment disrtribution coefficient to organic carbon content of the sorbent yields a new coefficient, K_{OC}.

$$K_{OC} = \frac{K_d}{OC} \quad or \quad \frac{K_f}{OC} \tag{1-7}$$

where K_d and K_f are the linear and Freundlich sorption coefficients specific to a particular sorbent and chemical combination, and OC is the fraction organic carbon of that sorbent (g OC/g dry soil). It is an important parameter in environmental fate modeling for

estimating the mobility and bioavailablity of a compound. The average log K_{OC} of $^{14}C_{12}H_{20}Cl_6$ mixtures was reported in Table 1.1 as 4.88 for particulate organic carbon (POC) obtained from freshwater sediments and filtered lake water [18]. The K_{OC} values of PCAs are, therefore, relatively high and are expected to increase with increasing K_{OW} [25]. These results indicate that the more hydrophobic PCAs would be expected to be mainly sorbed to particles in most environmental situations.

1.3.2. Chemical Properties

Little experimental data is available on environmentally important chemical properties or degradation processes of chlorinated *n*-alkanes such as photolysis, hydrolysis, oxidation, and biodegradation as shown in Table 1.2. Photolysis can occur either by direct absorption of UV radiation (λ>290 nm) or by indirect transfer of this energy from other excited species, a process known as sensitized photolysis. A previous study [26] reported that PCAs do not absorb UV light, and therefore no direct photolysis was noted. Although indirect photolysis reactions of PCAs in aquatic environments involving free radicals [10] have not been studied extensively, Sadek et al. [27] studied the photodegradation of 1,12-dichlorododecane (D_2C_{12}) in different aquatic media using a 150-watt xenon lamp as a light source. The results indicated that direct photolysis of D_2C_{12} was insignificant, however, psuedo-first-order rate constants (k) for indirect photodegradation ranged from 0.12 ± 0.01 to 0.17 ± 0.01 h^{-1} in several natural water systems. Also, theoretical half-lives of PCAs in the troposphere have been reported by Atkinson [28] as 1.2 to 1.8 days for short chain (C_{10}-C_{13}), 0.85 to 1.1 days for medium chain (C_{14}-C_{17}), and 0.5 to 0.8 days for long chain PCAs (C_{18}-C_{30}) congeners (see

Table1.2). The rates of hydrolysis and oxidation of PCAs in the aqueous phase are considered very slow at ambient temperature [29]. In aquatic environments the presence of natural catalysts might enhance hydrolysis or oxidation reactions, but unfortunately to date there is no data available for PCAs. However, dehydrochlorination of PCAs with activated alumina [30] was reported for the reaction with sodium in an ammonia-diethyl ether solution producing *n*-alkanes and *n*- alkenes as products [31].

1. 4. Uses and Applications

The first large-scale usage of PCAs occurred in 1932 in the preparation of an antiseptic solution [10]. Later on, the high chemical stability of these compounds lead to their high demand in industry. PCAs are used as effective extreme pressure (EP) additives for oil lubricants used in a wide range of machining and engineering operations [32], with an estimated consumption of 38-50 kt/year in 1961 [33], growing to 300 kt/year by 1993 (Table 1.3) [34]. The major use of these compounds is as high temperature metal cutting fluids and in other metal working operations such as drilling and machining [32]. Short chain chloroparaffins (SCCPs) are effective additives in the fluids used in heavy duty metal working, to remove the heat produced between the tool and the metal work piece. Chlorine is released from the chloroparaffin at the point of contact and reacts with the bare metal surface to form a metal chloride layer on the surface. This surface has a lower friction factor than an untreated surface and helps the metal to expand [34]. PCAs are used as halogenated flame-retardants due to their high chlorine content, which increase their thermal stability. However, the high concentration of hydrogen ions released in the fire zone, are responsible for breaking down large organic molecules into smaller, volatile radicals. Chloride ions released from chlorinated paraffins will form HCl and scavenge free hydrogen ions. In the same time chloride ions

Table 1.2: Estimated photolysis half-lives of short-chain PCAs in the atmosphere and in the presence of $^{\bullet}OH$ [10,34].

Carbon Chain	%Cl	Photolysis half-life (d)	Method
$C_{10} - C_{13}$	NA[a]	1.2-1.8	Est[b]
$C_{14} - C_{17}$	NA	0.81-1.1	Est
$C_{18} - C_{26}$	NA	0.5-0.8	Est
$C_{18} - C_{26}$	NA	Negligible	Direct[c]

[a]NA = not available.

[b]Estimated on basis of reaction with OH radical [34].

[c]Direct photolysis in the troposphere [28].

Table 1.3: % Usage of PCAs in the USA, Canada and the Western Europe in the 1990s, the total use estimated to be 300 kt/year.

	Country and % usage		
Use Pattern	USA [13]	Canada [13]	Western Europe [29]
Lubrication additives	45	20	70
Plastics	20	65	4.0
Rubber	13	8.0	10
Paints	9.0	3.0	8.0
Adhesives and Sealant	6.0	2.0	4.0
Miscellaneous	7.0	2.0	4.0

will react with and deactivate the volatile free radicals to prevent distribution of the fire [35]. On the other hand plasticizers are additives used to increase the softness, flexibility, and extension properties of plastics, rubbers, coatings and polyvinyl chloride (PVC) and other polymers. PCAs may be used as secondary plasticizers, with low cost, replacing conventional plasticizers such as phthalate and phosphate esters [10]. These characteristics as well as the similarity in the structure of PCAs to PVC resin, offer flame retardancy as well as resin flexibility [35]. Chlorinated paraffins are used as secondary plasticizers with a maximum loading level of 10% of the additives's package [35].

1. 5. Environmental Release

The short chain PCAs are of particular concern because they have the greatest potential for environmental release and the highest aquatic and mammalian toxicity of all PCAs [34]. In the United States, short chain PCAs have been placed on the Environmental Protection Agency (EPA) Toxic Release Inventory (TRI), and in Canada they are listed as "Priority Toxic Substances" under the Canadian Environmental Protection Act [36].

In Europe, industry has voluntarily implemented restrictions on the use of short chain PCAs. With the phasing out of many persistent organic pollutants (POPs) such as DDT and toxaphene over the past 20 years, PCAs are among the last high molecular weight organochlorine compounds still in industrial production [37].

Release of PCAs into the environment could potentially occur during production, storage, transportation, industrial use and leaching from landfill or waste disposal sites. The majority of release occurs from production and industrial usage, and can result from improper disposal of used lubricants and storage drums [37]. Landfilling of PCA products such as PVC, textiles, paint cans and oils may also result in slow leaching out of

the product matrix [38]. In Sweden, it is estimated that about 227 t/year (55%) of the C_{10}-C_{13} PCAs used in high-pressure lubricants are discharged directly into the environment [39]. Waterborne releases from production sites occur from spills or during facility wash-downs and cleaning of reactor vessels [32]. In 1995, effluents of a PCA manufacturing plant on the St. Lawrence River in Cornwall, Ontario, were found to contain 12.7 μg/L C_{10}-C_{17} PCAs [38]. Atmospheric emissions from PCA production sites are also an environmental concern [24]. In 1988, emissions at a PCA manufacturing plant in Germany were found to be 30-mg/m^3 total PCAs [34].

1. 6. Environmental Levels

A variety of analytical methods are used for determining residues of PCAs, in order to make comparisons of environmental concentrations at different sites. The total PCA concentrations (∑PCAs) detected in water are summarized in Table 1.4 [32,33,37-38]. In the US the concentrations of PCAs are reported as 0.15 to 8.3 μg/L, where the effluent of PCAs come from the production plant in Dover, OH. In the UK and Germany the concentrations of PCA with chlorine content of 45-52% ranged from 0.07 to 4.0 μg/L. The highest concentrations of PCA were the result of sampling near industrial activity. The concentration of C_{10}-C_{13} in Canada (sampling was from the Red River, downstream of the city of Winnipeg) ranged from 0.02 to 0.05 μg/L [9].

Environmental ∑PCAs reported in sediments and sewage sludge are provided in Table 1.5 [9,31,32,33,36,37]. Sewage sludge sampled near industries (such as an impoundment drainage ditch) in the U.S., were commonly found to contain higher PCA concentrations (1,200-40,000 μg/kg, dry wt) than those further away from industrial

Table 1.4: Environmental concentration (μg/L) of PCAs in water.

PCA measured	Location	Country	Conc. [μg/L]
C_{10}-C_{13}, 60% Cl	Impound drainage ditch	US[a]	<0.5-3.3
C_{14}-C_{17}, 52% Cl	Impound drainage ditch	US	<0.15-3.8
C_{20}-C_{30}, 42% Cl	Impound drainage ditch	US	<0.15-8.3
C_{10}-C_{13}, 60% Cl	Sugar Creek, OH	US	0.20-0.30
C_{14}-C_{17}, 52% Cl	Sugar Creek, OH	US	0.16-0.24
C_{20}-C_{30}, 42% Cl	Sugar Creek, OH	US	0.35-0.62
C_{10}-C_{30}, 45-52% Cl	Irish Sea	UK[b]	<0.5-1.0
C_{10}-C_{30}, 45-52% Cl	North Sea	UK	<0.5
C_{10}-C_{30}, 45-52% Cl	Bala Lake	UK	1.5
C_{10}-C_{30}, 45-52% Cl	River Dee	UK	<0.5
C_{10}-C_{30}, 45-52% Cl	River Wnion	UK	<0.5
C_{10}-C_{30}, 45-52% Cl	Manchester tap water	UK	<0.5
C_{10}-C_{30}, 45-52% Cl	River Trent	UK	1.0-6.0
C_{10}-C_{30}, 45-52% Cl	River Aire	UK	2.0
C_{10}-C_{30}, 45-52% Cl	River Thomas	UK	1.0-2.0
C_{10}-C_{30}, 45-52% Cl	Mersey Estuary	UK	3.0-4.0
C_{10}-C_{30}, 45-52% Cl	Wyre Estuary	UK	0.5-1.5
C_{10}-C_{30}, 45-52% Cl	River Lea	UK	<0.5
C_{10}-C_{30}	River Lech, Gersthofen	Germany[c]	0.10-0.60
C_{10}-C_{13}	River Lech, Rain	Germany	0.12
C_{10}-C_{30}	River Danube	Germany	0.10-1.2
C_{10}-C_{13}, 62% Cl	Sewage plant runoff	Germany	0.12
C_{10}-C_{13}, 62% Cl	Upstream sewage plant	Germany	0.08
C_{10}-C_{13}, 62% Cl	Downstream plant	Germany	0.07
C_{10}-C_{13}, 50-70% Cl	Red River, Selkirk	Canada[d]	0.02-0.05
C_{14}-C_{17}, 52% Cl	St. Lawrence River	Canada	<1.0

[a]HRGC/ECNI-MS (High Resolution Gas Chromatography coupled with Electron Capture Negative Ion Mass Spectrometry) [33]

[b]Tlc-ar (Thin-layer chromatography with argentation) [31]

[c]HRGC/ECNI-MS [36,37]

[d]HRGC/ECNI-HRMS (High Resolution Gas Chromatography coupled with Electron Capture Negative Ion High Resolution Mass Spectrometry) [9,32]

Table 1.5: Environmental concentration (μg/kg, dry wt) of PCAs in sediments and sewage sludge. [9,31,32,33,36,37].

PCA measured	Location	Country	Conc.
C_{10}-C_{13}, 60% Cl	Impound drainage ditch	US[a]	1,200-40,000
C_{14}-C_{17}, 52% Cl	Impound drainage ditch	US	760-50,000
C_{20}-C_{30}, 42% Cl	Impound drainage ditch	US	3,600-170,000
C_{10}-C_{13}, 60% Cl	Sugar Creek, OH	US	<1.5-7.3
C_{14}-C_{17}, 52% Cl	Sugar Creek, OH	US	<1.5-8.2
C_{20}-C_{30}, 42% Cl	Sugar Creek, OH	US	8-11
C_{10}-C_{30}, 45-52% Cl	Irish Sea	UK[b]	<0.0005-600
C_{10}-C_{30}, 45-52% Cl	North Sea	UK	<0.0005-350
C_{10}-C_{30}, 45-52% Cl	Bala Lake	UK	
C_{10}-C_{30}, 45-52% Cl	River Dee	UK	350
C_{10}-C_{30}, 45-52% Cl	River Wnion	UK	<0.0005
C_{10}-C_{30}, 45-52% Cl	Manchester tap water	UK	
C_{10}-C_{30}, 45-52% Cl	River Trent	UK	3000-14,000
C_{10}-C_{30}, 45-52% Cl	River Aire	UK	10,000
C_{10}-C_{30}, 45-52% Cl	River Thomas	UK	1,000
C_{10}-C_{30}, 45-52% Cl	Mersey Estuary	UK	3,000-8,000
C_{10}-C_{30}, 45-52% Cl	Wyre Estuary	UK	<0.0005-4,800
C_{10}-C_{30}, 45-52% Cl	River Lea	UK	1000
C_{10}-C_{13}	River Lech, Gersthofen	Germany[c]	<5-700
C_{10}-C_{13}	River Elbe, Hamburg	Germany	17-25
C_{10}-C_{13}	River Main	Germany	25-50
C_{10}-C_{13}	River Rhein	Germany	26-83
C_{10}-C_{13}	Hamburg Harbor	Germany	17
C_{10}-C_{13}, 62% Cl	Sewage sludge	Germany	1,000-65,000
C_{10}-C_{13}, 60-70% Cl	Lake Winnipeg	Canada[d]	21-135
C_{14}-C_{17}, 52% Cl	St. Lawrence River	Canada	<3500

[a]HRGC/ECNI-MS (High Resolution Gas Chromatography coupled with Electron Capture Negative Ion Mass Spectrometry)

[b]Tlc-ar (Thin-layer chromatography with argentation)

[c]HRGC/ECNI-MS

[d]HRGC/ECNI-HRMS (High Resolution Gas Chromatography coupled with Electron Capture Negative Ion High Resolution Mass Spectrometry)

activity such as Lake Winnipeg (176 μg/ kg, dry wt). However, there may be exceptions, as PCAs may also accumulate primarily in biota, instead of sediment [40].

The reported ∑PCA concentrations in aquatic organisms are shown in Table 1.6 [9,31,32,33,38]. Although PCA levels were small in catfish (350 μg/kg) in Detroit River, PCA concentrations were high (1148, 1205 μg/kg) in the yellow perch and zebra mussels respectively, from the same location. The concentration of C_{10}-C_{30}, with 45-52% Cl content in dogfish was 200 μg/kg, but mackerel in the same location was found to contain 100-1200 μg/kg. Walrus blubber was found to contain detectable levels of PCA as far north as Greenland, indicating long-range transport [10].

The reported ∑PCA concentration in birds and terrestrial mammals are shown in Table 1.7 [31,38]. While kittiwake in Puffin Isle were found to contain <5 μg/kg PCAs, guillemot in the same location contained 300 μg/kg. Campbell and McConnell reported ∑PCA levels from <0.05 to 2 μg/g in seabird eggs collected from UK coastal species, and mammals collected from areas close to industrial activity [38]. In Sweden the highest concentrations of C_{10}-C_{13} were in moose and rabbit. The ∑PCA concentration in tissue of humans and their foodstuffs are shown in Table 1.8 [9,31,39]. Although some levels were detected in dairy products and vegetable oils, they were not detected in non-dairy beverages. Human breast milk, from Inuit women living in communities in Northern Quebec, was found to contain PCA levels from 11 to 17 μg/kg. The ∑PCA concentrations in air and paving stones are shown in Table 1.9 [7,9,15,37]. In Germany, atmospheric emissions of PCAs were measured either as vapor or sorbed onto dust particles. In Canada during the summer of 1990, PCA samples were collected daily during a 4 month period on polyurethane foam plugs and measured as vapor phase[10].

Table 1.6: Environmental concentration (μg/kg, dry wt) of PCAs in aquatic organism [9,31,32,33,38].

PCA measured	Location	Species	Conc. (μg/kg, dry wt)
C_{10}-C_{13}, 60% Cl	Detroit River, US[a]	Yellow perch	1,148
C_{14}-C_{17}, 52% Cl	Detroit River, US	Catfish	305
C_{20}-C_{30}, 42% Cl	Detroit River, US	Zebra mussel	1,205
C_{10}-C_{13}, 60% Cl	Sugar Creek, US	Mussel	<7-180
C_{14}-C_{17}, 52% Cl	Sugar Creek, US	Mussel	<7-280
C_{20}-C_{30}, 42% Cl	Sugar Creek, US	Mussel	<7-170
C_{10}-C_{30}, 45-52% Cl	Irish Sea, UK[b]	Plaice	50
C_{10}-C_{30}, 45-52% Cl	North Sea, UK	Mussel	200
C_{10}-C_{30}, 45-52% Cl	Torbay, UK	Dogfish	200
C_{10}-C_{30}, 45-52% Cl	Torbay, UK	Mackerel	100-1,200
C_{10}-C_{30}, 45-52% Cl	Torbay, UK	Shrimp	50-500
C_{10}-C_{30}, 45-52% Cl	Liverpool Bay, UK	Pike	<50
C_{10}-C_{30}, 45-52% Cl	Vale Royal, UK	Pike	<50
C_{10}-C_{30}, 45-52% Cl	Farne Islands, UK	Grey seal	40-100
C_{10}-C_{30}, 45-52% Cl	Mersey Estuary, UK	Mussel	100
C_{10}-C_{30}, 45-52% Cl	Wyre Estuary, UK	Mussel	1,000-12,000
C_{10}-C_{13},60% Cl	L.Vatten, Sweden[c]	Arctic char	570
C_{10}-C_{13},60% Cl	L.Storvindeln,Sweden	Whitefish	1,000
C_{10}-C_{13},60% Cl	Kongsfjorden, Sweden	Ringed seal	130
C_{10}-C_{13},60% Cl	Baltic Sea, Sweden	Grey seal	280
C_{10}-C_{13},60% Cl	Bothnian Sea, Sweden	Herring	1,400
C_{10}-C_{13},60% Cl	Baltic Proper, Sweden	Herring	1,500
C_{10}-C_{13}, 60-70% Cl	S.W.Ellesmere Isl.,Canada[d]	Ringed seal	374-767
C_{14}-C_{17}, 52% Cl	St. Lawrence River,Canada	Zebra	<3,500

[a]HRGC/ECNI-MS.

[b]Tlc-ar.

[c]HRGC/ECNI-MS.

[d]HRGC/ECNI-HRMS.

Table 1.7: Environmental concentration (μg/kg) of PCAs in birds and terrestrial mammals [31,38].

PCA measured	Location	Species	Conc. (μg/kg)
C_{10}-C_{30}, 45-52% Cl	Weton Point, UK[a]	Sheep	<5-300
C_{10}-C_{30}, 45-52% Cl	Welsh, UK	Sheep	<5
C_{10}-C_{30}, 45-52% Cl	Isle of Scilly, UK	Guillemot	<100-1100
C_{10}-C_{30}, 45-52% Cl	Isle of Scilly, UK	Guillemot	<300-1400
C_{10}-C_{30}, 45-52% Cl	Isle of Scilly, UK	Heron (liver)	100-2700
C_{10}-C_{30}, 45-52% Cl	Skomer, UK	Shag (eggs)	<5-200
C_{10}-C_{20}, 45-52% Cl	Shiant Isle, UK	Manx (eggs)	<5
C_{10}-C_{20}, 45-52% Cl	Alia Craig, UK	Puffin (eggs)	nd-100
C_{10}-C_{20}, 45-52% Cl	Puffin Isle, UK	Kittiwake	<5
C_{10}-C_{20}, 45-52% Cl	Puffin Isle, UK	Shag (eggs)	50-250
C_{10}-C_{20}, 45-52% Cl	Puffin Isle, UK	Guillemot	300
C_{10}-C_{20}, 45-52% Cl	Bass Rock, UK	Gannet (eggs)	<10-600
C_{10}-C_{13},60% Cl	Sweden[b]	Opsrey	530
C_{10}-C_{13},60% Cl	Ottsjo,Sweden	Reindeer	140
C_{10}-C_{13},60% Cl	Grimso, Sweden	Moose	4400
C_{10}-C_{13},60% Cl	Revingeshed, Sweden	Rabbit	2900

[a]Tlc-ar.

[b]HRGC/ECNI-MS.

Table 1.8: Environmental concentration (μg/kg) of PCAs in humans and in human foodstuffs [9,31,39].

PCA measured	Location	Country	Conc. (μg/kg)
C_{10}-C_{30}, 45-52% Cl	Dairy products	UK[a]	300
C_{10}-C_{30}, 45-52% Cl	Vegetable oils	UK	150
C_{10}-C_{30}, 45-52% Cl	Fruits and vegetables	UK	25
C_{10}-C_{30}, 45-52% Cl	Beverages	UK	<50
C_{10}-C_{30}, 45-52% Cl	Human brain	UK	<50-80
C_{10}-C_{30}, 45-52% Cl	Human liver	UK	<50-1500
C_{10}-C_{20}, 45-52% Cl	Human kidney	UK	<50-200
C_{10}-C_{20}, 45-52% Cl	Human adipose tissue	UK	<50-540
C_{14}-C_{18}, 52% Cl	Human adipose tissue	Switzerland[b]	200
C_{14}-C_{18}, 52% Cl	Human breast milk	Canada[c]	11-17

[a]Tlc-ar.

[b]HRGC/ECNI-MS.

[c]HRGC/ECNI-HRMS.

Table 1.9: Environmental concentration of PCAs in other media [7,9,15,37].

PCA measured	Sample	Location	Conc.
C_{10}-C_{30},	Air	Manufacturing plant, Germany[a]	30 x10^9 pg/m^3
C_{10}-C_{13}, 56% Cl	Paving Stones	Metal plant Germany[b]	582 x10^9pg/kg
C_{14}-C_{13}, 60% Cl	Air	S. Ontario, Canada[c]	543 pg/m^3

[a]NA.

[b]HRGC/EI-MS.

[c]HRGC/ECNI-HRMS.

1. 7. Toxicity

Toxicity of PCAs has recently been evaluated in a number of risk assessments [41]. This data is based on commercial PCA mixtures, and poses some degree of uncertainty due to the complexity of the mixtures. For example, PCA mixtures consist of thousands of different compounds with different properties and toxicities. Stabilizers are also added to commercial PCA products, which may cause false results in many of the toxicity tests. The data available on toxicity of PCAs indicated that microorganisms appear fairly resistant to the toxic effects of PCAs. Tests done on sewage sludge bacteria showed that PCAs did not affect oxygen utilization at 1-200 mg/L [28], and there were no indications of effects on strains of *Salmonella typhimurium* [41]. Many aquatic toxicity studies can be misleading since they usually examine gross toxicological effects such as mortality and neglected reproductive effects. Sublethal effects of PCAs such as histology and enzyme function have been found in mammals [44]. Toxicity appears to be inversely related to carbon chain length for PCAs. However, since water was the exposure medium, the relatively higher solubilities of the shorter chain PCAs lead to greater exposure. Significant growth inhibition occurred to a species of freshwater alga (*Selenastrum capricornutum*) when exposed to short chain chloroparaffins (SCCPs) with average chlorine content of 58% (w/w) at 570 µg/L [45]. Because of the low water solubility of the intermediate and longer chain PCAs, fish show no significant mortality or abnormalities during a long-term exposure [45].

PCA toxicity to birds was studied using mallard ducks (Anas platyrhynchos) and ring-necked pheasants (*Phasanius colchius*). Medium chain PCAs (52% Cl) was spiked in their food at a concentration of 24 mg/g resulting in no significant toxicological effects [46]. Mallard ducks were also used in a one generation reproductive study with adult

ducks exposed to dietary concentrations of 0, 28, 166, and 1000 μg/g. No abnormalities were observed, however, eggshell thinning was noted for ducks exposed to the two higher concentrations [28].

Acute and chronic toxicity of PCAs to mammals is low, with the most common effect being an increase in liver weight at very high doses [47]. This can be attributed to CYP 450-enzyme induction, peroxisomal proliferation, smooth endoplasmic reticulum proliferation, and an increase in cell proliferation [48]. One study was conducted on the reproductive effects of PCAs [49]. Rats were fed medium chain PCAs (52% Cl), at concentrations of 0, 100, 1000, and 6250 mg/kg, for 28 days before mating, during mating and 21 days postnatal. Pups were also exposed to the same concentrations for 70 days following weaning. No pups from the highest exposure group survived to weaning, and all pups from the mid- to high-exposure group experienced labored breathing, discoloration and/or blood around the orifices.

Results of a number of studies using a brackish water fish suggest that narcosis (i.e., nonspecific toxic action) is the acute toxic mechanism of PCAs. However, some data suggests that PCAs have specific toxic actions on the liver, kidney and thyroid organs [50]. The authors concluded that three nongenotoxic mechanisms were responsible, namely, hepatic peroxisome proliferation, perturbation of the thyroid homeostasis, and protein-mediated nephropathy specific to male rats [50]. A two year gavage (introducing the food by tube into the stomach) study of mice and rats also indicated that the shorter chain, more highly chlorinated paraffins have a greater potential for chronic toxicity and carcinogenicity than the longer chain, lower chlorinated paraffins [51].

1.8. Analysis of Polychlorinated *n*-Alkanes

The determination of PCAs is very important to study their level and fate in different environmental compartments. In the past their analysis was very difficult because of the complex mixture in which they exist, which it was one of the reasons why they have so seldom been determined. Understanding the environmental behavior of that mixture will require economical and environmentally friendly methods. Two methods such as dehydrochlorination to the parent hydrocarbons [52] and gas chromatography/Mass Spectrometry (GC/MS) based on selected ion monitoring (SIM) of positive ions [53-54] have been used for monitoring PCA mixtures in environmental samples. Most GC/MS methods have relied on electron capture negative ionization (ECNI) low-resolution MS to determine PCA mixture [53]. Due to the lack of specificity of these methods any chlorohydrocarbon present in the environmental matrices could interfere with PCA fragments [53]. Also, other chemicals with molecular mass similar to PCAs such as PCBs, toxephene and chlorodane-related compounds have potential interference when monitor PCAs at nominal mass. While this mixture elutes through the chromatographic column over a wide range of retention times due to the multitude of isomeric compounds, the separation into single peaks for the definite identification of the components of the PCA mixture is not possible.

Consequently, using high resolution MS in electron capture negative ion mode (ECNI) offers a valuable tool to detect PCAs at trace levels while avoiding most of these problems. Gyos and Gustavsen [54] used ECNI-MS for the first time to determine two C_{10}-C_{13} PCAs with 59 and 70% chlorine content. Detailed information about the composition and the retention times of the isomers can be obtained from the interpretation of ECNI mass spectra of single GC-fractions in the mixtures. Both factors

are necessary to develop sensitive and selective methods to analyze PCAs in environmental samples by MS in the selective ion mode. So far there is little data available about the fragmentation behavior of PCA in ECNI-MS because of the complexity of their mass spectra and the lack of single reference compounds. Recently Tomy et al.[53] illustrated a selective, specific, and sensitive method for quantifying PCAs in environmental mixtures. In contrast to other studies, high-resolution gas chromatography/electron capture negative ion-high resolution mass spectrometry (HRGC/ECNI-HRMS) was used in the SIM mode. At a resolution of 12000, no interferences between PCAs and other organochlorine compounds were observed. The detection of $[M\text{-}Cl]^-$ ions from C_{10}-C_{13} PCAs was performed in seven windows. Two commercially available C_{10}-C_{13} PCAs with 60 and 70% chlorine content were used as standards. In this method the integrated SIM response covred the range 0.5 -500 ng. The analytical detection limit is ~ 60 pg of injected PCA at a signle-to-noise ratio of 4:1. The levels of PCAs in fish and sediment samples from the Trenton Channel of the Detroit River, near its entry to Lake Erie, and in zebra mussels from Lake Erie have been determined by this method [53].

The ion source temperature affected the detection of the monitored ions in the ECNI mass spectra of PCAs [53]. For example, at ion source temperature of 220°C the molecular ion peak is not detected, but the $[M\text{-}Cl]^-$ is observed clearly. Also small quantities of $[M\text{-}HCl]^-$ and of $[M+Cl]^-$ are present. Decreasing the ion source temperature to 120°C resulted in maximizing the abundance of both the $[M\text{-}Cl]^-$ and the $[M\text{-}HCl]^-$ ions. The *m/z* values of the ions to be used for selected ion monitoring are determined from the most abundant ion group in the spectrum, which is $[M\text{-}Cl]^-$. The most abundant

m/z value was used as a quantitation ion for SIM and the next most abundant ion as a confirming ion. For example, the most abundant *m/z* value of hexachlorodecane ($[M-Cl]^-$ = 313 *amu)*, is used as a quantitation ion, while the next most abundant ion (314 *amu*) is used as a confirming ion.

1.9. Primary Transformation Processes of Organic Pollutants

Organic pollutants may be transported long distances on local to global scales by volatilization, transport to surface water and sediment or penetration through the soil profile. Organic pollutants may cause serious problems in various environmental compartments due to their toxicity, persistence and bioaccumulation. [55]. To predict the fate of organic pollutants in the natural environment and to assess their risk, it is necessary to understand their chemical reactions under environmental conditions [55].

The primary processes for transforming pollutants in the environment include biotic (biological) as well as abiotic (non-biological) action. Both biotic (biodegradation) and abiotic (oxidation, hydrolysis and photolysis) actions [56], are responsible for reducing the contaminated materials and/or diminishing their toxicity. Many environmental pollutants such as pesticides [55], chlorinated solvents, and PCBs [56a] are transformed under the effect of biotic and abiotic degradation.

For example, zero-valent iron metal Fe^0 [56a] reduces a variety of groundwater contaminants such as trichloroethylene (TCE), chromate and nitrate, resulting in degradation of the contaminant and dissolution of the Fe^0 to Fe^{2+}. Reductive elimination of TCE by Fe^0 resulted in the production of the nontoxic chloroacetylene (Cl-C ≡ C -H) [56a]. Treatment of drinking water with chloramines produced cyanogen chloride (ClCN) as a toxic disinfection by-product. Hydrolysis of ClCN [56b] was studied at a pH range

of 9.54-10.93 and at a temperature of 21.0°C. The alkaline hydrolysis pathway was predominant resulting in transformtion of ClCN to equimolar amounts of cyanate and chloride ions. Chlorsulfuron (1-(2-chlorophenylsulfonyl)3-(4-methoxy-6-methyl-1,3,5-triazen-2-yl) urea is a herbicide used to control many broadleaf weeds and some annual grass weeds [56c]. At pH 5 chlorsulfuron hydrolysis exhibited pseudo-first-order degradation kinetics with a half-life of 24 days at 25°C. Aerobic soil degradation of chlorsulfuron at 25°C in a Keyport silt loam soil at pH 6.4 and 2.8% organic matter resulted in rapid degradation with a half-life of 20 days.

Hydrolysis and biodegradation processes transformed chlorsulfuron to a variety of degradation products, which ultimately degraded further to form carbon dioxide and fragments that are incorporated into the soil. Another report [55] shows the phototransformation of aromatic pollutants such as ethiofencarb, 4-chloro-2-methylphenol, nitrobenzene, propiconazole, acifluorfen and thiobencarb (Figure 1.1) in various aqueous media irradiated for 95 hr with sunlight. Both ethiofencarb and 4-chloro-2-methylphenol absorbed very small amounts of sunlight, and degraded mainly by photosensitized reaction with half-lives of 40 ± 5 and 18 ± 4 h respectively. The main photoproducts of 4-chloro-2-methylphenol were due to ring opening not hydroxy benzoquinone confirming the effect of photosensitizers. Other compounds degraded mainly by direct photolysis with half-lives of 85 ± 10, 120 ± 15, 133 ± 15 and 320 ± 30 hr for propiconazole, nitrobenzene, acifluorfen and thiobencarb, respectively. All compounds studied were degraded more rapidly in natural water than in pure water due to the effect of sensitizers.

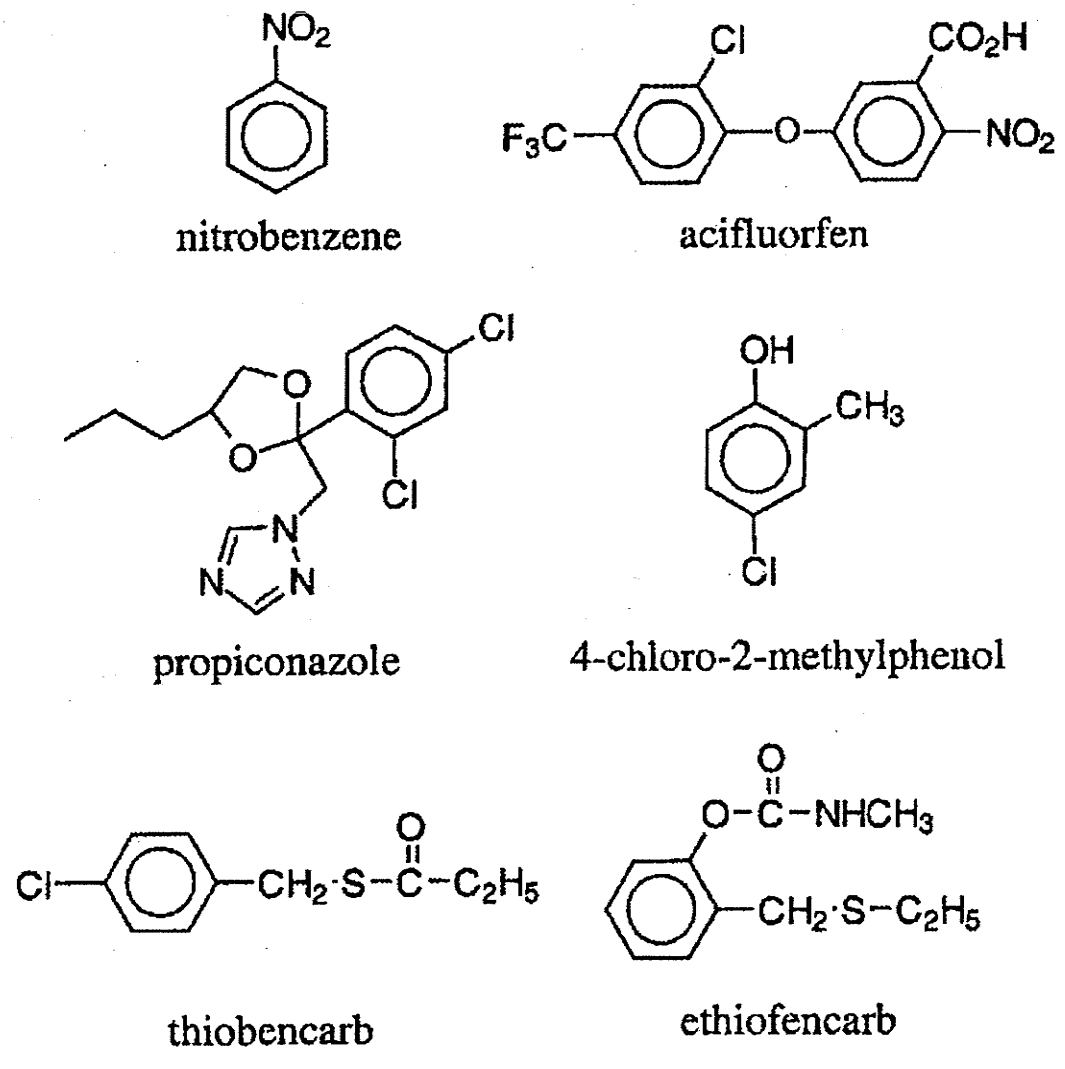

Figure 1.1: Structures of aromatic pollutants.Reproduced from reference 55.

1.9.1. Biodegradation Reactions

In biodegradation processes, degrading the chemical is mainly by the action of living organisms [56]. The most important organisms involved in biodegradation reactions are bacteria and fungi. Primary, ultimate and acceptable biodegradation are the main three types of biodegradation [56]. In the primary biodegradation, minimum change in the identity of the compound occurred, while mineralizing the compound to carbon dioxide, water and inorganic ions is the ultimate biodegradation. Removing some undesirable property of the compound such as foaminess or toxicity is called acceptable biodegradation.

1.9.2. Oxidation Reactions

An oxidation reduction reaction (redox) is a reaction in which electrons are transferred between two reactants. Whenever a substance is oxidized, another substance must be reduced. The reduced substance is the oxidizing agent, while the reducing agent is the compound oxidized [56]. In the absence of living biota (biological activity) redox reaction is considered an abiotic reaction [57].

Aquatic systems with significant amounts of dissolved oxygen will result in oxidation of the pollutants. Environmental pollutants such as aliphatic and aromatic hydrocarbons, alcohols, aldehydes, ketones, phenols, hydroquinones, sulfoxides, nitrogen and sulfer heterocyclic compounds are susceptible to oxidation reaction [56]. On the other hand, reductive degradation of organic chemicals may involve reduction of nitroaromatic compounds, azo compounds, quinines, sulfoxides and reductive dehalogenation of chlorinated aliphatic or aromatic contaminants [58]. In the natural environment, the pollutant is oxidized by oxygen or another oxidizing chemical such as oxides of iron and

manganese, ozone, hydrogen peroxide H_2O_2, singlet oxygen ($^{\bullet}O$), and $^{\bullet}OH$ radicals, producing a more oxidized product [56]. Also, sulfide (HS^-, H_2S), Fe(II), and Mn(II) are the most common environmental reducing agents for organic compounds [56]. Oxidation reactions are very important in the atmosphere, where oxygen, ozone and other oxidizing agents are present in large concentrations. Whereas in aquatic systems, oxygen and oxidizing agents are present in much lower concentrations and the reaction depends on the pH as well as the natural redox state of the particular water body [56].

One of the objectives in this study was to determine the hydrolytic and photolytic reactivity of PCAs in the environment.

1.9.3. Hydrolysis

Overall hydrolysis is a transformation of an organic chemical with water molecules or hydroxide ion (OH^-) resulting in the formation of a new R-O bond and cleaveage of a R-X bond in the original molecule:

$$R\text{-}X + H_2O \longrightarrow R\text{-}OH + HX \qquad (1\text{-}8)$$

where X represents a leaving group which readily undergoes hydrolysis.

Presence of OH groups in the products of hydrolysis reactions increases their polarity which reduces their environmental concern more than that of the parent compounds.

Dark degradation of chemicals in the absence of organisms and redox species is mainly the result of hydrolysis processes [56]. Hydrolysis may occur by nucleophilic substitution at sp^3 carbon centers or by acyl substitution at sp^2 carbon centers in carbonyl groups. Hydrolytic nucleophilic substitution reactions could follow S_N1 or S_N2 mechanisms as described below.

$$S_N1: \quad RX \longrightarrow R^+ + X^- \text{ (slow) ionization step} \qquad (1\text{-}9)$$

$$R^+ + H_2O \longrightarrow R\text{-}OH + H^+ \text{ (fast)} \quad (1\text{-}10)$$

$$S_N2: \quad RX + H_2O \longrightarrow R\text{-}OH + X^- + H^+ \quad (1\text{-}11)$$

In most cases, the particular mechanism involved in hydrolysis (nucleophilic substitution) is a hybrid of the two mechanisms (S_N1 and S_N2). Compounds such as halogenated hydrocarbons, epoxides and phosphorus esters may be hydrolyzed by nucleophilic substitution reactions. While carboxylic acid derivatives and carbonic acid derivatives undergo nucleophilic acyl substitution.

Rate of the hydrolysis reaction is pH dependent, where hydrolysis may occurs by acid, neutral, or basic reaction and the overall reaction rate is represented in equation (1-12).

$$-\frac{d[X]}{dt} = k_{H+}[H^+][X] + k_{H_2O}[H_2O][X] + k_{OH-}[OH^-][X] \quad (1\text{-}12)$$

where, k_{H+} [H+][X] is acid-catalyzed hydrolysis, k_{H_2O} [H_2O][X] is neutral hydrolysis and k_{OH^-} [OH^-][X] is base-catalyzed hydrolysis; and k_{H+}, k_{H_2O}, k_{OH-} are the acidic, neutral, and basic hydrolysis rate constants respectively. The relationship between the hydrolysis rate constant (k) and the reaction temperature is represented by the Arrhenius equation:

$$\ln k = \ln A - \frac{E_a}{RT} \quad (1\text{-}13)$$

where, A (s^{-1}) is the frequency factor which is related to entropic effects (the probability that a given collision involving sufficient energy will be successful), E_a is the activation energy (J/mole), which is the energy the molecules must have in order to react, R (8.314 x 10^{-3} kJ mol/K) is the gas constant and T (K) is the absolute temperature. A plot of ln k

versus $\frac{1}{T}$ will provide a straight line with a slope of $-\frac{E_a}{RT}$ and an intercept of ln A. The rate (k) is typically dependent on temperature.

The terms in equation (1-12) are more complex because both elimination and substitution pathways may operate. In addition, the anions used in preparation of the buffer solution may be involved in the degradation of the parent compounds by nucleophilic attack [56]. Organic compounds undergo transformation through hydrolysis reactions following mechanisms depending on the pH of the reaction medium. For example, epoxides ($R_1R_2C(O)CR_3R_4$) undergo neutral, acid-catalyzed and/or base-catalyzed reactions, which lead in most cases to the formation of diols. In some cases, ketones are formed as products of epoxide hydrolysis [56]. Carboxylic acid esters (RCOOR) undergo acid catalyzed, neutral, and base catalyzed hydrolysis. Generally, esters have larger k_{OH} than k_{H+} values at pH 5-6 [59]. Amides degrad primarily by base-catalyzed hydrolysis while carbonyl carbon atoms are not activated in low pH solutions. Also, organophosphorus and carbamate compounds undergo primarily base-catalyzed hydrolysis. A variety of nucleophilic substitution and elimination (dehydrochlorination) reactions of polyhalogenated hydrocarbons demonstrated the effect of halogen on the hydrolytic stability [56] as F > Cl > Br > I. Competing pathways resulted in mixed products. The multiple hydrolysis reactions and products for 1,2,3-trichloropropane are summarized in Figure (1.2) [56]. Nucleophilic substitution produced glycerol, while, 2-chloro-3-hydroxy-1-propene resulted from an elimination reaction. Both neutral and base- catalyzed reactions are favored over acid-catalyzed hydrolysis for polyhalogenated compounds. [56]. Reaction rate is dependent on C-Cl bond strength and steric hindrance. The products of the hydrolysis reaction may differ depending on pH.

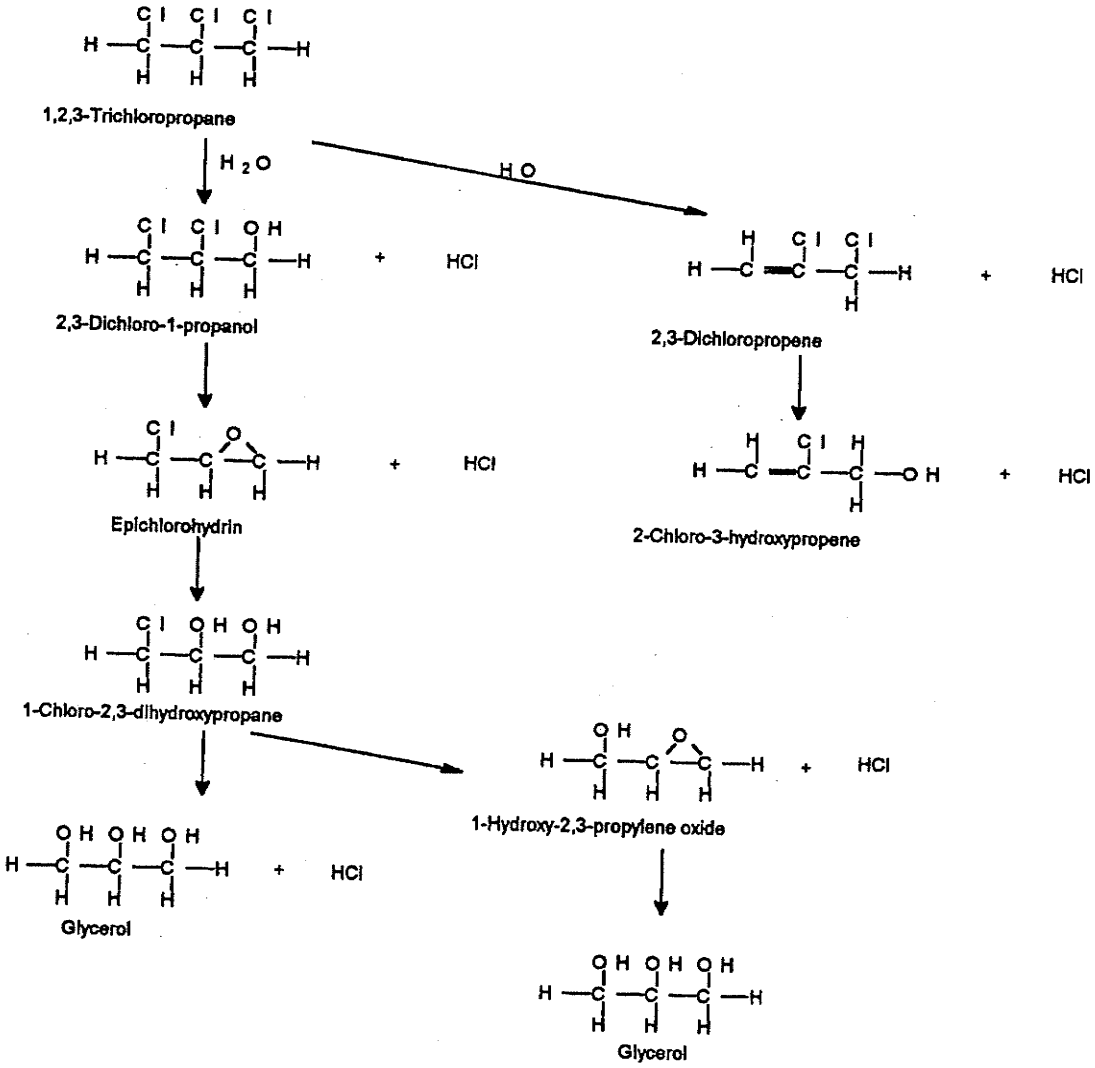

Figure 1.2: Proposed hydrolysis pathway for 1,2,3-trichloropropane and its intermediate products. Reproduced from reference 56.

For example, 1,2-dichloroethane hydrolyzes by the nucleophilic attack of H_2O in neutral to acidic solution to produce ethylene glycol, while in basic solution, the main product was vinyl chloride, formed by the elimination of HCl by the hydroxide ions [56]. Hydrolysis rates the for organic compounds may be estimated in the environment have been developed by different methods such as quantitative structure activity relationships (QSARs) [56]. The basic assumption of QSARs is that there are some quantitative relationships between the microscopic (molecular structure) and the macroscopic (empirical) properties (particularly biological activity) of a molecule. The term structure does not necessarily mean the spatial arrangement of atoms in a molecule itself, but rather the chemical and physicochemical properties in that arrangement. Another method is based on comparison of the reactivity of target compound with that of an analogous compound containing similar structure and functional groups for which the rate constants are known [56].

1.9.4. Photolysis

Photolysis is a chemical reaction that is initiated by absorption of energy from light sources [56]. According to the Grotthus-Draper law only light, which is absorbed by a molecule can be effective in producing a chemical transformation of the molecule. The Stark-Einstein law states that only one molecule is activated to an excited state for each quantum of light absorbed [60]. The rate of a photolysis reaction, which depends on the concentration of the chemical can be described by first-order kinetics:

$$\frac{d[C]}{dt} = -k_P [C] \qquad (1\text{-}14)$$

where [C] is the concentration, t is the time of irradiation and k_p is the first-order photolysis rate constant (t^{-1}).

The first-order photolysis half-life is given by:

$$t_{1/2} = \frac{0.693}{k_P} \qquad (1\text{-}15)$$

Under the influence of sunlight, chemicals may undergo transformation in air, water and soil, by direct and indirect photoreactions. In direct photoreactions, the absorption of light by the chemical leads to transformation, while in indirect photoreaction the chemical reacts with photolytically generated reactive species.

The overall photolysis rate is the summation of both direct and indirect photolysis rates [60]:

$$\frac{d[C]}{dt} = -k_P[C] = -\{k_d + k_s\}[C] \qquad (1\text{-}16)$$

where, k_P is the overall photolysis rate constant, k_d is the direct photolysis rate constant and k_S is the indirect photolysis rate constant.

1.9.4.1. Direct Photoreaction

In direct photolysis, the rate depends only on the rate of light absorbed (I_A) by the compound C and the efficiency of the chemical transformation process as described by the reaction quantum yield Φ:

$$\text{rate} = -\frac{d[C]}{dt} = \Phi\ I_A \qquad (1\text{-}17)$$

The quantum for the photoreaction yield is the ratio of the number of excited molecules undergoing a transformation process to the number of photons absorbed.

Although a number of studies [56] have reported quantum yields for several types of photoreactions in aerated water, few reliable procedures are available for estimating quantum yields even among closely related compounds. The magnitude of the reaction

quantum yield will depend on the efficiency of other mechanisms for deactivating the exicited state species [56], making its estimation difficult.

The Beer-Lambert law (exponential form) describes the absorption of light by a chemical in solution:

$$I_T = I_o \times 10^{-\varepsilon \ell C} \tag{1-18}$$

$$\text{Log } I_T = \log I_o - \varepsilon \ell C \tag{1-19}$$

$$A = \text{Log } \frac{I_o}{I_T} = \varepsilon \ell C \tag{1-20}$$

where I_o is the intensity of incident light, I_T the intensity of transmitted light, ε the molar absorptivity, ℓ the optical path length of the solution (cm) and C is the concentration of the absorbing substance. The amount of light absorbed (I_A) is the difference between the incident light and the transmitted light:

$$I_A = I_o - I_T \tag{1-21}$$

From equation (1-18)

$$I_A = I_o - I_o \times 10^{-\varepsilon \ell C} \tag{1-22}$$

$$I_A = I_o (1 - 10^{-\varepsilon \ell C}) \tag{1-23}$$

When the optical path length (ℓ) is 1 cm and the absorbance ($A = \varepsilon \ell C$) is low, equation (1-23) can be simplified to:

$$I_A = I_o \varepsilon C \ln 10 \tag{1-24}$$

or

$$I_A = 2.3 I_o \varepsilon C \tag{1-25}$$

Substituting the value of I_A into equation (1-17) provides an expression for the direct photolysis rate in water [60]:

$$-\frac{dC}{dt} = \frac{2.3}{jD}\ \Phi\, I_o\, \varepsilon\, [C] = k_d\, [C] \qquad (1\text{-}26)$$

where j is the factor (6×10^{20}) which converts photons to Einsteins for compatibility with molar concentration units, D is the depth of the water body (cm) and k_d is the direct photolysis rate constant at wavelength λ.

The rate constant of direct photolysis in the environment [60] with sunlight (k_{dE}) can bedetermined by suming the rate constants over all wavelengths above 290 nm where $\varepsilon > 0$, assuming that Φ is independent of wavelength:

$$k_{dE} = \frac{2.3}{jD}\,\Phi \sum I_o \varepsilon \qquad (1\text{-}27)$$

The average solar irradiance in the solution ($E_{o\lambda}^{av}$) is a function of the flux of the incident light (I_o) and the optical path length (l):

$$E_{o\lambda}^{av} = I_o\, l \qquad (1\text{-}28)$$

Equation (1-27) becomes:

$$k_{dE} = \frac{2.3}{jD}\ \Phi \sum E_{o\lambda}^{av}\, \varepsilon \qquad (1\text{-}29)$$

The average solar irradiance or flux ($E_{o\lambda}^{av}$) is the number of photons per unit area per unit time. A computer program called GC-SOLAR [60] has been developed to estimate the values of $\frac{E_{o\lambda}^{av}}{D}$ as a function of wavelength, time of day, year and latitude using light flux terms called Z_λ with units of photons $cm^{-2}\ s^{-1}$.

Substituting $Z_\lambda = \frac{I_0 l}{D} = \frac{E_{o\lambda}^{av}}{D}$ in equation (1-28) the rate constant can be writen as:

$$k_{dE} = \frac{2.3}{j} \Phi \sum \varepsilon_\lambda Z_\lambda \qquad (1\text{-}30)$$

Because photoreaction of chemicals in sunlight may take place over time periods of days, Mabey et al [56] computed diurnal (24-hr) light intensity terms, $L_\lambda = 2.3 \frac{I_0 l}{D}$ for four seasonal dates at specific decadic latitudes in shallow water. L_λ values have units of millieinsteins cm^{-2} day^{-1}. Thus the direct photolysis rate constant is simplified as:

$$k_{dE} = \Phi \sum \varepsilon_\lambda L_\lambda \qquad (1\text{-}31)$$

Direct photoreaction is possible only when the chemical absorbs light quanta of UV/visible light (wavelength range 290-800 nm) which are energetic enough to break bonds in a molecule. Therefore, chemicals that absorb light significantly only in the UV region below 290 nm and in the infra-red above 800 nm cannot undergo direct photolysis in the water compartment [60].

Whether a chemical has the potential for direct photolysis will depend on the degree of overlap between the ultraviolet/visible absorption spectrum of the chemical and the emission spectrum of the sunlight above the solar cut-off of 290 nm. For example, the overlap of the solar spectrum (L_λ) with the absorption spectrum (ε_λ) of *p*-nitroanisole (PNA) is shown in Figure (1.3) [56].

1.9.4.2. Indirect Photoreaction

Under natural conditions, chemicals at very low molar concentration [C] with weak absorbance ($A < 0.02$) do not undergo rapid direct photolysis [60]. However, the

phototransformation of these chemicals may occur rapidly in water containing dissolved humic substances, by indirect photoreaction with natural sensitizers [60]. Indirect photolysis by the sensitizers can be generalized by two mechanisms [61]. One of these is the energy transfer process, that is, the sensitizer absorbs light and transfers the energy to another chemical which then undergoes photochemical reactions. In the second mechanism light absorption results in homolytic cleavage of a chemical bond with formation of radicals and subsequent reaction of the radicals. A hypothesized sensitized photoreaction pathway by humic acid (sensitizer) to produce a reactive intermediate (oxidant) such as singlet molecular oxygen ($^1O_2$) is given below:

$$\text{Humic acid} + \text{photon} \longrightarrow \text{Humic acid}^{\bullet}\ (\text{excited state}) \qquad (1\text{-}32)$$

$$\text{Humic acid}^{\bullet} + {}^3O_2 \longrightarrow {}^1O_2 \qquad (1\text{-}33)$$

$${}^1O_2 + \text{chemical of interest} \longrightarrow \text{degradation products} \qquad (1\text{-}34)$$

The rate of indirect photolysis is described by bimolecular kinetic equations involving the concentration of both sensitizer [S] and the chemical of interest [C]:

$$-\frac{d[C]}{dt} = \frac{2.3}{j}\sum(E_{o\lambda}^{av}\,\varepsilon_{S\lambda}\,Q)\,[S]\,[C] \qquad (1\text{-}35)$$

where, Q is the proportionality constant between photosensitizer quantum yield and compound concentration [C]. If the concentration of the sensitizer remains constant [60], the indirect photolysis rate constant (k_S) is expressed as:

$$k_S = \frac{2.3}{j}\sum(E_{o\lambda}^{av}\,\varepsilon_{S\lambda}\,Q)\,[S] \qquad (1\text{-}36)$$

Substituting equation (1-36) into equation (1-35) yields the rate of indirect photolysis as a first-order differential equation:

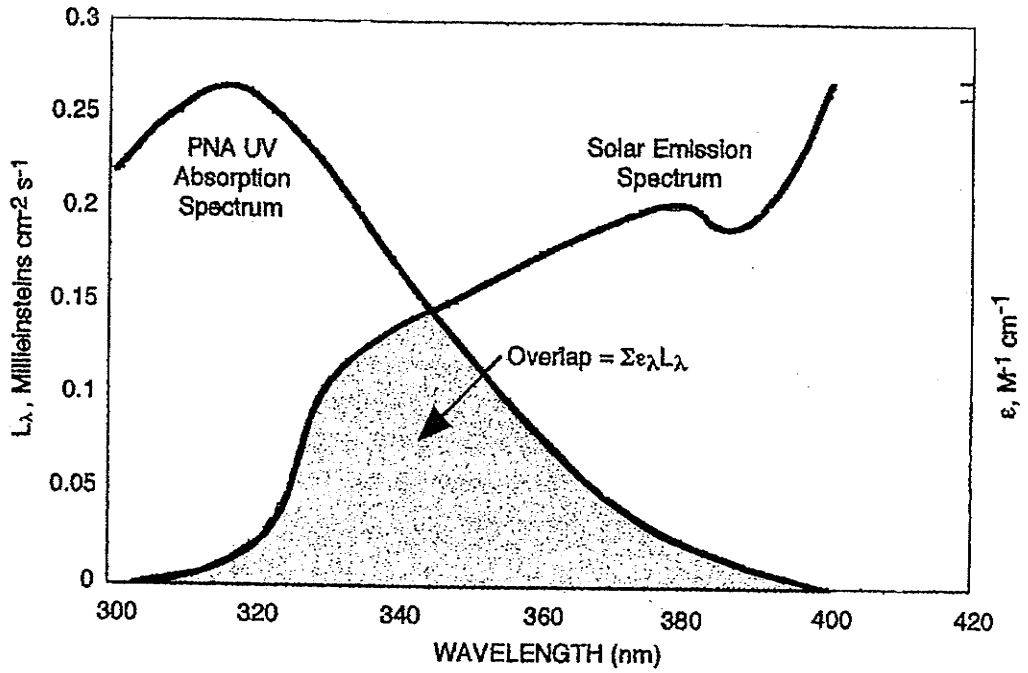

Figure 1.3: The overlap of the UV spectrum of *p*-nitroanisole (PNA) with the solar spectrum at the earth's surface. The overlap of the two curves represents the photoactive region for PNA defined as $\sum \varepsilon_\lambda L_\lambda$. Reproduced from reference 56.

$$-\frac{d[C]}{dt} = k_S\ [C] \tag{1-37}$$

Integrating this equation yields

$$\ln\frac{[C_o]}{[C_t]} = k_S\ t \tag{1-38}$$

where, k_S is first-order indirect photolysis rate constant (t^{-1}), C_o is the initial concentration and C_t is the concentration at time t.

Dissolved organic material (DOM) in the form of humic substances such as humic acid, fulvic acid, phenylalanine, tyrosine and tryptophan in natural water are well known sensitizers. These materials absorb sunlight and produce reactive intermediates that include hydroxyl radicals ($HO^{\cdot}$) [62-63] singlet molecular oxygen ($^1O_2$) [64-70], alkylperoxy radicals ($RO^{\bullet}_2$), superoxide anion ($O_2^{-\bullet}$) , hydroperoxy radicals ($HO^{\bullet}_2$) [71-72, 64-65] and triplet excited states of the humic substances [66-67,73] .The concentrations of the major photooxidants in surface waters diurnally averaged over 24 hours are summarized in Table (1.10) [56]. Also, the rate constants for various photooxidants in their reaction with major classes of organic compounds are listed in Table (1.11) [56]. Structure-activity relationships (SARs) have been used to estimate the rate constants for oxidation by several photooxidants. In developing these SAR it is assumed that, a number of reaction pathways by the oxidant exist and that these can be separated and treated individually and then summed to give the total molecular rate constant. For example, Atkinson [74] developed an additivity SAR to estimate the rate constant for the reaction of a large number of organic molecules with hydroxyl radicals (k_{OH}) in air.

Table 1.10: Time-averaged summer oxidant concentrations in insolated surface waters [a] [56].

Oxidant	Average concentration (M)
$^1O_2$	3×10^{-14}
RO_2	3×10^{-11}
HO	$6 \times 10^{-17} - 1 \times 10^{-18}$[c]
[b]DOM^3	6×10^{-14}
O_2^-	3×10^{-9}
H_2O_2	3×10^{-9}
CO_3^-	1×10^{-14}
e^- (Aq)	2×10^{-17}

[a]Values, averaged over 24 h, assume clear sky conditions at 40-50° N latitude with 5 mg/L DOM and 1 mg/L NO_3^-

[b]Triplet excited states.

[c]In seawater.

Table 1.11: Rate constants (M^{-1} s^{-1}) for oxidation of major classes of organic compounds in insolated surface waters [56].

Class	OH (10^{-9})	RO_2	$^1O_2$ (10^{-6})	$^at_{1/2}$
Alkanes	1-3	<0.01	<0.01	44d
Alcohols	2-4	0.1	<0.01	40d
Acids	1-2	<0.1	<0.01	130d
Aromatics	3-6	0.1-0.5	<0.01-10	22d
Olefins	3-20	0.05-1.0	10-100	600h
Phenols	10-20	10^3-10^5	1-20	13d
Aromatic amines	10-20	10^5	10-300	30d
Furans	10	10^4	100-1000	2.7d
Sulfides	20	<0.1	50	5d

$^at_{1/2}$ observed half-lives.

The main transformation processes involving •OH radicals are the abstraction of reactive hydrogen atoms (k_H), addition to nonaromatic multiple bonds and aromatic rings (k_E) and reactions with nitrogen, sulfur and phosphorus atoms (k_A). The over-all molecular rate constant k_{OH} is the sum of the rate constants for each of these reaction pathways and is given by:

$$k_{OH} = k_H + k_E + k_A \quad (1\text{-}39)$$

The abstraction of reactive hydrogen atoms results in formation of alkyl radicals that react with oxygen to give alkylperoxy radicals, which can yield the corresponding aldehyde or ketone. The addition of OH radicals to aromatic rings results in the formation of hydroxyaromatic compounds, hydroperoxy radicals or cleavage of the aromatic ring. Radicals formed can also react with nitrogen oxides and sulfur oxides present in the atmosphere.

1. 10. Remediation Techniques

Industrial development and intensive use of pesticides, herbicides and other agrochemicals have resulted in emission of large amounts of contaminants into the environmental. Many of these compounds are resistant to degradation by primary transformation processes and accumulate in surface and groundwater. In 1984, the Environmental Protection Agency (EPA) reported that 22% of approximately 466 randomly sampled drinking water samples contained detectable levels of volatile organic chemicals (VOCs) from agricultural sources [75]. As a response, EPA proposed maximum contaminant levels for VOCs and semivolatile organic chemicals (SOCs) in groundwater [75], and developed treatment processes. Several remediation technologies,

granular activated carbon (GAC) and packed tower aeration (PTA), have been field-tested for feasibility of removing organic contaminants from groundwater, with cost and performance playing an important role.

1. 10.1. Granular Activated Carbon

Carbon treatment for removing VOCs and SOCs from groundwater uses granular activated carbon (GAC) with on-site regeneration of the GAC. The contaminated water is passed through a stationary column or filter bed containing GAC until the influent concentration is in equilibrium with the adsorber unit. Additional head-space is provided above the carbon bed for periodic back washing. Activated carbon was effective in removing non-polar compounds from water, but the efficiency of removal was dependent on the adsorptive characteristics of the contaminant [75]. Conversely, GAC was not efficient in removing polar or low and very high molecular weight compounds from the water.

1.10.2. Packed Tower Aeration

Packed tower aeration technology also proved to be effective in removing VOCs from water [46]. The efficiency of PTA for removing contaminant is dependent on the ease of transfer of the contaminant from liquid phase to gas phase. The process uses an air stripping technique that involves mass transfer of VOCs from water to air by mixing the contaminated water with uncontaminated air in a countercurrent flow pattern. Contaminated water is pumped to the top of a column then trickled down through a bed of packing material. Uncontaminated air is pushed through the bottom of the column, VOCs partition from water to air passing to the top of the column. This method was successful for removing many of the VOCs including TCE, benzene, toluene, xylene and methylene chloride from ground water [46].

Those methods have been criticized since they only transfer VOCs from one phase to another. In the case of PTA, VOCs are discharged into the air resulting in air pollution, which can only be remedied by some form of off-gas control system. The most common control system is GAC adsorption that not only raises the cost of the PTA method, but also consequently gives rise to the problem of dealing with contaminant sorbed to the stationary phase of the GAC method. Sorbate saturated with halogenated compounds is considered hazardous and must be transported and disposed of according to explicit regulations [76].

1.10.3. Advanced Oxidation Techniques

In recent years, researchers have focused on new processes for water purification involving chemical destruction of the contaminant as opposed to processes which simply involve a phase transfer of the contaminant (e.g., from liquid to solid as in GAC, or from liquid to gas in the case of PTA). These new processes, called Advanced Oxidation Technologies (AOTs), include heterogeneous photocatalytic oxidation [77-78] and homogeneous photodegradation [79], using ultraviolet light (UV). AOTs have been used to destroy VOCs in contaminated water without posing a hazard to another medium [80]. In principle, oxidation processes transform water contaminants such as halogenated compounds into carbon dioxide, water and halide ions by reaction with hydroxyl radical [81]. Hydroxyl radicals are generated either by absorbing light via oxidants in homogeneous photodegradation processes or by the photocatalysts in photocatalytic processes. In the following sections both homogeneous and heterogeneous processes will be discussed in more detailed

1.10.3.1. Homogeneous Photodegradation

A homogenous photodegradation (single-phase system) process is one of the advanced oxidation processes (AOPs) which have been used for treatment of water contaminated with persistent organic chemicals [82]. In this process the oxidant absorbs UV and generates hydroxyl radicals ($^{\bullet}OH$), the powerful oxidizing species which can attack most organic pollutants [83-93]. The most important oxidants used in this process are ozone (O_3), hydrogen peroxide (H_2O_2) and Fenton's reagent (Fe/H_2O_2).

1.10.3.1.1. Ultraviolet Ozone (O_3/UV) System

Ozone, generated as a gas in air or oxygen, has the ability to absorb light strongly at 260 nm with $\varepsilon_\lambda = 3000\ M^{-1}\ cm^{-1}$ [82]. The UV/O_3 system for the treatment of organic pollutants was first investigated by Prengle *et al* and Garrison *et al* [82]. Around the same time Hoigne and Bader [94] identified the $^{\bullet}OH$ radical as the reactive species in that system, having the ability to degrade many priority pollutants such as aromatic hydrocarbons [95-99]. Generation of $^{\bullet}OH$ in the O_3/UV system has been proposed by two different mechanisms. Light induced homolysis of O_3 forming singlet oxygen O (^1D), which reacts with water to produce $^{\bullet}OH$ is the basis of one proposed mechanism [100]:

$$O_3 \xrightarrow{h\nu < 310} O_2 + O(^1D) \qquad (1\text{-}40)$$

$$O(^1D) + H_2O \longrightarrow 2\,^{\bullet}OH \qquad (1\text{-}41)$$

Secondly, it has been proposed that ozone/H_2O_2 photolysis generates the main precursor of $^{\bullet}OH$ [101].

$$O_3 + H_2O \xrightarrow{h\nu} H_2O_2 + O_2 \qquad (1\text{-}42)$$

In aqueous solution the conjugate base of H_2O_2 (HO^-_2) reacts with the remaining O_3 to form $^{\bullet}OH$ according to the following equations.

$$H_2O_2 + H_2O \longrightarrow HO^-_2 + H_3O^+ \qquad (1\text{-}43)$$

$$HO^-_2 + O_3 \longrightarrow O^-_3 + HO^{\bullet}_2 \qquad (1\text{-}44)$$

$$O^-_3 + H_2O \longrightarrow HO^{\bullet}_3 + OH^- \qquad (1\text{-}45)$$

$$HO^{\bullet}_3 \longrightarrow {}^{\bullet}OH + O_2 \qquad (1\text{-}46)$$

On the other hand, addition of H_2O_2 to O_3 even in the absence of UV light enhances the thermal production of $^{\bullet}OH$ radicals [80, 102-106] as in reactions 1-47 to 1-51.

$$O_3 + H_2O_2 \longrightarrow O_2 + {}^{\bullet}OH + HO^{\bullet}_2 \text{ (very slow)} \qquad (1\text{-}47)$$

$$H_2O_2 + H_2O \longrightarrow H_3O^+ + HO^-_2 \qquad (1\text{-}48)$$

$$O_3 + HO^-_2 \longrightarrow {}^{\bullet}OH + O^{\bullet -}_2 + O_2 \qquad (1\text{-}49)$$

$$O_3 + O^{\bullet -}_2 \longrightarrow O^{\bullet -}_3 + O_2 \qquad (1\text{-}50)$$

$$O^{\bullet -}_3 + H_2O \longrightarrow {}^{\bullet}OH + OH^- + O_2 \qquad (1\text{-}51)$$

Although O_3 reacts directly with H_2O_2 to produce $^{\bullet}OH$ radicals (eq. 1-47), this step is very slow. Further ionization of H_2O_2 to yield HO^-_2 increases the production rate of $^{\bullet}OH$ radicals. Oxidation of persistent organic pollutants in ground water has been accelerated by addition of H_2O_2 to O_3 in the dark [107]. Furthermore the presence of UV light in that system enhanced the photochemical production of $^{\bullet}OH$ radicals [108] making it suitable

for industrial development [109]. Other reports have shown that O_3 in general is efficient at generating $^{\bullet}OH$ radicals in water at high pH and of high inherent UV absorbency [82].

Although previous discussion indicated the importance of the O_3 system as a source of $^{\bullet}OH$ radicals, production of H_2O_2 as the precursor step is an expensive method of generating $^{\bullet}OH$ radicals [101]. Furthermore, ozone does not dissolve in water in high concentration, and in the presence of volatile organics air stripping of the components can occur [110], increasing the drawbacks of the ozone system.

1.10.3.1.2. H_2O_2/UV System

Photolysis of H_2O_2 with UV light [111-112] is an alternative method of formation of $^{\bullet}OH$ studied since the 1960s. In the presence of UV light (below 360 nm) one mole of H_2O_2 dissociates to two moles of $^{\bullet}OH$ radicals:

$$H_2O_2 \xrightarrow{h\nu} 2\ ^{\bullet}OH \qquad (1\text{-}52)$$

Previous studies [113-115] have determined the overall quantum yield of this reaction as 0.98 ± 0.05 in the gas phase. In aqueous solutions the presence of $^{\bullet}OH$ radical scavengers such as organic compounds reduces the quantum yield [116]. The degradation reaction of organic substrates by $^{\bullet}OH$ may proceed by three different mechanisms [80,117]. Hydrogen abstraction (equation 1-51) from the organic substrate (RH) may produce an organic radical ($R^{\bullet}$), which may further degrade in the presence of oxygen.

$$^{\bullet}OH + RH \longrightarrow R^{\bullet} + H_2O \qquad (1\text{-}53)$$

For unsaturated organic compounds, $^{\bullet}OH$ reacts by electrophonic addition (reaction 1-54) to the π-system producing an organic radical.

$$^{\bullet}OH + R_2C=CR_2 \longrightarrow R_2{}^{\bullet}C=CR(OH) \quad (1\text{-}54)$$

Finally an organic radical may be formed by an electron transfer reaction (equation 1-55), which is of particular interest when the previous reactions are disfavored by steric hindrance or multiple halogen substitution.

$$^{\bullet}OH + RX \longrightarrow OH^- + RX^{\bullet+} \quad (1\text{-}55)$$

Hydrogen peroxide is commonly used in the treatment of contaminated water because it is readily available, easy to handle, thermally stable and dissolves in water in a wide range of concentrations. H_2O_2 produces no air emissions, which is the problem with ozone treatment. The H_2O_2/UV process also produces $^{\bullet}OH$ with a high efficiency (quantum yields typically around 0.5) [82] and is more efficient than the O_3/UV process for the degradation of chlorinated hydrocarbons such as tetrachloroethylene [118]. The sequence of reactions resulting in photoxidation of organic contaminants during the H_2O_2/UV process [80] is shown in Figure 1.4. In the initial step H_2O_2 is photolyzed by UV light to yield $^{\bullet}OH$ (a), which reacts with an organic contaminant (HRH) to produce an organic radical ($RH^{\bullet}$) as in step (b). In the presence of dissolved oxygen, $RH^{\bullet}$ may form an organic peroxyl radical ($RHO^{\bullet}{}_2$) (c), which is heterolyzed to produce RH^+ as well as superoxide anion ($O^{-\bullet}{}_2$) (d). Peroxyl radical $RHO^{\bullet}{}_2$ may be homolyzed into $^{\bullet}OH$ and carbonyl compound (RO) (e) or back react to $RH^{\bullet}$ and O_2 (f). Also the remaining HRH may react by hydrogen abstraction with $RHO^{\bullet}{}_2$ (g) to initiate a chain of thermal oxidation reactions. In the presence of an unsaturated organic cation, polymerization reaction may take place if there is no oxygen in the reaction medium (h). The H_2O_2/UV process has been used as a method of oxidative degradation of organic pollutants during the last few decades [119] including hydrocarbon derivatives

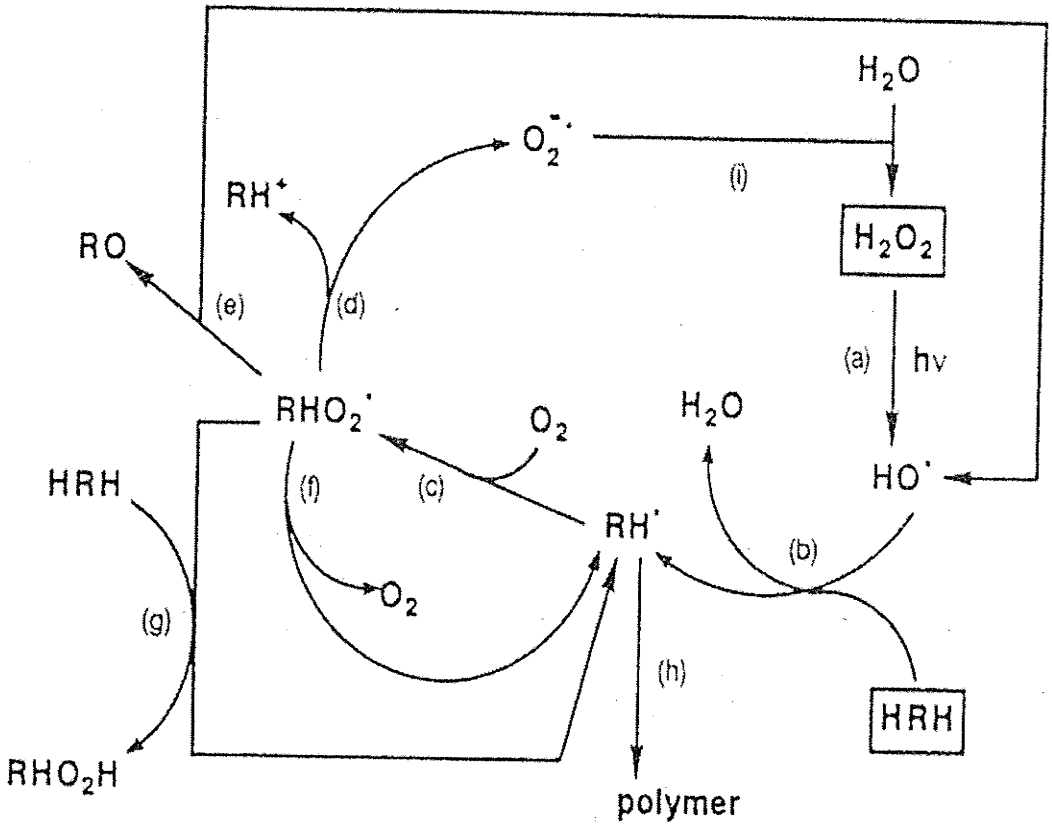

Figure 1.4: Reaction pathways in the H_2O_2/UV degradation of organic compounds (HRH). Reproduced from reference 94.

nitrotoluenes, nitrobenzenes and nitrophenols [127-128]. For example, direct photolysis of formic acid or sodium formate in the presence of UV light at 254 nm was negligible, while addition of 0.01M H_2O_2 lead to 60% decomposition of formic acid and complete mineralization of formate ion within three hours [120]. On the other hand, 1mM 2-propanol nearly disappeared within 12 minutes in the presence of 3 mM H_2O_2 at 254 nm. The reaction intermediates, such as acetone, acetic acid and formic acid reached complete mineralization within 12 hours [121]. Although thermal degradation of phenol (1mM aqueous solution), in the presence of 14 mM H_2O_2 did not take place in the dark, photodegradation with a Hg lamp (400-W high pressure) lead to complete mineralization of phenol [122]. Homogeneous photodegradation of halophenols such as 2-chlorophenol [123] and 4-chlorophenol [124] was very efficient utilizing the H_2O_2/UV process. Pesticides such as atrazine [125] directly photolyzed under UV light with a first order rate constant of $2x10^{-4}$ s^{-1}. Addition of $\leq$ 2mM H_2O_2 in acidic and neutral solution enhanced the degradation with the rate constant reaching (20-50) $x10^{-4}$ s^{-1}. The photodegradation of atrazine was strongly accelerated by the optimum concentration of H_2O_2 (10 mM) and inhibited by the presence of humic substances [126]. The presence of 2 mM H_2O_2 with irradiation at 254 nm increased the first-order rate constant for the disappearance of the herbicide metazachlor [126] from 2.2 x 10^{-4} s^{-1} to 150 x 10^{-4} s^{-1}. Decomposition of nitrotoluenes [127] and nitrophenols [128] were also enhanced by the presence of 8 mM H_2O_2, reaching complete mineralization to carbon dioxide and nitric acid in the case of 2,4-dinitrotoluene [127]. Another report has shown that using 1% (v/v) H_2O_2 with UV light for oxidative degradation of 1,2-dimethyl-3-nitrobenzene and nitro-*o*-xylene contained in industrial wastewaters [80] resulted in 95% removed of total organic

carbon (TOC) in 40 minutes of irradiation. The H_2O_2/UV process utilizing both batch and flow reactors has been studied for a variety of aliphatic compounds [80] such as trichloroethylene, chloroform and dibromoethane, and aromatic compounds such as benzene, dichlorobenzene, chlorophenol and diethyl phthalate. The results indicated mass balance between chloride ions and the original aliphatic chlorinated compounds. In genenral the rate of degradation was dependant on the concentration of H_2O_2, UV light intensity and the chemical structure of the substrate.

Another report [129] shows that the presence of carbonate and bicarbonate in the reaction medium decrease the efficiency of the H_2O_2/UV process. This may be due to the competition between the substrate and carbonate ions for the reaction with $^{\bullet}OH$ radical. The destruction rate of phenol in the presence of H_2O_2 and UV light, was inversely proportional to the relative radiant power as reported in another study [80].

Conversely, a continuous-flow stirred tank reactor (CSTR) was used to investigate the effect of water quality parameters such as humic material, pH, and CO_3^{2-} /HCO_3^- ion on the removal of *n*-chlorobutane from aqueous solutions. It was found that the process was affected by water quality parameters and the rate of degradation was directly proportional to the photolysis rate of H_2O_2. Degradation of ground water samples contaminated with hazardous aliphatic compounds [80] in pilot scale equipment was also investigated. Using 50 mg/L H_2O_2 in the presence of a Hg lamp (30 kW), tetrachloroethylene level decreased from 3700-4000 ug/L to 0.7-0.8 ug/L at a liquid flux of 230 L/min in 50 seconds.

The above discussion has shown that the H_2O_2/UV process is a promising technique for the degradation of most organic pollutants. The disadvantage of using

hydrogen peroxide is its low molar absorptivity (ε_λ) in the ultraviolet region, which ranges from 18 to190 M^{-1} cm^{-1} at 254 and 200 nm, respectively [130]. Thus, a high concentration of hydrogen peroxide relative to that of pollutant is necessary in order for significant degradation to occur. Finally the use of solar energy with the H_2O_2/UV process remains under investigation [130].

1.10.3.1.3. Photo-Fenton Systems (H_2O_2/Fe/UV)

Another way of generating $^{\bullet}OH$ radicals in homogeneous techniques is via the photo-Fenton reaction. A mixture of iron (II) and hydrogen peroxide in the dark, known as Fenton's reagent, is a recognized source of $^{\bullet}OH$ radicals [131]. Addition of Fe^{+2} catalyzes the decomposition of hydrogen peroxide to $^{\bullet}OH$ [132]:

$$Fe^{+2} + H_2O_2 \longrightarrow OH^- + {}^{\bullet}OH + Fe^{+3} \qquad (1\text{-}56)$$

While the original Fenton's reagent uses ferrous ion (Fe^{+2}/H_2O_2), numerous reports have proposed that addition of ferric ion (Fe^{+3}) also enhances the catalytic decomposition of H_2O_2 to generate $^{\bullet}OH$ [133]. This mixture (Fe^{+3}/H_2O_2) is frequently referred to as the modified Fenton or Fenton-like reagent [133]. Combining hydrogen peroxide and ferric ion in aqueous solution at lower pH enhances the thermal (dark) production of hydroxyl radicals by a free radical chain mechanism [134]:

$$Fe^{3+} + H_2O_2 \longrightarrow Fe^{2+} + HO^{\bullet}_2 + H^+ \qquad (1\text{-}57)$$

$$Fe^{2+} + H_2O_2 \longrightarrow Fe^{3+} + {}^{\bullet}OH + OH^- \qquad (1\text{-}58)$$

$$Fe^{+2} + {}^{\bullet}OH \longrightarrow Fe3+ + OH^- \qquad (1\text{-}59)$$

$$H_2O_2 + {}^{\bullet}OH \longrightarrow HO^{\bullet}_2 + H_2O \qquad (1\text{-}60)$$

$$Fe^{+2} + HO^{\bullet}_2 + H^+ \longrightarrow Fe^{3+} + H_2O_2 \qquad (1\text{-}61)$$

$$Fe^{+3} + HO^{\bullet}_2 \longrightarrow Fe^{2+} + O_2 + H^+ \qquad (1\text{-}62)$$

The above series of reactions (for simplicity no complexing agent is shown in the coordinated sphere) starts with the initiation step in which the ferric ion reacts with hydrogen peroxide to produce the ferrous ion; along with the hydroperoxy radical. The hydroperoxy radical is relatively unreactive with organic chemicals compared to the hydroxyl radical [118, 135-139]. However, the ferrous ion that is formed in the initiation step (1-57) goes on to react with hydrogen peroxide (1-58) to produce the desired hydroxyl radicals. Although the hydroperoxy radicals that form in the initiation step do not significantly act directly as $^{\bullet}OH$, they do react with the ferric ion in reaction (1-60) to produce additional ferrous ion that feeds into reaction (1-56) to produce more of the hydroxyl radical. In acidic solutions ferrous ions react with hydroperoxy radicals ($HO^{\bullet}_2$) as in reaction (1-59) to produce H_2O_2 and Fe^{3+}, which generates more ferrous ions to enhance production of $^{\bullet}OH$ radicals. Numerous studies have investigated the reactivity of $^{\bullet}OH$ generated from (Fe^{2+}/H_2O_2) [140-142] and (Fe^{3+}/H_2O_2) [133], towards the degradation of organic pollutants. The oxidation of alcohols, ethers, dyes, chlorinated phenols, chlorobenzene, and other chlorinated organics in aqueous solutions and in wastewaters, were quite effective by the thermal production of $^{\bullet}OH$ [143-147].

In contrast, irradiation of Fenton-type systems with UV or UV/visible light can greatly enhance its oxidizing power [147-150]. These reactions are termed photo-Fenton ($Fe^{2+}/H_2O_2/UV$) and modified photo-Fenton ($Fe^{3+}/H_2O_2/UV$) reactions [141,144]. Enhanced generation of $^{\bullet}OH$ in the case of photo-Fenton is due to oxidation of Fe^{2+} to Fe^{3+} by H_2O_2, producing one $^{\bullet}OH$ as in reaction 1-63. Fe^{3+} then acts as a light absorbing

species producing another $^{\bullet}OH$, regenerating Fe^{2+} (reaction 1-64):

$$Fe^{2+} + H_2O_2 \longrightarrow Fe^{3+} + {}^{\bullet}OH + OH^- \qquad (1\text{-}63)$$

$$Fe^{3+} + H_2O \xrightarrow{h\nu} Fe^{2+} + {}^{\bullet}OH + H^+ \qquad (1\text{-}64)$$

To avoid artifacts that can result from locally high concentrations of the reagents, photochemical generation of Fe^{2+} *in situ* from Fe^{3+} is used in a modified photo-Fenton reaction [151].

$$Fe^{3+} + H_2O_2 \xrightarrow{h\nu} Fe^{2+} + HO^{\bullet}{}_2 + H^+ \qquad (1\text{-}65)$$

The Fe^{2+} formed from reaction 1-65 reacts with H_2O_2 to produce $^{\bullet}OH$ radicals as in reaction 1-63. Both photo-Fenton and modified photo-Fenton reactions play an important role in the degradation of a wide variety of organic pollutants [152-157].

1.10.3.2. Heterogeneous Photocatalysis

Heterogeneous photocatalysis reactions are relatively new techniques in the field of advanced oxidation methods, but appear very promising for the destruction of potentially toxic organic compounds (PTOC) present in aquatic environments [158-160]. These reactions are heterogeneous in nature due to the catalyst being either immobilized, or a suspension of fine solid particles in aqueous solutions [161]. In the 1970s, a number of reports suggested that band-gap illuminated *n*-type semiconductors such as metal oxides (TiO_2, ZnO_2) or metal sulfides (CdS), might have the potential for the activation of stable molecules and ions of PTOC at ambient or near ambient conditions [162].

1.10.3.2.1. Theory of Semiconductors

Semiconductors are crystalline materials with an electrical conductivity (typically 10^5 to 10^{-7} siemens per meter) intermediate between that of a conductor (up to 10^9 S/m) and an insulator (as low as 10^{-15} S/m) [163]. According to molecular orbital (MO) theory, the energy of electrons in isolated atoms is defined by the energy of the atomic orbitals (AO). However, because of the very large number of atoms that interact in solid materials such as a semiconductor, the atoms are close together and their AOs will combine to form new molecular orbitals. The difference in energy levels of these orbitals is small, and the electrons will distribute among the same number of molecular orbitals [164]. Due to overlap, the molecular orbitals will form continuous bands (Figure 1.5) instead of energy levels and the electrons will occupy these bands according to their energy [165]. The filled bonding orbitals form bands called valence bands (VB), while the empty antibonding orbitals form bands called conduction bands (CB) [165]. Between these two bands there is a region with no orbitals called a band gap (or forbidden region), which can act as a barrier to electronic mobility as illustrated in Figure 1.6 [165].

Therefore, the energy bands of a solid-state semiconductor crystal consist of a conduction band (CB), a valence band (VB), and an energy gap (E_{gap}). The charge carrier electrons exist in the conduction band, while the charge carrier holes exist in the valence band and the two bands are separated in energy by the energy gap. The lowest energy of the CB is called the conduction band edge (Ec) and is equal to the top of the energy gap; the highest energy of the VB is called the valence band egde (Ev), and is equal to the bottom of the energy gap. The difference between metals, semiconductors and insulators is the size or energy of the band gap (E_{gap}) (Figure 1.7) [166].

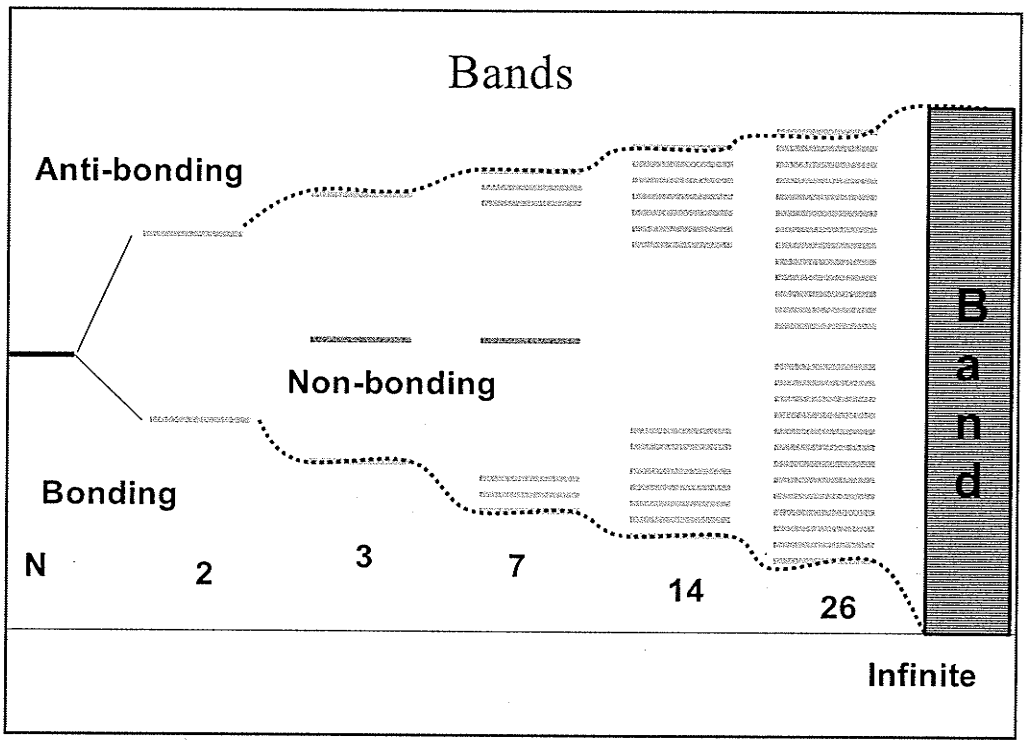

Figure 1.5: Formation of continuous bands in a semiconductor where N represents the number of molecular orbitals.

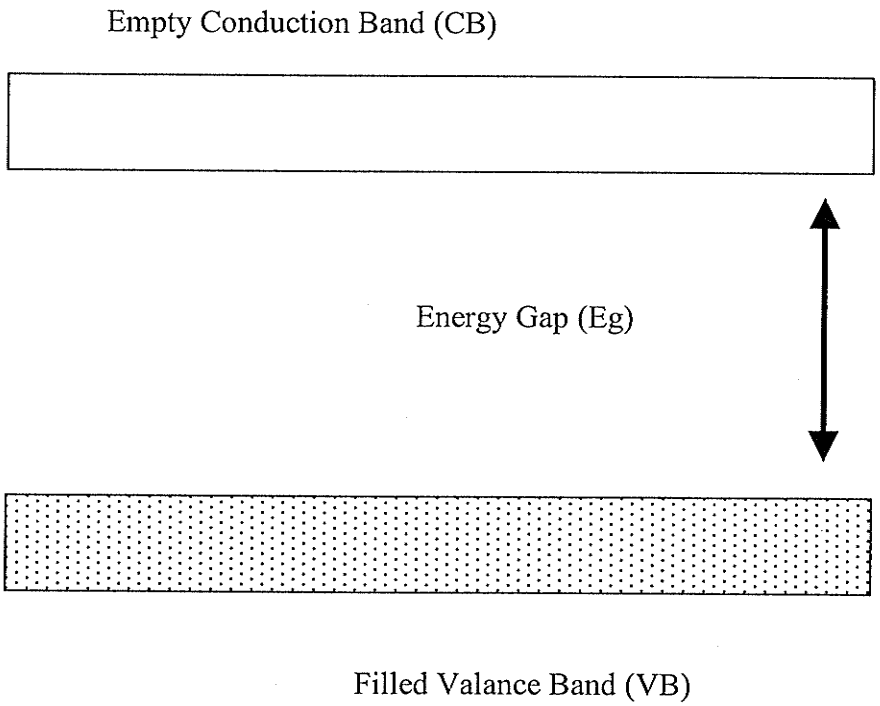

Figure 1.6: Valence and conduction bands in a semiconductor particle.

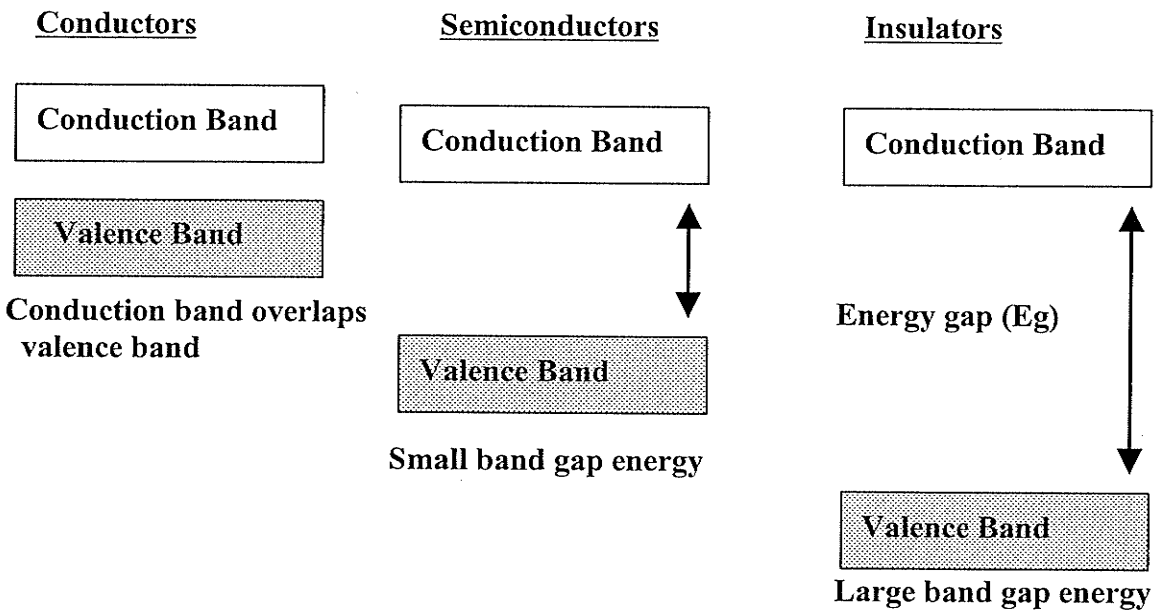

Figure 1.7: The difference in the band gap energy in conductors, semiconductors and insulators.

In metals, the band gap is small leading to overlap between the conduction band and the valence band, such that the electrons can easily move between the two bands. The band gap in insulators is quite large, so the electrons can not promote from the valence band into the conduction band under normal conditions. The band gap in semiconductors is somewhere between metals and insulators which allows the electrons to be promoted from the valence band to the conduction band much more easily [166].

Semiconductors may be of two types; intrinsic or extrinsic. An intrinsic semiconductor is one in which the number of electrons in the conduction band is equal to the number of holes created in the valence band. In the extrinsic semiconductor, the number of electrons and holes are controlled by added donor or acceptor impurities. Donor semiconductors, called n-type, are those in which the electrical conduction is mainly due to electrons, while acceptor semiconductors, called p-type, are those in which the electrical conduction is mainly due to holes [167]. A Fermi level (in other contexts, referred to as the electron chemical potential) term is used to describe the top of the collection of electron energy levels at absolute zero temperature. While the free energy of the redox couple in solution is described by its redox potential (E_{redox}), the free energy of the electrons in semiconductors is described by the Fermi level (E°_{f}). For an intrinsic semiconductor the Fermi level lies at the center of the band gap, but for n-type semiconductors, it lies just below the conduction band. For p-type semiconductors it lies just above the valence band [165,168] as described in Figure 1.8.

In *n*-type semiconductors, as the temperature increases or upon absorption of a photon with an energy equal to or higher than the band gap energy (E_{gap}) a band-to-band

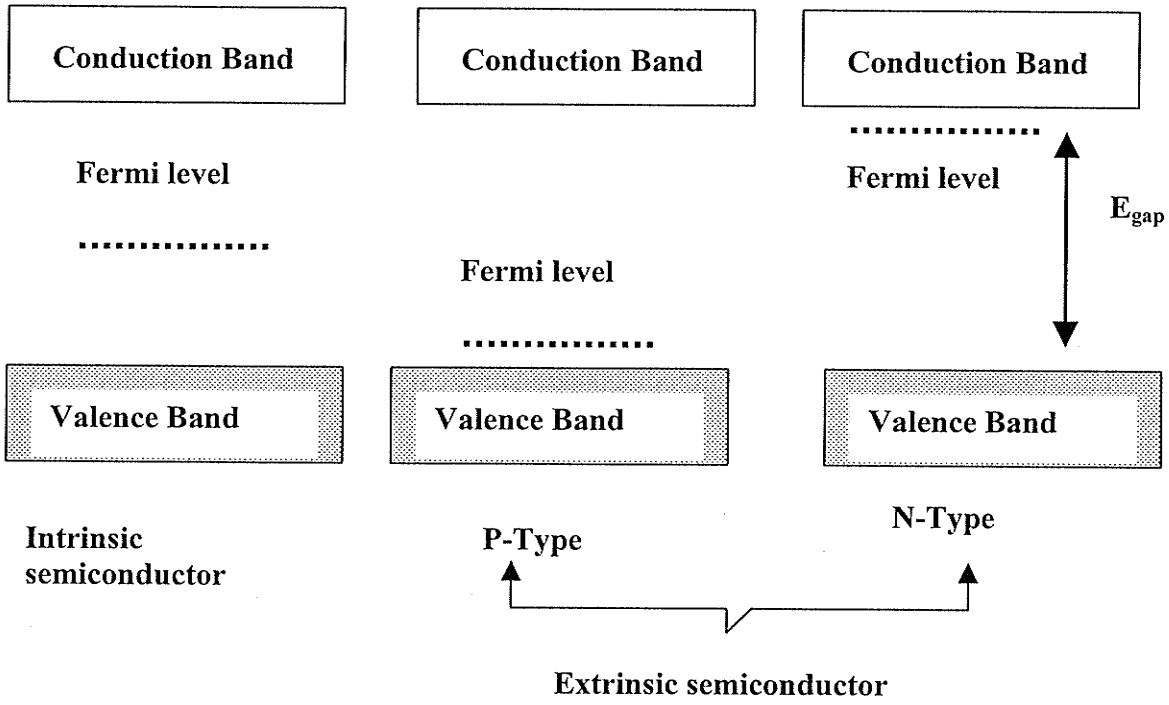

Figure 1.8: Position of Fermi level in intrinsic and extrinsic semiconductors.

transition occurs. The photogenerated electron-hole pair (e.p) is formed by promotion of an electron from the filled valence band (vb) into the vacant conduction band (cb) leaving behind an electron vacancy in the valence band called a hole, (h^+_{vb}). The potential energies of the resulting electron-hole pair can be defined by the thermodynamic levels represented as E_{cb} for the electrons and E_{vb} for the holes, whereas E_{cb}-E_{vb} = ΔE_{gap} [168].

1.10.3.2.2. Basic Principles of Semiconductor Photocatalysis

The term photocatalysis consists of the combination of photochemistry and catalysis. The photocatalyst is a substance that can be activated by a photon to accelerate a chemical transformation rather than by heat (thermal catalyst) [169]. In the photocatalytic reaction, the light-activated substance (sensitizer or photocatalyst) absorbs the suitable photon to promote electrons into the excited (antibonding) orbitals. Whereas these electrons are much more weakly held, they can transfer into oxidative processes much more easily than the electrons in the corresponding ground states [170]. On the other hand, the photoexcitation of electrons from the ground state will leave vacancies (holes) in the valence band. This hole will be in an orbital that is energetically lower than the corresponding orbital of the ground state. As a result of this electronic excitation by light, the powerful oxidizing holes h^+_{vb} and strongly reducing electron e^-_{cb} are formed [171]. Their oxidation and reduction potentials are determined by the energy of the top of the valence band and the bottom of the conduction band, respectively. A sufficiently long excited-state lifetime to allow for interaction with the substrate, and sufficient oxidizing and reducing power to induce oxidations or reductions of the substrate are the two critical features in the photocatalyst substances [165,170-171].

1.10.3.2.3. Excitation of Photocatalyst Particles

Figure 1.9 summerizes the possible reactions that may occur when the photocatalyst particle is illuminated with light of equal or greater energy than that of the band gap. Photoexitation of the particle promots an electron from the valence band to the conduction band (1) leaving a hole (positive charge) in the valence band. In the absence of a suitable trap the electron-hole pair may recombine (2), releasing the absorbing photon as heat and no electron transfer reaction will take place. In the presence of traps such as organic pollutants, hydroxyl ions, water molecules and oxygen, the charges can move to trap sites and participate in redox reactions. Direct oxidation can occur between the valence-band hole (h^+) and the adsorbed organic pollutant (electron donor) (3), while direct reduction may take place between the conduction band electrons (e^-) (4) and electron acceptor pollutants. Numerous studies [165,170-171] have reported that the valence band hole oxidizes adsorbed hydroxy ions generating a hydroxy radicals ($^{\bullet}OH$) (5). These powerful oxidizing agents can attack most organic pollutants. On the hand, oxygen molecules present in most systems, can scavenge conduction band electrons producing superoxide ion radicals ($O_2^{\bullet-}$) (6) which have the ability to reduce many pollutants.

1.10.3.2.4. Photocatalytic Degradation of Organic Substrates

In photocatalytic degradation of organic substances, the photoinduced electron transfer between the photocatalyst and the organic substance depends on their redox potential (E_{redox}), and the energy of the valence band hole and conduction band electrons, relative to that of a standard electrode (either NHE or SCE). The relative energy

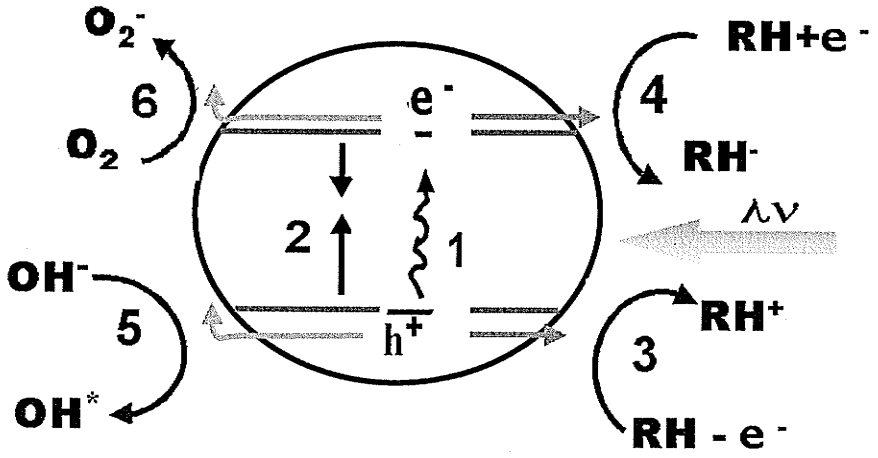

Figure 1.9: Possible reactions occuring during photoexcitation of a photocatalyst particle.

positions of common semiconductors and the corresponding wavelengths are summarized in Table (1.12) [169].

The redox potentials of some organic substances are represented in Table (1.13) [172-177], to illustrate the potential for redox reactions of the organic substances by semiconductor photocatalysts. If the organic substrate has an oxidation potential (E_{ox}) lower (less positive) than the valence band energy (E_{vb}) (i.e. $E_{ox} < E_{vb}$), oxidative processes may take place. In this case the electron will transfer from the organic substrate (donor) into the valence band hole resulting in the formation of an organic radical cation, which is readily degraded. Also, the reductive process may occur if the reduction potential (E_{red}) of the substrate is higher (less negative) than the conduction band energy (E_{cb}) (i.e. $E_{red} > E_{cb}$). The substrate will act as an acceptor, gaining electrons from the conduction band forming a radical anion.

Most organic and inorganic photodegradation reactions by semiconductors utilize either the oxidizing power of holes (either directly or indirectly), or the reducing power of electrons. The application of illuminated semiconductor photocatalysis, [178-188] as an advanced oxidation technology for remediation of contaminants, has been tested successfully for a wide variety of compounds. The efficiency of photocatalytic reactions (photooxidations or photoreductions) by semiconductors is affected by the recombination process of the electron-hole pair. Whenever the semiconductor particle absorbs photons of suitable wavelength, the charges are distributed near the surface. The electrons migrate towards the bulk of the semiconductor, whereas the holes migrat to the surface in the direction of the surface where oxidation can occur [189-194]. If electron-hole traps are not present on the surface of the irradiated semiconductor, the photogenerated electron-hole pair recombines and the energy absorbed will be lost as heat.

Table 1.12: Band gap energies[a] (V vs. SCE ± 0.1V) and corresponding wavelengths of light for some common semiconductors [169].

Semiconductor	Valence Band	Conduction Band	Band Gap (eV)	Wavelength (nm)
TiO_2	+3.1	-0.1	3.2	376-413
SnO_2	+4.1	+0.3	3.8	354
ZnO	+3.0	-0.2	3.2	365
WO_3	+ 3.0	+0.2	2.8	459
CdS	+2.1	-0.4	2.5	512
GaAs	+1.0	-0.4	1.4	885
GaP	+2.2	-1.0	2.3	539
Sic	+1.6	-1.4	3.0	413

[a]Band energies in water at pH =1.0

Table 1.13: Oxidation potentials of sample organic compounds.

Compound	Oxidation Potential, $E_{ox}^{1/2}$ (V *vs* SCE in CH_3CN)	Ref.
cis-Stilbene	1.63	[172]
trans-Stilbene	1.49	[173]
Hexamethyl(Dewar)benzene	1.58	[174]
Hexamethyl benzene	1.62	[174]
Phenyl vinyl ether	1.28[a]	[175]
Dianthracene	1.55	[176]
1,1-Diphenyl ethylene	1.80	[177]
1,1-Di-p-anisyl ethylene	0.78[a]	[177]

[a]Determined *versus* Ag/AgCl

The rate of recombination of the electron-hole pair in colloidal TiO_2 particles has been determined by the second order rate equation to be 3.2×10^{11} $cm^3 s^{-1}$ corresponding to a lifetime of 30 ns [195]. Experiments carried out at low laser fluence showed that hole trapping at the surface can compete with recombination. The hole trapping rate constant of colloidal TiO_2 has been determined by laser photolysis experiments as 4×10^5 s^{-1} [195-196].

Common traps of positive valence-band holes are hydroxide ions (OH^-) and water molecules (H_2O). Examples of conduction band electron traps are oxygen molecules [197], and methyl viologen (MV^{+2}) (1,1'-dimethyl-4,4'-bipyridylium chloride) [198].

$$MV^{2+} + e^-_{CB} \longrightarrow MV^{+\bullet} \qquad (1\text{-}64)$$

When colloidal TiO_2 comes into contact with the aqueous phase, the surface will be covered by hydroxide groups (OH^-). Although there are two types of OH^- groups, basic and acidic [199], the basic OH^- group has high electron density, which can act as a positive hole trap. Experiments have shown a rate constant of the trapping reaction of $4x10^5$ s^{-1} [200]. The hole trapped by the OH^- ion can be considered as a surface-bound hydroxyl radical represented as ($^\bullet OH$) or ($^\bullet O^-$) [201]. On the other hand, electron transfer from colloidal TiO_2 to acceptors such as O_2 or MV^{+2} has a rate constant of 10^{-7} cms^{-1} and 10^{-2} cms^{-1} respectively [198]. In general, the hole and electron traps play important role in the separation of the charges on the surface of the oxide semiconductor, to allow the redox processes to take place.

1.10.3.2.5. Identification of a Degradation Pathway

In general, to determine the pathway of photocatalytic degradation, experiments that affect the degradation are performed. For a given substrate, the photocatalytic degradation may proceed *via* oxidation or reduction. The use of scavengers of the oxidizing or reducing species can clarify whether the photodegradation is an oxidation or a reduction reaction. There are many scavengers that can be added to alter the degradation process. For example, the addition of some common inorganic anions will inhibit oxidations. Chloride, sulfate and phosphate all have detrimental effects on the rate of degradation. Chloride ion reacts with the oxidizing species such as $^{\bullet}OH$ radicals to produce the chloride radical, thus preventing the oxidation of a substrate. Sulfate and phosphate ions also prevent substrate oxidation by binding to the TiO_2 surface and blocking the oxidizing active sites. Conversely, the presence of nitrates and perchlorates do not effect the degradation rate [202].

In addition to inorganic ions, the presence of alcohols, in particular methanol and *tert*-butyl alcohol, will serve to inhibit a photocatalytic oxidation [203]. Methanol can be oxidized at the hole competing with the substrate for the oxidizing site [202]. Conversely, methanol does not affect a photoreduction, since it does not react with the conduction band electron. In fact, the scavenging of the hole would prevent charge recombination and allow the electron to exist for longer periods of time, which may enhance the rate of a photoreduction reaction.

Transition metals also greatly affect the rate of degradation of a compound, either increasing or decreasing the rate. A metal cation may react with the conduction band

electron thereby hindering photoreductions, and enhancing photooxidations by preventing charge recombination [204].

$$M^{n+} + e^-_{cb} \rightarrow M^{(n-1)+} \qquad (1\text{-}66)$$

The reduced product from equation (1-66) may react with the oxidizing site of the TiO_2 particle (1-67):

$$M^{(n-1)+} + h^+_{vb} \rightarrow M^{n+} \qquad (1\text{-}67)$$

Both reactions must be examined to explain the effects of a transition metal on a degradation rate. The above examples illustrate the importance of e^- and h^+scavengers in determining whether the degradation is an oxidation or reduction.

1.10.3.2.6. Photooxidation Pathway

The majority of degradation reactions proceed through an oxidation process, although photoreductions are observed in select cases, such as the reduction of methyl viologen [205]. Photooxidations occur primarily via a reaction between the substrate and the trapped hole present on the semiconductor surface (indirect oxidation) or via the h^+_{vb} species itself (direct oxidation). Mechanisms vary according to the substrate, but the trapped hole can be viewed as removing a hydrogen from saturated compounds or adding to carbon double bonds [206]. Direct oxidation occurs less frequently than oxidation via the trapped hole, but is important in the degradation of certain types of compounds, such as oxalate and trichloroacetate ions [206]. In addition, replacement of water with a redox inert solvent prevents the formation of trapped holes; therefore, any oxidation would be due to a reaction at the h^+_{vb} itself. Oxidations have been observed with organic substrates present in acetonitrile and in the photooxidation of toluene solvent [207]. However, without water present, complete mineralization will not occur, and only partial oxidations

are observed [207]. With respect to indirect photooxidation, the process may proceed in four different ways, depending on the sorption behavior of the substrate [208]. Table 1.14 lists the four possibilities, with regard to an indirect photooxidation reaction of a substrate with a hydroxyl radical.

The four possibilities must be accounted for if a pathway is to be ascribed to a given photooxidation. Determination of which of the four is the dominant route is not always straightforward. Product identification can prove to be of little use, since the same products can result from each possibility [207]. Experiments must be performed which can attribute the photooxidation to one of the above cases. A common method used to determine the importance of dissolved hydroxyl radicals is to use a powerful oxidizing agent which can effectively block the creation of free hydroxyl radicals [209] thereby removing reactions 2 and 4 from contention. Similarly the sorption behavior of the substrate can help determine which of reactions 1 or 3 is more important. If a substrate moves preferentially to the photocatalyst, surface reaction 1 will be dominant, while reaction 3 will dominate if the opposite is true.

The kinetics of photomineralization of organic substrates in the presence of TiO_2 on steady-state illumination is described by the Langmuir-Hinshelwood (L-H) model i.e.

$$R_{LH} = -\frac{d[C]_i}{dt} = \frac{K\,k\,[C]_i}{1 + K\,[C]_i} \qquad (1\text{-}68)$$

where R_{LH} is the initial rate of substrate removal, $[C]_i$ is the initial concentration of the organic substrate and traditionally K is taken to be the Langmuir adsorption constant of the substrate on the surface of TiO_2 and k is a proportionality constant which provides a measure of the intrinsic reactivity of the photoactivated surface with the substrate.

Table 1.14: Photooxidation pathways [207].

	Type of Reaction
1	The photooxidation is heterogeneous and proceeds between an adsorbed hydroxyl radical and an adsorbed substrate molecule.
2	The photooxidation proceeds between a dissolved hydroxyl radical, existing in the bulk solution, and an adsorbed substrate.
3	The photooxidation proceeds between an adsorbed hydroxyl radical and a substrate molecule arriving at the particle surface.
4	The photooxidation is homogeneous and proceeds between a free hydroxyl radical and a free substrate molecule in the bulk solution.

Attributing the experimental data to the modified (L-H) kinetic model provides indirect evidence for a given pathway. The modified L-H model concerns the solid-liquid interface (i.e. TiO_2 surface/substrate interaction) and assumes that degradation is dependent on adsorption, with adsorption occurring prior to degradation, and that the adsorption occurs with similar heats of adsorption being independent of other molecules already adsorbed.

Furthermore, it is assumed that a constant number of active sites exist throughout the duration of the degradation process, and only one substrate molecule is present at a given site at a given moment [210]. With these assumptions, the model incorporates the degree of surface coverage, θ_x, into the rate of degradation (1-68), with θ_x given by [210]:

$$R_{LH} = k_{LH}\,\theta_x \qquad 1\text{-}69$$

$$\theta_x = \frac{KC}{1+KC} \qquad 1\text{-}70$$

The modified L-H model assumes adsorption to be important, and this assumption is tested with a plot of equation (1-71) [210].

$$\frac{1}{r} = \frac{1}{k} + \frac{1}{kKC} \qquad 1\text{-}71$$

where $\frac{1}{r}$ is the inverse initial rate of reaction and $\frac{1}{C}$ is the inverse initial concentration. ($\frac{1}{k}$), supports the L-H assumption, and gives indirect evidence that the substrate adsorbs to the photocatalyst surface. This would imply that the pathway is a heterogeneous one. However, this evidence is indirect and as such must be substantiated with additional experimental evidence. Since a kinetic study by itself is not sufficient to determine the pathway of degradation [206], experiments should be performed which illustrate the

sorption behavior of the substrate, the results of which should substantiate the results obtained from the L-H model.

1.10.3.2.7. TiO_2 Photocatalysis

Even though all the photocatalysts listed in Table 1.12 operate under the same principles, a comparison reveals that TiO_2 is the most versatile. Titanium dioxide is chemically inert, stable over prolonged use, inexpensive, and has a redox range (-0.2 V and + 2.9 V) [212] which covers the $H_2O/OH^{\bullet}$ redox potential of 2.8 eV ($OH^{\bullet} + e^- \rightarrow OH^-$), which is thought to be an essential reaction for the redox degradation of aqueous organic chemicals [211]. The other photocatalysts do not perform as well as titanium dioxide for various reasons. The metal sulfides, such as ZnS, and the iron oxides, such as α-Fe_2O_3, are susceptible to photoanodic and photocathodic corrosion, respectively, and as such cannot be used for prolonged periods of time [206]. The remaining photocatalysts are suitable, but do not match the effectiveness of TiO_2, unless the pollutant is loaded directly onto the dried photocatalyst prior to irradiation [207]. Furthermore, in aqueous media ZnO forms $Zn(OH)_2$ on its surface, which deactivates ZnO by changing the surface chemistry of the particle [209-213]. However, it has been demonstrated that the acid-base properties of the metal oxide surfaces influence their reactivity. On the other hand, adsorption of water at the surface of the semiconductor leads to coverage by OH^- groups [214] which promots formation of metal hydroxide (M-OH). The amphoteric behavior of metal hydroxide is depectid by the following equilibria [215]:

$$M\text{-}OH + H \xrightarrow{K1} M\text{-}OH_2^+ \qquad (1\text{-}72)$$

$$M\text{-}OH \xrightarrow{K2} M\text{-}O^- + H^+ \qquad (1\text{-}73)$$

The zero-point charge (pH_{ZPC}) of the metal oxide is defined as the pH at which the concentration of protonated and deprotonated forms are equal:

$$pH_{ZPC} = \frac{1}{2}(pK_1 + pK_2) \quad (1\text{-}74)$$

According to pH_{ZPC} the metal oxide surface is positively charged below pH_{ZPC} and negatively charged above pH_{ZPC}. Although this surface charge will influence the reactivity of the photocatalyst [216] the pH_{ZPC} of TiO_2 has a wide range of 3.5 to 6.7 as shown in Table 1.15 [216]. Since, TiO_2 does not suffer from these drawbacks, it is the photocatalyst of choice for the photodegradation of many aqueous pollutants. TiO_2 exists in two primary forms, rutile and anatase. Of the two, anatase is far superior for photocatalytic degradations, forming a more uniform suspension in aqueous media that facilitates interaction with a substrate. Excitation of the anatase TiO_2 particle (maximum absorption band at around 340 nm) [165,170-171], requires UV light, and creates photo-formed e^-_{CB} and h^+_{vb} species. These species may undergo a number of different reactions as shown in Table 1.16. These reactions occur in competition with each other, and two reactions, the recombination and the trapping reactions, are of primary importance. Recombination occurs when the electron and hole species recombine to produce an unexcited TiO_2 particle which dose not have the ability to catalyze reactions Thus, TiO_2 will only be an effective photocatalyst if the rate of recombination is not significantly greater than the rate of charge trapping or the rate of reaction with an organic chemical present in solution [217]. Charge trapping arises from interactions between the solvent and the redox species. In an aqueous system, the solvent is water, and the species responsible for the trapping is the hydroxide ion.

Table 1.15: The zero-point charge of common semiconductor [216].

Semiconductor	pH_{ZPC}
SiO_2	2.0
TiO_2	3.5- 6.7
$\propto$-Fe_2O_3	6.5-8.5
ZnO	9.0±0.3
$\propto$-Al_2O_3	9.1
CuO	9.5
MgO	12.5

Table 1.16: Fundamental reactions of an excited TiO_2 particle [217].

Reaction	Time
Charge Creation:	
1 $TiO_2 + h\nu \rightarrow h^+_{vb} + e^-_{cb}$	fs
Recombination:	
2 $h^+_{vb} + e^-_{cb} \rightarrow TiO_2 + \text{heat}$	Few ns
Charge Trapping:	
3: $h^+_{vb} + Ti^{IV}OH \rightarrow \{Ti^{IV}OH^\bullet\}^+$	10 ns
4: $e^-_{cb} + Ti^{IV}OH^\bullet \rightarrow \{Ti^{III}OH\}$	100 ps
also denoted as:	
3a: $h^+_{vb} + H_2O \rightarrow h^+_{vb}/OH^\bullet$	10 ns
4a: $e^-_{cb} \rightarrow e^-_{cb}$ (trapped)	100 ps
Trapped Species Recombination:	
5 $e^-_{cb} + \{Ti^{IV}OH^\bullet\}^+ \rightarrow Ti^{IV}OH$	100 ns
6: $h^+_{vb} + \{Ti^{III}OH\} \rightarrow Ti^{IV}OH$	10 ns
Reaction with halogenated alkane:	
7: $\{Ti^{IV}OH^\bullet\}^+ + RX \rightarrow Ti^{IV}OH + [RX]^+$	100 ns
8: $\{Ti^{III}OH\} + RX \rightarrow Ti^{IV}OH + R^\bullet + X^-$	ms
also denoted as:	
7a: $h^+_{vb}/{}^\bullet OH + RX \rightarrow [RX]^+$	100 ns
8a: $e^-_{cb} + RX \rightarrow R^\bullet + X^-$	ms

Water and hydroxide ions associate with the surface of the particle effectively covering it, and undergo reactions with the redox species to form electrons and trapped holes [209]. The rates of recombination are slowed by these electrons and trapped holes relative to the untrapped species, allowing the TiO_2 particle to catalyze oxidation or reduction reactions in aqueous media [209].

Table 1.16 [209, 218] provides the primary reactions involved with a TiO_2 particle illuminated in aqueous media. Note that the trapped hole, designated $\{Ti^{IV}OH^{\bullet}\}^{+}$, can also be written without the metal ion present as $h^{+}_{vb}/OH^{\bullet}$. Likewise, the trapped electron, $\{Ti^{III}OH\}$, is a site with an excess electron, and as such can simply be denoted as e^{-}_{cb}, although this e^{-}_{cb} is not intrinsically the same as the untrapped e^{-}_{cb} electron created when excitation occurs initially. The purpose of the OH, in the designation of the trapped species, is to clarify what is responsible for the trapping and to differentiate the trapped species from the original species, e^{-}_{cb} and h^{+}_{vb} (for which the rate of recombination is faster). Once trapping occurs, the photocatalyst is able to react with organic compounds present in the solution. The notation of "RX" in the table refers to a generic halogenated alkane, which is capable of reacting with the trapped species. The short form reactions (omitting the $Ti^{III}OH$ and $Ti^{IV}OH^{\bullet+}$) are also provided in Table 1.16. In order for TiO_2 to be a useful photocatalyst for degrading chlorinated alkanes, reactions 7 and/or 8 must predominate. In particular, photooxidation reactions dominate over photoreduction reactions, since the oxidizing range of TiO_2 is greater than the reducing range [210,219].

TiO_2 is a stable, highly photoactive semiconductor material that has been used to photocatalytically degrade many different compounds which exist in the gas [220] or

liquid phase [216]. It has found use in the destruction of alkanes, [221] phenols, [222-224] aliphatic alcohols [225], dyes and surfactants [226], PCBs [218], and halogenated alkanes [227] to name a few general chemical categories [218]. In addition, a recent (1998) report has illustrated the feasibility of using TiO_2 to mineralize bacterial cell mass in air [228]. The process suggests a possible disinfection technique for air. Another similar report has shown that TiO_2 is capable of successfully degrading gaseous formaldehyde, a known indoor air pollutant [229]. The report provides a possible remediation method for what is referred to as the "sick building syndrome".

With regard to chlorinated alkanes, little work has been done; however, Pelizzetti *et al* [211] have successfully degraded 1-bromododecane. The degradation was a photooxidation observed to yield a stoichiometric amount of carbon dioxide upon mineralization of 1-bromododecane [211]. In addition to this work, Pelizzetti et al have used TiO_2 to photocatalytically destroy dodecane, toluene [212], dodecyl sulfate, 1-decanol [230], and many other compounds.

1.10.3.2.8. Photocatalytic Degradation of Various Classes of Pollutants by TiO_2

During the past two decades, photocatalytic process involving TiO_2 semiconductor particles under UV light illumination have been shown to be potentially advantageous and useful in the treatment of wastewater pollutants. For example, wastewater from the textile industry is highly colored and represents an increasing environmental danger due to their refractory nature. An aqueous solution of 250 mL of 0.18 mM triphenylmethane dye (gentian Violet) was irradiated in the presence of TiO_2 (P25, 1 g/L) with a 125-W medium pressure Hg lamp [231]. The absorbance of the dye was followed at 536 nm after 80% dilution of the irradiated solution. After 90 min of illumination, the results showed 99% decomposition of the parent compound with 85%

mineralization of the dye. Pyrene is a polycyclic aromatic hydrocarbon (PAH) containing four benzenoid rings, mostly derived from the incomplete combustion of some organic matter. The photocatalytic oxidation of pyrene [232] preadsorbed (surface coverage: 2 $x10^{-5}$ mol/g) on different photocatalyst particles (50 mg/50 mL water) such as TiO_2, Al_2O_3, SiO_2 were irradiated with UV light (100-W Hg lamp) at pH 5 and 20°C. Results indicated that the degradation rate of pyrene was fast in the presence of TiO_2. The chemical oxygen demand (CODCr) was measured using the potassium dichromate oxidation method. The results show the rapid decrease of CODCr with illumination time approaching zero at 120 min of irradiation, indicating that a complete mineralization of pyrene occurred.

Nitrobenzene (NB), a known priority pollutant [233] is used as a raw material and intermediate for many dyestuffs. Photocatalytic degradation of NB (300 mg/L) was carried out using 0.3% (w/v) TiO_2 and concentrated sunlight. Experiments were carried out in a cylindrical reactor (ID 8 cm) of 465-cm^3 capacity fitted with a centrally mounted sparger surrounded by a cooling coil (ID 4 cm), and a water cooled glass condenser for the outgoing gases/vapors. To study the scale up some experiments were carried out in three different diameter geometrically similar reactors (6, 9, 12 cm ID) with volumes of 0.25,1, and 2 L, respectively. Air was bubbled at sufficiently high velocity (>2 cm s^{-1}) to keep all the TiO_2 in suspension. Most experiments were carried out in a short period between October–December (2000) and on consecutive days when the climate was bright and sunny. Concentrations of NB and its intermediates were measured by HPLC using methanol:water (50:50 v/v) as the mobile phase. Major intermediates were *p*-nitrophenol and *o*-nitrophenol in acidic medium and *m*-nitrophenol, and *p*-nitrophenol in alkaline

solution. In general, photocatalytic degradation of NB in both acidic (pH 3.5 and 4.5) and alkaline (pH 9.5 and 10.5) solutions resulted in 95–98.5% removal of NB and 88–92% removal of TOC.

Black liquor [234] is one of the main byproducts discarded as waste in the manufacture of quality paper. Black liquor contains lignin (from 10 to 50%, by wt) that is highly resistant to microbial attack. Photocatalytic degradation of lignin was performed in a Pyrex reactor open to air equipped with a Phillips HPK 125-W lamp with an intensity of 6.67×10^{-7} einstein/s. Although direct photolysis of 1000 mL (90 mg/L) of lignin solutions at pH 8.2 showed only 3.3% disappearance of the parent compound, presence of 1 g/L of TiO_2 increased the degradation of lignin to reach 56% disappearance in 420 min. COD (dichromate method) removal by photocatalytic degradation of the lignin solution depends strongly on the initial concentration of the lignin and becomes higher (about 81%) at initial concentration of 39.4 mg/L. GC/MS analysis showed different lignin-derived compounds such as 3,4,5-trimethoxybenzaldehyde, which could be useful to the industry of aromas and perfumes. In contrast, early literature [235-236] has demonstrated the important role of TiO_2 as a photocatalyst, for conversions in continuous flow reactors of the light hydrocarbons, including methane, ethane, propane and isobutane. Photooxidation of the gas phase of the hydrocarbons on the surface of TiO_2 or ZnO, resulted in the oxidation of carbon monoxide to carbon dioxide [237], and the oxidation of cyanide ion [238-239]. Also, Karutler and Bard, [240-241] investigated decarboxylation of linear saturated carboxylic acids (acetic, propionic, butyric). The latter studies found total oxidation of methane and ethane, while isobutane could be converted to acetone and carbon dioxide with selectivities exceeding 90%, provided that oxygen

pressures were modest [242]. Photoassisted heterogeneous dehalogenations were also reported in this period. Thus chloride ion release into water occurs upon illumination of TiO_2 slurries in dilute solutions of chlorinated biphenyls [243] or *p*-dichlorobenzene [244], as does dechlorination of CF_2Cl_2 and $CFCl_3$ on illuminated ZnO [245]. Halide transfer from one molecule to another also takes place, for example, from carbon tetrachloride or fluorotrichloromethane or difluorochloromethane to ethane [245].

Almost every major class of organic or haloorganic water contaminant has now been examined , at least initially, for possible degradation (partial or to complete mineralization) or removal from the liquid phase. In general advanced oxidation techniques are promising methods for the treatment of polluted groundwater and industrial waste [219-220]. Important advantages of AOT processes have been defined as near ambient temperature treatment, and complete mineralization of organic compounds in many cases [215]. Many applications have used economic light sources such as sunlight to effectively oxidize the organic pollutants [246]. It can be concluded that, along with the growth knowledge and the advances in manufacturing industry, the applications of these technologies will be increased at a unique scale.

1.11. Objectives of This Study

As summarized in the above discussion polychlorinated *n*-alkanes containing isomers and congeners with different properties, are used in a wide variety of commercial and industrial applications. Although PCAs have been identified as somewhat toxic and relatively persistent contaminants, little is known about their environmental reactivity such as hydrolysis, oxidation, and photolysis. Furthermore, photocatalytic degradation techniques have not been applied to water contaminated with PCAs.

The objectives of this study were to assess the environmental persistence of short chain PCAs by investigating their hydrolytic and photolytic reactivity in both pure and natural water, and then to investigate the feasibility of employing homogeneous and heterogeneous photocatalysis for the degradation of simple PCA isomers and complex PCA mixtures in contaminated water. Although identification of degradation products and reaction pathways were not the emphasis of this study, the extent of dechlorination of PCAs and the degradation of total organic carbon will be determined in selected experiments.

The potential of two homogeneous photodegradation techniques, hydrogen peroxide and the photo-Fenton system, will be investigated for the degradation of PCAs in aqueous solutions. For degradation with hydrogen peroxide the optimum conditions for degradation, the identification of the major oxidant, the effect of natural water on reactivity and the extent of mineralization will be determined. The efficiency of Fenton systems containing Fe^{+2} or Fe^{+3} for the degradation of PCAs will be investigated in the presence and absence of ultraviolet light. The effect of natural water on the degradation of PCAs will be examined under both Fenton and photo-Fenton conditions.

The heterogeneous photocatalytic system based upon TiO_2 will be applied to the degradation of PCAs in both pure and natural water. In this study the optimum concentrations of both PCA and the photocatalyst, the identification of the reactive species, and the site of the reaction will be determined. In all of the photocatalytic studies the effect of chlorine number and carbon chain length on reactivity will be assessed for a series of short chain polychlorinated *n*-alkanes with carbon chain lengths from C_{10} to C_{13} and chlorine number from Cl_2 to Cl_8.

Since only 1,10-dichlorodecane and 1,12-dichlorododecane are commercially available, a further objective of this study was to synthesize several additional isomers, including tetra and hexa chlorinated decanes and a tetrachlorinated undecane.

Microsoft Excel software was used to present the data. Triplicate experiments were generally conducted to establish the precision of the analytical method. In these experiments results were reported statistically with standard deviations. Due to good precision of the methods, catalytic experiments were simply duplicated and results reported as arithmetic means. The objectives of these experiments were to determine the efficiency of the remediation techniques rather than to report rate constants or half-lives.

CHAPTER 2

Synthesis and Characterization of Polychlorinated *n*-Alkanes (C_{10}-C_{13})

2.0. Introduction

Determining the environmental fate of polychlorinated *n*-alkanes has received less attention due to the difficulty associated with the analysis of PCA mixtures as discussed previously. Studying the environmental behavior of individual isomers and simple mixtures of PCAs, will aid in understanding the behavior of commercial PCA mixtures. Both individual PCA isomers and mixtures with high chlorine number are not commercially available. Synthesis of PCA congeners was the first requirement of this study and was carried out by chlorine addition at the double bonds of the respective *n*-alkenes. PCA mixtures were synthesized by free radical chlorination of the respective *n*-alkanes.

2.1. Experimental

2.1.1. Chemicals and Reagents

Two chlorinated n-alkanes 1,10-dichlorodecane and 1,12-dichlorododecane were purchased from Aldrich Chemical (Milwaukee, WI). Chlorine gas, 1,9-decadiene and 1,5,9-decatriene, used in the synthesis of individual isomers of *n*-decanes, were purchced from Aldrich. For synthesis of tetrachloroundecane, 1,10-undecadiene purchased from Wiley-Organics (Ohio) was used as precursor. Glass-distilled dichloromethane (DCM) and hexane used in the synthesis were obtained from EM Science (NJ, USA). Florisil used in the clean-up of samples was purchased by Fisher Scientific (NJ, USA). Nitrogen

gas (99.99%) used in concentrating solutions was purched from BOC Gases (Mississauga Ontario, Cananda.). All organic solvents used in the sample work-up and analysis were HPLC and/or spectrophotometric grade.

2.1.2. Synthesis of Polychlorinated *n*-Alkanes (PCAs)

2.1.2.1. Synthesis of PCA Isomers

Individual polychlorinated *n*-alkane isomers were synthesized by chlorine addition to the respective *n*-alkenes. In the synthesis of 1,2,9,10-tetrachlorodecane (T_4C_{10}), 1,2,5,6,9,10-hexachlorodecane (H_6C_{10}) and 1,2,10,11-tetrachloroundecane (T_4C_{11}), the respective *n*-alkenes 1,9-decadiene, 1,5,9-decatriene, and 1,10-undecadiene were used. For instance, 1,2,9,10-tetrachlorodecane (T_4C_{10}) was synthesized by bubbling chlorine gas into 1,9-decadiene dissolved in dichloromethane, using a variation of the procedure reported by Tomy et al.[247]. To remove excess chlorine gas from the reaction medium to minimize production of higher chlorinated decanes (i.e. chlorine number higher than four) approximately 10 mL of 0.05 M NaOH was layered over 40 mL of dichloromethane (DCM) in a round bottom flask. The round bottom flask was wrapped in aluminum foil to prevent light penetration thus minimizing free radical reactions. Chlorine gas was gently bubbled through the layered solution for several minutes at room temperature with gentle shaking. Then 1,9-decadiene (0.0325g) dissolved in another 10 mL of DCM was introduced into the lower DCM layer by pipet. After several minutes, the solution was periodically shaken over a 3 to 5 min period.

2.1.2.2. Extraction and Purification

The mixture was transferred into a separatory funnel and gently shaken with 20 mL of NaOH (0.05 M) for clean-up. After 15 min the layers were separated and the lower

(DCM) layer was dried by passing through pre-heated $MgSO_4$. To eliminate any residual, unreacted 1,9-decadiene, 1 mL was treated with 5 mL of 1:1 H_2SO_4:HNO_3 concentrated reagents at 70°C to transform decadiene into water soluble products. The solution of the two strong acids produces a nitronium ion (NO^+_2)

$$HNO_3 + 2H_2SO_4 \longrightarrow NO^+_2 + H_3O^+ + 2HSO_4^- \quad (2\text{-}1)$$

which reacts with 1,9-decadiene to form water soluble products that are removed with the water layer [248-249]. After 20 min the mixture was cooled in an ice-bath, 2 mL was transfered to a small round bottom flask, to which approximately 7 mL of Milli-Q water was added. The mixture was gently shaken, the products were extracted with 4 ml of hexane and concentrated to 1 mL before clean-up on florisil. Florisil (reagent grade 60-100 mesh) was heated to 200°C for 6 h and allowed to cool. Florisil (10g) was deactivated by turning with 0.12 mL Milli-Q water (1.2 % w/w) until a uniform powder resulted. A glass column was filled with 9 g of deactivated florisil and tapped down. The product mixture (1 mL) was added to the column which was then eluted with a solvent sequence consisting of 40 mL of hexane (F1), 50 mL of 15:85 dichloromethane:hexane (F2), and 60 mL of 1:1 dichloromethane:hexane (F3). T_4C_{10} was found in fractions F2 and F3, which were combined and concentrated under reduced pressure on a rotary evaporator leaving the isomers in hexane for analysis.

In the same manner 1,2,5,6,9,10-hexachlorodecane and 1,2,10,11-tetrachloro-undecane were synthesized by chlorine addition at the double bonds of 1,5,9-decatriene and 1,10-undecadiene respectively. In each case free radical chlorination reactions were minimized by controlling the amount of chlorine gas (by opening the valve of the chlorine tank for 5 secconds).

2.1.2.3. Synthesis of PCA Mixtures

Mixtures of short chain polychloro-*n*-alkanes (sPCA) used in these studies included decanes (C_{10}), undecanes (C_{11}), dodecanes (C_{12}) and tridecanes (C_{13}) each containing Cl_5 to Cl_8 isomers. sPCA mixtures were synthesized and supplied by Dr.Gregg Tomy, Freshwater Institute, Department of Fisheries and Oceans, Winnipeg, MB. Briefly, the separate sPCA mixtures were synthesized by free radical chlorination of the parent *n*-alkane (decane, undecane, dodecane and tridecane) under reflux at 70°C with sulfuryl chloride (SO_2Cl_2) in the presence of UV-light (Hg lamp 550-W) [17]. Reaction flasks were cooled in an ice-bath and dried by bubbling with nitrogen for 5 min. sPCA mixtures were purified by diluting each reaction mixture with hexane, chromatographing on florisil and eluting with different solvents including hexane and 1:1 hexane:dichloromethane. Unreacted *n*-alkanes were eluted first with hexane whereas the products were eluted with mixed solvents. Full scan high resolution gas chromatography coupled with mass spectrometry (HRGC/MS) in electron ionization (EI) and negative chemical ionization (NCI) modes were used to characterize both isomers and PCA mixtures.

2.2. Instrumentation

Characterization of isolated fractions were performed on a Hewlett-Packard (HP) 5890 series II gas chromatograph, fitted with a 30 m x 0.25 mm x 0.25 μm high resolution column (Supelco), containing PTE-5 stationary phase. Samples were injected (1 to 2 uL) as solutions in hexane, using a 7673 HP autosampler. The splitless injection port temperature was 200°C. Column head pressures were 14 psi, with an overall helium flow rate of approximately 55 mL/min. The column temperature program was as follows: initial 90°C (2 min), 10 °C/min to 180°C (2 min), 7°C/min to 250°C (5 min). The

capillary column was interfaced with a HP 5889 mass spectrometer (MS) with a transfer-line temperature of 280°C. Positive electron ionization (EI) mass spectra of GC effluents were scanned usually from *m/z* 50 to 500 at a rate of 0.9 sec per decade, with ion source temperature of 250°C measured by a thermocouple located in the ion source body. Mass spectra were produced with an electron energy of 70 eV. Perfluorotributylamine (PFTBA), introduced through an inlet valve system, was used for tuning the instrument.

The characterization of PCA mixtures was carried out using the same GC/MS but in negative chemical ionization (NCI) mode. The GC temperature program was slightly modified as follows: initial 50°C (2 min), 7°C/min to 180°C (5 min), 7°C/min to 250°C (15 min), with a total run time of 50.57 min. NCI mass spectra were scanned at 0.8 sec per decade over the range *m/z* 15 to 550, with methane as a moderating gas at a pressure of ~ 1 $x10^{-4}$ torr, as recorded by the source ion gauge. Ion source temperature was 150°C and electron beam current 230 μA.

2.3.Characterization of Polychlorinated *n*-Alkanes (PCAs)

2.3.1. Characterization of PCA Isomers

The total ion chromatogram of synthesized 1,2,9,10-tetrachlorodecane (T_4C_{10}) produced one dominant peak with a retention time of 13.7 min as shown in Figure 2.1(A). The total ion chromatogram of 1,9-decadiene (starting material) is shown in Figure 2.1(B) indicating that acid teatment effectively removed unreacted starting material. Small amounts of higher chlorinated decane isomers identified as pentachloro-decanes (P_5C_{10}) are evident in the chromatogram indicating that free radical substitution reactions were not entirely eliminated. The electron ionization (EI) mass spectrum matched the reported spectrum of tetrachlorodecane [247] confirming this as the identity of the

product due to the presence of a characteristic ion $[M-2HCl]^+$ at *m/z* 206 (Figure 2.2). The chromatograms of the synthesized hexachlorodecane and tetrachloroundecane showed negligible free radical chlorination (Figures 2.3 and 2.4, respectively). Hexachlorodecane (Figure 2.3) shows two peaks with very similar retention times of 33.60 and 33.69 min indicating the presence of two H_6C_{10} isomers. The identities of the products were again confirmed by matching with corresponding spectra available in the literature [247].

EI mass spectra of individual PCA congeners are represented in Figures 2.5 to 2.8. Examination of these spectra reveals a number of even-electron odd-mass ions of low *m/z* common to all of the congeners. Although molecular ions M^+ are not detected in EI mass spectra of PCA isomers, the characteristic $[M-2HCl]^+$ ions were observed for each congener except for D_2C_{12} (Table 2.1). $[M-HCl]^+$ ions decompose during the ionization and were observed only for hexachlorodecane (Figure 2.7) consistent with previous reports [247].

2.3.2. Characterization of PCA Mixtures

Individual PCA mixtures were characterized by GC/NCIMS using methane as reagent gas. Due to the complexity of these mixtures, there is severe overlap and hence poor resolution [250]. Total ion chromatograms (TICs) of decane, undecane, dodecane and tridecane mixtures were obtained by GC/MS in separate runs as shown in Figures 2.9A to 2.12A.

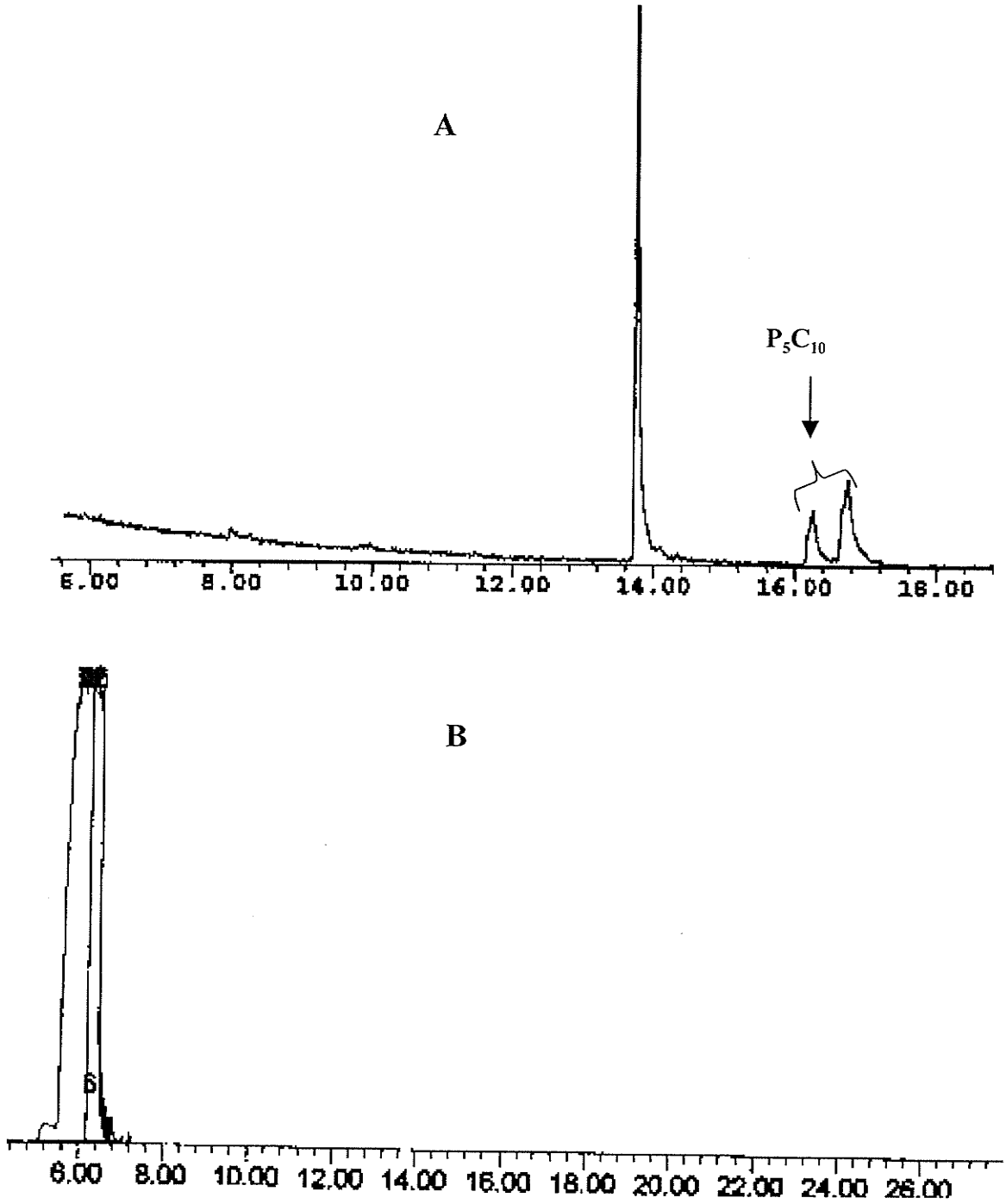

Figure 2.1: Total ion chromatograms of the purified 1,2,9,10-tetrachlorodecane (A) and of the starting material 1,9-decadiene (B).

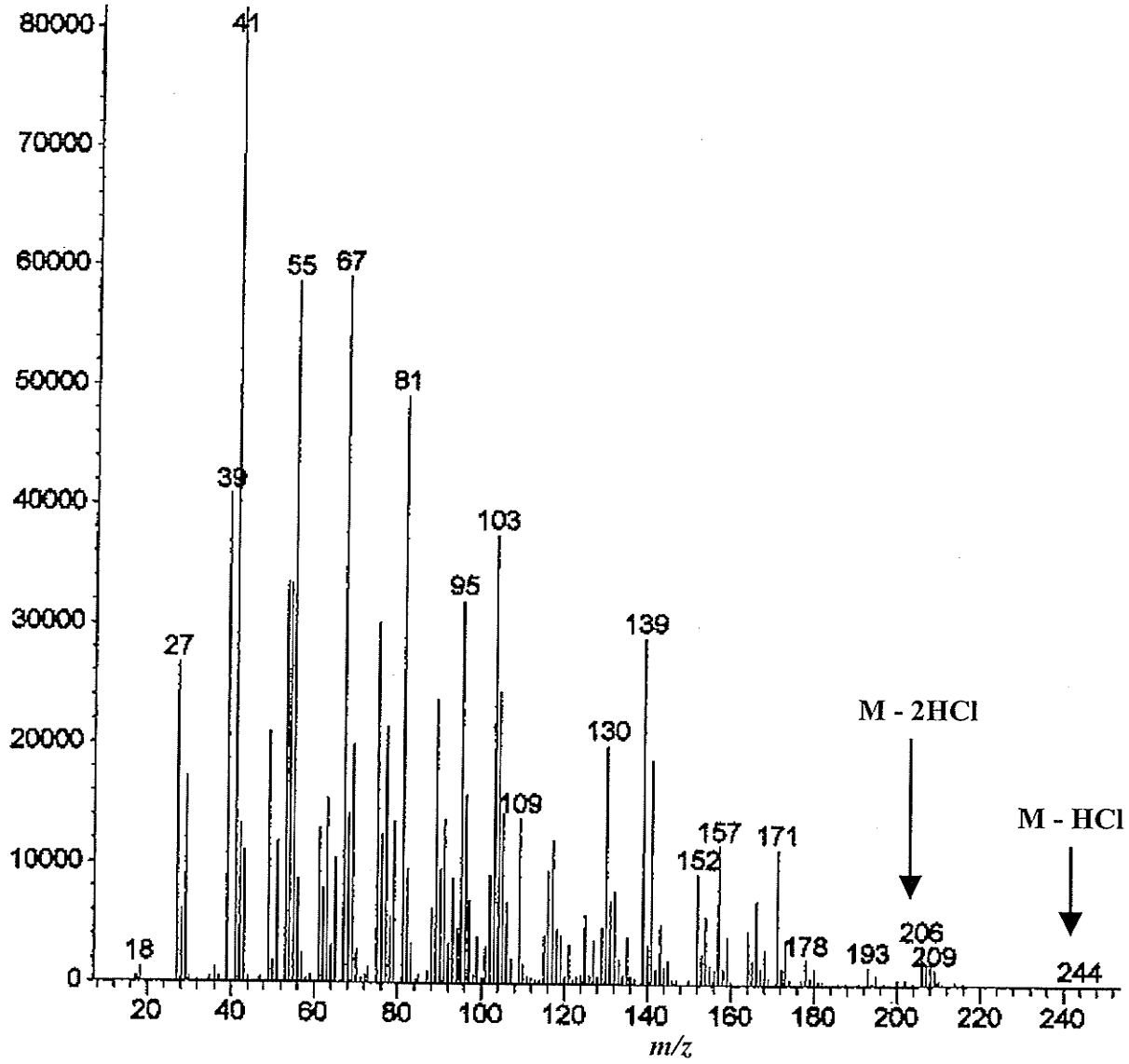

Figure 2.2: Electron ionization positive ion mass spectrum of 1,2,9,10 tetrachlorodecane.

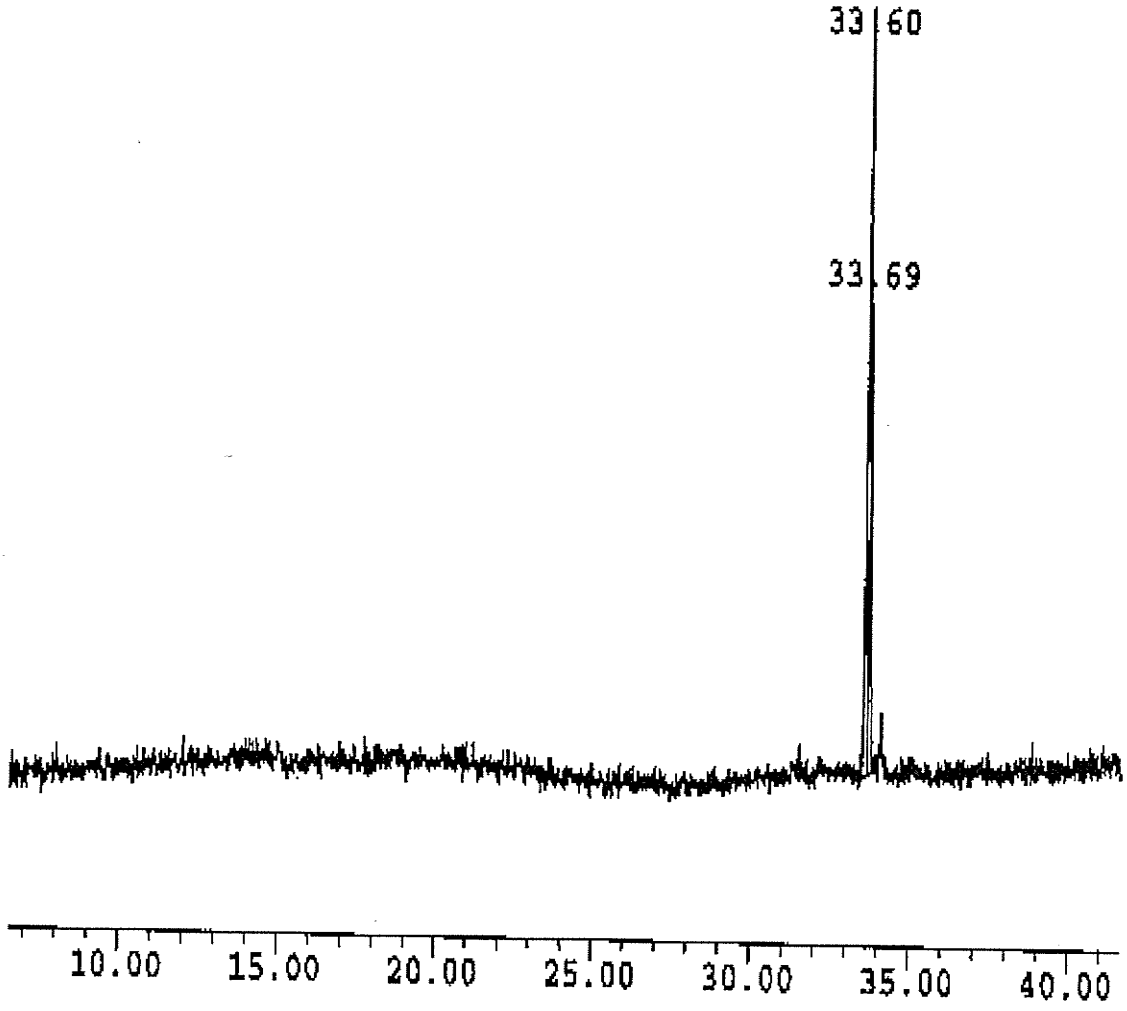

Figure 2.3: Total ion chromatogram of 1,2,5,6,9,10-hexachlorodecane.

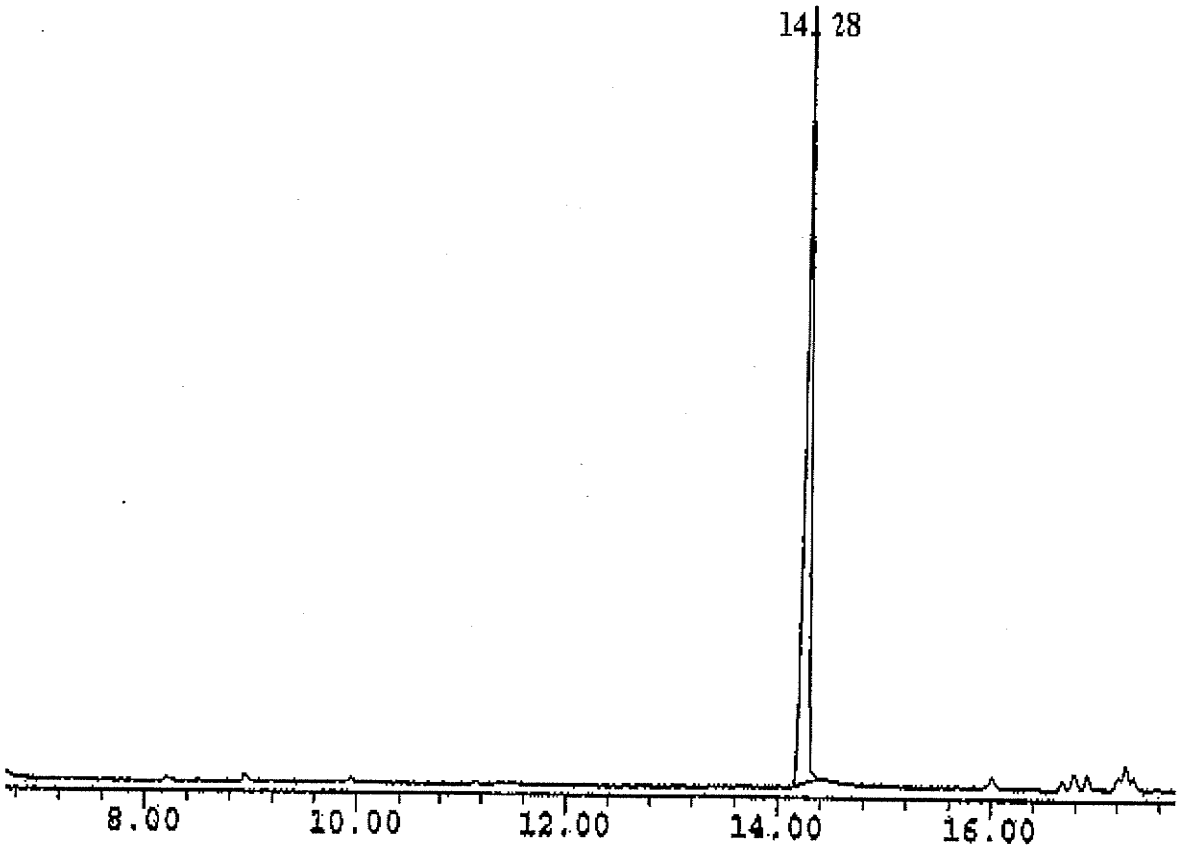

Figure 2.4: Total ion chromatogram of 1,2,10,11-tetrachloroundecane.

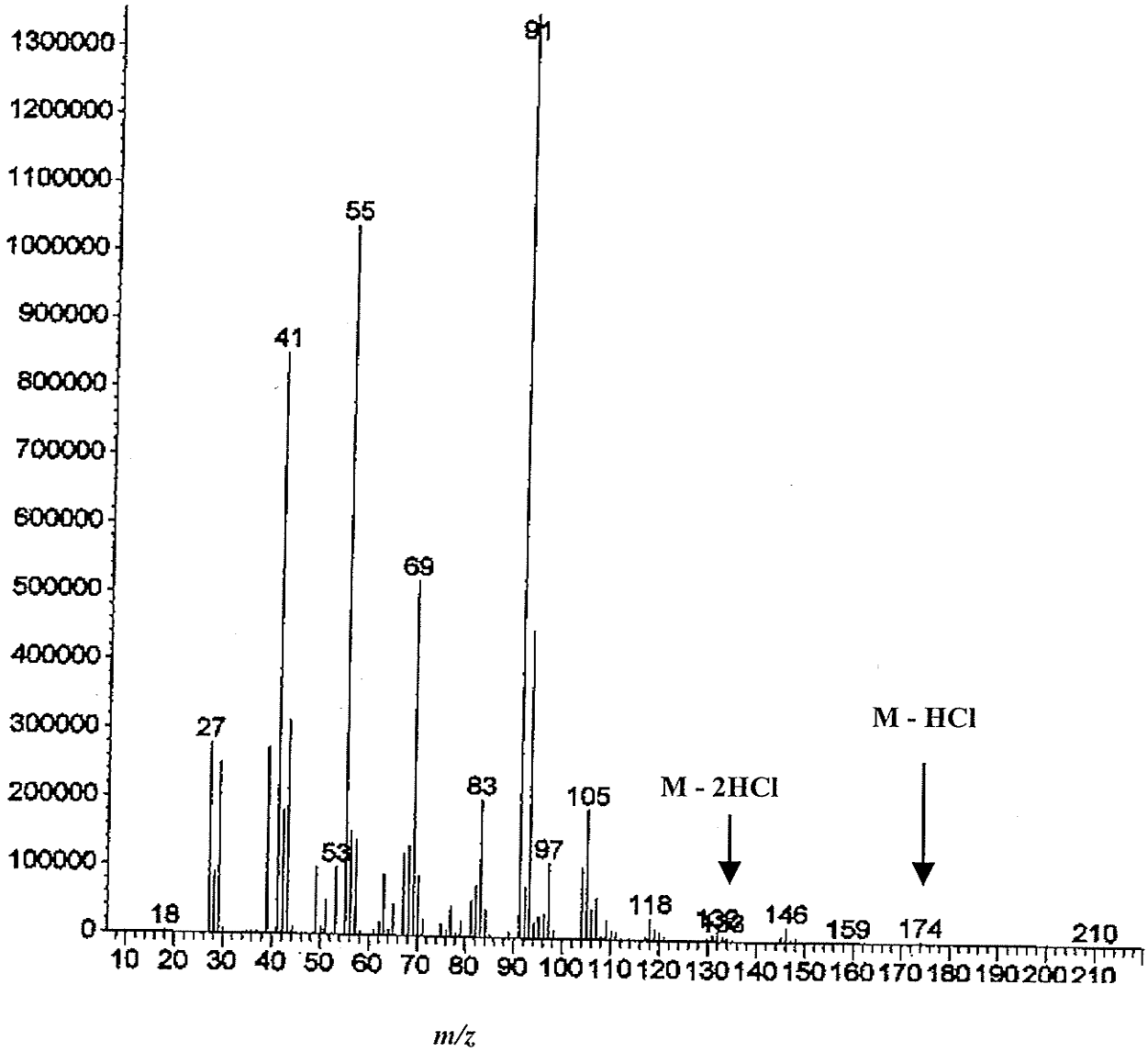

Figure 2.5: Electron ionization positive ion mass spectrum of 1,10-dichlorodecane.

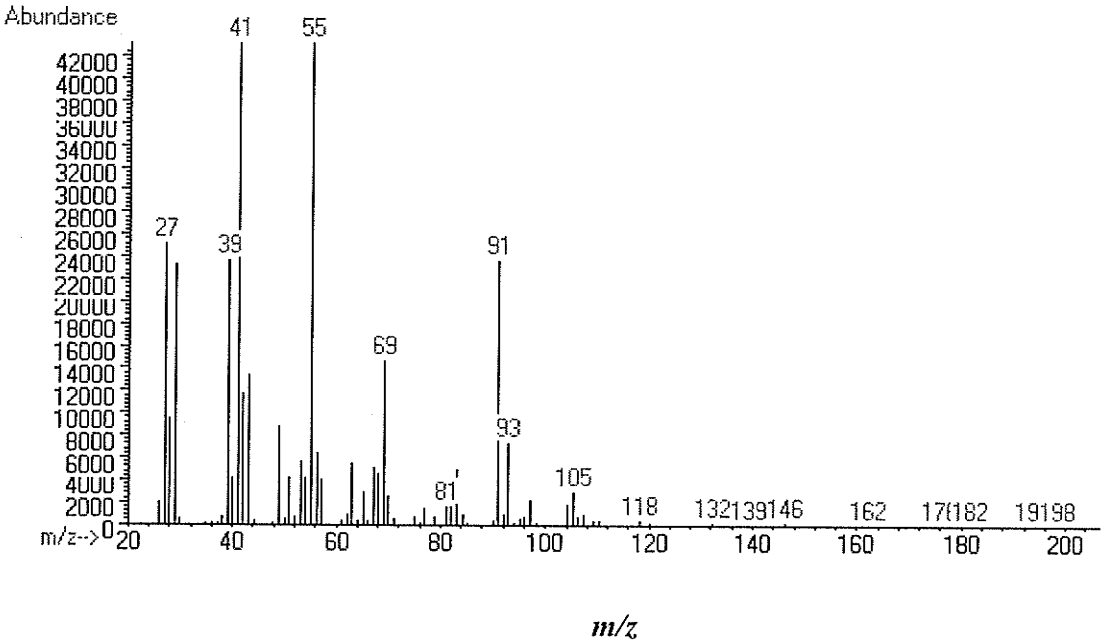

Figure 2.6: Electron ionization positive ion mass spectrum of 1,12-dichlorododecane.

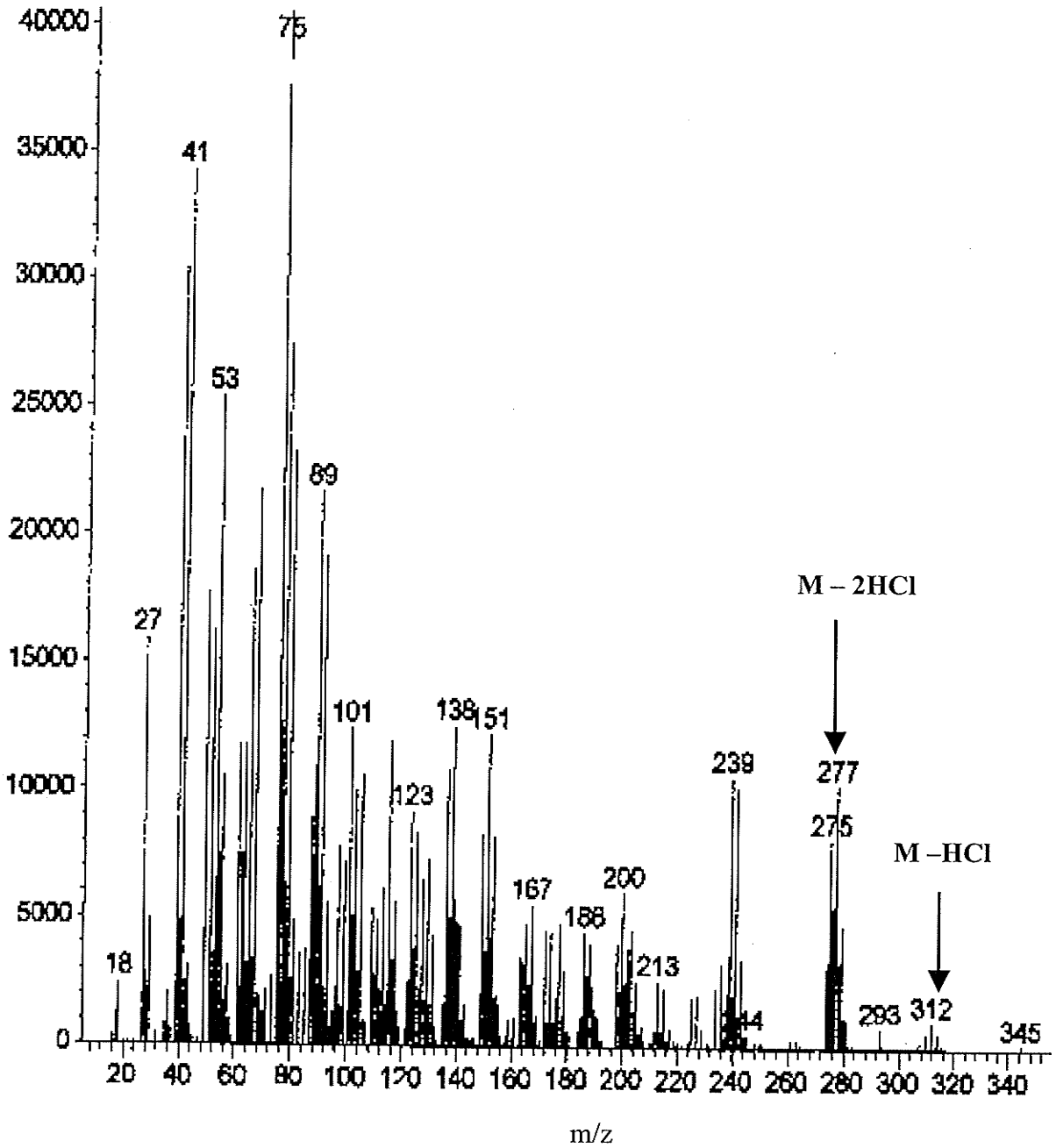

Figure 2.7: Electron ionization positive ion mass spectrum of 1,2,5,6,9,10-hexachlorodecane.

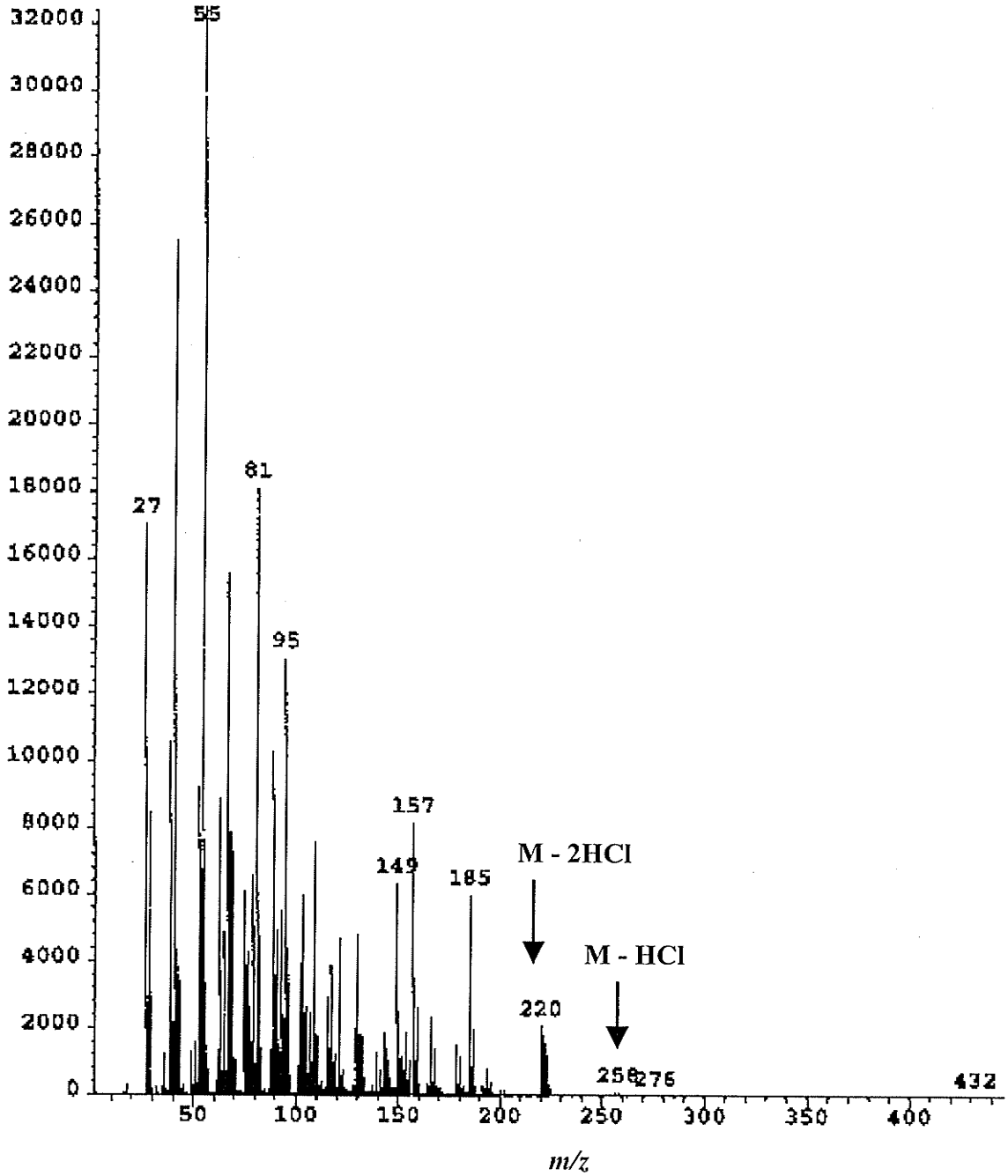

Figure 2.8: Electron ionization positive ion mass spectrum of 1,2,9,10-tetrachloroundecane.

Table 2.1: Molecular[a] and fragment ions of individual PCA isomers formed by electron ionization (EI).

Isomer	M^+	Observed fragment ions[b]	
		$[M-HCl]^+$	$[M-2HCl]^+$
Dichlorodecane	210	ND	138
Tetrachlorodecane	278	ND	206
Hexachlorodecane	346	310	274
Tetrachloroundecane	292	ND	220
Dichlorododecane	238	ND	ND

[a] Molecular ions are not detectable

[b] ND = not detected

Reconstructed chromatograms show the elution profiles for the dominant Cl_5 to Cl_8 congener groups of each mixture (Figures 2.9B to 2.12B). Mass chromatograms were reconstructed by extracting the most abundant ion in the $[M\text{-}HCl]^-$ cluster for each congener group. For example, the M-HCl ions for penta-, hexa-, hepta- and octachlororodecane have *m/z* values of 276, 310, 344 and 378, respectively. The most abundant ions in each cluster are the [M-HCl+2] isotope peaks at 278, 312, 346 and 380, respectively (Table 2.2). Each reconstructed chromatogram shows a complex pattern of peaks due to the large number of isomers in each congener group.

In general, the total elution time of each mixture varied under identical GC conditions. Although the chlorinated decanes are the shortest of all the mixtures it had the longest elution time of approximately 20.5 min (Figure 2.9). The PCA mixture with the longest carbon chain, the chlorinated tridecane, eluted in a shorter time (11.5 min). Both chlorinated undecanes and dodecanes eluted over a period of 13.5 to 14 min. Table 2.3 summarizes the overlap between chlorinated decanes and the other mixtures, measured by calculating the retention time range of individual mixtures in separate runs under the same temperature program. Undecanes overlap with 68% of the elution time of chlorinated decanes. The % interference decreased with increasing alkane chain length, with the least interference from chlorinated tridecanes (56%). As illustrated in Figure 2.13, isomers with a short carbon chain and a high degree of chlorination such as $C_{10}Cl_8$ elute over the same time period as long carbon chain isomers with a lower degree of chlorination such as $C_{13}Cl_5$. The total ion chromatogram of a composite mixture of all of the individual PCA mixtures (C_{10}-C_{13}) is shown in Figure 2.14. The complexity of the mixture results in elution of isomers over a wide range of retention times (~23.5 min) consistent with earlier reports [223].

2.4. Quantification of Polychlorinated *n*-Alkanes (PCAs)

2.4.1. Concentration of PCA Isomers

Standard solutions of individual PCA isomers, 1,10-dichlorodecane (D_2C_{10}) and 1,12-dichlorododecane (D_2C_{12}) were prepared by carefully weighing a known amount of the isomer and dissolving in 1:1 acetonitrile:water in a 10 mL volumetric flask. These solutions, with concentrations of 800 and 100 ng/μL for D_2C_{10} and D_2C_{12} respectively, were used for preparation of stock solutions for all subsequent experimental work.

The concentrations of the synthesized PCA isomers, tetrachlorodecane (T_4C_{10}), hexachlorodecane (H_6C_{10}) and tetrachloroundecane (T_4C_{11}), were determined using the internal standard (IS) calibration method. In this method a solution of two chlorinated aliphatic compounds, lindane (γ-HCH) and 1,10-dichlorodecane (D_2C_{10}), were prepared gravimetrically and analyzed under full scan (*m/z* range of 15 to 500) GC/MS conditions.

The response of D_2C_{10} (S) relative to that of lindane (IS), the relative response factor or RRF, is determined using 38 and 15 ng/uL of each, respectively.

$$\text{RRF} = \frac{m_S / A_S}{m_{IS} / A_{IS}} \qquad (2\text{-}1)$$

Assuming that the RRF of other PCAs is similar to that of D_2C_{10}, D_2C_{10} was used as the internal standard to establish the concentrations of each PCA isomer. For example, the amount of T_4C_{10} in the standard is calculated after establishing the area ratio chromatographically, according to:

$$m_S = \text{RRF} \times \frac{A_S}{A_{IS}} \times m_{IS} \qquad (2\text{-}2)$$

where: m_S and m_{IS} are the amounts of T_4C_{10} and D_2C_{10} (38 ng/uL) respectively, and A_S and A_{IS} are their respective peak areas.

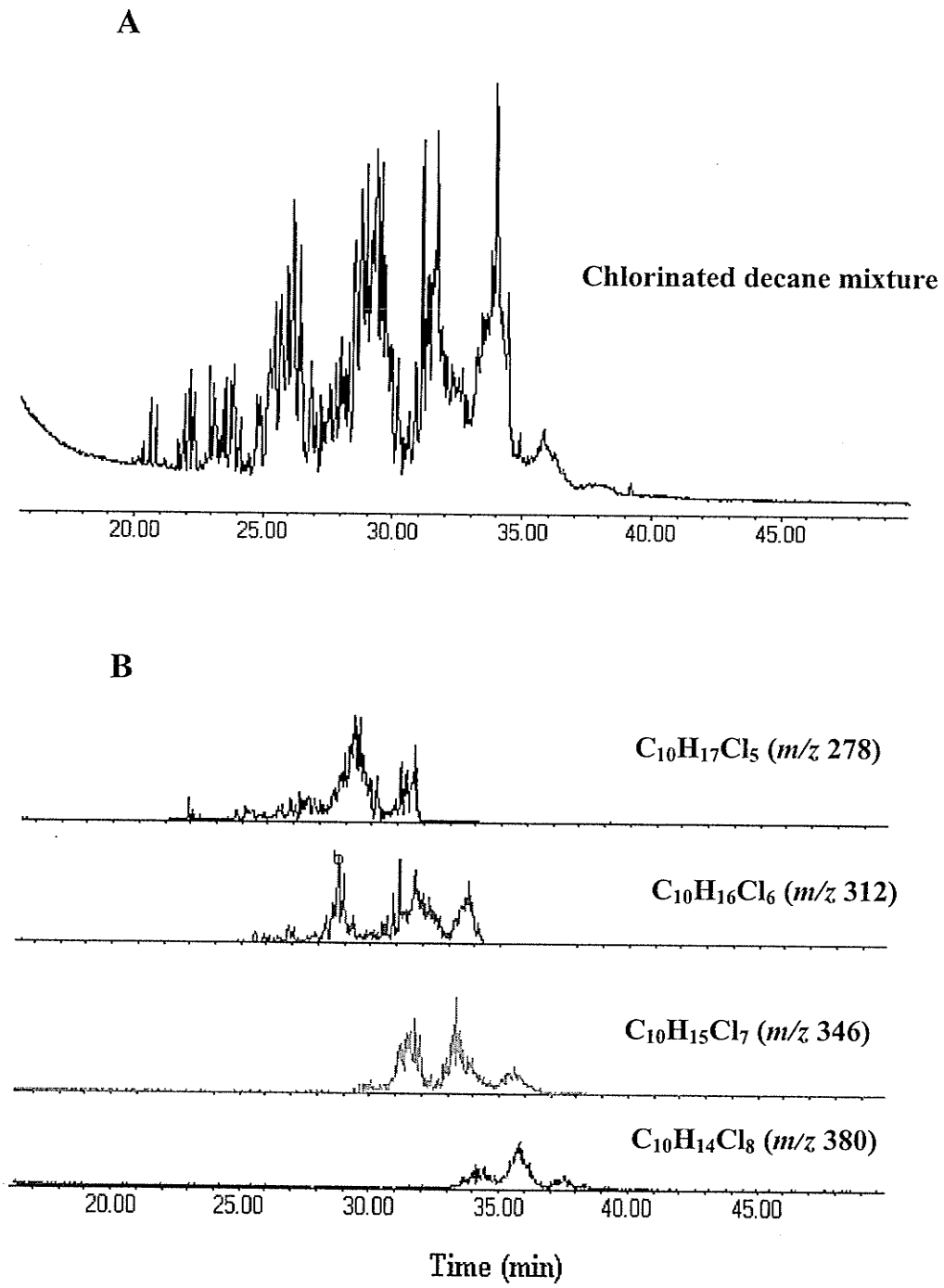

Figure 2.9: Total ion chromatogram of the chlorinated decane mixture (A) and elution profiles of the extracted ions representing the Cl_5, Cl_6, Cl_7 and Cl_8 congener groups (B).

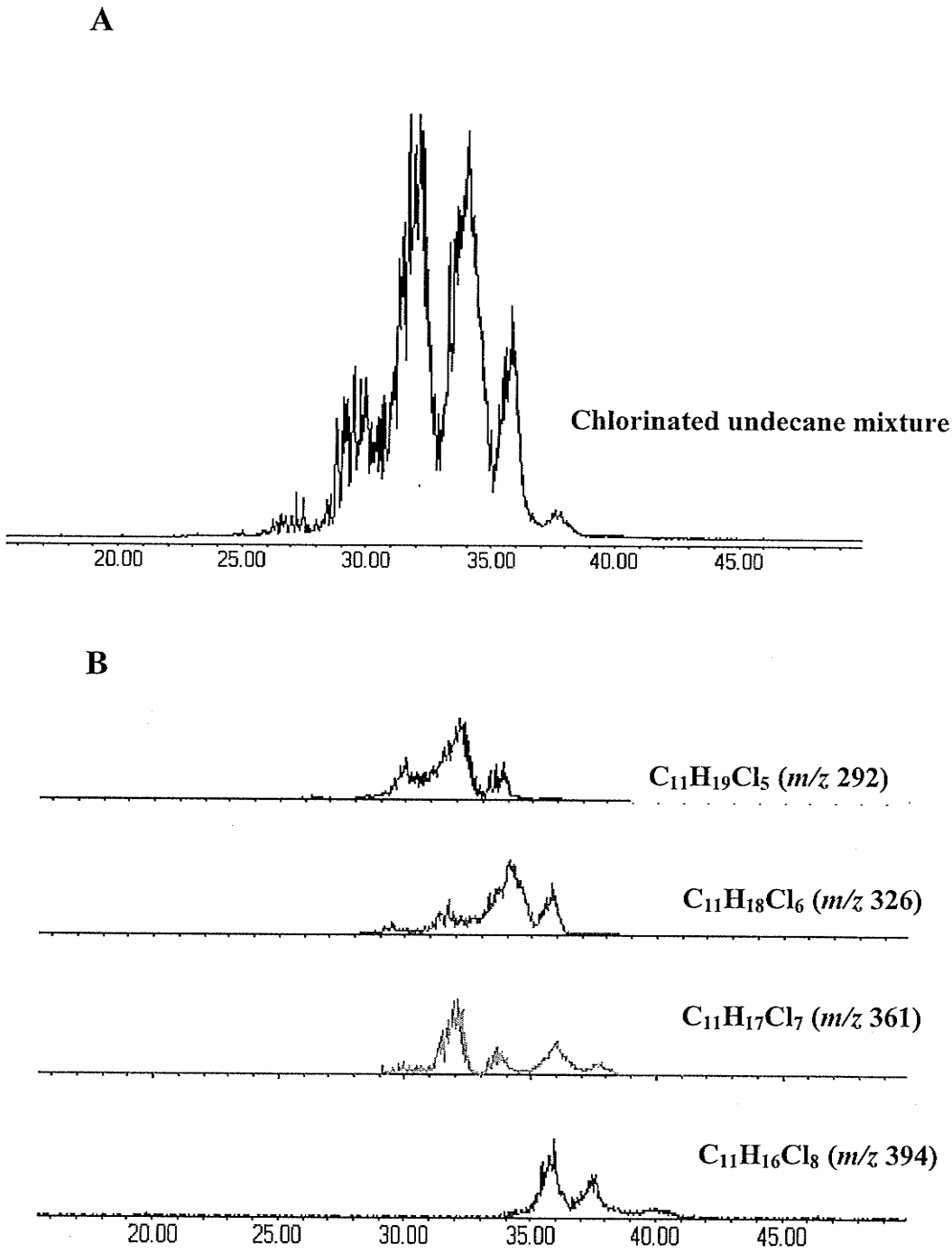

Figure 2.10: Total ion chromatogram of the chlorinated undecane mixture (A) and elution profiles of the extracted ions representing the Cl_5, Cl_6, Cl_7 and Cl_8 congener groups (B).

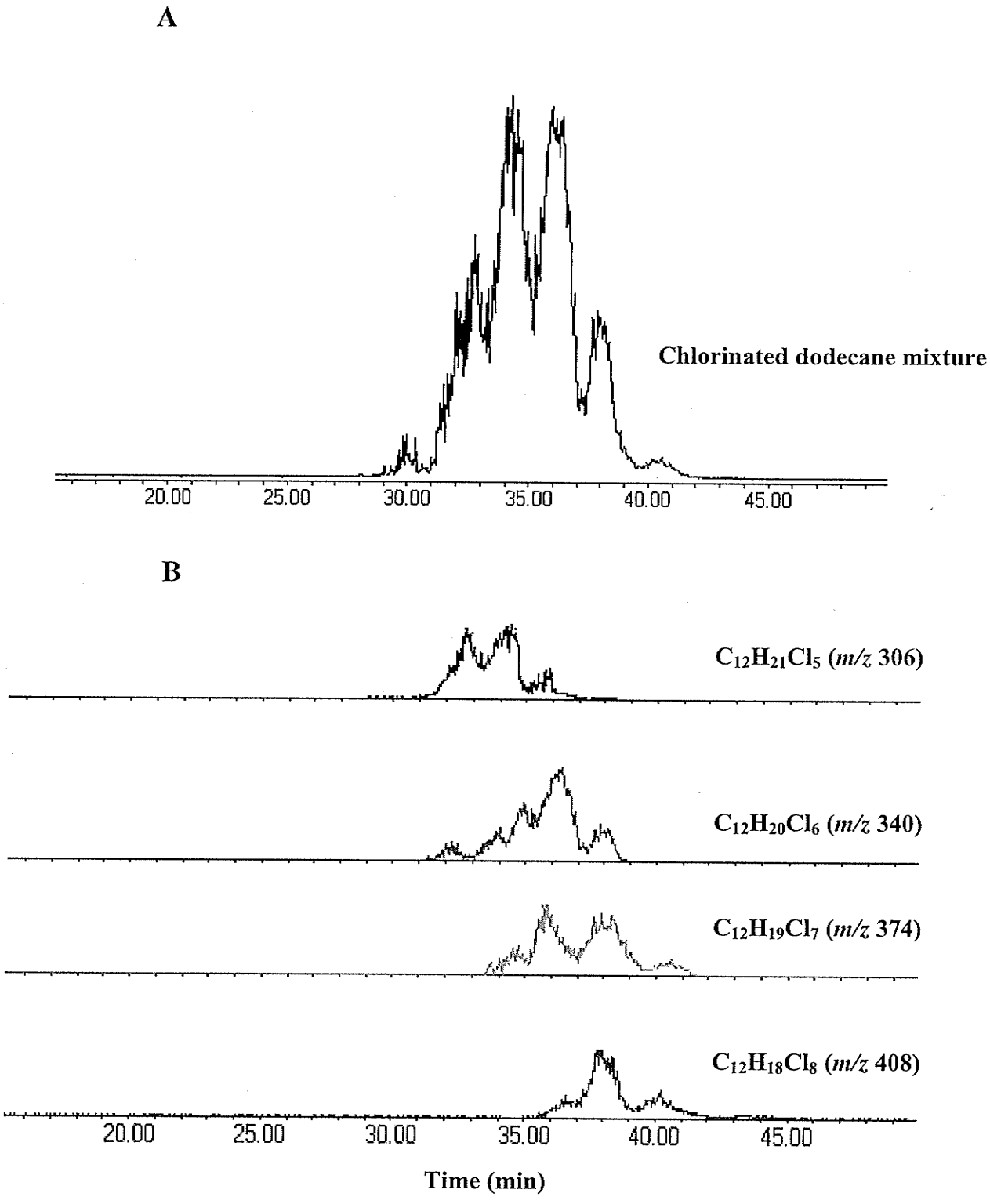

Figure 2.11: Total ion chromatogram of the chlorinated dodecane mixture (A) and elution profiles of the extracted ions representing the Cl_5, Cl_6, Cl_7 and Cl_8 congener groups (B).

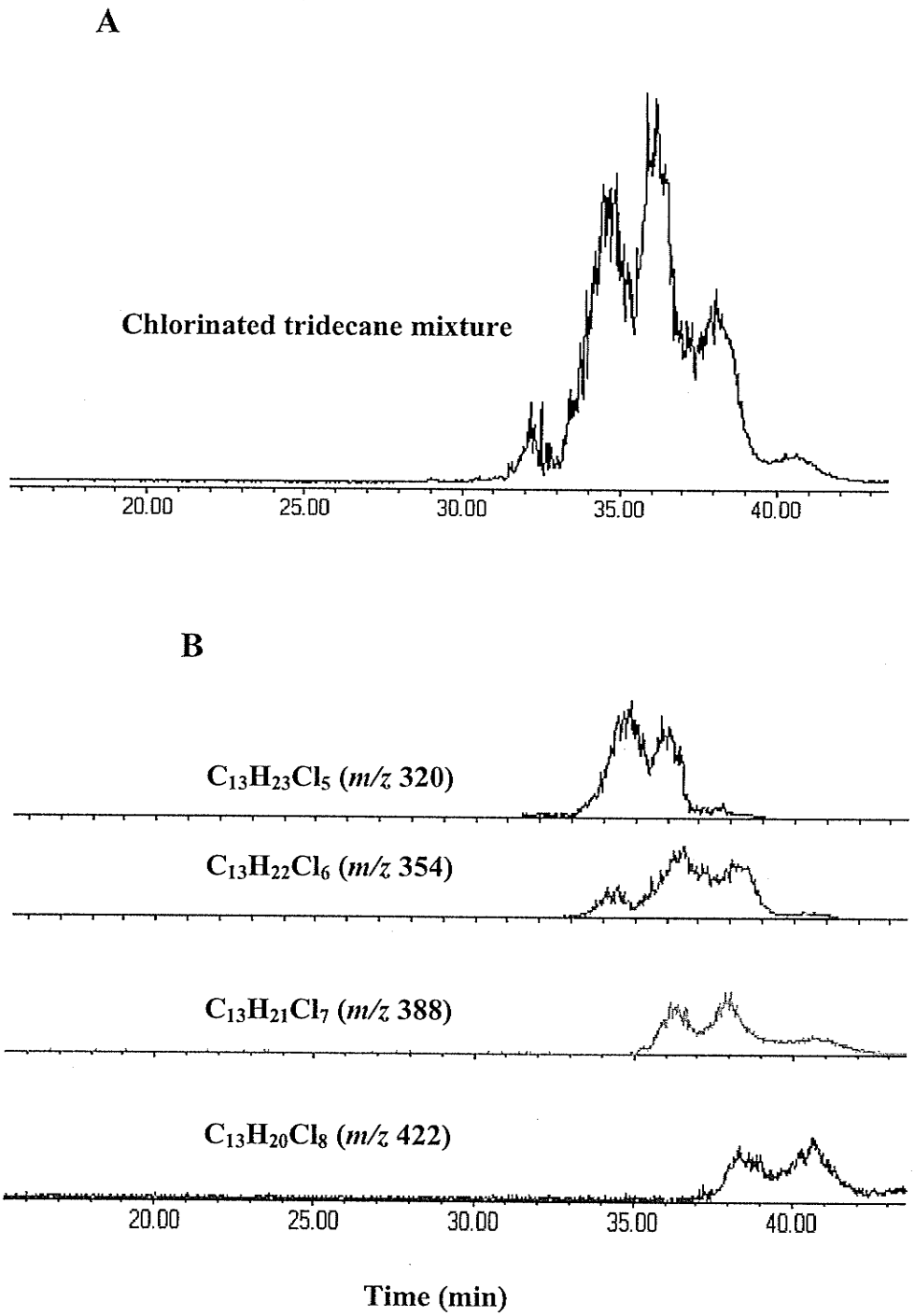

Figure 2.12: Total ion chromatogram of the chlorinated tridecane mixture (A) and elution profiles of the extracted ions representing the Cl_5, Cl_6, Cl_7 and Cl_8 congener groups (B).

Table 2.2: The two prominent ions in the $[M-HCl]^-$ cluster for each congener groups and the most abundant ion (in boldface) used for SIM.

Mix./Cl number	Cl_5	Cl_6	Cl_7	Cl_8
C_{10}	276/**278**	310/**312**	344/**346**	378/**380**
C_{11}	290/**292**	324/**326**	358/**360**	392/**394**
C_{12}	304/**306**	338/**340**	372/**374**	406/**408**
C_{13}	318/**320**	352/**354**	386/**388**	420/**422**

Table 2.3: Percentage interference of individual PCA mixtures with chlorinated decanes during their elution time (min).

PCAs mix.	Start time	End time	Elution time	% interference
Decanes	19.5	40.0	20.5	
Undecanes	25.0	39.0	14.0	68.3
Dodecanes	29.0	42.0	13.5	65.9
Tridecanes	30.5	42.0	11.5	56.1

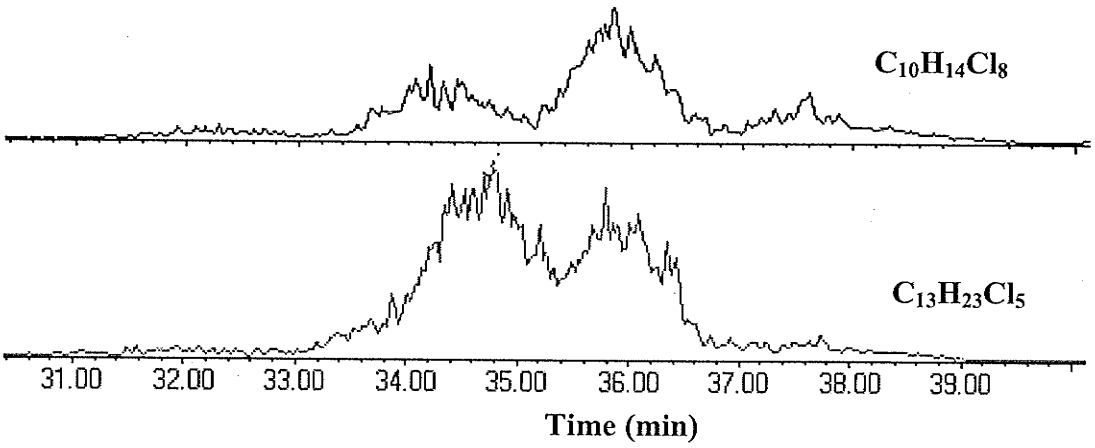

Figure 2.13: Mass chromatograms (GC/NCI-MS) showing the similarity in the elution profiles of octachlorinated decanes ($\sum C_{10}Cl_8$) with pentachlorinated tridecanes ($\sum C_{13}Cl_5$).

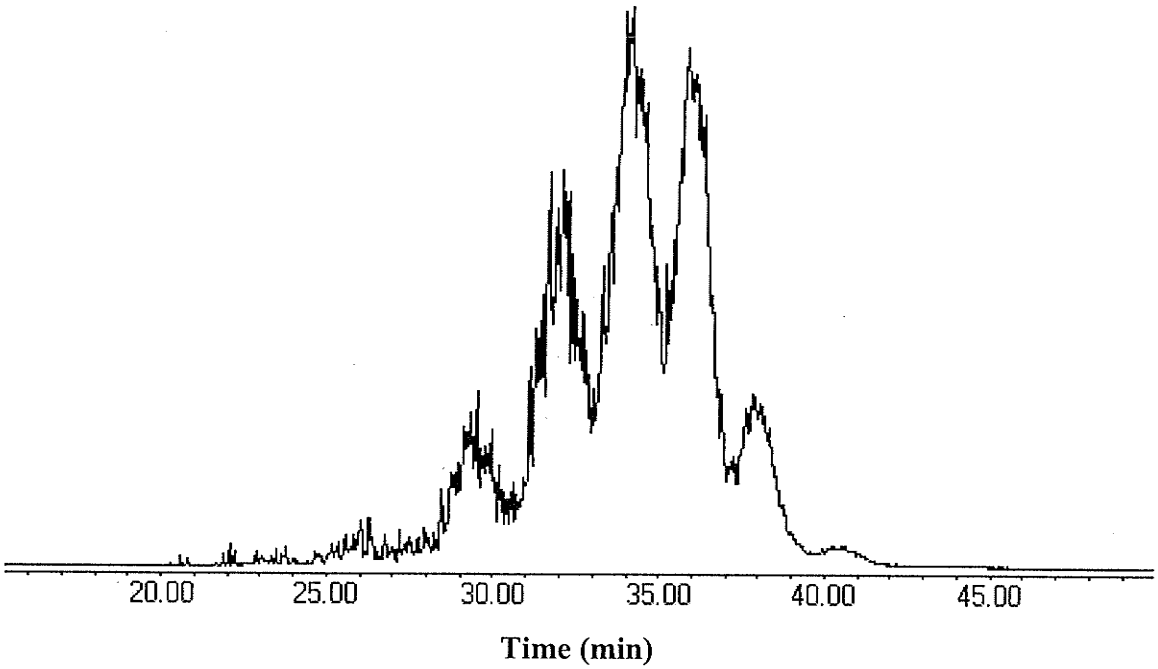

Figure 2.14: Negative chemical ionization full scan (*m/z* 50-550) total ion chromatogram of a composite mixture of PCAs (Σ $C_{10}Cl_{5\text{-}8}$ to Σ $C_{13}Cl_{5\text{-}8}$)

In determining the concentrations of tetrachlorodecane in any solution, it was assumed that the ionization efficiency of the chlorinated alkane congeners are the same [18], hence the relative response factor for tetrachlorodecane would be identical to that of D_2C_{10}. Using this assumption, the concentrations of stock solutions of synthesized PCA isomers were determined to be 328.7, 400 and 366.5 ng/uL for tetrachlorodecane, hexachlorodecane and tetrachloroundecane, respectively.

2.4.2. Concentration of PCA Mixtures

Mixtures of PCAs were provided as neat liquids. Working solutions were prepared by carefully weighing individual amounts of each mixture, dissolving in acetone in a 1 mL volumetric flask and storing at 4°C. The concentrations of the standard solutions, representing the sum of all isomers in each mixture, were 44.0, 112.6, 100.0 and 204.3 μg/μL for $\sum C_{10}Cl_{5\text{-}8}$ (chlorinated decanes), $\sum C_{11}Cl_{5\text{-}8}$ (chlorinated undecanes), $\sum C_{12}Cl_{5\text{-}8}$ (chlorinated dodecanes) and $\sum C_{13}Cl_{5\text{-}8}$ (chlorinated tridecanes), respectively.

In degradation studies of both PCA isomers and mixtures, analyses were performed by GC/MS in selected ion monitoring (SIM) mode. In the analysis of PCA isomers, positive electron ionization (EI) was used and the selected ions were 91/93 for both D_2C_{10} and D_2C_{12}, and 139/141, 239/241 and 157/159 for T_4C_{10}, H_6C_{10} and T_4C_{11}, respectively. In the analysis of PCA mixtures, NCI was used and the $[M\text{-}HCl]^-$ fragment ions were monitored as illustrated for sevsral pentachlorinated isomers in Figure 2.15.

To determine the concentration of each congener group ($\sum Cl_5$ to $\sum Cl_8$) in each PCA mixture, standard solutions of individual mixtures were analyzed by GC/NCI-MS in SIM mode. The fraction of each congener group ($\sum Cl_5$ to $\sum Cl_8$) was calculated using the ratio of the peak area for that group to the total integrated area of the mixture (Table 2.4). The

concentrations of each congener group were determined by multiplying the fraction composition by the weight of the PCA mixture.

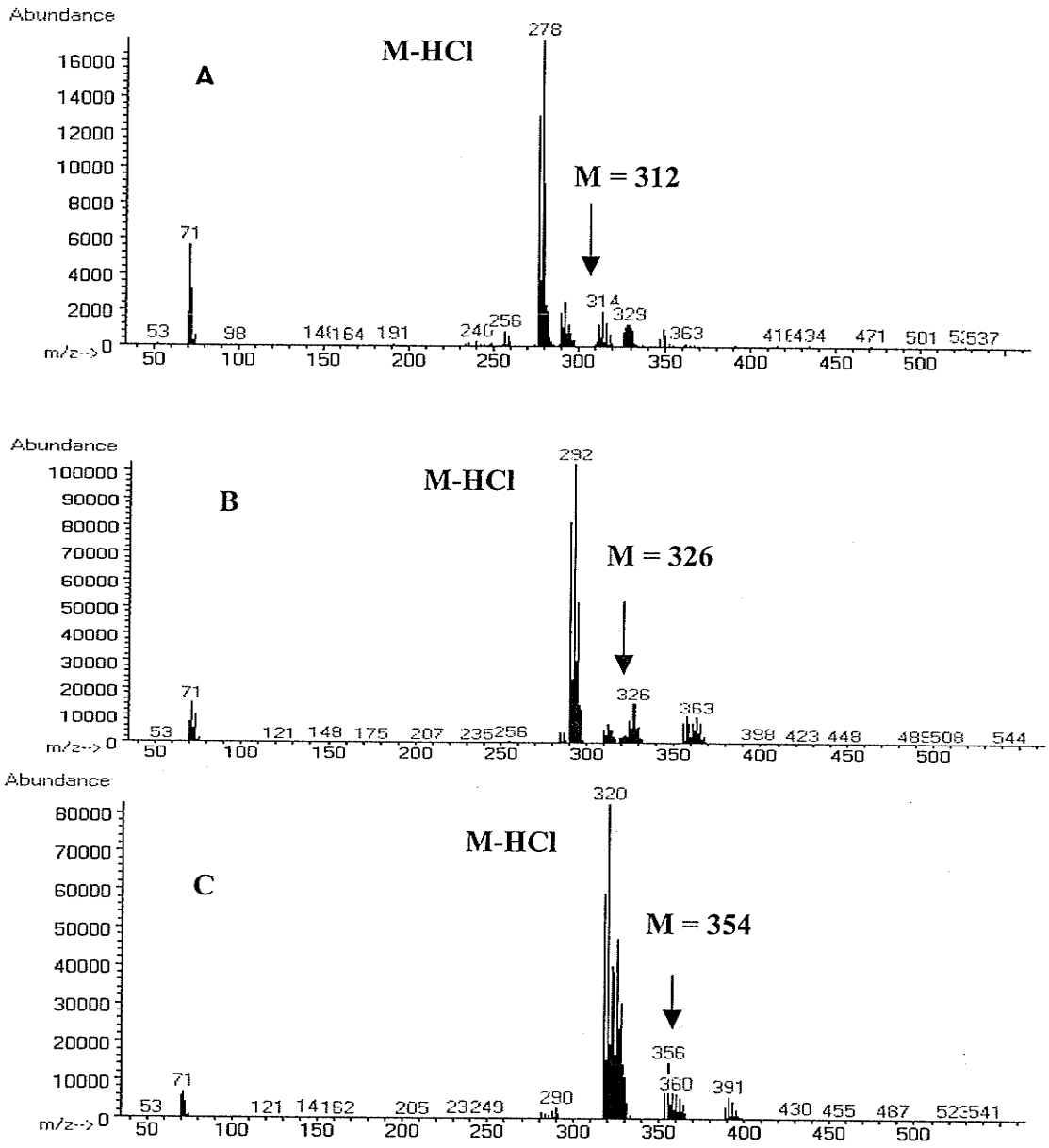

Figure 2.15: NCI mass spectra obtained for (A) $C_{10}Cl_5$, (B) $C_{11}Cl_5$ and (C) $C_{13}Cl_5$

CHAPTER 3

Hydrolysis and Photolysis of Polychlorinated *n*-Alkanes (C_{10}-C_{13})

3.0. Introduction

As discussed in Chapter 1 short chain chloroparaffins (SCCPs) are of particular concern because they have the greatest potential for environmental release and the highest aquatic and mammalian toxicity of all PCAs. No data is currently available on the actual rates of environmental transformation reactions of SCCPs. Understanding the photolytic and hydrolytic behavior of SCCPs is valuable in assessing their persistence and environmental fate.

In this study the environmental reactivity of PCA isomers including D_2C_{10}, T_4C_{10}, H_6C_{10}, T_4C_{11} and D_2C_{12} as well as individual mixtures of polychlorinated decanes (C_{10}), undecanes (C_{11}), dodecanes (C_{12}) and tridecanes (C_{13}) were examined. Hydrolytic reactivity of both isomers and mixtures of the PCAs were investigated in pure water at different pHs (4, 7 and 9) and at different temperatures (15, 20 and 30°C). Furthermore, the direct and indirect photolysis of these isomers and mixtures were examined in pure and natural water using a xenon lamp as a simulated sunlight source.

3.1. Experimental

3.1.1. Water Sources

Milli-Q water (18 M Ω cm^{-1}) and water from Lake Winnipeg (collected in May 2000, pH 8.6) and Lake 375 of the Experimental Lakes Area (collected May 2002, pH 6.8) were used in this study. Suspended particles were removed from natural water by filtration through glass fiber filters (1.2μm, Whatman GF/C filters) to eliminate the

potential for sorbents [251]. Water analyses, performed by the water chemistry lab at the Freshwater Institute (Winnipeg MB), are summarized in Table 3.1.

3.1.2. Chemicals and Reagents

Commercial and synthesized PCA isomers used for this investigation included 1,10-dichlorodecane, 1,2,9,10-tetrachlorodecane, 1,2,5,6,9,10-hexachlorodecane, 1,2,10,11-tetrachloroundecane and 1,12-dichlorododecane. PCA mixtures included decanes (C_{10}), undecanes (C_{11}), dodecanes (C_{12}) and tridecanes (C_{13}) each containing Cl_5 to Cl_8 isomers. Sodium azide purchased from Anachemia was used to sterilize solutions in the hydrolytic study. Boric acid, potassium hydrogen phthalate, hydrochloric acid (BDH), potassium phosphate monobasic and potassium chloride (Mallinckrodt) were used to adjust solution pHs to 4, 7 and 9. Organic solvents (acetone, hexane, dichloromethane, chloroform) used for preparation and extractions were HPLC grade.

3.1.3. Sample Preparation

All glassware was washed prior to use with dilute nitric acid and thoroughly rinsed with pure water, followed by an acetone-hexane-acetone wash sequence. Glassware was sterilized by heating at 180°C for 24 hours. Glassware was marked for use with individual congeners to prevent cross-contamination.

Aqueous solutions of PCAs (with initial concentrations of 10^{-6} to10^{-8} M) were prepared by pipeting from stock solutions into buffer solutions in sterilized 1L round bottom flasks and stirred to facilitate equilibration. Total equilibration time before experiments was approximately 15 minutes to ensure homogeneity. Then 40 mL aliquots were removed from the stock solution and placed into sterile 50 mL Pyrex tubes. For both hydrolysis and photolysis, samples were tightly sealed to prevent volatilization [252].

Table 3.1: Analysis of natural and pure water.

Water content	Lake Winnipeg	Lake 375	Milli-Q
$N\text{-}NO_3$ (mg/L)	127	NA	<1
$N\text{-}NO_2$ (mg/L)	18	NA	<1
$N\text{-}NH_4$ (mg/L)	15	NA	<5
Total Dissolved N (mg/L)	770	NA	<5
Total Dissolved P (mg/L)	60	NA	<1
Dissolved Inorganic C (mmol /L)	2350	420	<10
Dissolved Organic C (mmol/L)	990	430	20

After the allotted time of hydrolysis or photolysis, the samples were transferred to 125 mL separatory funnels. The empty Pyrex tubes were then rinsed with two 30 mL portions of the extraction solvent to recover any chemical sorbed to the walls of the tube and added to the separatory funnel.

3.1.4. Hydrolysis

After adjusting to the required pH (4, 7 and 9) solutions were sterilized with 0.01g/L sodium azide [253] and oxygen was removed by gently bubbling with N_2. Preliminary tests were carried out for each of the isomers at 50°C in order to determine the potential for hydrolytic degradation. Compounds with hydrolytic half-lives at 50°C longer than one year are considered stable [254] and do not require further investigation at lower temperatures. When this condition was not met, more detailed studies were performed. Hydrolysis experiments at 15 and 20°C were performed in the dark in a temperature controlled environment chamber. For studies at 30 and 50°C, samples were placed in a VWR Model 1217 water bath which regulated the temperature to ± 0.1°C.

3.1.5. Photolysis

Photolytic experiments were conducted with a Xe-lamp (intensities of 3.0×10^{-5} Ein L^{-1} min^{-1}) [255] as simulated sunlight source with solutions at pH 9 and 38°C. Solutions wrapped with aluminum foil served as a dark control to account for chemical degradation. Indirect photolysis was conducted at the natural pH of 6.8 and 8.6 for Lake 375 and Lake Winnipeg water, respectively, and at a temperature of 38°C. Direct photolysis was investigated for all PCA isomers in Milli-Q water at pH 9 and a temperature of 38°C. Samples were generally irradiated in duplicate in the photoreactor, which had been thermally equilibrated for 10 min. In sets with Milli-Q and natural water, samples were typically removed after irradiation times of 0, 7, 17, 27, 34, 40 and 48

hours. In all cases solutions were transferred to a 125-mL separatory funnel for extraction.

3.1.6. Extraction of PCAs

Both liquid-liquid and solid-liquid extraction were evaluated at each pH to establish the optimum conditions for the extraction of PCAs from the aqueous solutions. Liquid-liquid extraction was carried out with either 85:15 hexane:dichloromethane or 95:5 Hexane:chloroform, while C-18 Sep-pak (SEP) extraction cartridges were used for solid-liquid extraction. Salting out was also tested with 100 g L^{-1} of NaCl added to the aqueous layer prior to extraction. In liquid-liquid extraction the solutions were shaken for 30 min and the organic layer was transferred to a 100 mL round bottom flask containing 2 mL of hexane spiked with 10 ng μL^{-1} lindane. Lindane was used as an internal standard to correct for any losses during sample work-up, as well as variability in injection volumes in gas chromatographic analysis. Experiments with D_2C_{12} used D_2C_{10} as the internal standard since lindane and D_2C_{12} had similar GC retention times under the column temperature program used. After extraction the solution was transferred into a round bottom flask. The separatory funnel was washed with 10 mL hexane, and the rinsings were also added to the round bottom flask.

Samples were evaporated to approximately 5 mL by rotoevaporation and transferred to 15 mL tapered Pyrex centrifuge tubes. The round bottom flasks were washed with 10 mL of hexane, with the solvent added to the centrifuge tubes. The samples were then concentrated to 150-300 μL by slow evaporation using nitrogen gas. After concentration, samples were transferred to 0.15 mL glass inserts placed inside a 2 mL sample vial and analyzed by GC/MS.

3.1.7. Analysis of PCAs

PCAs were analyzed with HP 5890 GC interfaced with 5989A MSD in EI and NCI modes. NCI analysis utilized methane as the moderating gas and an ion source temperature of 150°C. The column temperature program and the ions used for selected ion monitoring (SIM) were discussed in Chapter 2.

3.1.7. Kinetic Treatment of Degradation

The rate of disappearance of PCA isomers and mixtures in both the hydrolysis and photolysis investigations was determined by monitoring the concentration of parent PCAs as a function of time using GC/MS analysis. Samples (n = 2) were removed at specific times, liquid-liquid extracted using (85:15) hexane:dichloromethane, spiked with an internal standard (usually γ-lindane) and analyzed by GC/MS. Data were treated with a first-order kinetic model providing first-order rate constants (k)

$$-\frac{d[PCA]}{dt} = k[PCA] \qquad (3\text{-}1)$$

and corresponding first-order half-lives ($t_{1/2}$):

$$t_{1/2} = \frac{\ln 2}{k} \qquad (3\text{-}2)$$

3.2. Results and Discussion

3.2.1. Extraction Efficiency

Several tests were done on the extraction efficiency of the different PCA isomers from water. The results of both liquid-liquid and liquid-solid extraction are shown in Table 3.2. Results indicate high efficiency of extraction (83.5 %) for D_2C_{10} using liquid-solid extraction. However, as the chlorine number increased, the efficiency of C-18 SPE method decreased, while the hexane:dichloromethane efficiency remained relatively

Table 3.2: Extraction efficiencies of chlorinated decane isomers and mixtures using liquid-solid (C-18 Sep-pak) and liquid-liquid (85:15 hexane:dichloromethane) extraction at pH 7.

Isomer	Sep-Pak	Liquid-liquid
$C_{10}H_{20}Cl_2$	83.5	82.8
$C_{10}H_{18}Cl_4$	63.2	76.7
$\Sigma C_{10}H_{17}Cl_5$	NA	72.4
$C_{10}H_{16}Cl_6$	37.9	74.1
$\Sigma C_{10}H_{15}Cl_7$	NA	71.1
$\Sigma C_{10}H_{14}Cl_8$	NA	68.5

constant. Thus, liquid-liquid extraction was used for extraction of PCAs in this study. Since hydrolysis experiments were performed at different pHs (4, 7 and 9), experiments were carried out to investigate the effect of pH on the extraction efficiency of D_2C_{10}, The results, summarized in Table 3.3, indicate that the extraction efficiency varied between 71 and 83% in the pH range of 4 to 9 but decreased dramatically with increasing basicity with only 40% recovery at pH 13. Salting out with 100 g L^{-1} NaCl reduced the extraction efficiency of D_2C_{10} to 27% at pH 7. The extraction efficiency of PCAs was dependent on the time of contact of the solvent with the aqueous solution. The results in Figure 3.1 indicate that with 85:15 hexane:dichloromethane maxium recovery of H_6C_{10} at pH 4 required a minimum 20 min extraction time.

3.2.2. Hydrolysis of PCA Isomers

US OECD (Organization for Economic Co-operation and Development) guidelines suggest that a chemical is considered hydrolytically stable when the degradation half-life at 50°C exceeds one year [254]. Preliminary tests at 50°C over a 5 to 8 day period indicated that all of the isomers degraded sufficiently (see Table 3.4) to necessitate further study. Hydrolysis rates appeared to decrease with increasing chlorine number and carbon chain length. Detailed studies of all congeners were conducted over the environmentally significant pHs of 4, 7 and 9 and temperatures of 15 to 30°C. All pH adjustments were made using the buffer mixtures outlined in Table 3.5. Hydrolysis half-lives of PCA isomers at different pHs and temperatures are summarized in Tables 3.6 to 3.8. In general hydrolysis rates were dependent on chlorine number, carbon chain length, temperature and pH. The rate of hydrolysis of chlorinated decanes decreased dramatically from Cl_4 to Cl_6. For example, hydrolysis half-lives increased from 19.5 to 49.0 d for T_4C_{10} to H_6C_{10} at pH 4 and 15°C.

Table 3.3: Extraction efficiency of D_2C_{10} as a function of pH (liquid-liquid extraction, 85:15 hexane:dichloromethane).

pH	% Efficiency
4.0	73.9
7.0	82.8
9.0	70.8
10.0	68.2
12.5	60.4
13.1	40.1
Salting out (at pH 7)	27.10

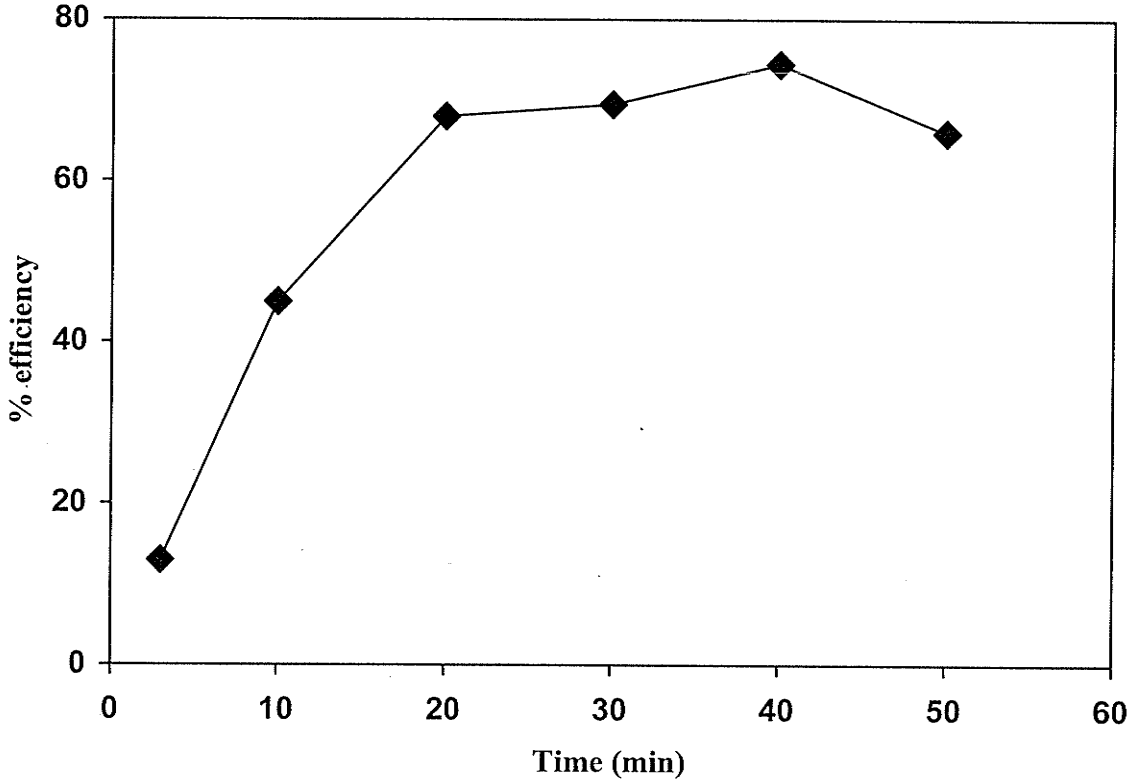

Figure 3.1: Extraction efficiency of H_6C_{10} using liquid-liquid (85:15 hexane:dichloromethane) extraction at pH 4 as a function of time.

Table 3.4: Hydrolysis of PCA isomers at different pH (as percent hydrolyzed in 5-8 days at 50°C).

Isomer	Time (d)	Percent Hydrolyzed		
		pH 4	pH 7	pH 9
1,10-dichlorodecane	5	29.1	29.7	38.5
1,2,9,10-tetrachlorodecane	5	21.1	35.7	46.1
1,2,5,6,9,10-hexachlorodecane	5	58.6	64.8	65.9
1,2,10,11-tetrachloroundecane	8	50.0	73.5	68.5
1,12-dichlorododecane	8	56.5	72.5	70.5

Table 3.5: Buffer mixtures used to adjust the pH of all solutions.

Composition	Final Volume (mL)	pH
10 mL 0.1M HCl + 50 mL 0.1M 1-$KOCOC_6H_4$-2-COOH	100	4.0
30 mL 0.1 M NaOH + 50 mL 0.1M KH_2PO_4	100	7.0
50 mL 0.1 M NaOH + 50 mL 0.1M H_3BO_3 in 0.1M KCl	100	9.0

Table 3.6: Hydrolysis half-lives of PCA isomers at 15°C.

Isomer	Hydrolysis half- lives (d)		
	pH 4	pH 7	pH 9
1,10-dichlorodecane	16.8	16.6	22.5
1,2,9,10-tetrachlorodecane	19.5	15.8	19.9
1,2,5,6,9,10-hexachlorodecane	49.0	47.0	48.0
1,2,10,11-tetrachloroundecane	28.9	25.3	13.5
1,12-dichlorododecane	30.4	18.0	17.0

Table 3.7: Hydrolysis half-lives of PCA isomers at 20°C.

Isomer	Hydrolysis half- lives (d)		
	pH 4	pH 7	pH 9
1,10-dichlorodecane	4.9	8.7	14.4
1,2,9,10-tetrachlorodecane	3.3	5.0	5.5
1,2,5,6,9,10-hexachlorodecane	46.2	45.0	46.5
1,2,10,11-tetrachloroundecane	22.5	20.2	10.3
1,12-dichlorododecane	16.0	8.5	9.0

Table 3.8: Hydrolysis half- lives of PCA isomers at 30°C.

Isomer	Hydrolysis half- lives (d)		
	pH 4	pH 7	pH 9
1,10-dichlorodecane	5.1	13.0	6.8
1,2,9,10-tetrachlorodecane	2.9	3.2	2.9
1,2,5,6,9,10-hexachlorodecane	43.0	40.0	44.0
1,2,10,11-tetrachloroundecane	17.7	11.9	12.6
1,12-dichlorododecane	11.8	9.3	7.8

The data for the lowest chlorinated isomer (D_2C_{10}) do not show a clear trend. Hydrolysis rates appear to decrease with increasing carbon chain length; for example, half-lives of tetrachlorinated congeners increased from 19.5 to 28.9 d for T_4C_{10} to T_4C_{11} at pH 4 and at 15°C. This trend is again not apparent for the lower chlorinated congeners (D_2C_{10} and D_2C_{12}). In general increasing temperature resulted in expected increases in hydrolysis rates. For example, the half-lives of tetrachloroundecane (T_4C_{11}) decreased from 25.3 to 20.2 d with an increase in temperature from 15 to 20°C at pH 7. In general hydrolysis rates increased with increasing pH; suggesting the importance of nucleophilic attack by OH^- in a base-catalyzed hydrolysis [56]. This trend, which was not obvious for the lower chlorinated decanes, requires further study.

3.2.3. Hydrolysis of PCA mixtures

The hydrolytic reactivities of a series of PCA mixtures (C_{10}, C_{11}, C_{12} and C_{13}) were studied at pH 9 and a temperature of 15°C. The hydrolysis of the chlorinated decane (C_{10}) mixture containing Cl_5 to Cl_8 congener groups was extended to pH 4 and 7. Hydrolysis half-lives of the chlorinated decanes generally increased with chlorine number (see Table 3.9) in acidic and neutral media. For example, half-lives increased from 70.5 to 78.6 d at pH 7 as chlorine number increased from Cl_5 to Cl_8 (see Figure 3.2). A similar trend was noted at pH 4. Little variation in hydrolysis rates was observed at pH 9, possibly due to the high concentrations of OH^-. Hydrolysis rates of higher chlorinated decanes (Cl_7 and Cl_8) increased with increased basicity indicating the importance of base-catalyzed hydrolysis. The hydrolysis half-lives of the $C_{10}Cl_8$ congener group decreased from 81.4 d at pH 4 to 73.5 d at pH 9. Hydrolysis rates of the lower chlorinated decanes (Cl_5 and Cl_6) showed little variation with pH.

Table 3.9: Hydrolysis half-lives (d) of the congener groups in the chlorinated decane (C_{10}) mixture as a function of pH at 15°C.

Group/pH	pH 4	pH 7	pH 9
Cl5	74.2	70.5	72.2
Cl6	75.4	73.4	75.3
Cl7	79.7	75.2	74.5
Cl8	81.4	78.6	73.5

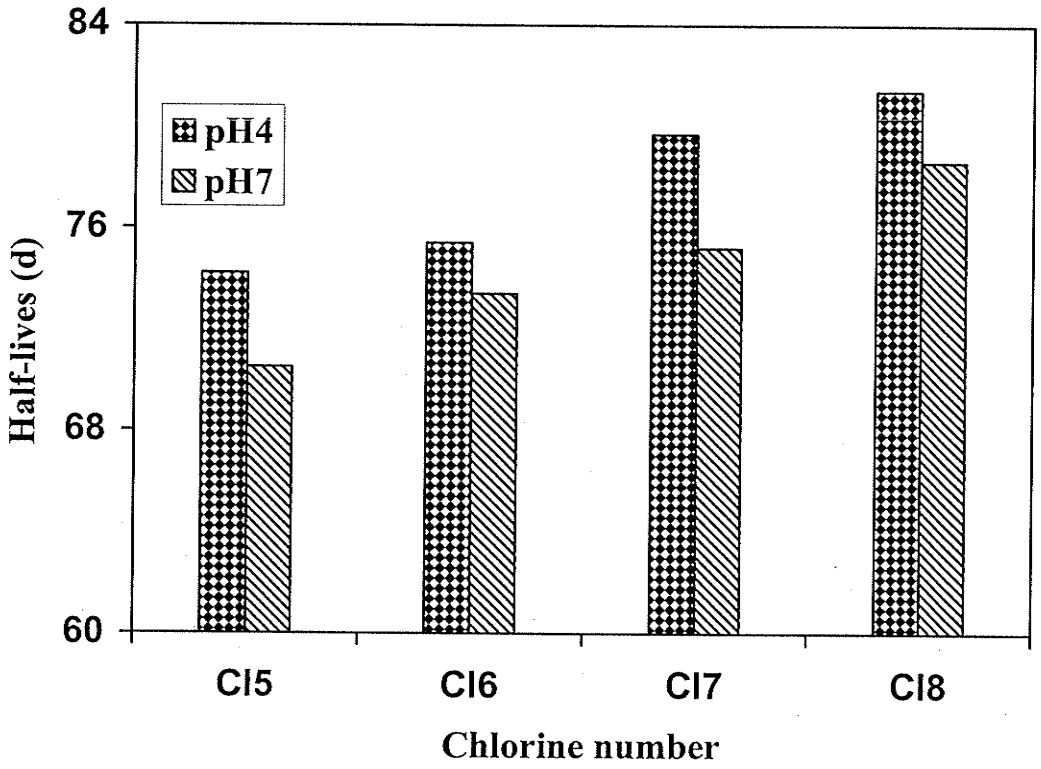

Figure 3.2: Hydrolysis half-lives (d) of the congener groups in the chlorinated decane (C_{10}) mixture at acidic and neutral pH at 15°C.

The hydrolysis half-lives of all of the PCA mixtures (C_{10}, C_{11}, C_{12} and C_{13}) are summarized in Table 3.10. Generally, the hydrolysis rates of the congener groups decreased with increasing carbon chain length. Figure 3.3 illustrates this trend for the Cl_7 congener group, with an overall increase in the hydrolysis half-life from 74.5 to 110.5 d as the carbon chain length increased from the decane (C_{10}) to the tridecane (C_{13}). Trends with respect to chlorine number are not clear.

3.2.4. Photolysis of PCA Isomers

PCA isomers underwent slow photolysis at pH 9 and at 38°C in both Milli-Q water and water from Lake Winnipeg with photolysis half-lives ranging from 5 to 12 d (see Table 3.11). Photolysis rates decreased with increasing chlorine number from Cl_2 to Cl_6 for the chlorinated decanes in both Milli-Q and Lake Winnipeg water. The transformation rate decreased moderately with increasing carbon chain length in both types of water. For example, photolysis half-lives of 7.2 and 8.8 d were observed for T_4C_{10} and T_4C_{11}, respectively in Lake Winnipeg water. The transformation rate of all PCA isomers is somewhat enhanced in natural water, likely due to the presence of natural sensitizers in the lake water.

3.2.5. Photolysis of PCA Mixtures

The PCA mixtures degraded slowly in pure water with half-lives ranging from 22 to 33 d (see Table 3.12). In general, a tendency of decreased photolysis rates with increasing chlorine number and carbon chain length is observed, although there are anomalies. For example, increasing carbon chain length from C_{10} to C_{13} resulted in an increase the photolysis half-life from 23.1 to 32.1 d for the Cl_7 congener group (see

Table 3.10: Hydrolysis half-lives (d) of PCA mixtures at pH 9 and at 15°C.

Isomer/Mixture	C_{10}	C_{11}	C_{12}	C_{13}
Cl_5	72.2 ± 1.6	85.4 ± 2.1	84.6 ± 1.1	89.5 ± 0.95
Cl_6	75.3 ± 1.2	91.1 ± 1.9	92.2 ± 0.78	95.2 ± 0.65
Cl_7	74.5 ± 1.3	86.3 ± 1.5	98.2 ± 1.7	110.5 ± 2.4
Cl_8	73.5 ± 0.97	88.5 ± 1.6	96.9 ± 1.1	105.4 ± 1.9

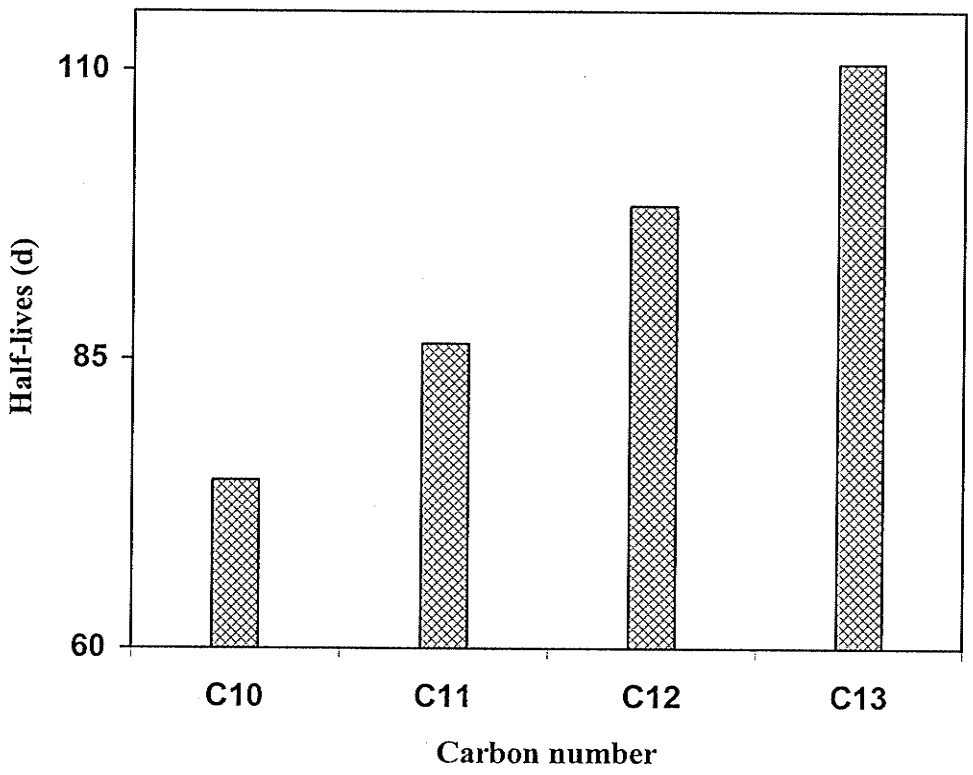

Figure 3.3: Hydrolysis half-lives of the heptachlorodecane (Cl_7) mixtures with different carbon chain lengths (C_{10} to C_{13}) at pH 9 and 15°C.

Table 3.11: Photolysis half-lives (d) of PCA isomers at pH 9 and at 38°C in lake water and pure water.

Isomer	Lake Winnipeg	Milli-Q Water
1,10-dichlorodecane	5.0 ± 0.35	5.4 ± 0.16
1,2,9,10-tetrachlorodecane	7.2 ± 0.25	7.7 ± 0.57
1,2,5,6,9,10-hexachlorodecane	10.3 ± 0.43	11.5 ± 0.27
1,2,10,11-tetrachloroundecane	8.7 ± 0.17	8.9 ± 0.13
1,12-dichlorododecane	6.2 ± 0.22	6.8 ± 0.15

Table 3.12: Aqueous photolysis half-lives (d) of PCA mixtures at pH 9 and at 38°C in Milli-Q water.

Isomer/Mixture	C_{10}	C_{11}	C_{12}	C_{13}
Cl5	22.0	24.1	23.1	22.4
Cl6	24.7	27.5	25.3	26.7
Cl7	23.1	30.4	31.4	32.1
Cl8	22.4	29.2	30.7	32.8

Figure 3.4). Increasing chlorine number from Cl_5 to Cl_8 increased the half-life of the chlorinated tridecanes from 22.4 to 32.8 d.

Photolysis rates of PCA mixtures were greater in Lake 375 water than in Milli-Q water. This is again attributed to indirect photolysis due to the presence of sensitizers in natural water. The effects of chlorine number and carbon chain length were similar to those observed in pure water (see Table 3.13). For example, increasing carbon chain length from C_{10} to C_{13} resulted in an increase the photolysis half-life from 20.7 to 23.7 d for the Cl_6 congener group. Increasing chlorine number from Cl_5 to Cl_8 increased the half-life of the chlorinated tridecanes from 22.1 to 26.9 d.

3.3. Conclusions

The hydrolysis half-lives ranged from 17 to 49 d for the PCA isomers and from 72 to 111 d for the PCA mixtures at 15°C. The slower hydrolysis for the mixtures is attributed to the presence of higher chlorinated congeners. Hydrolysis rates tended to decrease with increasing carbon chain length and chlorine number. In general increasing temperature resulted in expected increases in hydrolysis rates. Hydrolysis rates appeared to increase with increasing pH; suggesting the importance of nucleophilic attack by OH^- in a base-catalyzed hydrolysis [56].

The photolysis half-lives of the PCA isomers did not vary significantly between pure and natural water with half-lives in the 5 to 12 d range. For the PCA mixtures photodegradation rates were somewhat enhanced in natural water with half-lives of 20 to 27 d compared to 22 to 33 d in pure water. In general, the photolysis rates decreased with increasing chlorine number and carbon chain length.

Short chain PCAs are widespread environmental contaminants, which have been detected in both surface water and biota [10-11]. The relatively slow rates of hydrolysis and

photolysis determined in this study suggest that short chain PCAs are relatively persistent, accounting for their occurrence in remote locations in the environment. Effective methods must be developed for the remediation of water contaminated with PCAs. Advanced oxidation processes (AOPs) have been tested on most organic contaminants with encouraging results. Two different AOPs involving both homogeneous and heterogeneous photodegradation will be discussed for the degradation of short chain PCAs in the next chapters.

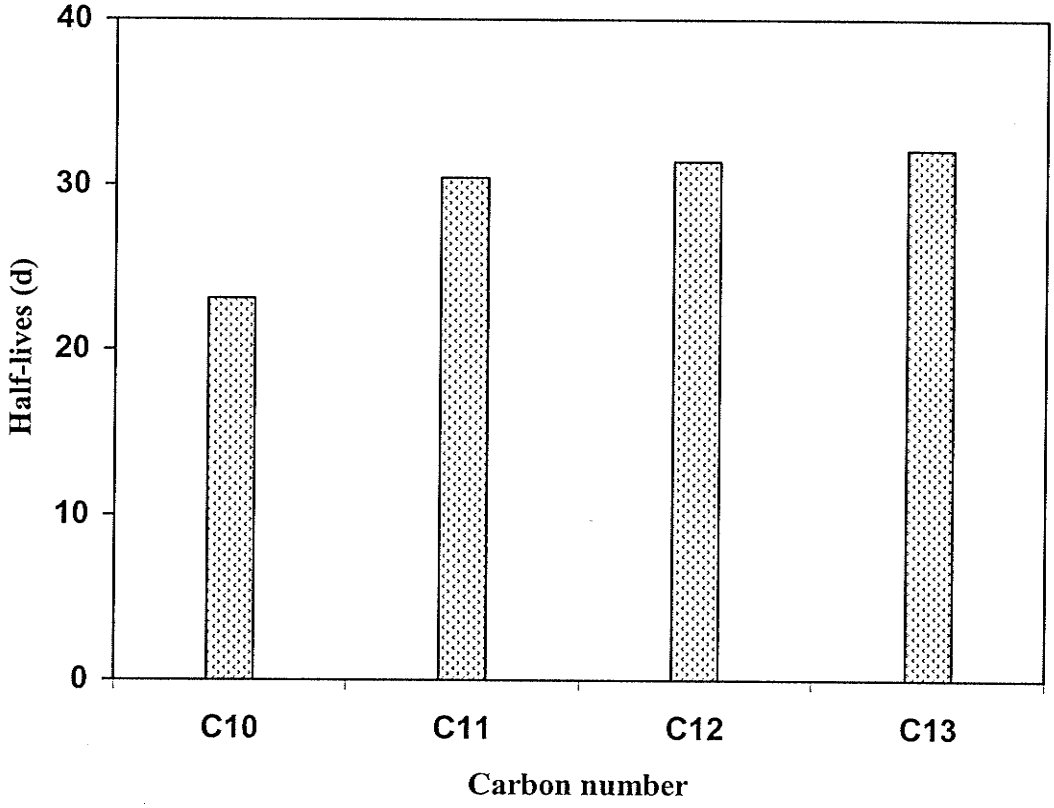

Figure 3.4: Photolysis half-lives of PCA mixtures as a function of carbon chain length at pH 9 and at 38°C in Milli-Q water.

Table 3.13: Aqueous photolysis half-lives (d) of PCA mixtures in Lake 375 at pH 9 and at 38°C.

Isomer/Mixture	C_{10}	C_{11}	C_{12}	C_{13}
Cl5	19.5 ± 0.95	21.1 ± 0.76	22.2 ± 0.88	22.1 ± 0.60
Cl6	20.7 ± 1.1	22.5 ± 0.97	22.8 ± 1.3	23.7 ± 0.8
Cl7	21.2 ± 0.87	25.4 ± 0.69	26.2 ± 1.1	24.1 ± 0.99
Cl8	21.0 ± 1.2	25.2 ± 0.66	26.5± 0.86	26.9 ± 0.75

Chapter 4

Homogeneous Photodegradation of Polychlorinated *n*-Alkanes using H_2O_2/UV and photo-Fenton Reaction

4.0. Introduction

Homogeneous photodegradation is one of the advanced oxidation processes used for the oxidation of persistent organic contaminants in water [82]. In this process the oxidant absorbs UV light initiating reactions that generate hydroxyl radicals ($^{\bullet}OH$), which are capable of oxidizing most organic pollutants [83-84]. The most important oxidants used in this process are ozone (O_3), hydrogen peroxide (H_2O_2) and Fenton's reagent (Fe/H_2O_2).

The production of $^{\bullet}OH$ radicals from H_2O_2 in the presence of UV light (below 360 nm) is relatively efficient with an overall quantum yield of 0.5 in aqueous solutions [116]. The H_2O_2/UV process has been used as a method of oxidative degradation of most organic pollutants during the last few decades [119]. The efficiency of $^{\bullet}OH$ radical production may be enhanced by irradiation of aqueous solutions of H_2O_2 containing iron salts [131]. In these photo-Fenton ($Fe^{2+}/H_2O_2/UV$) or modified photo-Fenton ($Fe^{3+}/H_2O_2/UV$) systems the contribution of multiple reactions including photolysis of H_2O_2, photolysis of Fe^{+3} and reaction of H_2O_2 with Fe^{+2} enhances the generation of $^{\bullet}OH$ radicals. To avoid artifacts that can result from locally high concentrations of the Fe^{+2}, the modified photo-Fenton reaction generates Fe^{2+} from Fe^{3+} *in situ* [151]. Both photo-Fenton and modified photo-Fenton reactions play an important role in the degradation of a wide variety of organic pollutants [152-157].

The objectives of this investigation are to determine the effectiveness of both H_2O_2/UV and photo-Fenton conditions for the oxidation of polychlorinated *n*-alkanes (PCAs) in aqueous solutions.

4.1. Experimental

4.1.1. Reagents

Individual PCA isomers were either available from Aldrich (D_2C_{10} and D_2C_{12}) or synthesized in the laboratory (T_4C_{10}, H_6C_{10} and T_4C_{11}) as described in Chapter 2. PCA mixtures, chlorinated decanes (C_{10}), undecanes (C_{11}), dodecanes (C_{12}) and tridecanes (C_{13}) were synthesized as described in Chapter 2. Hydrogen peroxide solutions were prepared by diluting 30 wt.% H_2O_2 (BDH) with Milli-Q purity and natural water to the desired concentration. DMP (2,9-dimethyl-1,10-phenanthroline) (Sigma Chemical), 0.01 M $CuSO_4$ $5H_2O$ (BDH) and phosphate buffer (prepared with K_2HPO_4 and NaH_2PO_4 and adjusted to pH 7 with 0.05 M H_2SO_4 and 1.0 M NaOH) were used in the spectrophotometric determination of H_2O_2. DMP reagent was dissolved in 100 mL of 95% ethanol, placed in a 100 mL flask wrapped with aluminum foil and refrigerated. Radical scavengers KI (BDH) and *t*-butyl alcohol (Mallinckrodt) and $NaClO_4$ as ionic strength adjuster (BDH) were used as received. Reagent grade iron salts, $Fe(ClO_4)_3$ $9H_2O$, $Fe(ClO_4)_2$ $6H_2O$ used in preparation of the Fenton reagent were supplied by Aldrich Chemical Co. All organic solvents used including hexane and dichloromethane were HPLC grade.

4.1.2. Sample Irradiation

The homogeneous photodegradation of PCAs was investigated in aqueous solutions of H_2O_2 alone and in aqueous solutions under Fenton conditions ($1x\ 10^{-3}$ M Fe and $1x10^{-2}$ M H_2O_2). In experiments with H_2O_2, aqueous solutions of PCA isomers (250 μg/L) and 1.0×10^{-2} M H_2O_2 were prepared in Milli-Q water and natural water. In studies of PCA mixtures (250 μg/L) in both Milli-Q and natural water, 2.0×10^{-2} M H_2O_2 was used. Experiments with Fenton and modified Fenton reactions were performed using $Fe(ClO_4)_2$ and $Fe(ClO_4)_3$ as sources of Fe(II) and Fe(III), respectively.

All photolytic experiments were performed using a Rayonet Photochemical reactor equipped with a carousel and 16 RPR 300 nm UV lamps emitting abroad band centered at 300 nm (Figure 4.1) with an intensity of 3.6×10^{-5} $EinL^{-1}min^{-1}$ as established by ferrioxalate actinometry. To avoid exceeding the water solubility of PCAs (Table 1.1) [15], concentrations of aqueous solutions did not exceed 250 μg/L. Three sources of natural water were utilized in photodegradation studies including bog water (pH 8.6) and lake water from Lake Winnipeg (pH 8.3) and from Lake 375 of the Experimental Lakes Area near Kenora, ON (pH 6.8). Perchloric acid ($HClO_4$) was used to adjust pH to 2.8 (the optimum pH of the Fenton reaction) in experiments with Milli-Q water, and to adjust the pH of natural water in investigation of the effect of pH on the photodegradation process.

4.1.3. Fenton and Modified Fenton Reactions

Stock solutions of ferrous and ferric perchlorate (1 mM) were prepared daily in acidic solution of perchloric acid ($HClO_4$) to prevent the maturation of monomeric Fe(III) species to polymeric Fe(III) species [111]. The perchlorate salts were

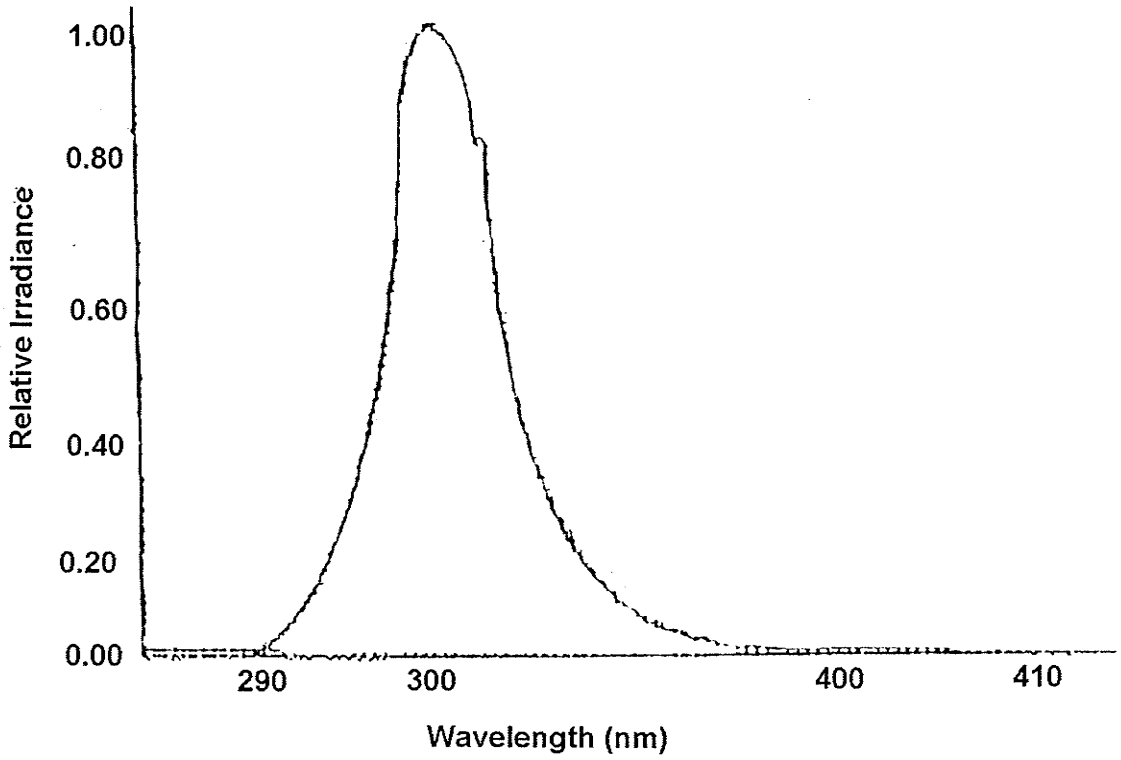

Figure 4.1: Spectrum of emission from 300 nm lamps used in the Rayonet RPR Photochemical Reactor.

chosen in this study to avoid metal ion complexation, light absorption and chemical and photochemical reactions involving the counter ion [112]. Sodium perchlorate (100 mM) was added to the solutions to keep the ionic strength constant. Photolysis reactions of PCAs were initiated by adding H_2O_2 and after stirring (to keep the solution homogeneous and well-aerated), the iron solutions were added in quick succession. The pH was then adjusted with $HClO_4$ and/or NaOH and the samples were subjected to irradiation in the photoreactor. Samples were collected at various times and analyzed for PCAs, H_2O_2 and Fe ions.

4.1.4. Control Experiments

Dark control experiments (with tubes wrapped with aluminum foil) were carried out under Fenton and modified Fenton conditions in order to ascertain whether PCAs degraded in the absence of light. Another control without H_2O_2 was used to assess the extent of direct and indirect photolysis of PCAs.

4.1.5. Hydroxyl Radical Scavenging

Different $^{\bullet}OH$ radical scavengers were used to prove its role as a primary oxidant for the degradation of PCAs in the presence of H_2O_2 and photo-Fenton systems. Experiments were performed in the presence of 10 mM iodide (I^-) ion (KI) and 10 mM tert-butyl alcohol as well-known $^{\bullet}OH$ radical scavengers.

4.1.6. Determination of Reaction Kinetics

The photoreactor lamps were turned on at least 10 min in advance to insure constant output. Normally duplicate solutions (40 mL) were simultaneously irradiated in the photoreactor and removed at intervals for analysis. In experiments with aqueous

hydrogen peroxide, samples were typically removed after irradiation times of 0, 10, 20, 30, 40,50, 60, 90, 120 and 180 min. In experiments with Fenton conditions samples were typically removed after 0, 10, 20, 30, 40, 50, 60, 75 and 90 min. For the analysis of PCAs, the samples were removed from the photoreactor and mixed immediately with 1 mL of *tert*-butyl alcohol to prevent production of further $^{\bullet}OH$ radicals prior to analysis. In all cases PCA samples were transferred to a 125-mL separatory funnel and extracted (liquid-liquid extraction) immediately with (85:15) hexane:dichloromethane.

In liquid-liquid extraction slow inversion of samples proceeded for 30 minutes, and then the organic layer was transferred to 100 mL round bottom flasks containing 2 mL hexane spiked with 10 $ng\mu L^{-1}$lindane. Lindane was used as an internal standard to correct for any losses during subsequent transfer or evaporation and to correct for differences in injection volumes. After extraction, solutions were evaporated and concentrated to 300 μL by a gentle stream of nitrogen gas. After concentration, samples were transferred to 0.15 mL glass inserts placed inside a 2 mL sample vial and prepared for analysis as described previously.

The rate of disappearance of PCAs was determined by monitoring the concentration of PCAs after each irradiation time using HP GC/MSD in EI and NCI modes for isomers and mixtures, respectively. Negative chemical ionization (NCI), in selected ion monitoring (SIM) mode with methane as the moderating gas and ion source temperature 150°C was used for analysis. The column temperature program and SIM ions were described in Chapter 2.

Plots of ln [PCAs] versus time were typically linear with high correlation coefficients, suggesting that the homogeneous photodegradation of PCAs followed

a first-order process expressed by:

$$-\frac{d[PCA]}{dt} = k\,[PCA] \qquad (4\text{-}3)$$

where k is the observed first-order rate constant (min^{-1}) for overall photodegradation, [PCA] is the concentration of PCA at irradiation time t. First-order photodegradation half-lives are calculated from:

$$t_{1/2} = \frac{\ln 2}{k} \qquad (4\text{-}4)$$

4.2. Analytical Methods

4.2.1. Chemical Actinometry

Chemical actinometry requires a solution that undergoes a chemical change (such as a redox reaction) with a known quantum yield. Ferrioxalate actinometry is a classical method [257] used to determine the intensity of UV radiation emitted by the source of irradiation. In acidified solutions ferric ion (Fe^{+3}) is reduced to ferrous ion (Fe^{+2}) by UV light following first-order kinetics. The sequence of this reaction is shown below:

$$[Fe(C_2O_4)_3]^{-3} + H_3O^+ \longrightarrow [Fe(C_2O_4)_3]^+ + C(C_2O_4)^{-2} \qquad (4\text{-}5)$$

$$[Fe(C_2O_4)_3]^+ \xrightarrow{h\nu} Fe^{+2} + (C_2O_4)^- \qquad (4\text{-}6)$$

$$(C_2O_4)^- + [Fe(C_2O_4)_3]^+ \longrightarrow 2CO_2 + Fe^{+2} + (C_2O_4)^{-2} \qquad (4\text{-}7)$$

Free ferrous ions (Fe^{+2}) form a complex with 1,10-phenanthroline which is detected by measuring the absorbance at 510 nm.

Potassium ferrioxalate, $K_3Fe(C_2O_4)_3\ 3H_2O$, was prepared by the procedure described by Hatchard and Parker (1956) [257] by mixing 1.5 M ferric chloride and 1.5 M potassium oxalate in a 1:3 volume ratio. Solutions were mixed with vigorous stirring

and recrystallized from warm water two times. The resulting crystals, green in color, were stored in the dark at room temperature. A 6 mM solution was prepared by dissolving the appropriate amount of ferrioxalate in 0.1 N H_2SO_4, following which 20 mL was irradiated in the photoreactor.

Analysis consisted of removing a 4 mL aliquot of the ferrioxalate solution (which was now faint green to colorless) following irradiation at 0,15, 25, 30, 35, and 40 sec adding 1 mL of 0.1% 1,10-phenanthroline, 2 mL of a 0.6 M sodium acetate buffer and diluting to 20 mL with Milli Q water. The mixture was allowed to stand in the dark for thirty min. The absorbance of the phenanthroline-Fe^{2+} complex was measured at 510 nm and the concentration of Fe^{+2} was determined using a standard calibration curve (see Figure 4.2). A background solution was prepared for each set of trials consisting of the same volume of solution but without ferrioxalate. This solution, prepared by adding 1,10-phenanthroline and the buffer to 0.1 N H_2SO_4 and diluting to 20 mL with water, served as a reference in absorbance measurements.

The total output of UV light emitted by the photoreactor was calculated according to [257]:

$$I_{\lambda o} = \frac{k_P}{(2.303)\,(\Phi_p)\,(\varepsilon_{p\lambda})\,(l)} \qquad (4\text{-}8)$$

where $I_{\lambda o}$ represents the intensity of the incident light, k_p is the first-order rate constant for the reduction of Fe^{3+} to Fe^{2+}, Φ_p is the quantum yield of the reaction (1.22 mol/Ein) [257], $\varepsilon_{p\lambda}$ is the molar absorptivity of ferrioxalate (1.11 x 10^{-4} L/mol.cm) and l is the path length of the tube used in the photolysis experiments (2.476 cm as determined with caliper measurements). A plot of the concentration of Fe^{+2} (from Figure 4.2) versus the

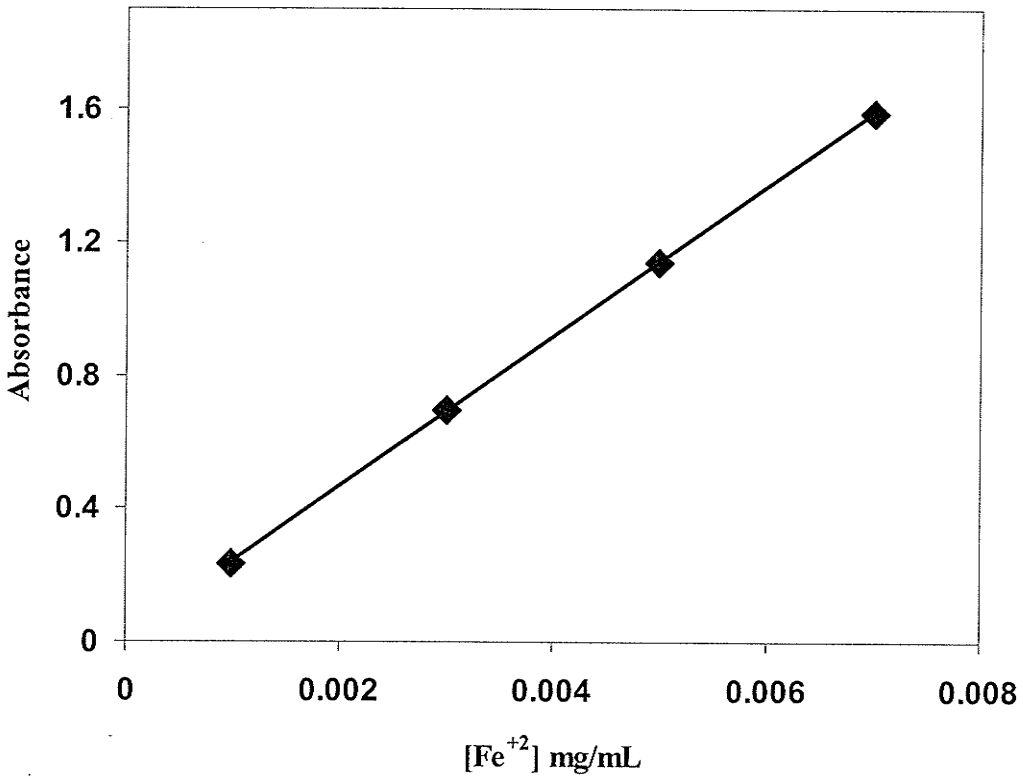

Figure 4.2: Calibration Curve for spectrophotometric determination of Fe^{+2} during the determination of UV light intensity by Ferrioxalate actinometry.

exposure time yielded the first-order rate constant (k_p) of 0.0464 s^{-1} for the actinometer, providing a UV light intensity of 3.6 x 10^{-5} $EinL^{-1}min^{-1}$ (equation 4-8).

4.2.2. Determination of Hydrogen Peroxide Concentration

The concentration of hydrogen peroxide was determined spectrophotometrically by using copper (II) and the 2,9-dimethyl-1,10-phenanthroline (DMP) method with absorbance measurements at 454 nm [258]. In this method Cu^{2+} is reduced by H_2O_2 in the presence of DMP forming $CU(DMP)^{+}_2$ complex:

$$2\ Cu^{2+} + 4\ DMP \longrightarrow 2\ Cu(DMP)^{+}_2 + O_2 + 2H^{+} \qquad (4\text{-}1)$$

The $Cu(DMP)^{+}_2$ complex is stable and absorbs strongly at 454 nm. A series of solutions containing different concentrations of H_2O_2 were used to establish the calibration curve. Five mL aliquots of H_2O_2 were added to 10 mL volumetric flasks containing 1 mL each of DMP, Cu^{2+} and phosphate buffer (pH 7) solutions. Solutions were diluted to volume with Milli Q water and the absorbance was measured at 454 nm. The slope of the calibration curve was used to determine the molar concentrations of H_2O_2 in the irradiated samples according to the following equation:

$$\Delta A_{454} = \varepsilon [H_2O_2] x \frac{V}{10} \qquad (4\text{-}2)$$

where, ΔA_{454} is the difference in the absorbance between the sample and the blank solution, V is the sample volume (mL) and ε is the slope of the calibration curve (M^{-1} cm^{-1}). Spectrophotometric measurements were performed with a Hewlett-Packard 8450A diode array spectrophotometer using a quartz cell of path length 1.0 cm.

4.2.3. Determination of Fe^{+2}

In experiments using modified photo-Fenton conditions ($H_2O_2/Fe^{+3}/UV$), Fe^{+3} produces Fe^{+2} during the photodegradation reaction (see equation 1-65). Samples were removed from the photoreactor and spiked with 1 mL of 0.1% 1,10-phenanthroline and 2 mL of a 0.6 M sodium acetate buffer to form phenanthroline-Fe^{2+} complex. The concentration of Fe^{+2} was determined spectrophotometrically using same Hewlett-Packard 8450A diode array spectrophotometer with a quartz cell of path length 1.0 cm at 510 nm wavelength and a previously prepared calibration curve.

4.2.4. Determination of Chloride Ion (Cl^-)

Two methods have used for determining chloride ion in solutions of both PCA isomers and mixtures. Chloride ion (Cl^-) released from PCA isomers during the photodegradation reaction was measured potentiometrically using an Orion 96-17B chloride selective electrode calibrated with NaCl standards. In order to reach a detectable concentration of Cl^- 1 L solutions were concentrated by rotary evaporation, adjusted to a volume of 5 mL, followed by addition of 2 mL of Orion ISA reagent prior to measurement. A Shimadzu LC- 10AD Liquid Chromatograph equipped with an auto-sampler, a conductivity detector and an anion-exchange column with a substituted styrene-divinylbenzene polymer stationary phase containing a quaternary amine ligand was used to determine chloride ion in experiments with PCA mixtures. This amine functional group separates anions (i.e. Cl^-, and SO_4^{2-}).

4.2.5. Determination of Dissolved Organic Carbon (TOC)

A model 700 TOC Analyzer (O.I. Corporation) equipped with an auto-sampler based on a 1.0 mL sample loop was used for TOC analysis. Samples were acidified with phosphoric acid and sparged with carbon free nitrogen to remove inorganic carbon. The

samples were then heated (100°C) and treated with potassium persulphate to oxidize DOC to CO_2 over the course of a 6-min digestion. CO_2 is stripped from the sample with carbon free nitrogen and trapped on a Molecular Sieve column at ambient temperature. At the completion of sample digestion, the column is heated to 200°C releasing the CO_2 which is quantified by infra-red (IR) detection.

4.3. Results and Discussion

4.3.1. Homogeneous Photodegradation of PCA Isomers with H_2O_2/UV

4.3.1.1. Effect of Hydrogen Peroxide Concentration

Although the photolysis of H_2O_2 is the main process to generate hydroxyl radicals ($^{\bullet}OH$), equation (1-52), H_2O_2 in high concentration can act as a self-scavenger of $^{\bullet}OH$ radicals [259-260] as shown in equation (1-60). On the other hand, very low concentrations of H_2O_2 will result in low concentrations of $^{\bullet}OH$ radicals which may slow the degradation of the organic substrate. The key is to utilize an optimum concentration of H_2O_2. Aqueous solutions of T_4C_{10} absorb very small amounts of UV light, hence direct photolysis of T_4C_{10} was minimal as expected. However, T_4C_{10} degradation was sensitized by the presence of hydrogen peroxide due to the favorable absorption spectrum of H_2O_2. The direct photolysis of H_2O_2 generates $^{\bullet}OH$ radicals according to equation (1-52). Hydroxyl radicals are known to react with saturated organic chemicals by H-abstraction from alkyl or hydroxy groups [261] or by an electron-transfer process [262]:

$$^{\bullet}OH + RH \longrightarrow R^{\bullet} + H_2O \qquad (4\text{-}9)$$

$$^{\bullet}OH + RH \longrightarrow [RH]^{+\bullet} + OH^{-} \qquad (4\text{-}10)$$

The rate of degradation of T_4C_{10} by reaction with $^{\bullet}OH$ radicals was dependent on the concentration of H_2O_2 as illustrated in Figure 4.3. At a pH of 2.8 and in 0.1 M $NaClO_4$ the largest degradation rate was observed with a H_2O_2 concentration of 1.0×10^{-2} M with 60% disappearance of the parent tetrachlorodecane in the first 20 min of photolysis. The rate decreased at lower H_2O_2 concentrations as a smaller fraction of incident light was absorbed, leading to a decrease in the rate of $^{\bullet}OH$ production. At high H_2O_2 (1.5 M) concentrations $^{\bullet}OH$ scavenging by H_2O_2 (equation 1-60) reduced the degradation rate of T_4C_{10}.

$$^{\bullet}OH + H_2O_2 \longrightarrow HO_2^{\bullet} + H_2O \qquad (4\text{-}11)$$

Therefore, in all subsequent experiments an initial H_2O_2 concentration of 1.0×10^{-2} M was used. However, even under these reaction conditions the reaction was incomplete with T_4C_{10} reaching a plateau at 82% disappearance in 40 min possibly due to the depletion of H_2O_2 during the reaction as will be discussed later.

4.3.1.2. Effect of $^{\bullet}OH$ Scavengers

The photodegradation of T_4C_{10} by H_2O_2 was inhibited by the presence of 0.01 M iodide (I^-) ion as illustrated in Figure 4.4. Hydroxyl radicals are known to oxidize iodide [94] according to

$$^{\bullet}OH + I^- \longrightarrow OH^- + I^{\bullet} \qquad (4\text{-}12)$$

This reaction is competitive [263] with T_4C_{10} oxidation hence decreasing the observed rate of degradation of T_4C_{10}. Iodide may also react directly with H_2O_2 to prevent the formation of $^{\bullet}OH$ radicals [264] according to

$$H_2O_2 + 2I^- + 2H^+ \longrightarrow I_2 + 2H_2O \qquad (4\text{-}13)$$

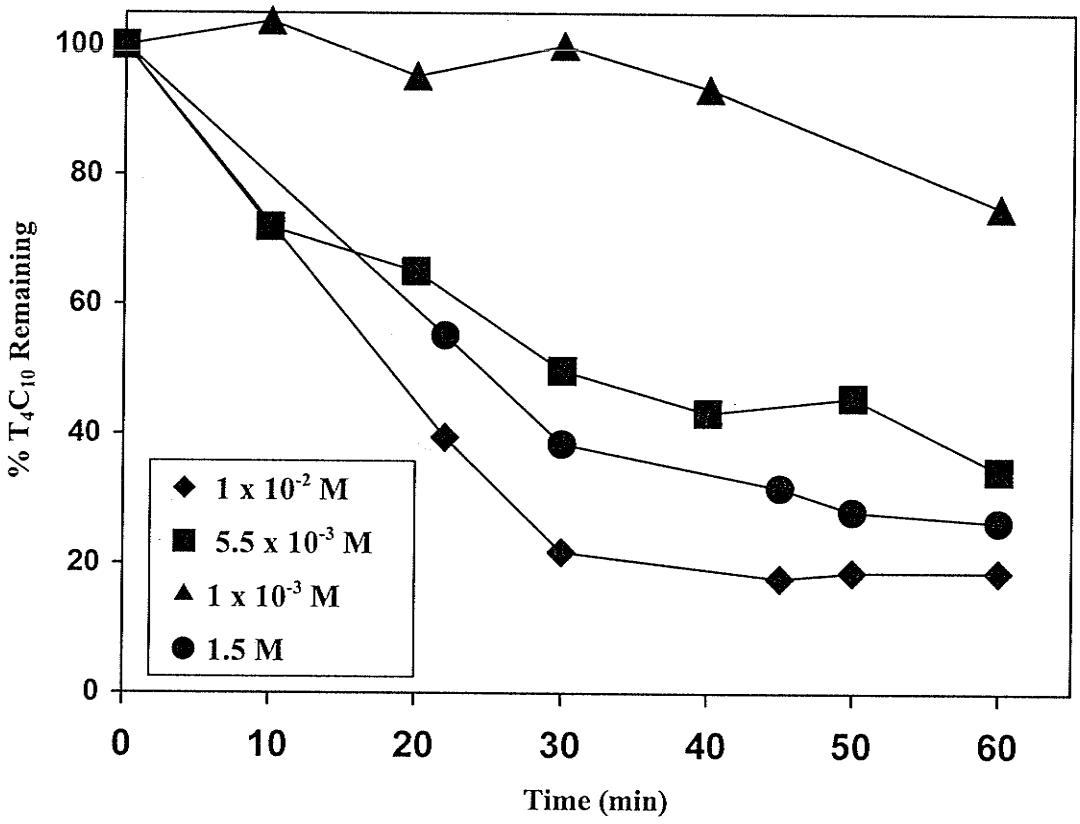

Figure 4.3: Homogeneous photodegradation of 1,2,9,10-tetrachlorodecane (250 μg/L) in 0.1M $NaClO_4$ and pH 2.8 using 300 nm UV with different concentrations of H_2O_2.

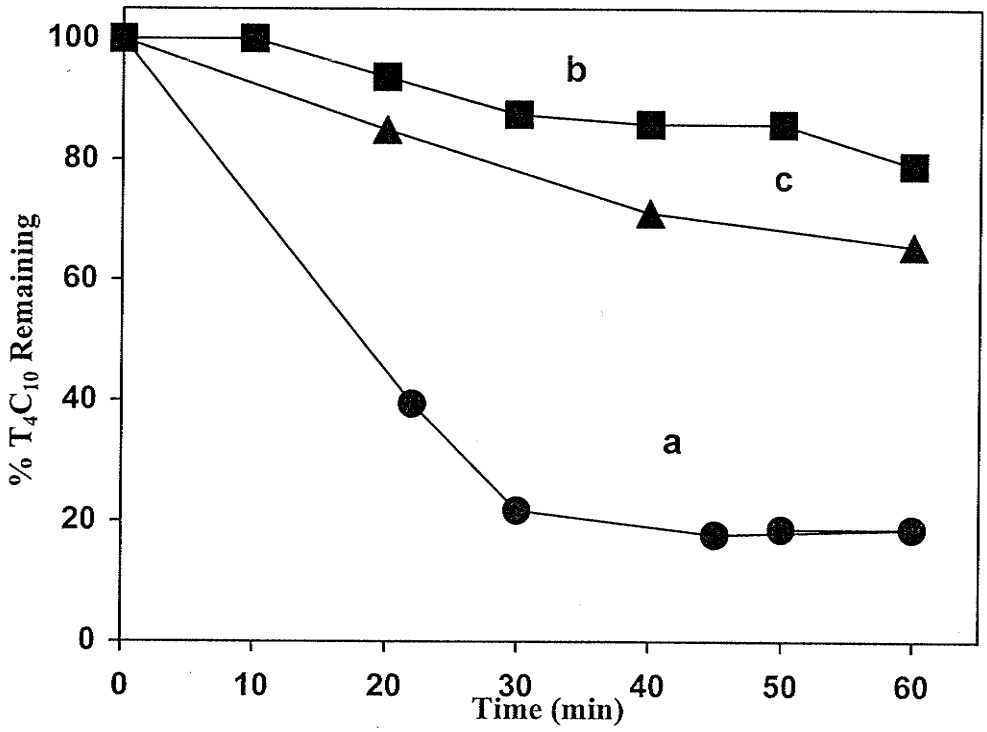

Figure 4.4: Homogeneous photodegradation of 1,2,9,10-tetrachlorodecane (250 μg/L) with 1.0 x 10^{-2} M H_2O_2 in 0.1M $NaClO_4$ and pH 2.8 using 300 nm UV light (a) without added hydroxyl radical scavengers, (b) in the presence of 0.01 M KI and (c) in the presence of 0.10 M *tert*-butyl alcohol.

thereby slowing the rate of oxidation of T_4C_{10}. The degradation of T_4C_{10} was also inhibited by the presence of 0.01 M *tert*-butyl alcohol (Figure 4.4), a well-known $^{\bullet}OH$ radical scavenger [265-266] confirming that the degradation of tetrachlorodecane proceeds by reaction with $^{\bullet}OH$ free radicals.

4.3.1.3. Photodegradation of PCA Isomers in Pure Water

To investigate the homogeneous photodegradation of PCA isomers in pure water experiments were performed in Milli Q water in the presence of H_2O_2 (1×10^{-2} M) at pH 2.8 and an ionic strength of 0.1M $NaClO_4$. The results indicated that photodegradation of PCA isomers (D_2C_{10}, H_6C_{10}, T_4C_{11} and D_2C_{12}) was quite effective; for example, 94 % disappearance of parent 1,10-dichlorodecane in the first 30 minutes (Figure 4.5).

However, increasing chlorine number from Cl_2 to Cl_6 decreased the degradation rate resulting in longer half-lives (Table 4.1); for example, $t_{1/2}$ increased from 9.4 to 24.3 min from D_2C_{10} to H_6C_{10}. As will be discussed later in this Chapter homogeneous photodegradation of PCAs in the presence of H_2O_2 resulted in dechlorination of the parent PCA, with chloride ion released rapidly and quantitatively. Release of chloride ion may inhibit the degradation of PCA isomers with high chlorine number by scavenging of $^{\bullet}OH$ according to [267]:

$$^{\bullet}OH + Cl^- \underset{(1)}{\overset{H^+}{\rightleftharpoons}} HOCl^{\bullet} \underset{(2)}{\rightleftharpoons} Cl^{\bullet} + H_2O \underset{(3)}{\overset{Cl^-}{\rightleftharpoons}} Cl_2^{\bullet-} \qquad (4\text{-}14)$$

Under the above conditions, the photodegradation reactions of chlorinated undecane (T_4C_{11}) and chlorinated dodecane (D_2C_{12}) are shown in Figures 4.6 and 4.7. The results indicate 71% degradation of T_4C_{11} in the first 30 min whereas; disappearance of D_2C_{12} reached 90 % in the same irradiation time. The greatest degradation occurred in

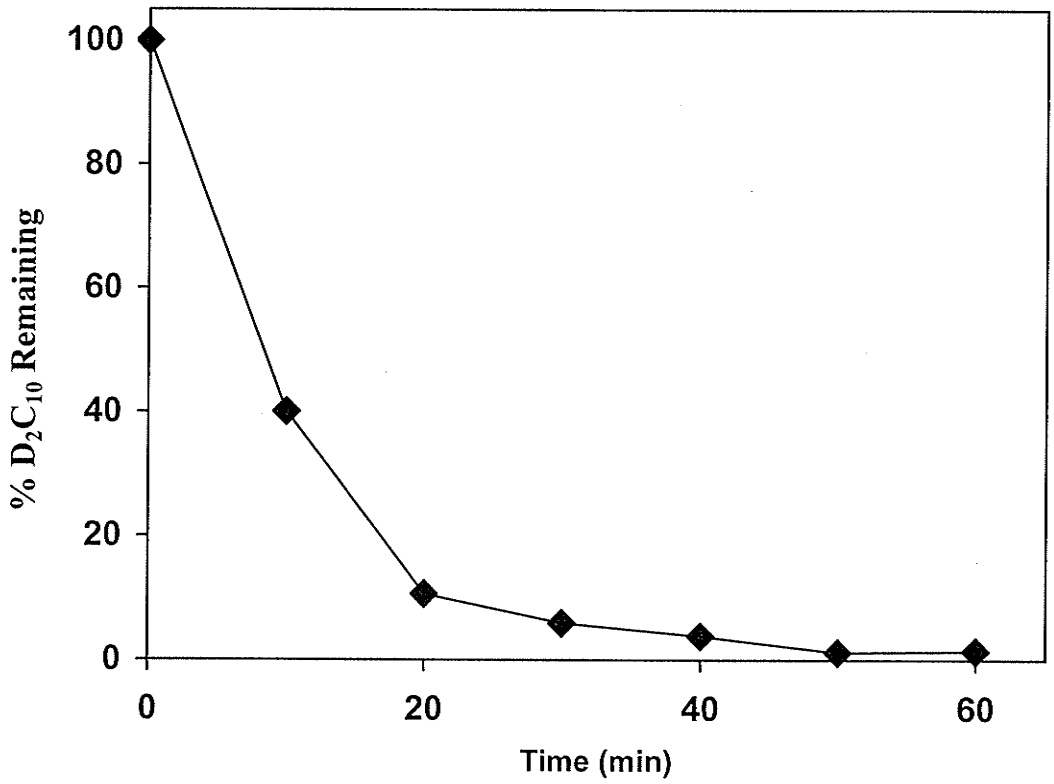

Figure 4.5: Homogeneous photodegradation of 1,10-dichlorodecane (250 μg/L) in Milli Q water in 0.1M $NaClO_4$ and pH 2.8 using 300 nm UV in the presence of 0.01M H_2O_2.

Table 4.1: Observed first-order rate constants and half-lives for the photodegradation of PCA isomers in Milli Q water in the presence of 1.0×10^{-2} M H_2O_2 at pH 2.8, 0.1M $NaClO_4$ and (300nm) UV light.

	D_2C_{10}	T_4C_{10}	H_6C_{10}	T_4C_{11}	D_2C_{12}
k (min^{-1})	0.074	0.042	0.029	0.031	0.059
$t_{1/2}$ (min)	9.4	16.7	24.3	22.4	11.8
R^2	0.948	0.815	0.824	0.942	0.972

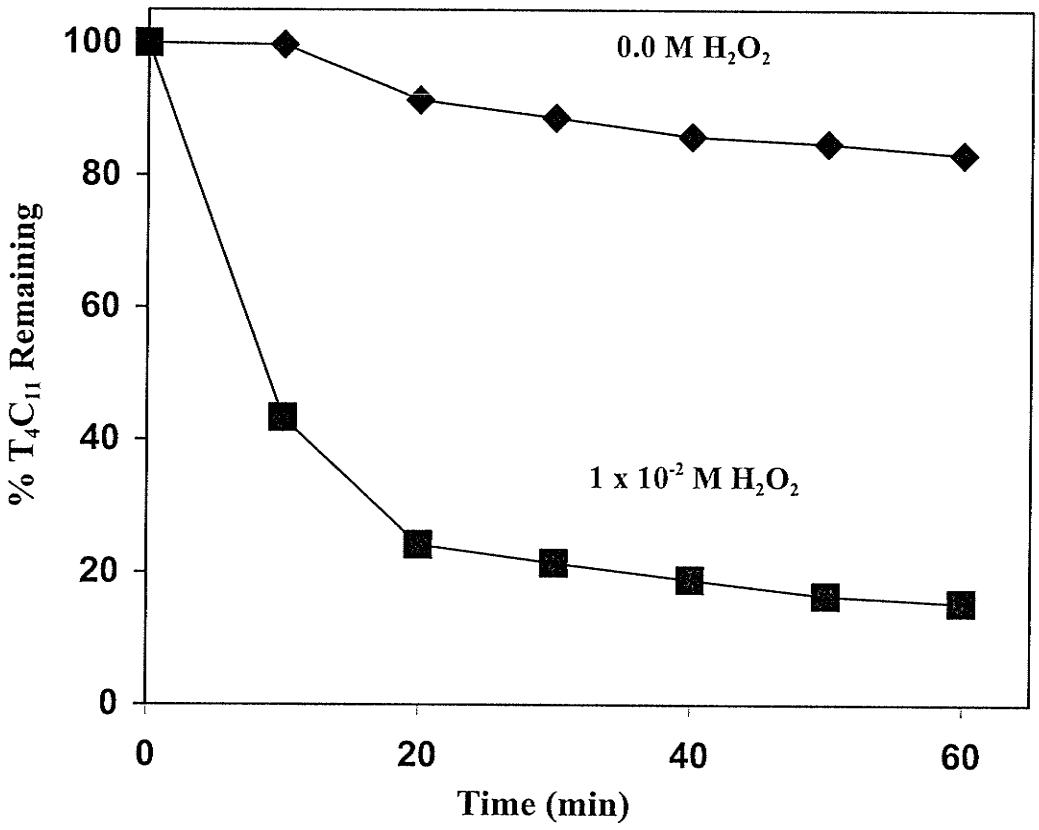

Figure 4.6: Homogeneous photodegradation of 1,2,10,11-tetrachloroundecane (250 µg/L) in Milli Q water in 0.1 M $NaClO_4$ and pH 2.8 using 300 nm UV in the presence of 0.01M H_2O_2.

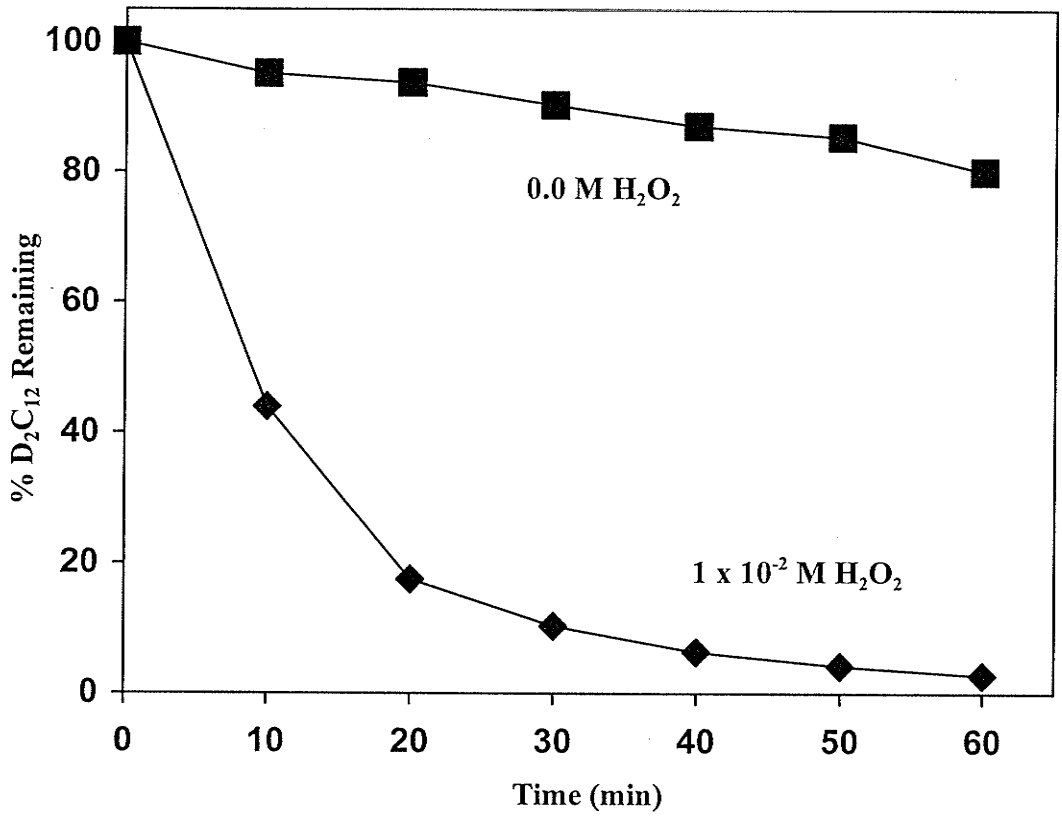

Figure 4.7: Homogeneous photodegradation of 1,12-dichlorododecane (250 μg/L) in Milli Q water in 0.1M $NaClO_4$ and pH 2.8 using 300 nm UV in the presence of 0.01M H_2O_2.

the first 40 min followed by slower reaction in the latter stages of irradiation or stop after about 50 min. This is explained by the consumption of hydrogen peroxide during the photolysis process [242] decreasing the rate of production of $^{\bullet}OH$ radicals.

On the other hand, increasing carbon chain length from C_{10} to C_{11} with four chlorine atoms (T_4C_{10} and T_4C_{11}) (Figure 4.8) resulted in decreased degradation rates, with 79 and 71% transformation of T_4C_{10} and T_4C_{11}, respectively in 30 min. Increasing carbon number from C_{10} to C_{12} (for D_2C_{10} and D_2C_{12} Figure 4.9) was expected to produce a larger decrease in the degradation rate if the carbon chain length has a significant effect. In fact the percent disappearance only decreased from 94 to 90% as the carbon chain length increased from D_2C_{10} to D_2C_{12}, suggesting that chloride scavenging of $^{\bullet}OH$ radicals is largely responsible for the decreased degradation rates.

4.3.1.4. Photodegradation of PCA Isomers in Natural Water

Lake Winnipeg Water. Figure 4.10 shows the first-order rate constants of the photodegradation of the chlorinated decanes, D_2C_{10}, T_4C_{10}, and H_6C_{10} by $1x10^{-2}$ M H_2O_2 in Lake Winnipeg water at its natural pH 8.3. As discussed above scavenging of $^{\bullet}OH$ radicals by chloride ion results in slower degradation with increasing chlorine number (from Cl_2 to Cl_6). The results summarized in Table 4.2, show that the degradation half-lives of chlorinated decanes increased from 14 to 31 min as the chlorine number increased from Cl_2 to Cl_6.

Increasing carbon chain length from C_{10} (D_2C_{10}) to C_{12} (D_2C_{12}) increased half-lives slightly from 14 to 18 min, while $t_{1/2}$ for T_4C_{11} was twice that of T_4C_{10}.

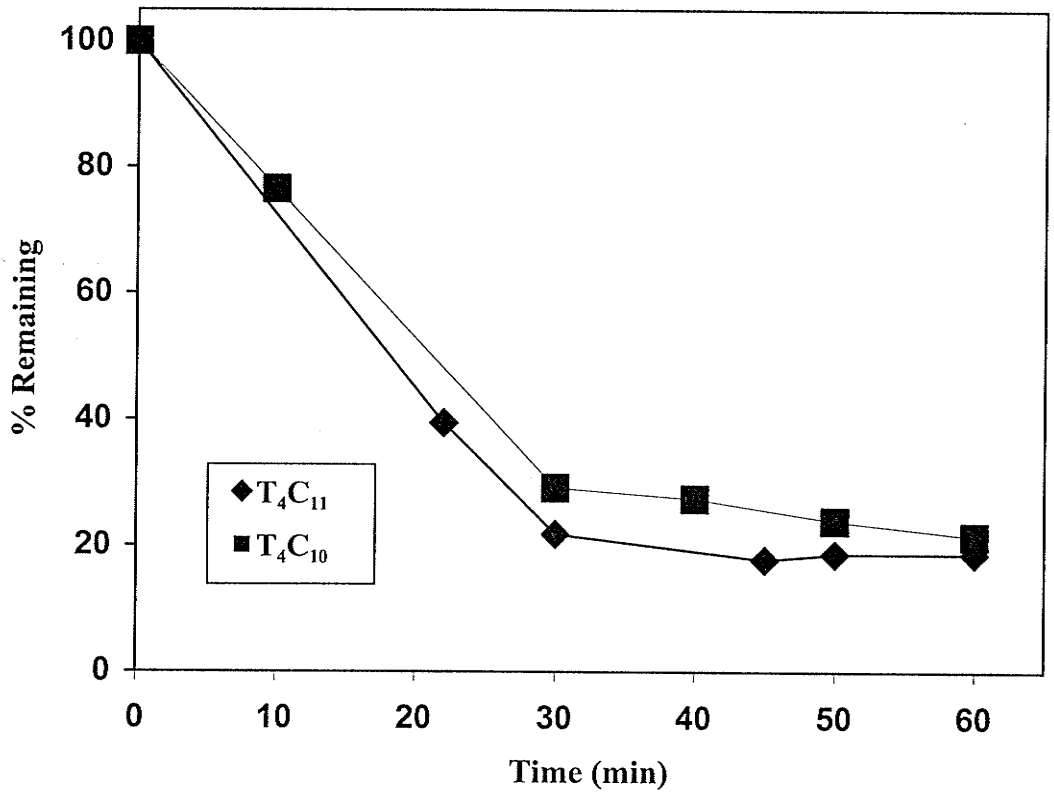

Figure 4.8: Effect of increased carbon chain length (from C_{10} to C_{11}) on the photodegradation of PCAs (250 μg/L) in Milli Q water in 0.1M $NaClO_4$ and pH 2.8 using 300 nm UV in the presence of 0.01M H_2O_2.

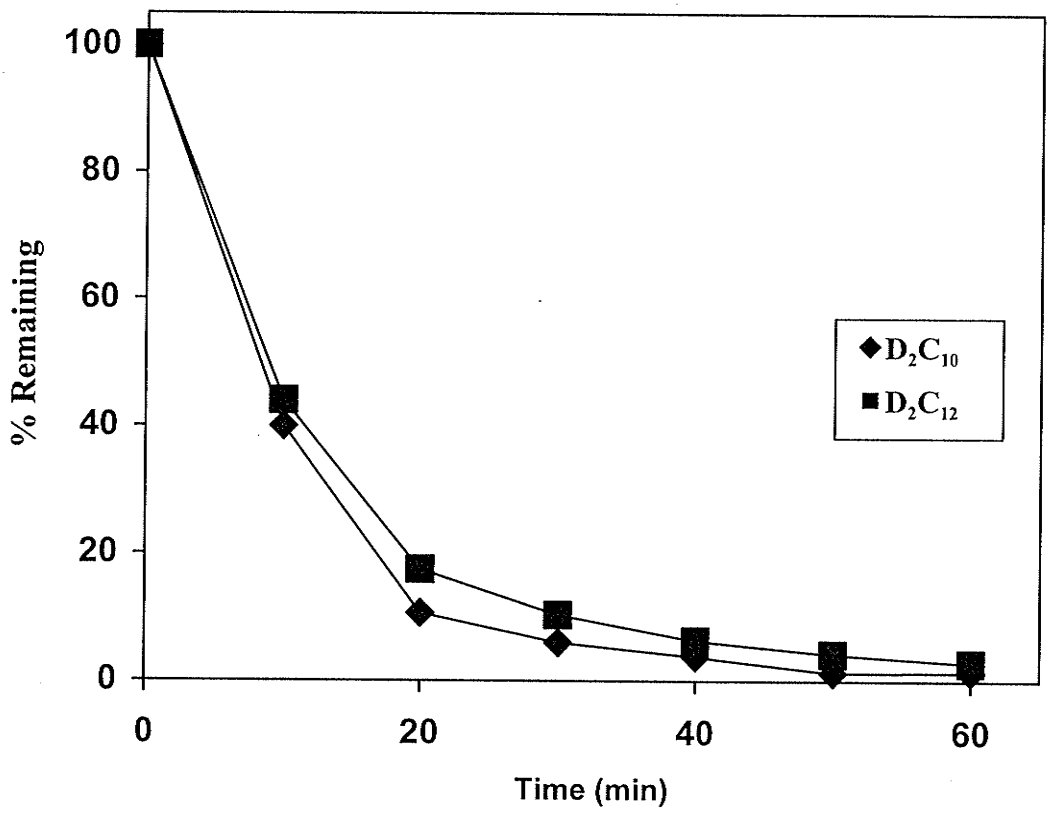

Figure 4.9: Effect of increased carbon chain length (from C_{10} to C_{12}) on the photodegradation of PCAs in Milli Q water in 0.1M $NaClO_4$ and pH 2.8 using 300 nm UV in the presence of 0.01M H_2O_2.

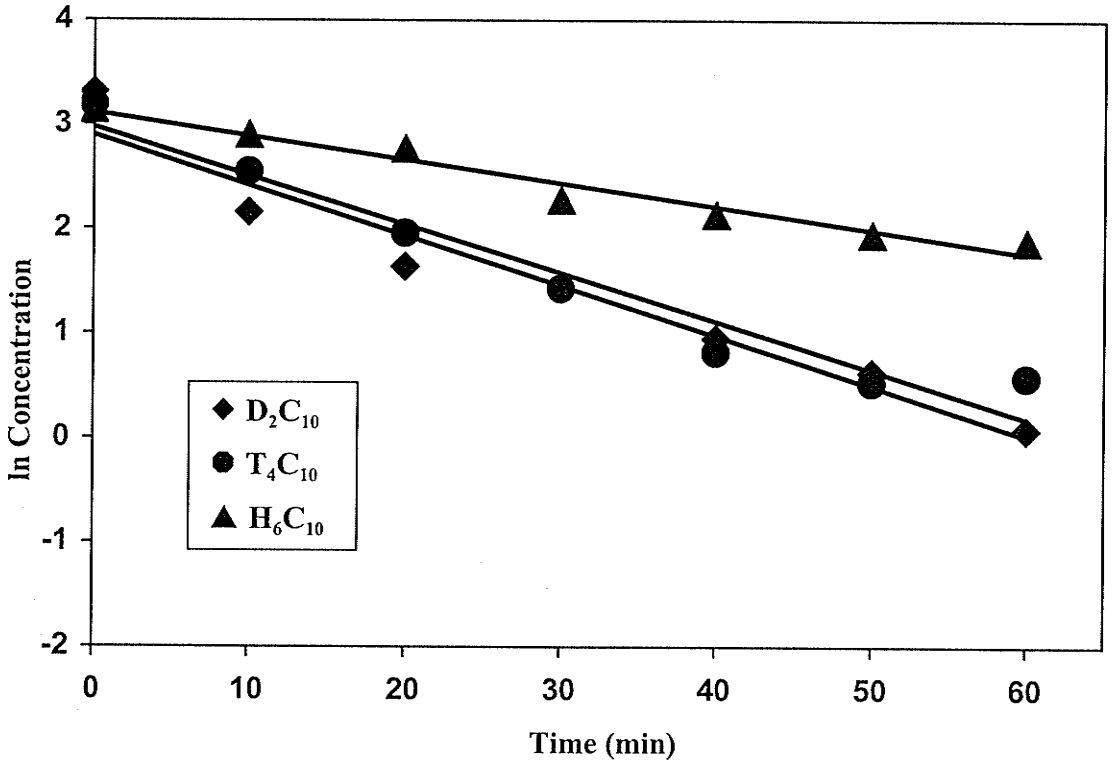

Figure 4.10: First-order plots for the degradation of chlorinated decanes (250 μg/L) in Lake Winnipeg water in 0.1M $NaClO_4$ and pH 8.3 using 300 nm UV in the presence of 0.01M H_2O_2.

Table 4.2: Observed first-order rate constants and half-lives for the photodegradation of PCA isomers in Lake Winnipeg water in the presence of 0.01M H_2O_2 at pH 8.3, 0.1M $NaClO_4$ and (300nm) UV light.

	D_2C_{10}	T_4C_{10}	H_6C_{10}	T_4C_{11}	D_2C_{12}
k (min^{-1})	0.048	0.046	0.022	0.023	0.039
$t_{1/2}$ (min)	14.4	14.9	30.9	30.4	18.0
R^2	0.950	0.950	0.960	0.972	0.910

As noticed in Milli Q water, increases in both chlorine number and carbon chain length contributed to decreased initial rates of photodegradation. However, natural organic carbon in lake water (990 μmol/L) is expected to consume hydrogen peroxide during the irradiation. Light attenuation due to presence of dissolved organic matter (DOM) may also reduce the rate of decomposition of hydrogen peroxide to $^{\bullet}OH$ radicals. The degradation of T_4C_{11} in Milli Q and lake water is compared in Figure 4.11. T_4C_{11}degrades more slowly in lake water with 66% disappeared in 30 min compared to 79% in Milli Q water. Absorption spectra of lake water and a mixture of PCAs in Milli Q water are shown in Figure 4.12. Although DOM absorbs UV light at 300 nm (the wavelength of maximum intensity of the light source) to a greater extent than the PCA mixtures, the kinetics do not support a photodegradation sensitized by excited state DOM. The decreased rate of photolysis in Lake Winnipeg water is therefore due to light attenuation by dissolved DOM.

Bog Water. The photodegradation of PCA isomers in bog water at pH 8.6 in the presence of H_2O_2 ($1x10^{-2}$ M) was considerably slower than in lake water. Although the isomers photodegrade in bog water, their half-lives are 1.3 to 2.1 times longer (Table 4.1). The slower reaction is attributed to a greater amount of dissolved organic carbon in bog water than in lake water which further attenuates the light available for photodegradation. First-order plots for the chlorinated decanes are illustrated in Figure 4.13. A significant decrease in the degradation rate with increased chlorine number was noted, with the degradation half-lives decreasing from 26 to 65 min for D_2C_{10} and H_6C_{10}, respectively, as summarized in Table 4.3. The photodegradation is also slowed by an increase in carbon chain length as illustrated in Figure 4.14 for T_4C_{10} and T_4C_{11}.

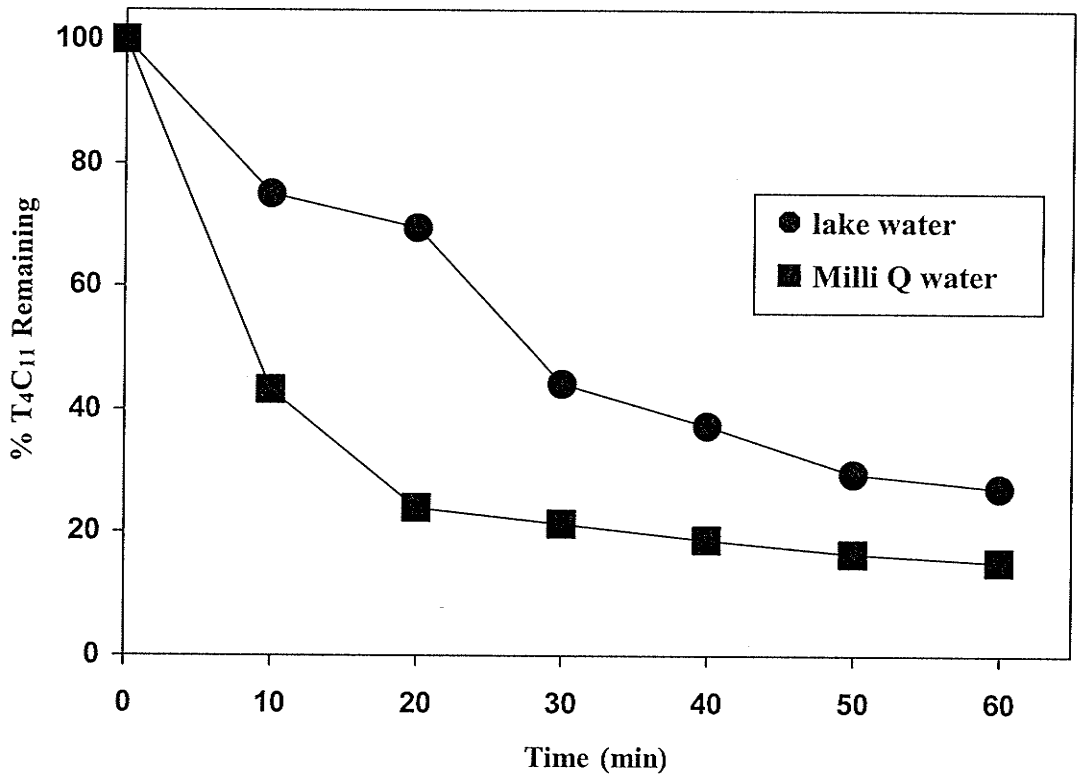

Figure 4.11: Effect of total organic carbon (TOC) on the homogeneous photodegradation of 1,2,10,11-tetrachloroundecane (250 μg/L) in the presence of 0.01M H_2O_2 in Lake Winnipeg water in 0.1M $NaClO_4$ and pH 8.3 using 300 nm UV light.

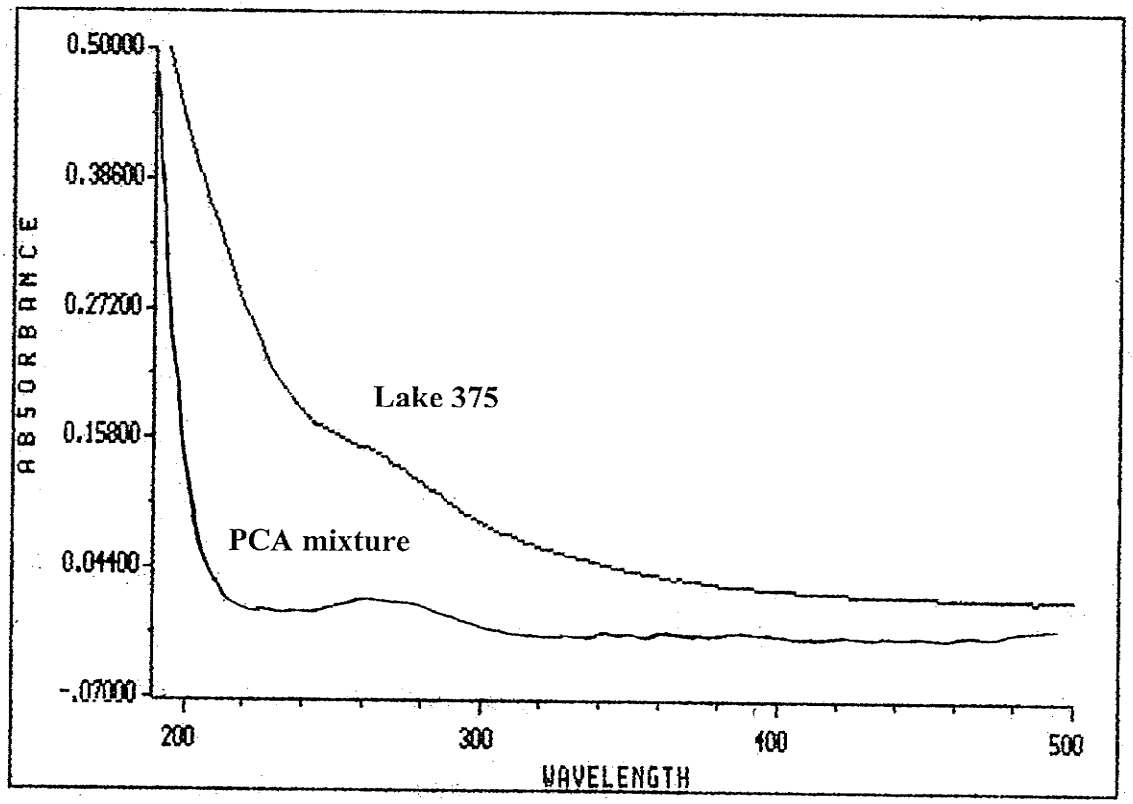

Figure 4.12: Absorption spectra of Lake Winnipeg water and an aqueous solution (250 μg/L) of a mixtures of PCAs in Milli Q water.

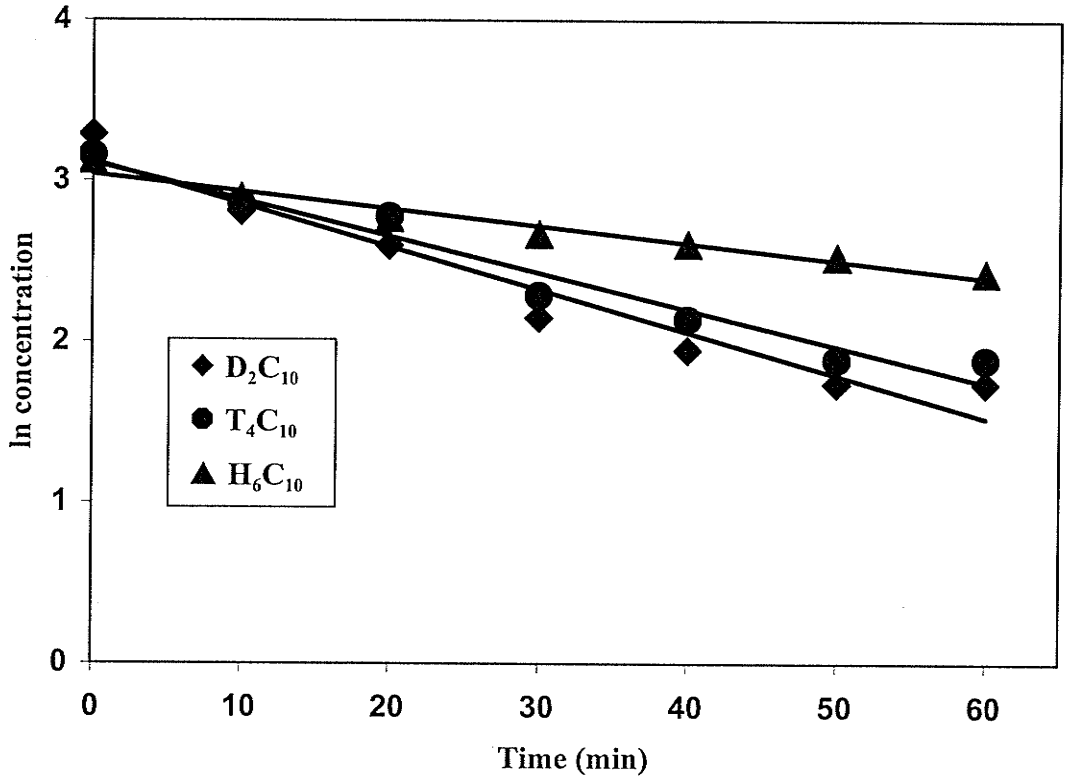

Figure 4.13: First-order plots for the degradation of chlorinated decanes (250 μg/L) in bog water in 0.1M $NaClO_4$ and pH 8.6 in the presence of 0.01M H_2O_2.using 300 nm UV light.

Table 4.3: Observed first-order rate constants and half-lives for the photodegradation of PCA isomers in bog water in the presence of 0.01M H_2O_2 at pH 8.6 and 0.1M $NaClO_4$.

	D_2C_{10}	T_4C_{10}	H_6C_{10}	T_4C_{11}	D_2C_{12}
k (min^{-1})	0.027	0.023	0.011	0.018	0.026
$t_{1/2}$ (min)	26.1	30.4	64.8	39.4	26.6
R^2	0.942	0.955	0.953	0.977	0.983

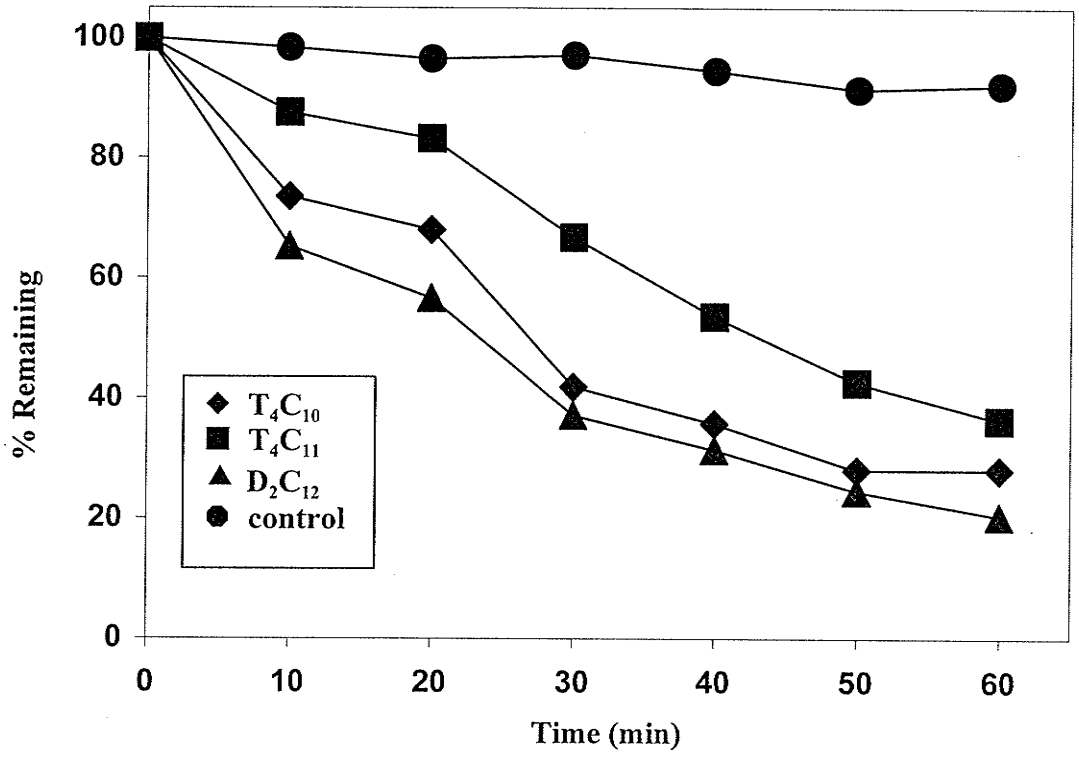

Figure 4.14: Photodegradation of PCAs (250 μg/L) of different chlorine number and carbon chain length in bog water in the presence of 0.01M H_2O_2 in 0.1M $NaClO_4$ and pH 8.6 using 300 nm UV. The control shows the degradation of D_2C_{12} in the absence of H_2O_2.

The effect of chlorine number is greater than the effect of carbon chain length, indicating that chloride scavenging of $^{\bullet}OH$ radicals is the dominant factor determining the degradation rate. For example, D_2C_{12} photodegrades faster than T_4C_{10} and T_4C_{11} (Figure 4.14). The effect of the water source on the homogeneous photodegradation of hexachlorodecane is summarized in Figure 4.15, illustrating the light attenuation effects of dissolved organic carbon.

4.3.2. Photodegradation of PCA Isomers Using Fenton and Photo-Fenton Systems

As discussed in the introduction, Fenton's reagent, a mixture of ferrous (Fe^{2+}) ion and hydrogen peroxide (in dark) which produces $^{\bullet}OH$ radicals by reaction (1-56) has been used extensively for the chemical oxidation of chlorinated aromatic hydrocarbons. On the other hand, a mixture of ferric (Fe^{3+}) ion and H_2O_2, known as modified Fenton conditions has been used to avoid the problems of high local concentrations of Fe^{2+} at the time of mixing of reagents [267] with the potential for scavenging $^{\bullet}OH$ radical:

$$Fe^{2+} + {}^{\bullet}OH \longrightarrow Fe^{3+} + OH^{-} \qquad (4\text{-}15)$$

Under these conditions Fe^{2+} is produced in situ from Fe^{3+} in aqueous H_2O_2 solutions (equation 1-57) to then react with excess H_2O_2 to generate $^{\bullet}OH$ radicals. Photo-Fenton reactions using either Fenton (Fe^{2+}/H_2O_2) or modified Fenton (Fe^{3+}/ H_2O_2) conditions and UV light often accelerate the decomposition of organic chemicals. With ferric ion in acidic solutions the dominant $Fe(OH)^{2+}$ complex photolyzes according to [141, 144]:

$$Fe(OH)^{2+} + h\nu \longrightarrow Fe^{2+} + {}^{\bullet}OH \qquad (4\text{-}16)$$

This enhances the production of $OH^{\bullet}$ radicals and promotes cycling of Fe^{3+} to Fe^{2+} for reaction with H_2O_2 (equation 1-56).

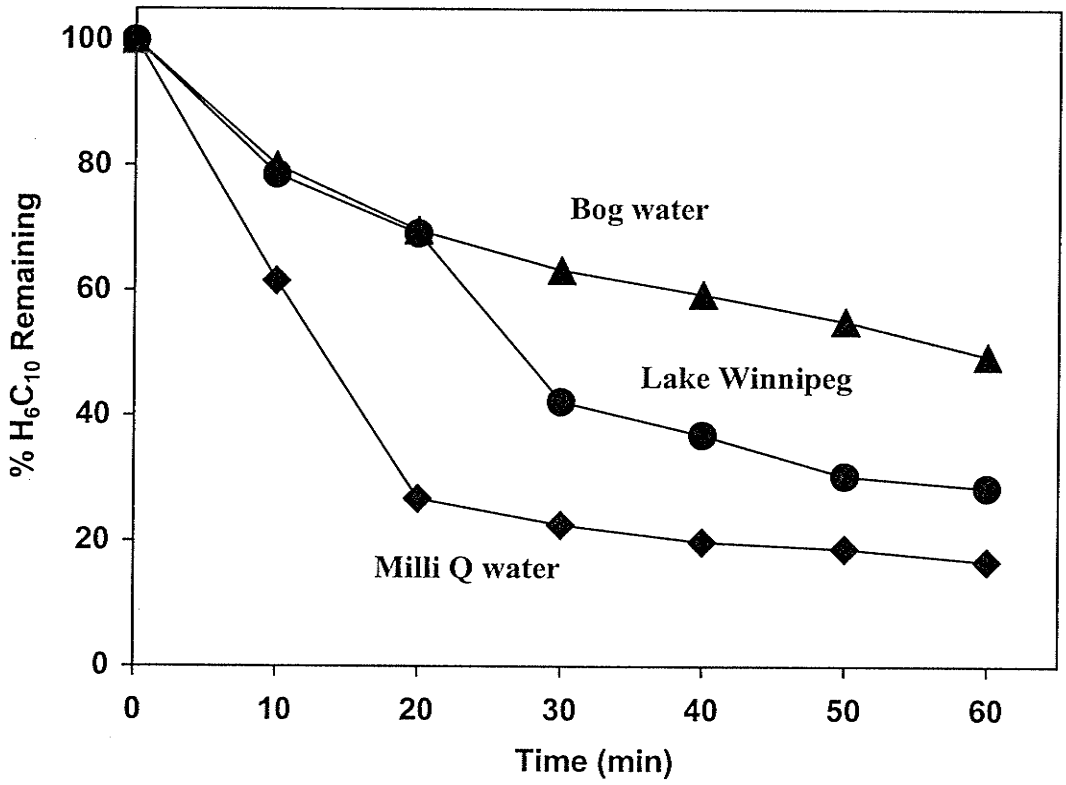

Figure 4.15: Effect of dissolved organic carbon (DOC) on the homogeneous photodegradation of 1,2,5,6,910-hexachlorodecane (250 μg/L) in the presence of 0.01M H_2O_2 in 0.1M $NaClO_4$ using 300 nm UV light.

4.3.2.1. Thermal Fenton Systems in Pure Water

Separate experiments were carried out at pH 2.8 with 1.0 x10^{-3} M $Fe(ClO_4)_2$ and $Fe(ClO_4)_3$ in the presence of 1.0 x 10^{-2} M H_2O_2 under dark conditions to investigate the thermal (dark) degradation of PCA isomers. As shown in Figure 4.16 tetrachlorodecane degraded very slowly under dark conditions under both Fenton and modified Fenton conditions with less than 17 % disappearance in 60 min. However, the thermal degradation of H_2O_2 in the presence of Fe^{+3} decreased its concentration significantly over the reaction period as will be discussed later in this chapter. The decreased H_2O_2 concentration does not reflect increased production of $^{\bullet}OH$ radicals, but is rather attributed to the catalytic effect of Fe^{3+} on the decomposition of H_2O_2 to H_2O and O_2 [110] for which a detailed mechanism is presented by Pignatello (1992) [266]. There is some evidence that Fe^{3+} and H_2O_2 react to produce several Fe^{III}-hydroperoxy complexes [268], $Fe^{III}(HO_2)^{2+}$ and $Fe^{III}(OH)(HO_2)^{+}$,which decompose to produce the hydroperoxy radical ($HO_2^{\bullet}$) and Fe^{2+}. However, the general lack of reactivity of PCAs under Fenton or modified Fenton conditions indicates that, if $HO_2^{\bullet}$ is formed, it is relatively nonreactive with T_4C_{10} and other PCA isomers.

4.3.2.2. Photo-Fenton System in Pure Water

Photodegradation of 1,2,9,10-tetrachlorodecane in the presence of photo-Fenton ($Fe^{2+}/H_2O_2/UV$) conditions is illustrated in Figure 4.17. The results shown that the photodegradation of T_4C_{10} was very effective with 67 % transformation in the first 20 min of irradiation. The photo-Fenton reaction is affected by the counter ion used in the iron salt. When 2.5 x10^{-4} M $FeSO_4$ is used in the photo-Fenton reaction, the extent of degradation of T_4C_{10} is somewhat decreased (Figure 4.18).

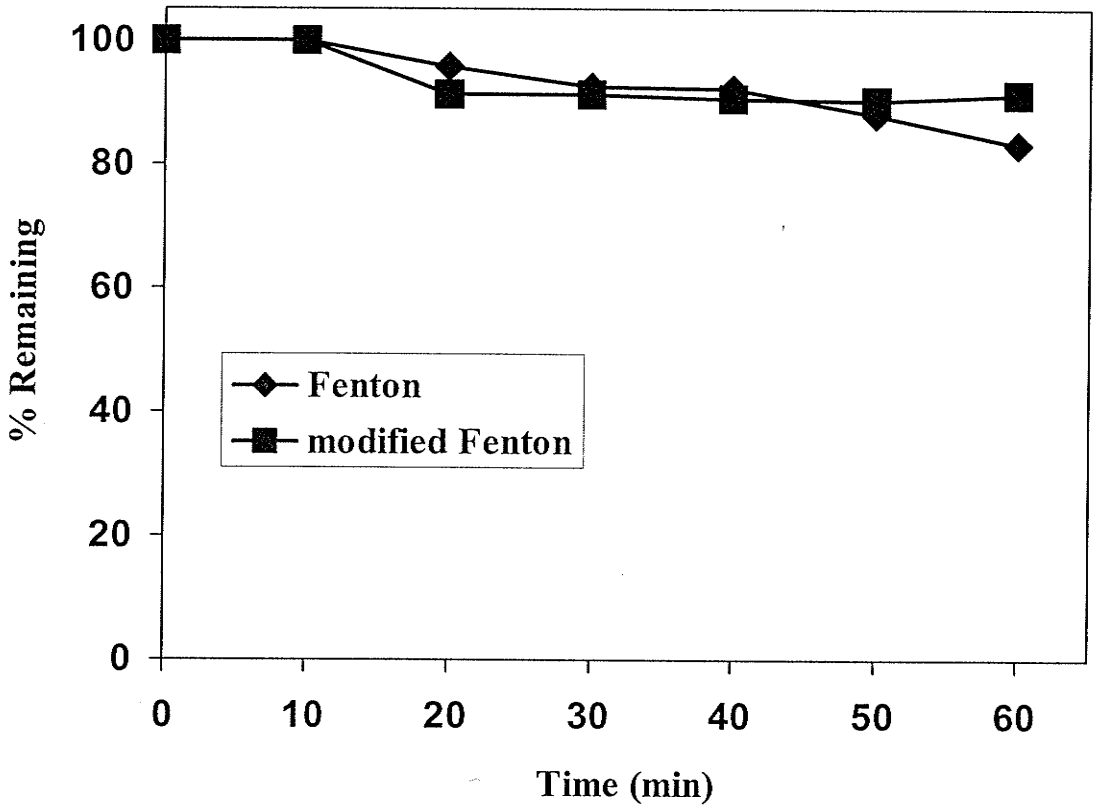

Figure 4.16: Thermal (dark) degradation of 1,2,9,10-tetrachlorodecane (250 μg/L) in Milli Q water under Fenton (1.0 x 10^{-3} M $Fe(ClO_4)_2$) and modified Fenton (1.0 x 10^{-3} M $Fe(ClO_4)_3$) conditions in the presence of 0.01M H_2O_2 in 0.1M $NaClO_4$ and pH 2.8 using 300 nm light.

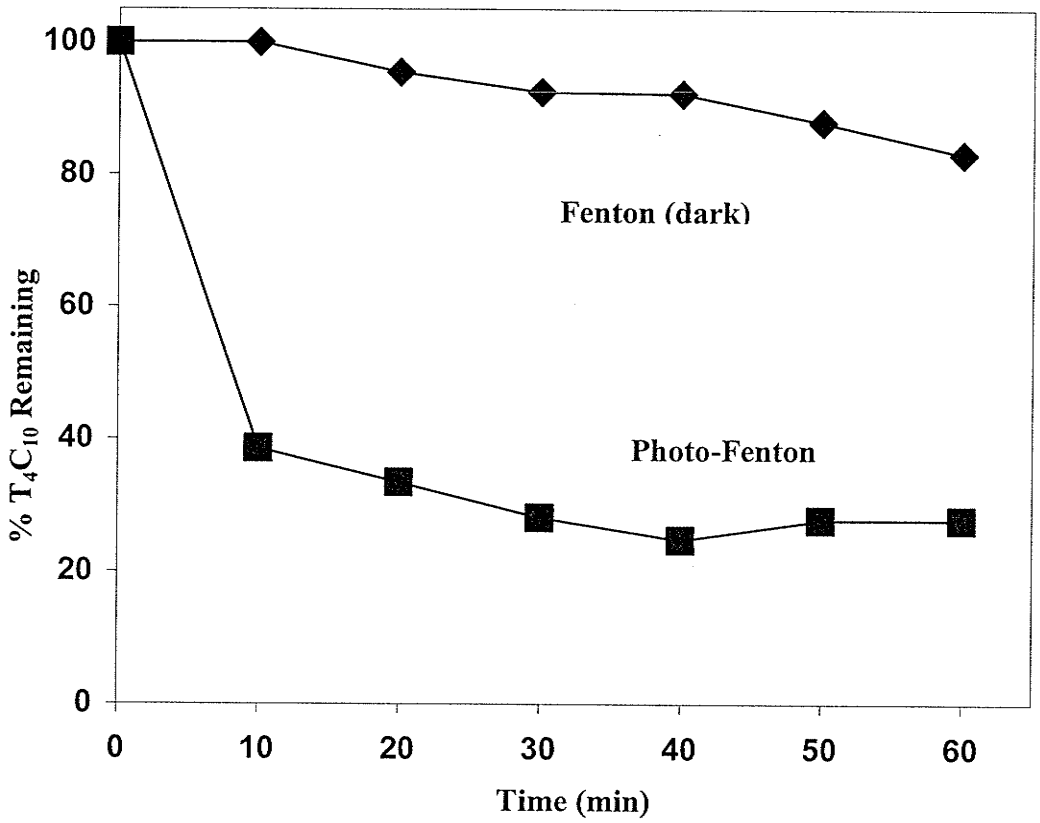

Figure 4.17: Photodegradation of 1,2,9,10-tetrachlorodecane (250 μg/L) in Milli Q water under Fenton and photo-Fenton (1.0×10^{-3} M $Fe(ClO_4)_2$/1×10^{-2} M H_2O_2) conditions in the presence of 0.1M $NaClO_4$ and pH 2.8 using 300 nm light.

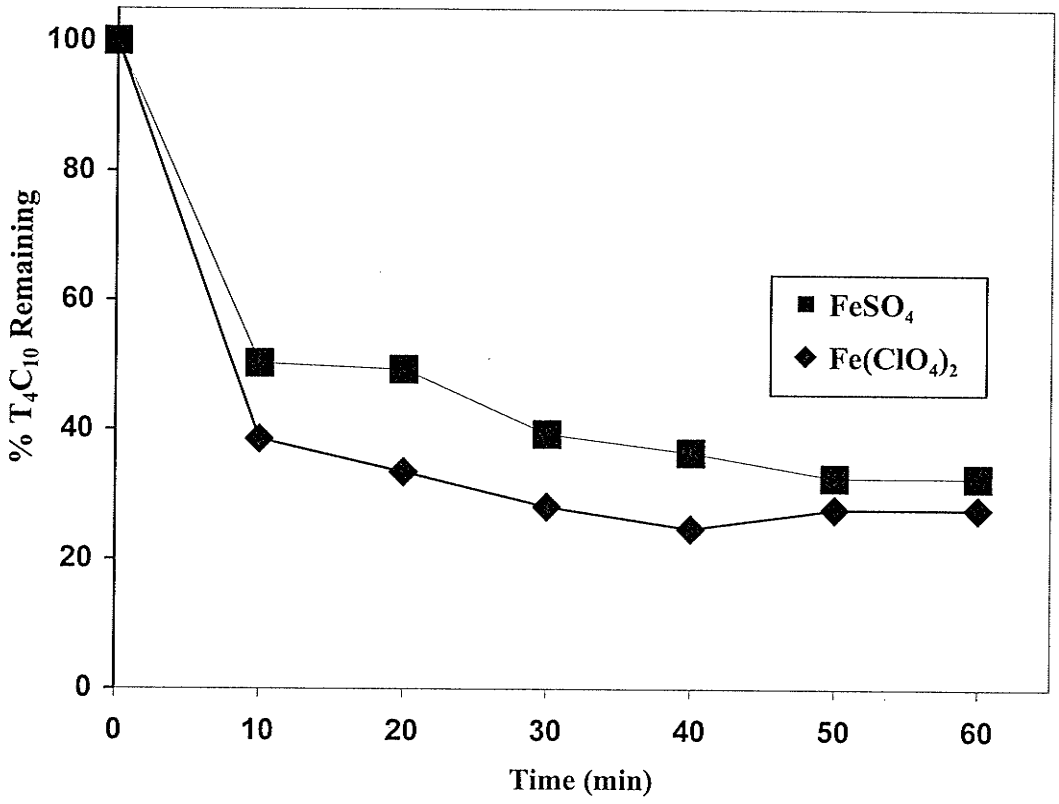

Figure 4.18: Photodegradation of T_4C_{10} by the photo-Fenton reaction at pH 2.8 and 0.1M $NaClO_4$ using (2.5 x 10_{-4} M $FeSO_4$ and 1 x10^{-3} M $Fe(ClO_4)_2$ using 300 nm light.

Several factors may be responsible for the decreased reaction rate. Sulfate scavenging of $^{\bullet}OH$ radicals would reduce the reactivity of $^{\bullet}OH$ for T_4C_{10}:

$$OH^{\bullet} + SO_4^{2-} \xrightarrow{H+} H_2O + SO_4^{2-} \qquad (4\text{-}17)$$

In the presence of SO_4^{2-} the distribution of iron complexes shifts away from $Fe(OH)^{2+}$ [266] which reduces the rate of $^{\bullet}OH$ production and hence the degradation of T_4C_{10}. However, the lower concentration of $Fe(SO_4)_2$ in this experiment (2.5×10^{-4} M), chosen to minimize this effect, may also have affected the production of $^{\bullet}OH$ radicals.

4.3.2.3. Modified Photo-Fenton Conditions in Pure Water

The degradation of T_4C_{10} was enhanced under modified photo-Fenton ($Fe^{3+}/H_2O_2/UV$) conditions, with 79% disappearance in the first 20 min compared to 67% under photo-Fenton conditions (Figure 4.19). Using Fe^{+3} in the modified photo-Fenton system minimizes the effect of high local concentrations of Fe^{+2} minimizing scavenging of $^{\bullet}OH$ radicals according to equation (4-15). Therefore, all the experiments throughout this study were performed with the modified photo-Fenton reagent ($Fe^{+3}/H_2O_2/UV$). The degradation of the PCA isomers D_2C_{10}, D_2C_{12}, T_4C_{10}, H_6C_{10} and T_4C_{11} under modified photo-Fenton conditions are shown in Figures 4.20 - 4.22. The results indicate that modified photo-Fenton conditions in acidic media significantly accelerates the degradation of PCA isomers. Under these conditions the rates of transformation of D_2C_{10} and D_2C_{12} are rapid (Figure 4.20) with 96 and 95% degradation, respectively, in the first 30 min of photolysis. Isomers with high chlorine number (Figure 4.21) slow the degradation rate, due to scavenging of $^{\bullet}OH$ radical by chloride ions as discussed earlier. Similar results have been reported by Pignatello [266], where chloride

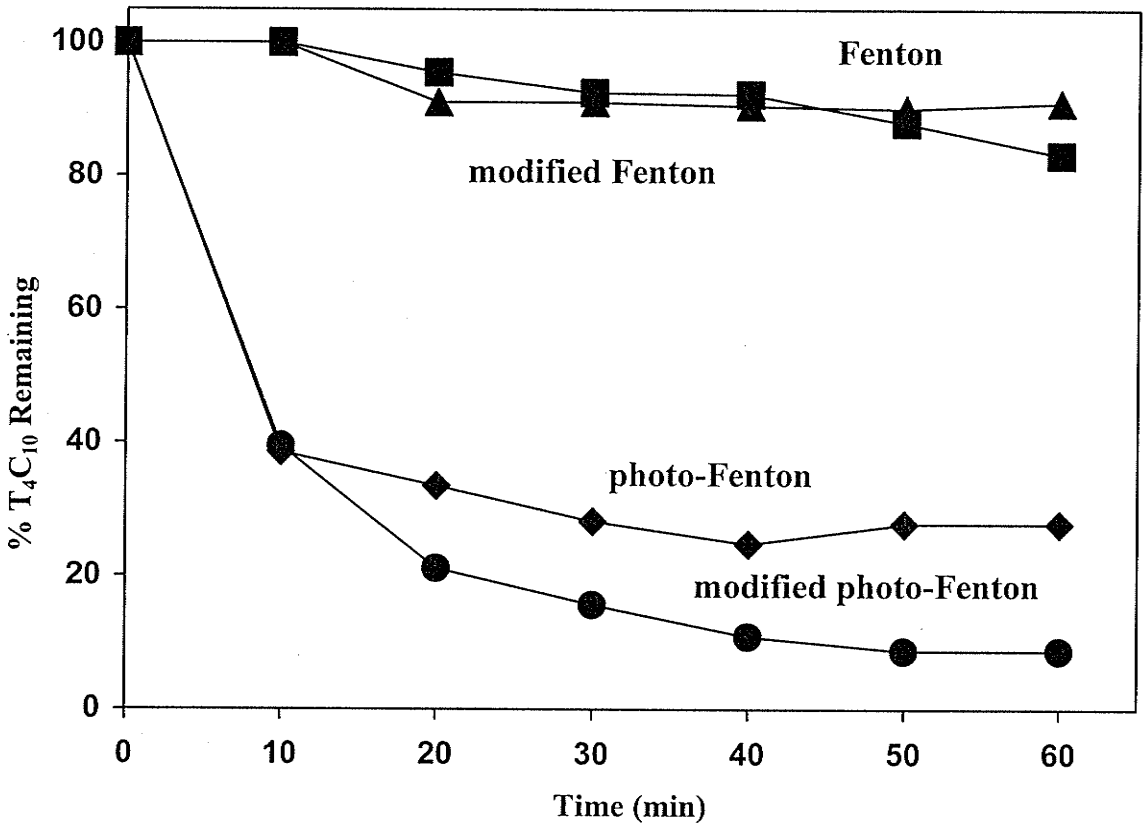

Figure 4.19: Photodegradation of 1,2,9,10-tetrachlorodecane (250 μg/L) in Milli Q water under photo-Fenton (1.0×10^{-3} M $Fe(ClO_4)_2$) and modified photo-Fenton (1.0×10^{-3} M $Fe(ClO_4)_3$) conditions in the presence of 0.01M H_2O_2 in 0.1M $NaClO_4$ and pH 2.8 using 300 nm light.

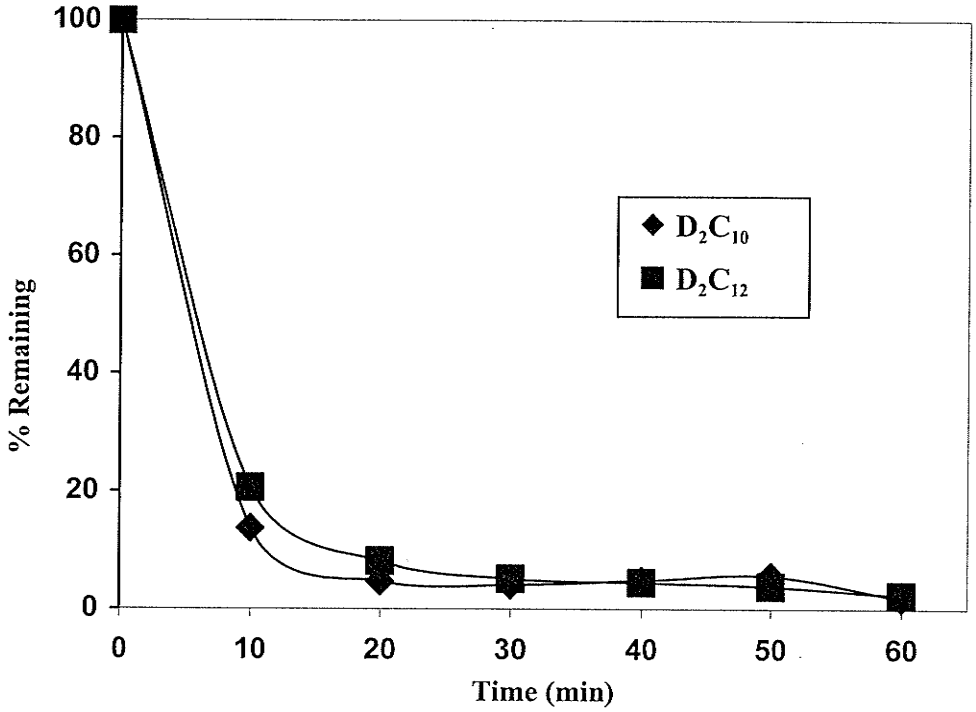

Figure 4.20: Photodegradation of 1,10-dichlorordecane and 1,12-dichlorododecane (250 μg/L) in Milli Q water under modified photo-Fenton conditions (1.0×10^{-3} M $Fe(ClO_4)_3$) in the presence of 0.01M H_2O_2 in 0.1M $NaClO_4$ and pH 2.8 using 300 nm light.

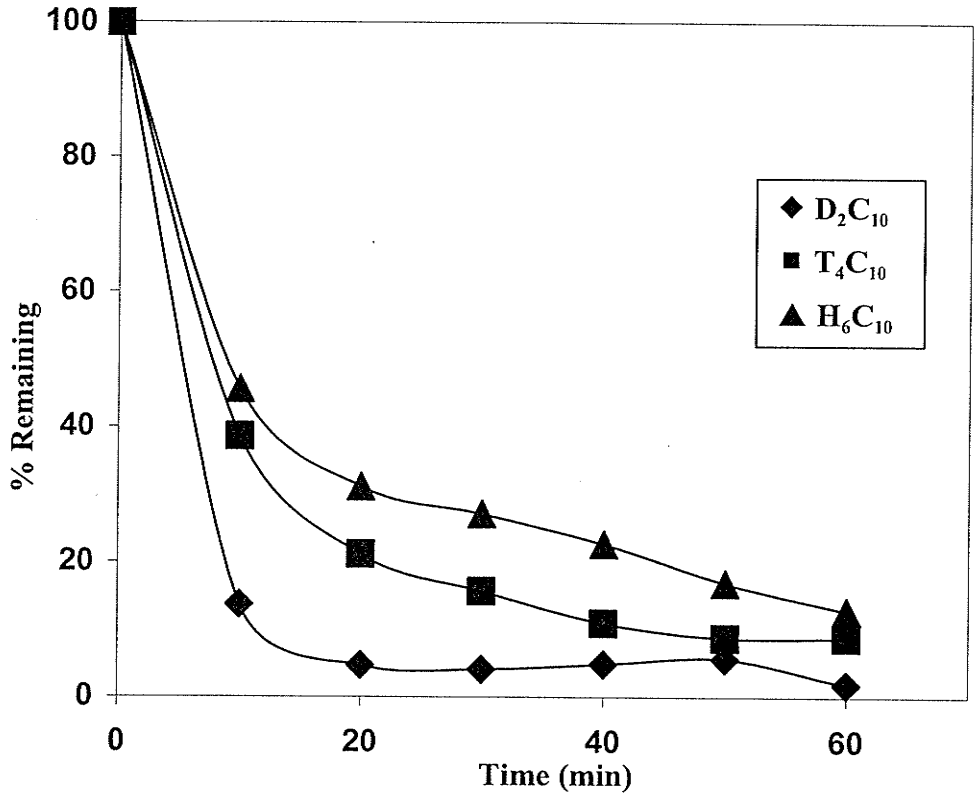

Figure 4.21: Photodegradation of chlorinated decanes (250 μg/L) in Milli Q water under modified photo-Fenton conditions (1.0×10^{-3} M $Fe(ClO_4)_3$) in the presence of 0.01M H_2O_2 in 0.1M $NaClO_4$ and pH 2.8 using 300 nm light.

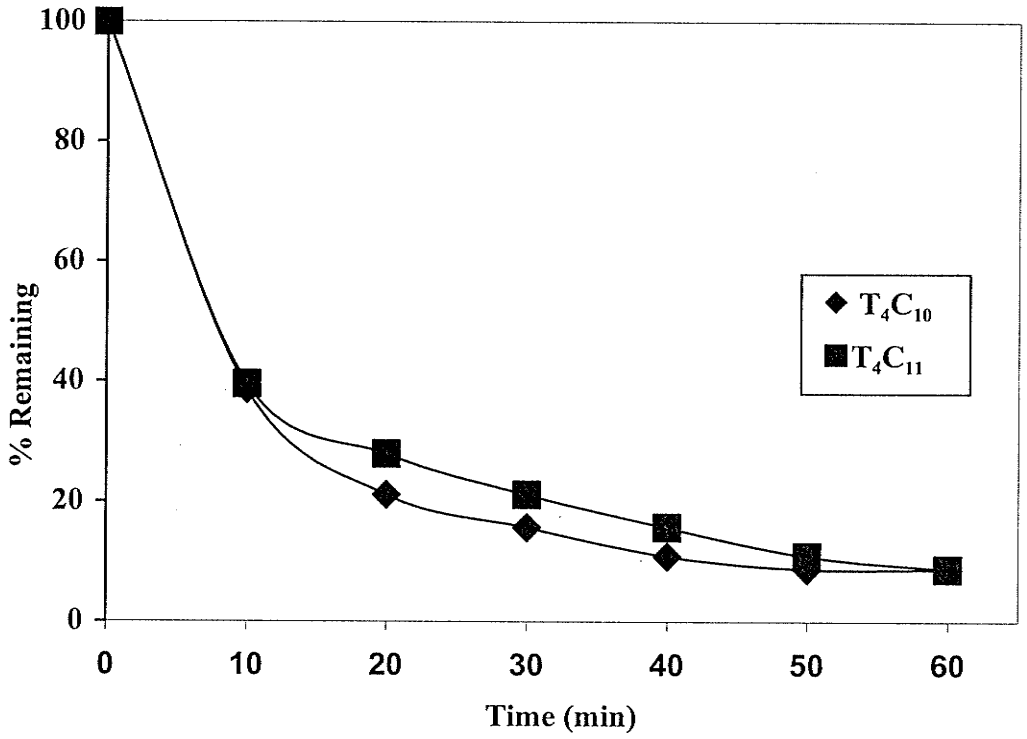

Figure 4.22: Homogeneous photodegradation of 1,2,9,10-tetrachlorodecane and 1,2,10,11-tetrachloroundecane (250 μg/L) in Milli Q water under modified photo-Fenton conditions (1.0×10^{-3} M $Fe(ClO_4)_3$) in the presence of 0.01M H_2O_2 in 0.1M $NaClO_4$ and pH 2.8 using 300 nm light.

ions inhibited the transformation of the herbicide 2,4-dichlorophenoxyacetic acid (2,4-D) under modified photo-Fenton conditions. Increasing the carbon chain length had minimal affect on the degradation rate as illustrated in Figure 4.20 for D_2C_{10}/D_2C_{12} and in Figure 4.22 for T_4C_{10}/T_4C_{11}. The rapid photodegradation of PCA isomers is attributed to the enhanced degradation of hydrogen peroxide and hence production of oxidizing $^{\bullet}OH$ radicals. This supports recent work by Bossmann et al.[167] and DeLaat et al.[168] suggesting that iron (IV) complexes may be the main precursors leading to the production of $^{\bullet}OH$ radicals. The presence of $^{\bullet}OH$ radical scavengers resulted in decreased degradation rates of PCAs isomers. The degradation of T_4C_{10} under modified photo-Fenton conditions (Figure 4.23) was inhibited by the presence of *tert*-butyl alcohol (0.1M), supporting a free radical reaction.

4.3.2.4. Photolysis of H_2O_2

The presence of Fe^{3+} has a dramatic effect on the rate of disappearance of hydrogen peroxide as illustrated in Figure 4.24. In the absence of Fe^{3+} the photodegradation of H_2O_2 (1.0×10^{-2} M) is very slow with the 300 nm light source used due to the recombination of $^{\bullet}OH$ radicals. However, this system is capable of degrading ($\sim 10^{-6}$ M) PCAs (for example, see Figure 4.5) without significant decreases in H_2O_2 concentration. The thermal degradation of H_2O_2 under Fenton-like conditions (1.0×10^{-3} M Fe^{3+}/dark) resulted in 50% disappearance in 30 minutes. However, the lack of reactivity of PCAs under these conditions (for example, see Figure 4.16) indicates that this decomposition does not involve significant production of $^{\bullet}OH$ radicals. Under modified photo-Fenton conditions (1.0×10^{-3} M Fe^{3+}/H_2O_2/UV) Fe^{+3} catalyzes the degradation of H_2O_2 to such an extent that

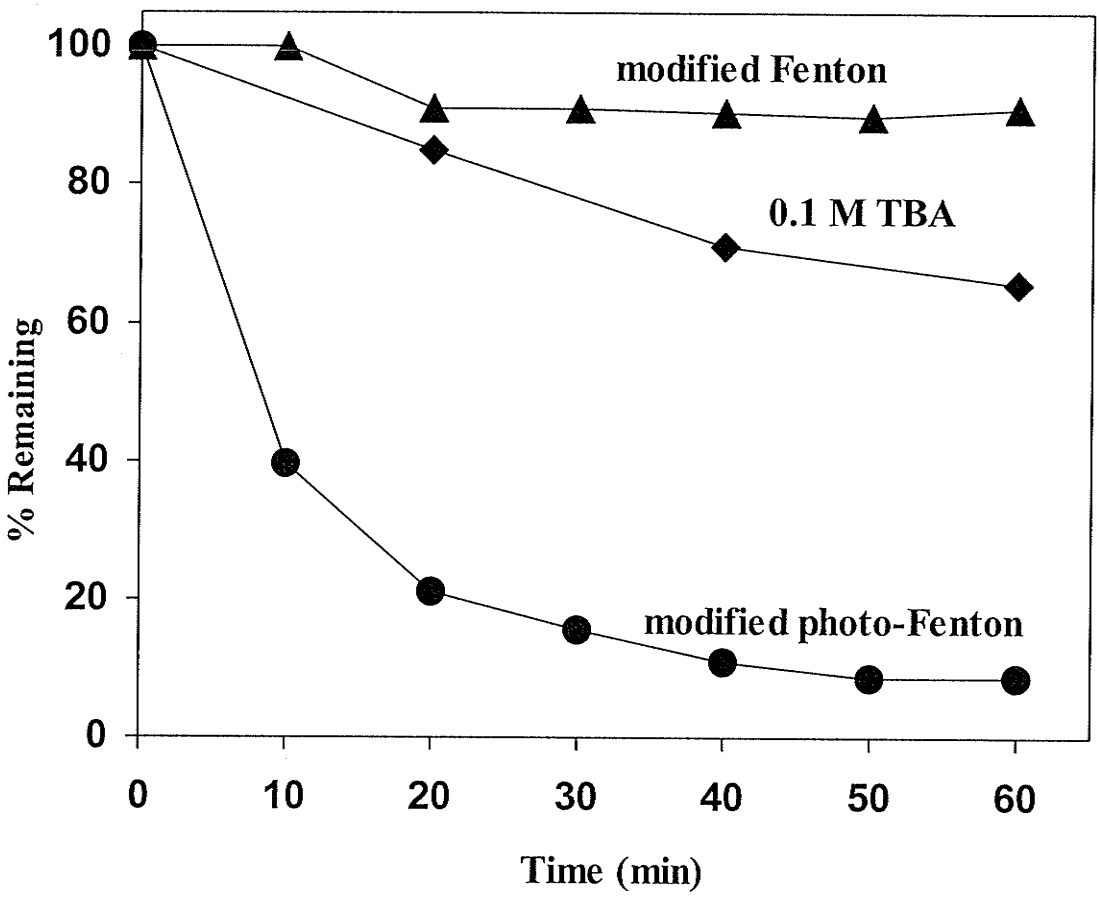

Figure 4.23: Effect of (0.1M) *tert*-butyl alcohol on the homogeneous photodegradation of 1,2,9,10-tetrachlorodecane in Milli Q water under modified photo-Fenton conditions ($1x10^{-2}$ M H_2O_2/$1x10^{-3}$ M Fe $(ClO_4)_3$) at pH 2.8 and 0.1M $NaClO_4$ using 300 nm light.

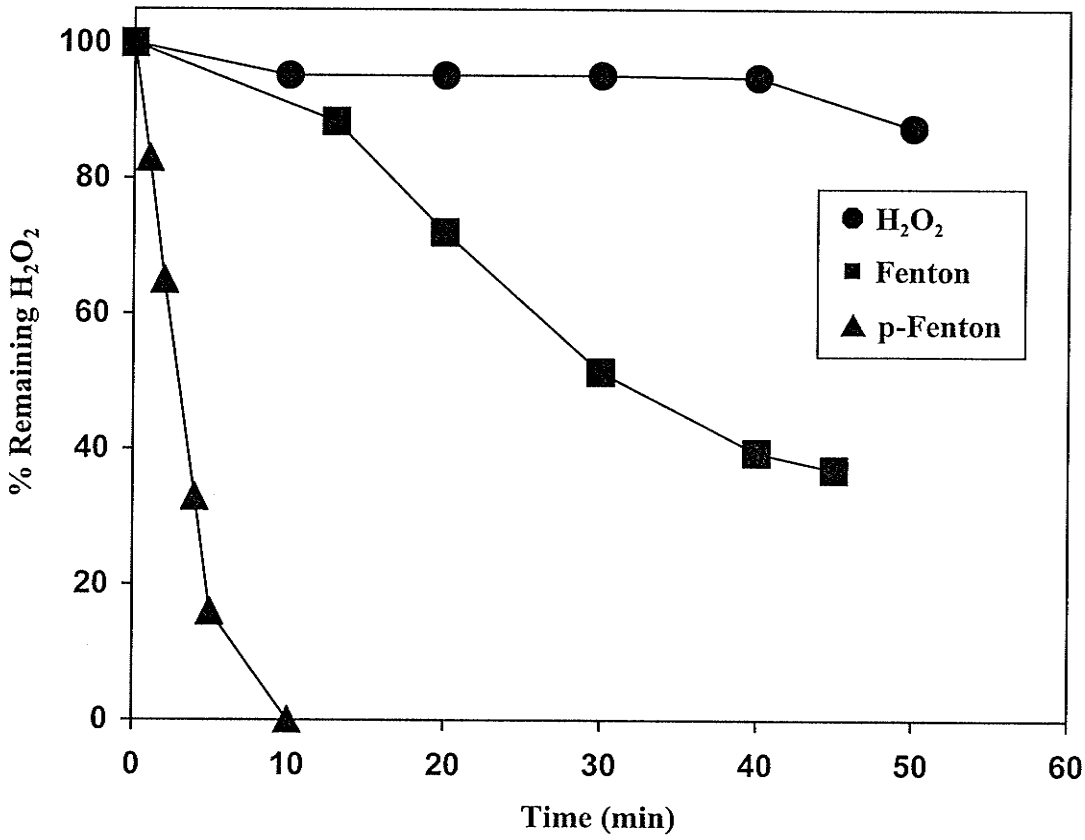

Figure 4.24: Degradation of H_2O_2 as a function of irradiation time in Milli Q water under modified Fenton (1.0×10^{-3} M $Fe(ClO_4)_3$/1.0×10^{-2} M H_2O_2/dark) and modified photo-Fenton (1.0×10^{-3} M $Fe(ClO_4)_3$/1.0×10^{-2} M H_2O_2/UV) conditions in 0.1M $NaClO_4$ and pH 2.8 using 300 nm light.

.

it is 85% depleted after 5 min of irradiation. The resultant increase in production of $^{\bullet}OH$ radicals produced a similar dramatic increase in the rate of destruction of PCAs. For example, the disappearance of T_4C_{10} reached 80% in 20 min of irradiation compared to 61% disappearance under H_2O_2/UV process as shown in Figure 4.25. The rapid degradation of T_4C_{10} is attributed to the enhanced degradation of hydrogen peroxide and hence production of oxidizing $^{\bullet}OH$ radicals (Figure 4.24). This supports recent work by DeLaat and Gallard [267], which suggested that iron (IV) complexes may be the main precursors leading to the production of $^{\bullet}OH$ radicals.

As discussed above, the modified photo-Fenton reaction enhanced the production of $^{\bullet}OH$ radicals due to the reduction of Fe^{+3} to Fe^{+2}. To further support this, the concentration of Fe^{+2} produced during the reaction was determined in the same manner as discussed previously. The results in Figure 4.26 indicated that 14% of Fe^{+3} was converted into Fe^{+2} in 60 min during the reaction. The results indicated that the reduced amount of Fe^{3+} resulted in production of a significant amount of $^{\bullet}OH$ radicals that dramatically enhanced the degradation of PCAs.

4.3.2.5. Modified Photo-Fenton Reactions in Natural Water

Photodegradation of PCA isomers in lake water at natural pH (pH 6.8) with 1.0×10^{-2} M H_2O_2 and 1.0×10^{-3} M Fe^{+3} in the presence of 0.1M $NaClO_4$ was quite efficient with more than 90% disappearance in the first 20 minutes for chlorinated decanes (D_2C_{10} and T_4C_{10}) as shown in Figure 4.27. As noticed from the results, increased chlorine content resulted in decreased degradation rates. For example, the percent transformation of H_6C_{10} reduced to 50% in the first 20 min due to scavenging of $^{\bullet}OH$ radicals by chloride ions.

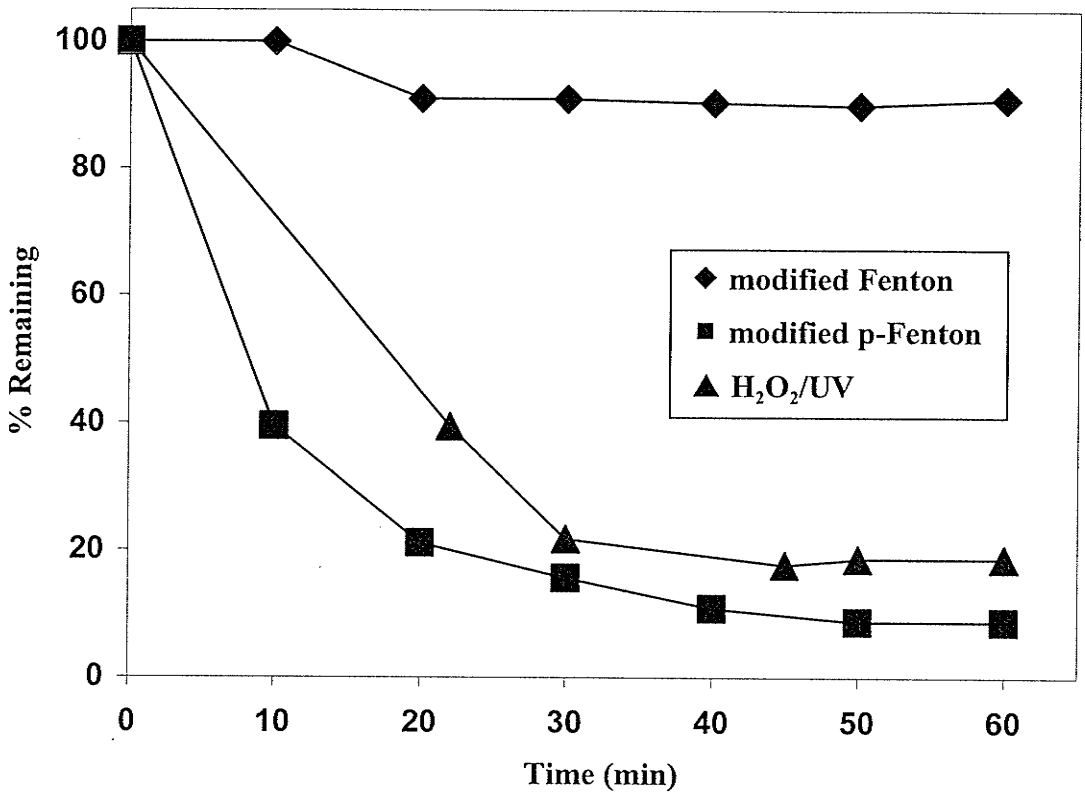

Figure 4.25: Photodegradation of 1,2,9,10-tetrachlorodecane (250 μg/L) in Milli Q water under modified Fenton (1.0×10^{-3} M $Fe(ClO_4)_3$/1.0×10^{-2} M H_2O_2/dark), modified photo-Fenton (1.0×10^{-3} M $Fe(ClO_4)_3$/1.0×10^{-2} M H_2O_2/UV) conditions and in the presence of 1.0×10^{-2} M H_2O_2 in 0.1M $NaClO_4$ and pH 2.8 using 300 nm light.

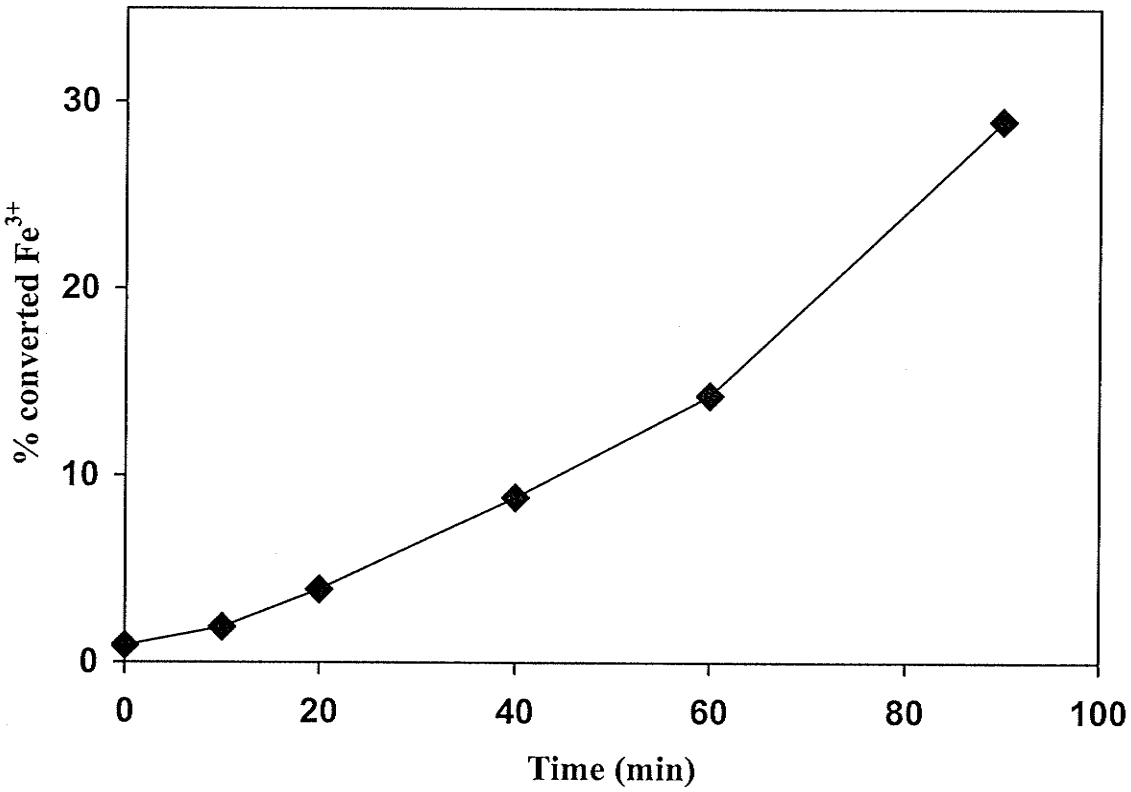

Figure 4.26: Formation of Fe^{+2} from reduction of Fe^{+3} by H_2O_2 during the modified photo-Fenton reaction.

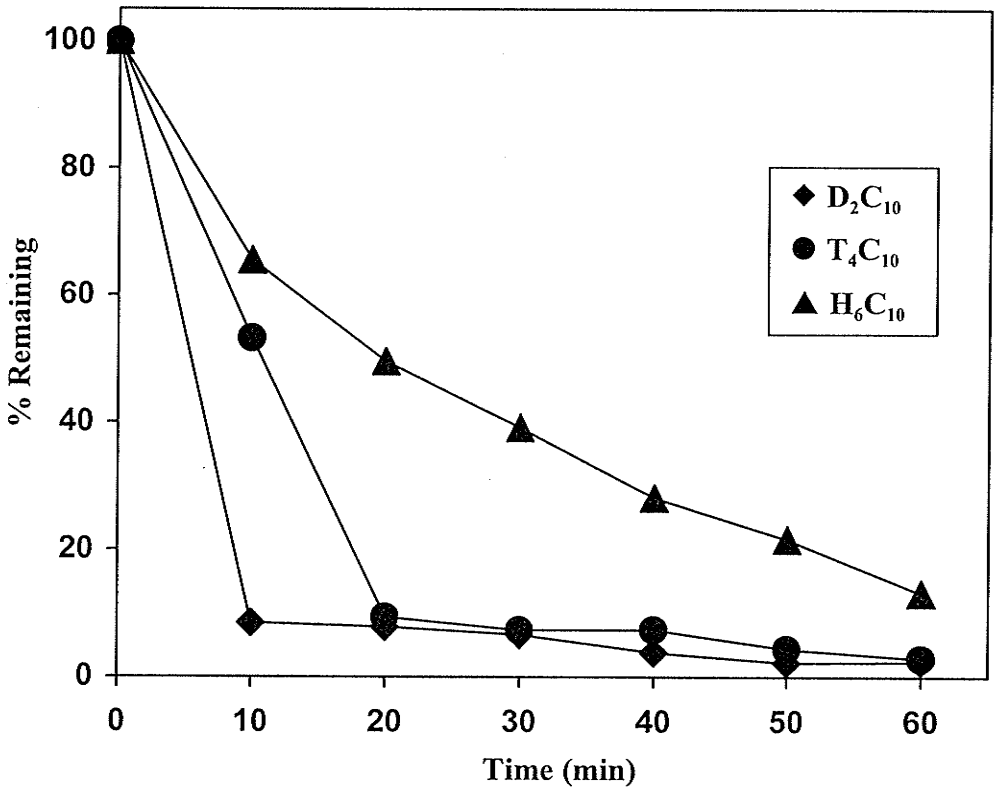

Figure 4.27: Homogeneous photodegradation of chlorinated decanes (D_2C_{10}, T_4C_{10} and H_6C_{10}) in lake water under modified photo-Fenton conditions ($1x10^{-2}$ M H_2O_2/1 $x10^{-3}$ M Fe $(ClO_4)_3$) at pH 2.8 and 0.1M $NaClO_4$ using 300 nm light.

Again carbon chain length appears to have minimal effect at low chlorine number as illustrated for D_2C_{10} and D_2C_{12} in Figure 4.28. At higher chlorine number the effect of carbon chain length is notable as illustrated for T_4C_{10} and T_4C_{11} (Figure 4.29). The water properties, specifically dissolved organic carbon, again affect the degradation of PCAs under photo-Fenton conditions. Figures 4.30 and 4.31 show the effect on T_4C_{11} in lake water and D_2C_{10} in lake and bog water. The results are explained by the competition between dissolved organic carbon in natural water and the PCA for $^{\bullet}OH$ radicals and/or the light attenuation effects of the natural water. Over all, these effects inhibited the degradation reactions in these natural waters.

4.3.3. Homogeneous Photodegradation of PCA Mixtures

PCA mixtures including chlorinated decanes, undecanes, dodecanes and tridecanes were synthesized by free radical chlorination of the respective *n*-alkane in the presence of UV light as discussed in Chapter 2. Each mixture consists of a complex mixture of optical isomers and congeners with chlorine numbers ranging from Cl_5 to Cl_8. Stock solutions of individual mixtures were prepared in acetone at concentrations of 250 μg/L. In all experiments with PCA mixtures the concentration of H_2O_2 was increased to 0.02 M from 0.01 M to increase the production of $^{\bullet}OH$ radicals. Experiments with $^{\bullet}OH$ radical scavengers were performed with *tert*-butyl alcohol to support the photooxidation reaction with $^{\bullet}OH$ radicals.

The effect of H_2O_2 consumption on the photodegradation reaction was investigated by the addition of 0.01 M H_2O_2 after 90 min of reaction.

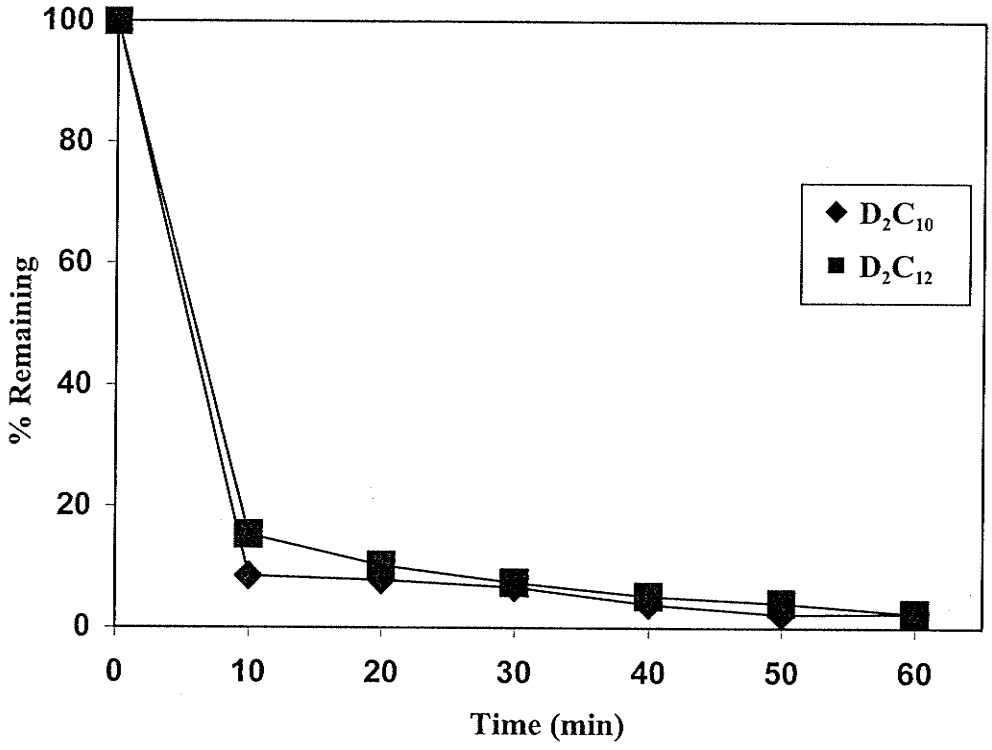

Figure 4.28: Effect of carbon chain length on the homogeneous photodegradation of 1,10-dichlorodecane and 1,12-dichlorododecane in lake water under modified photo-Fenton conditions ($1x10^{-2}$ M H_2O_2/$1x10^{-3}$ M $Fe(ClO_4)_3$) at pH 2.8 and 0.1M $NaClO_4$ using 300 nm light.

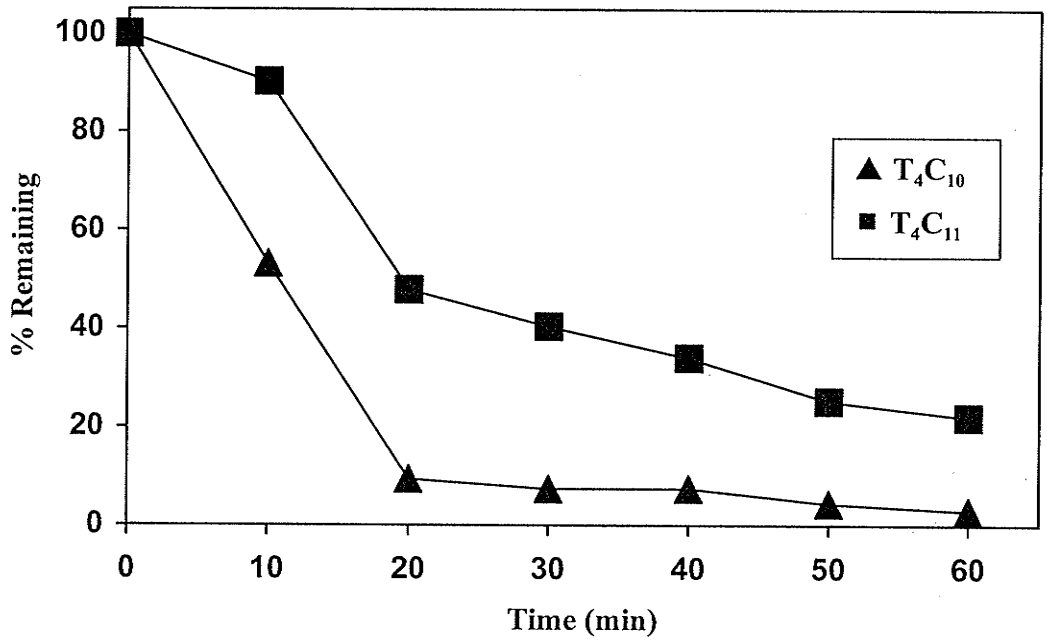

Figure 4.29: Effect of carbon chain length on the homogeneous photodegradation of 1,2,9,10-tetrachlorodecane and 1,2,10,11-tetrachloroundecane in lake water under modified photo-Fenton conditions ($1x10^{-2}$ M H_2O_2/$1x10^{-3}$ M $Fe(ClO_4)_3$) at pH 2.8 and 0.1M $NaClO_4$ using 300 nm light.

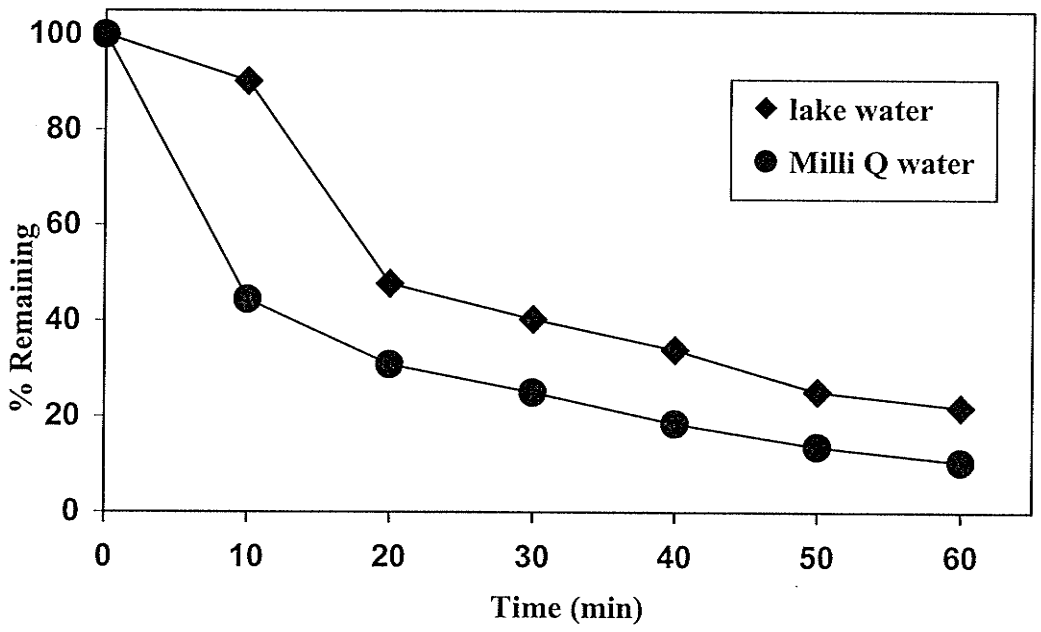

Figure 4.30: Effect of dissolved organic carbon on the homogeneous photodegradation of 1,2,10,11-tetrachloroundecane in lake water under modified photo-Fenton conditions ($1x10^{-2}$ M H_2O_2/$1x10^{-3}$ M $Fe(ClO_4)_3$) at pH 2.8 and 0.1M $NaClO_4$ using 300 nm light.

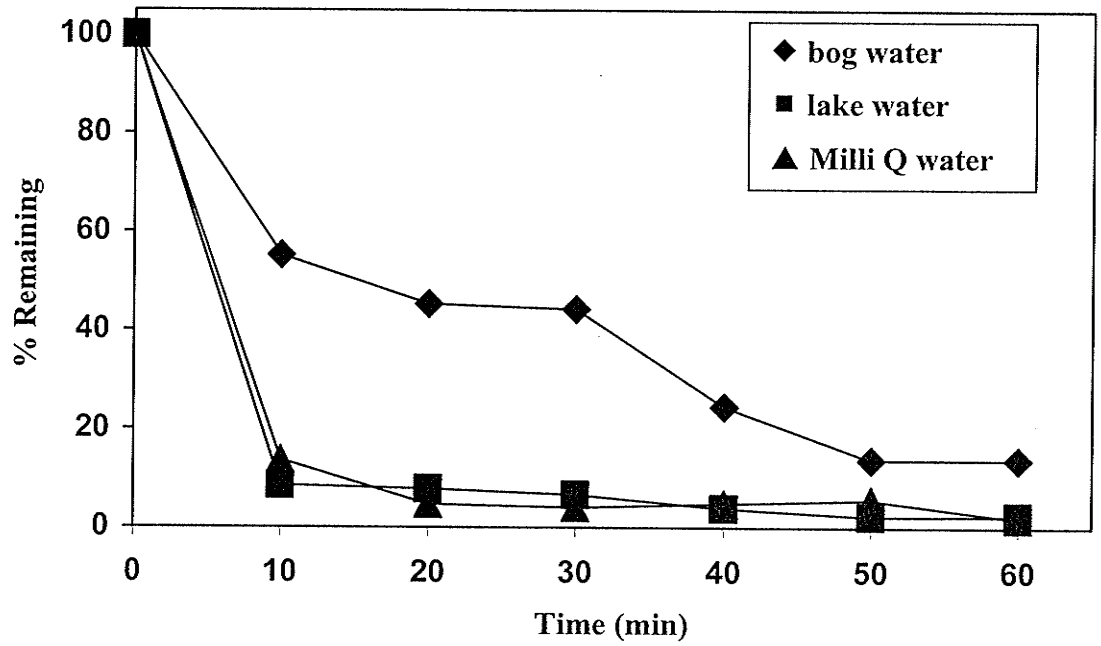

Figure 4.31: Effect of dissolved organic carbon on the homogeneous photodegradation of 1,10-dichlorodecane in bog water under modified photo-Fenton conditions ($1x10^{-2}$ M H_2O_2/$1x10^{-3}$ M $Fe(ClO_4)_3$) at pH 2.8 and 0.1M $NaClO_4$ using 300 nm light.

4.3.3.1. H_2O_2/UV in Pure Water

The photodegradation of all the PCA mixtures in the presence of 0.02 M H_2O_2 are illustrated in figures 4.32 to 4.35. The results indicated that aqueous solutions of 0.02M H_2O_2 were effective in photodegrading PCA mixtures. For example, chlorinated decane mixtures degraded rapidly with 64% disappearance in the first 90 minutes. However, increasing both the chlorine number and the carbon chain length lead to slower degradation in the first hour of the reaction period, due to scavenging of $^{\bullet}OH$ radicals by chloride ion and/or the competition between the parent PCA and the degradation products for $^{\bullet}OH$ radical. For the chlorinated decanes an increase in chlorine number decreased the percent transformation in the first 90 minutes from 70 to 59 % for Cl_5 to Cl_8, respectively (Figure 4.32).

Photodegradation of chlorinated undecanes (Figure 4.33) appeared to be inhibited by chlorine number. Degradation of chlorinated dodecanes (Figure 4.34) and trichlorodecanes (Figure 4.35) under the same conditions also showed the effect of chlorine number. Overall, aqueous solutions of 0.02 M H_2O_2 as a photooxidant are effective in degrading all of the PCA mixtures (C_{10}, C_{11}, C_{12} and C_{13}) (Figure 4.36) with 80% disappearance in 3 h of irradiation indicating the efficiency of aqueous solutions of (0.02 M) H_2O_2 as a photooxidant for PCAs.

4.3.3.1.1. Effect of $^{\bullet}OH$ Scavengers

The chlorinated decane mixtures were photolyzed with 0.02 M H_2O_2 in the presence and absence of 0.1M *tert*-butyl alcohol as $^{\bullet}OH$ radical scavenger. As expected (Figure 4.37) the degradation of chlorinated decanes was inhibited by 0.1M *tert*-butyl alcohol supporting free radical photooxidation of PCAs.

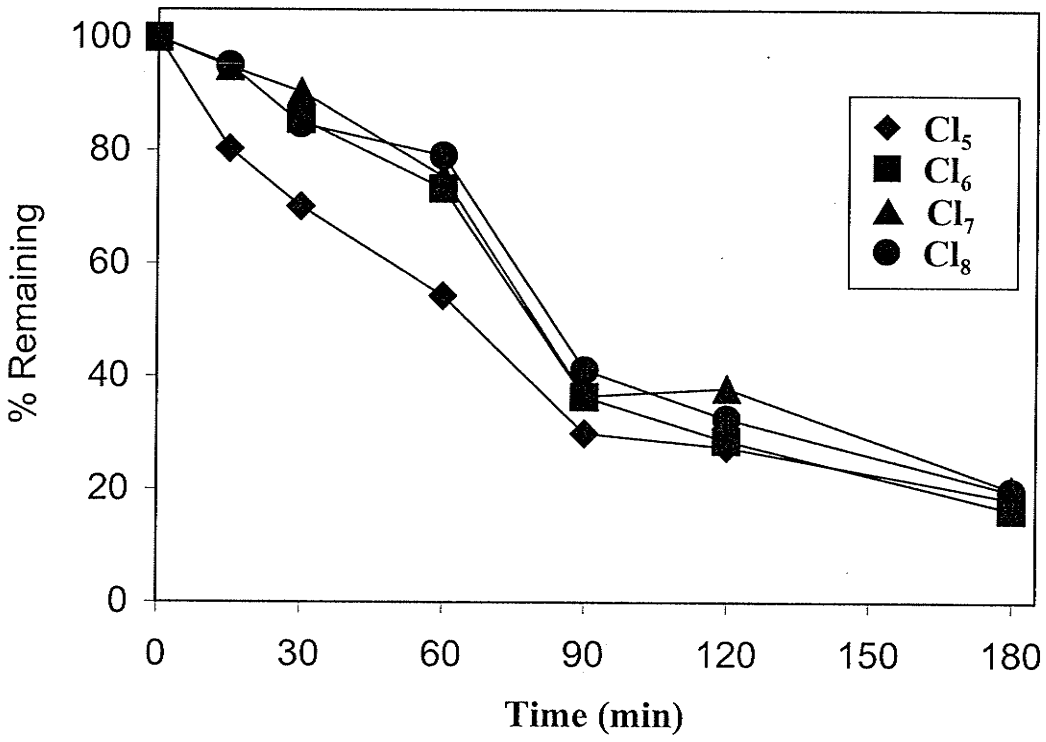

Figure 4.32: Homogeneous photodegradation of the chlorinated decane ($\Sigma C_{10}Cl_{5-8}$) mixture (250 μg/L) in Milli Q water in the presence of 2 $x10^{-2}$ M H_2O_2 in 0.1M$NaClO_4$ and pH 2.8 using 300 nm UV light.

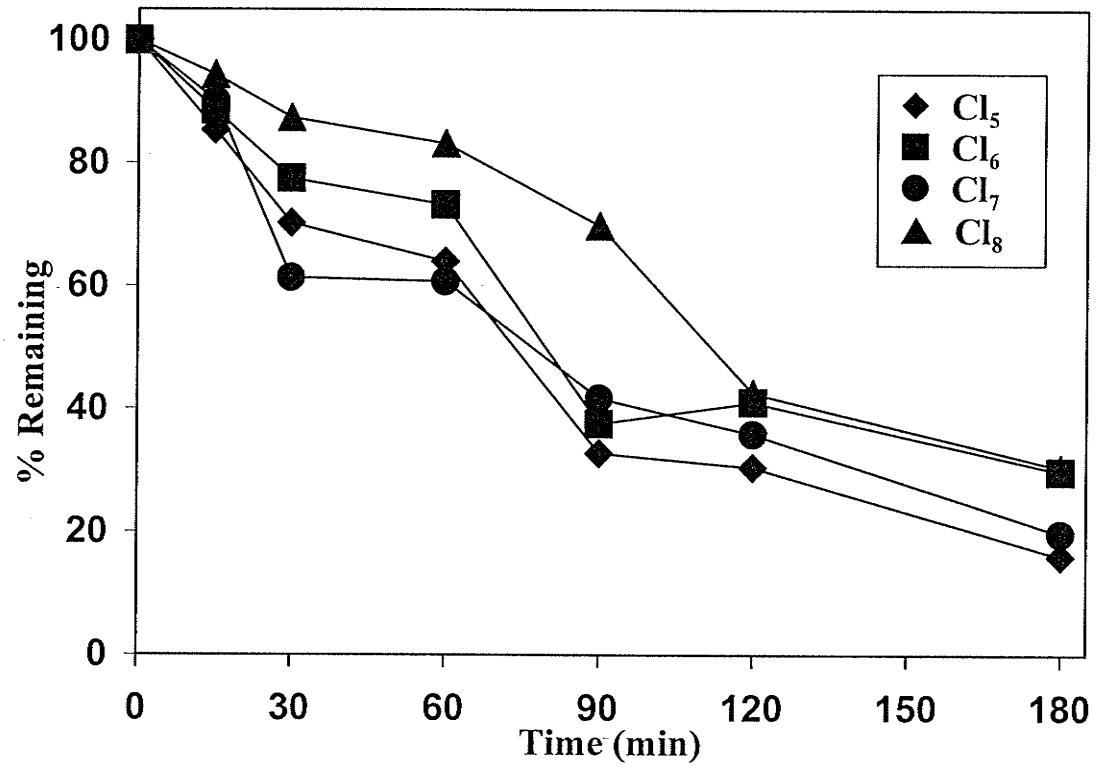

Figure 4.33: Homogeneous photodegradation of the chlorinated undecane ($\Sigma C_{11}Cl_{5\text{-}8}$) mixture (250 µg/L) in Milli Q water in the presence of 2 $x10^{-2}$ M H_2O_2 in 0.1MNaClO_4 and pH 2.8 using 300 nm UV light.

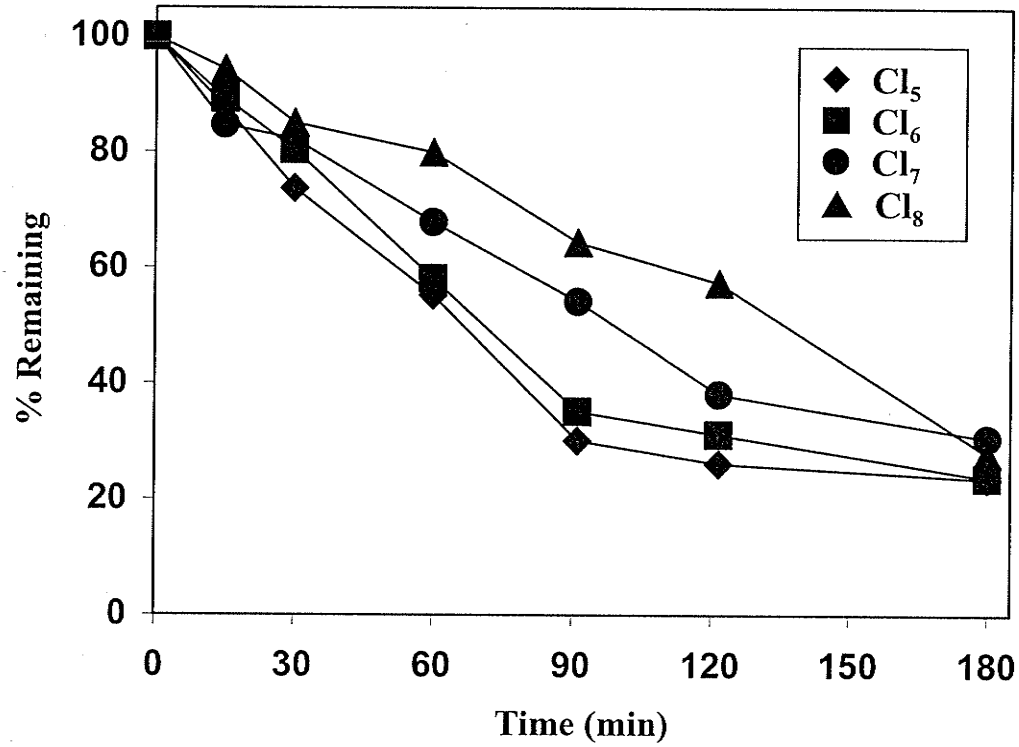

Figure 4.34: Homogeneous photodegradation of the chlorinated dodecane ($\Sigma C_{12}Cl_{5\text{-}8}$) mixture (250 µg/L) in Milli Q water in the presence of 2 $x10^{-2}$ M H_2O_2 in 0.1M$NaClO_4$ and pH 2.8 using 300 nm UV light.

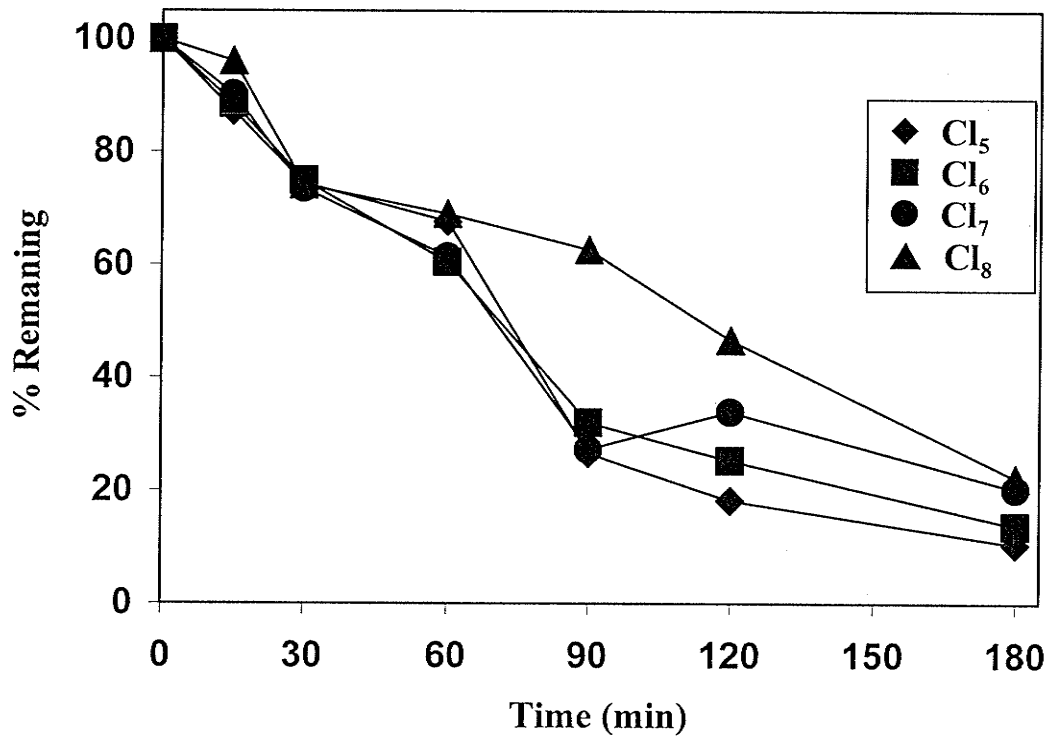

Figure 4.35: Homogeneous photodegradation of the chlorinated tridecane ($\Sigma C_{13}Cl_{5\text{-}8}$) mixture (250 μg/L) in Milli Q water in the presence of 2 $x10^{-2}$ M H_2O_2 in 0.1M$NaClO_4$ and pH 2.8 using 300 nm UV light.

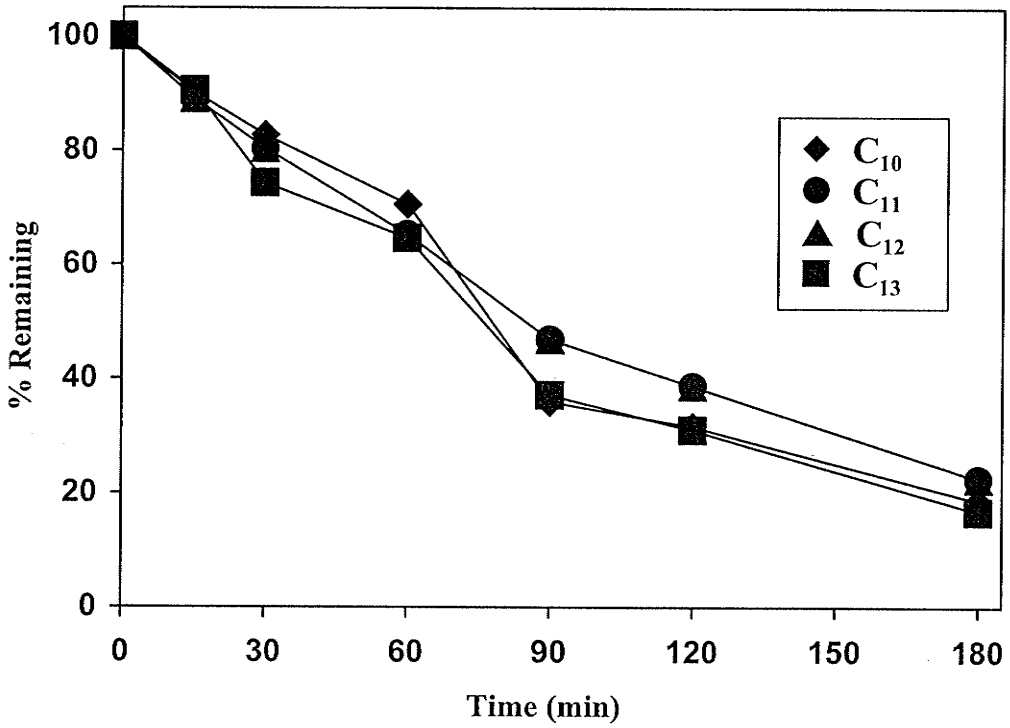

Figure 4.36: Homogeneous photodegradation of individual PCA mixtures ($\Sigma C_{10}Cl_{5\text{-}8}$ to $C_{13}Cl_{5\text{-}8}$) (250 µg/L) in Milli Q water in the presence of 2 $x10^{-2}$ M H_2O_2 in 0.1M$NaClO_4$ and pH 2.8 using 300 nm UV light.

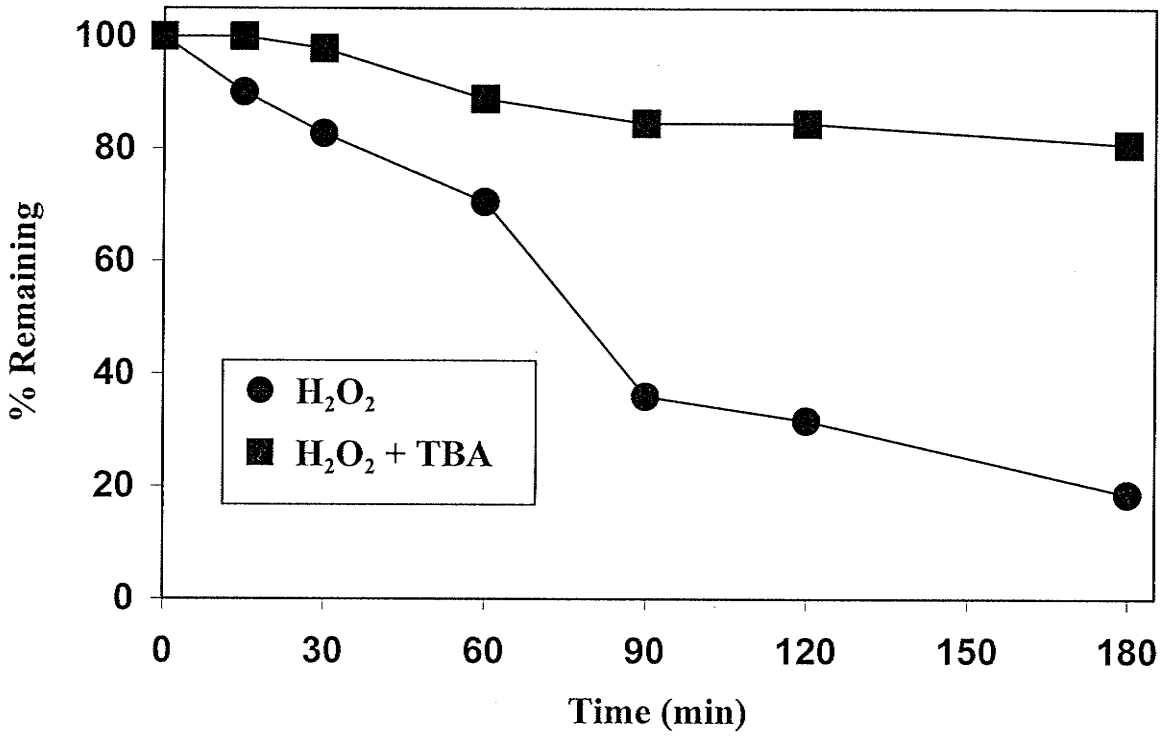

Figure 4.37: Effect of 0.1M *tert*-butyl alcohol on the photodegradation of the chlorinated decane ($\Sigma C_{10}Cl_{5\text{-}8}$) mixture (250 μg/L) in Milli Q water in the presence of 2 x10^{-2} M H_2O_2 in 0.1M$NaClO_4$ and pH 2.8 using 300 nm UV light.

4.3.3.1.2. The Effect of H_2O_2 Depletion

Decreasing the concentration of H_2O_2 to 0.001 M slowed the degradation of T_4C_{10}, due to the decreased concentration of $^{\bullet}OH$ radicals. Therefore, the depletion of H_2O_2 during the irradiation period is expected to slow down the reaction. This is supported by an observed increase in reaction rate upon addition of 0.01 M H_2O_2 after 60 min of irradiation (Figure 4.38). The dramatic increase in the degradation rate of the composite PCA mixture resulted from increased concentration of $^{\bullet}OH$ radical in the reaction medium. This result suggested that the degradation of PCA mixtures could be optimized by periodic addition of H_2O_2 during the reaction period.

4.3.3.2. H_2O_2/UV in Lake Water

Lake 375 water has been used to investigate the efficiency of the homogeneous photodegradation of PCA mixtures in natural water in the presence of 0.02 M H_2O_2. At pH 6.8, 0.02 M H_2O_2 was very effective in the degradation of PCA mixtures. The photodegradation of chlorinated decane (C_{10}), undecane (C11), dodecane (C_{12}) and tridecane (C_{13}) mixtures are shown in Figures 4.39 to 4.42. Although there is not a strong correlation between reactivity and the degree of chlorination, it appears that degradation slows as chlorine number increases. However, there was no clear trend in the effect of carbon chain length on the degradation rate as displayed in Figure 4.43.

The degradation of PCAs is slightly enhanced in lake water compared to Milli Q water as illustrated for the chlorinated decane mixture in Figure 4.44. This is attributed to sensitized photodegradation reactions in the natural water.

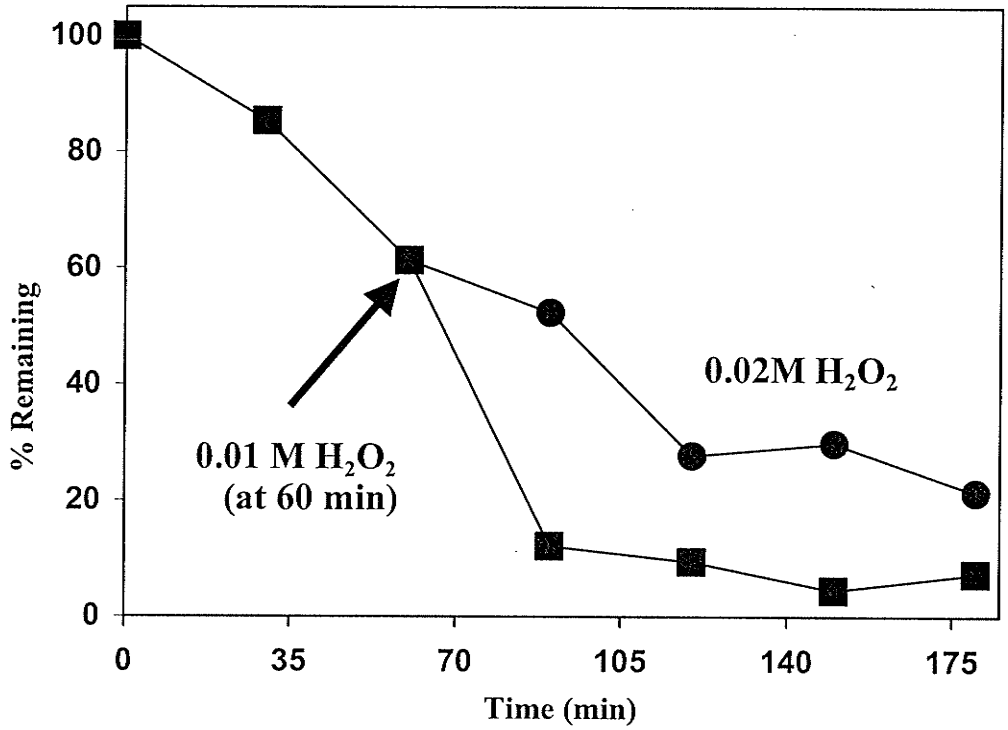

Figure 4.38: Enhancement of the degradation of the composite PCA mixture ($\Sigma C_{10}Cl_{5\text{-}8}$ to $C_{13}Cl_{5\text{-}8}$) (250µg/L) in Milli Q water with the addition of 0.01 M H_2O_2 after 60 min of irradiation.

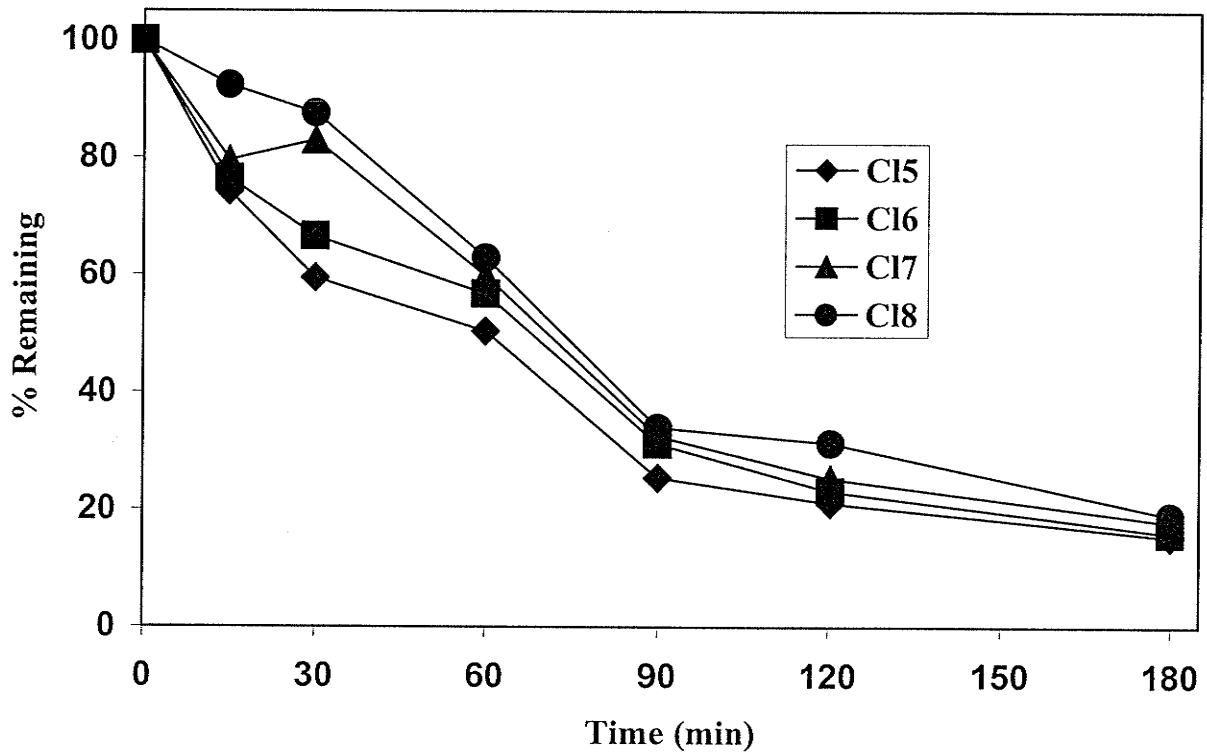

Figure 4.39: Homogeneous photodegradation of chlorinated congener groups in the chlorinated decane ($\Sigma C_{10}Cl_{5\text{-}8}$) (250 µg/L) mixture in Lake 375 water using 2 x10^{-2} M H_2O_2, 0.1 M $NaClO_4$ and pH 6.8 with 300 nm UV light.

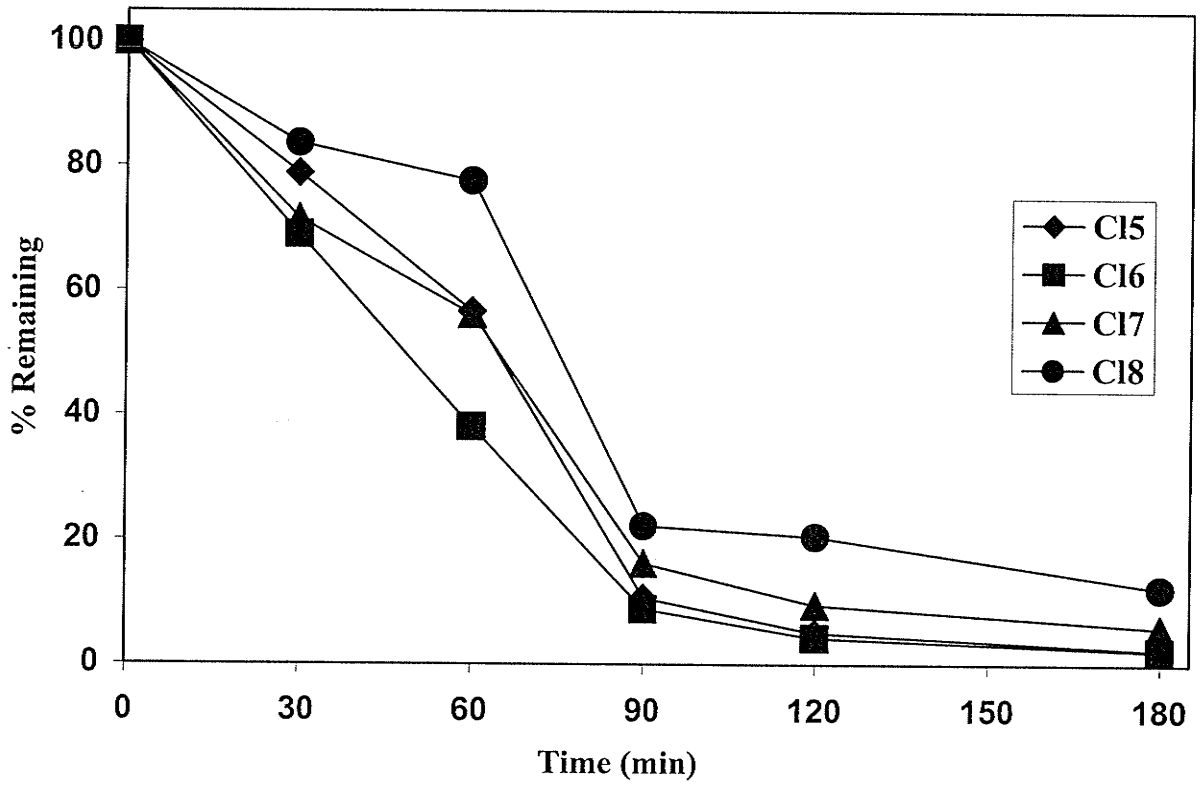

Figure 4.40: Homogeneous photodegradation of chlorinated congener groups in the chlorinated undecane ($\Sigma C_{11}Cl_{5\text{-}8}$) (250 µg/L) mixture in Lake 375 water using 2 x 10^{-2} M H_2O_2, 0.1 M $NaClO_4$ and pH 6.8 with 300 nm UV light.

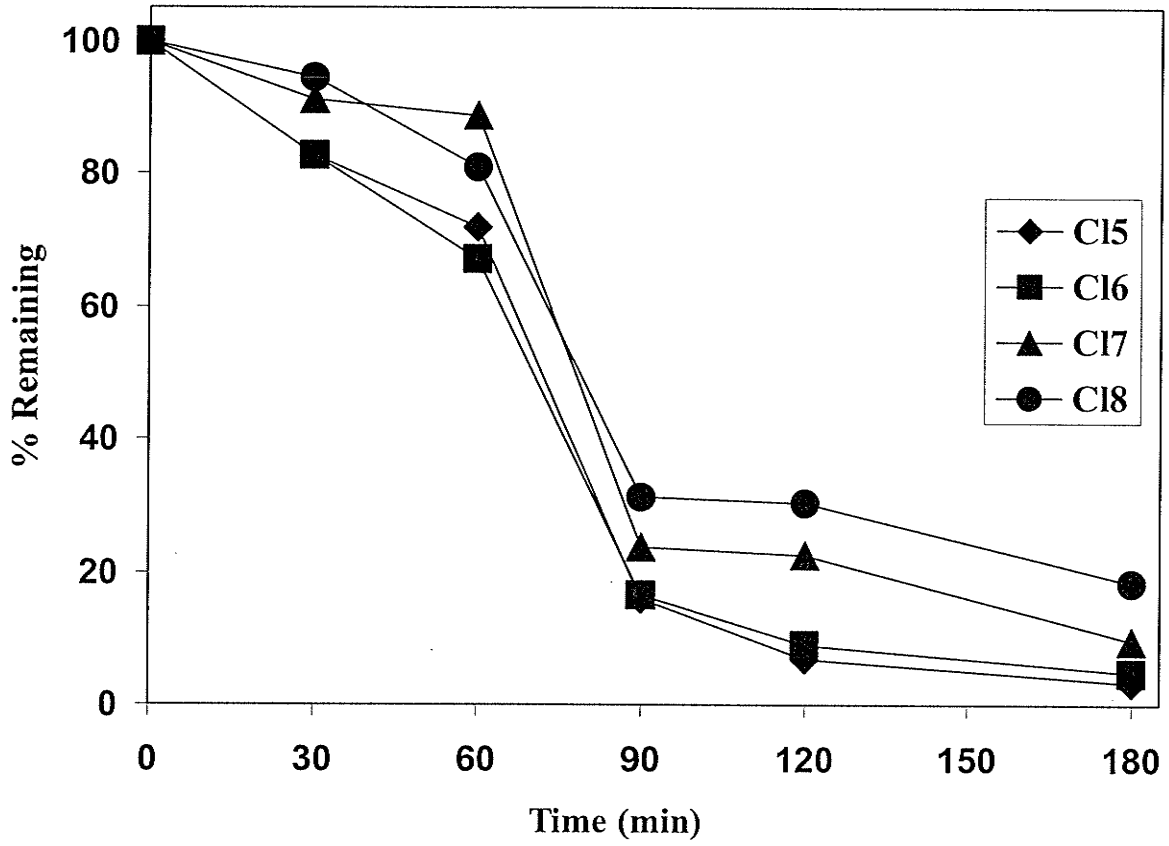

Figure 4.41: Homogeneous photodegradation of chlorinated congener groups in the chlorinated dodecane ($\Sigma C_{12}Cl_{5\text{-}8}$) (250 μg/L) mixture in Lake 375 water using 2 x10^{-2} M H_2O_2, 0.1 M $NaClO_4$ and pH 6.8 with 300 nm UV light.

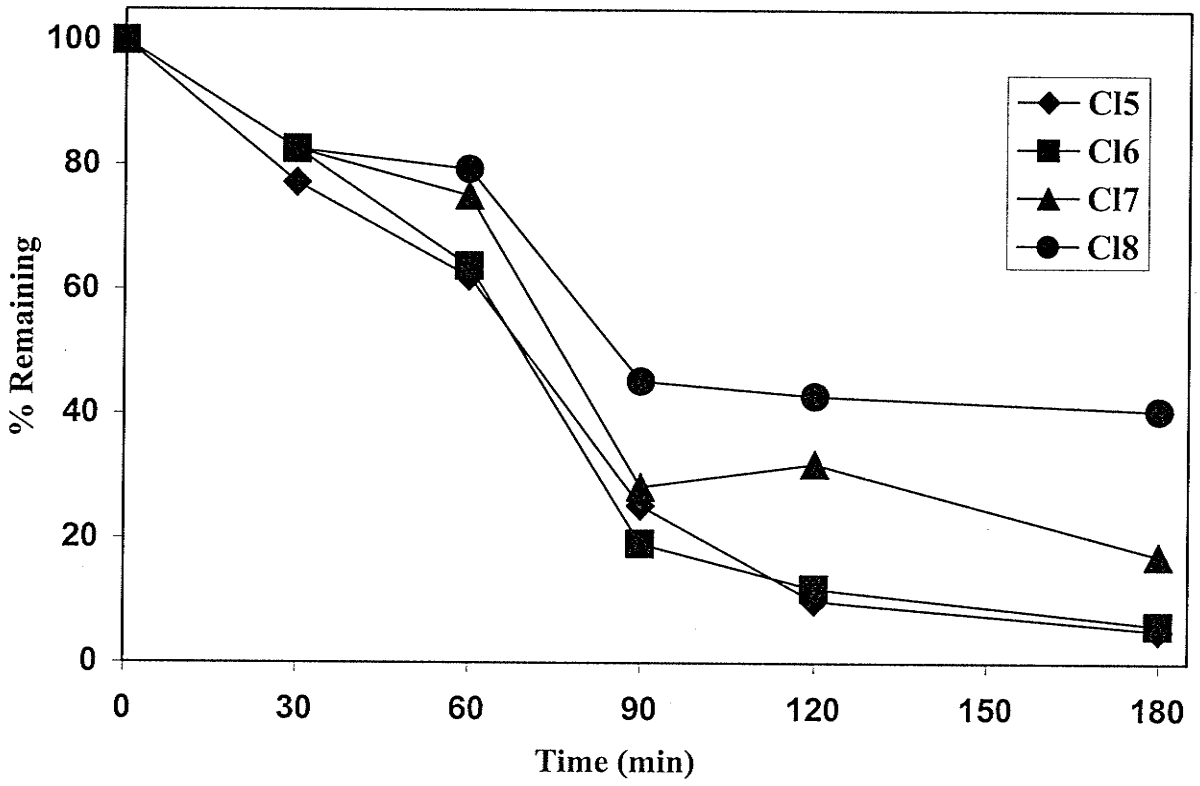

Figure 4.42: Homogeneous photodegradation of chlorinated congener groups in the chlorinated tridecane ($\Sigma C_{13}Cl_{5\text{-}8}$) (250 µg/L) mixture in Lake 375 water using 2 x10^{-2} M H_2O_2, 0.1 M $NaClO_4$ and pH 6.8 with 300 nm UV light.

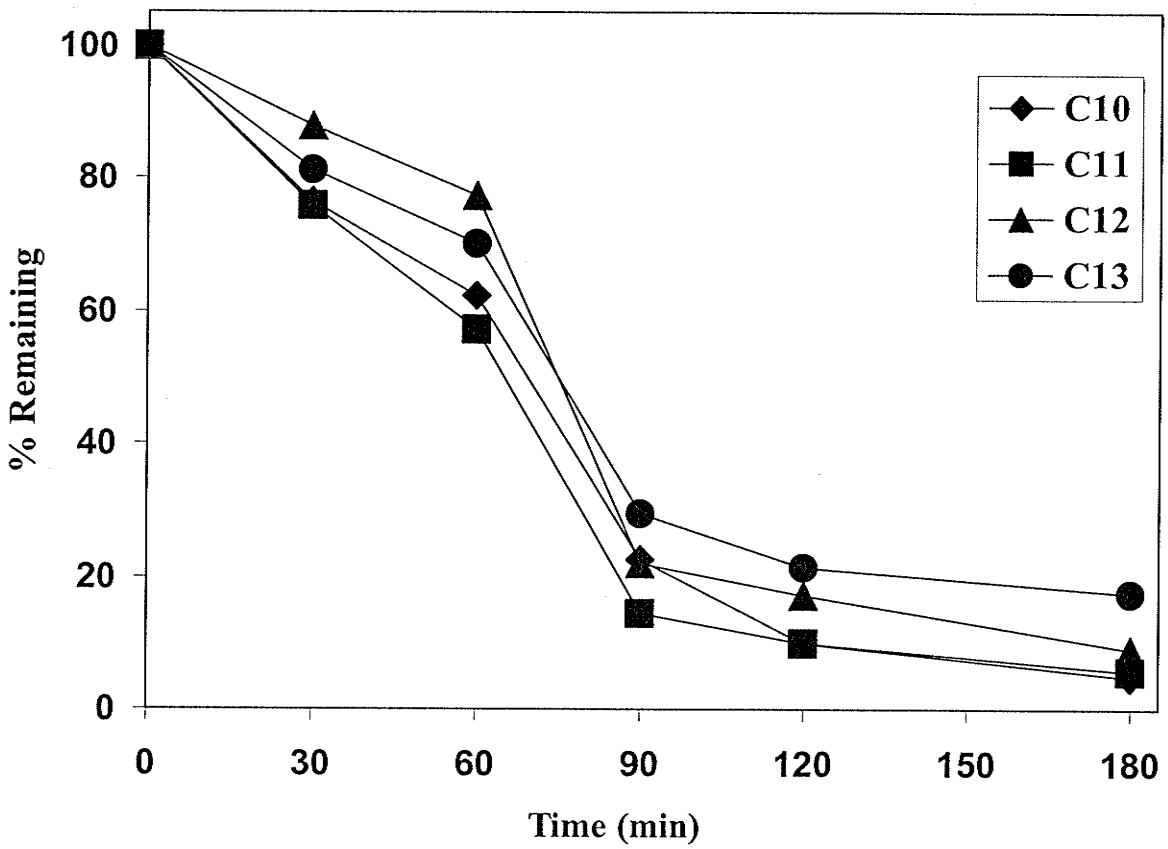

Figure 4.43: Homogeneous photodegradation of individual PCA (Σ $C_{10}Cl_{5\text{-}8}$ to Σ $C_{13}Cl_{5\text{-}8}$) mixtures (250 µg/L) in Lake 375 water using 2 x 10^{-2} M H_2O_2, 0.1 M $NaClO_4$ and pH 6.8 with 300 nm UV light.

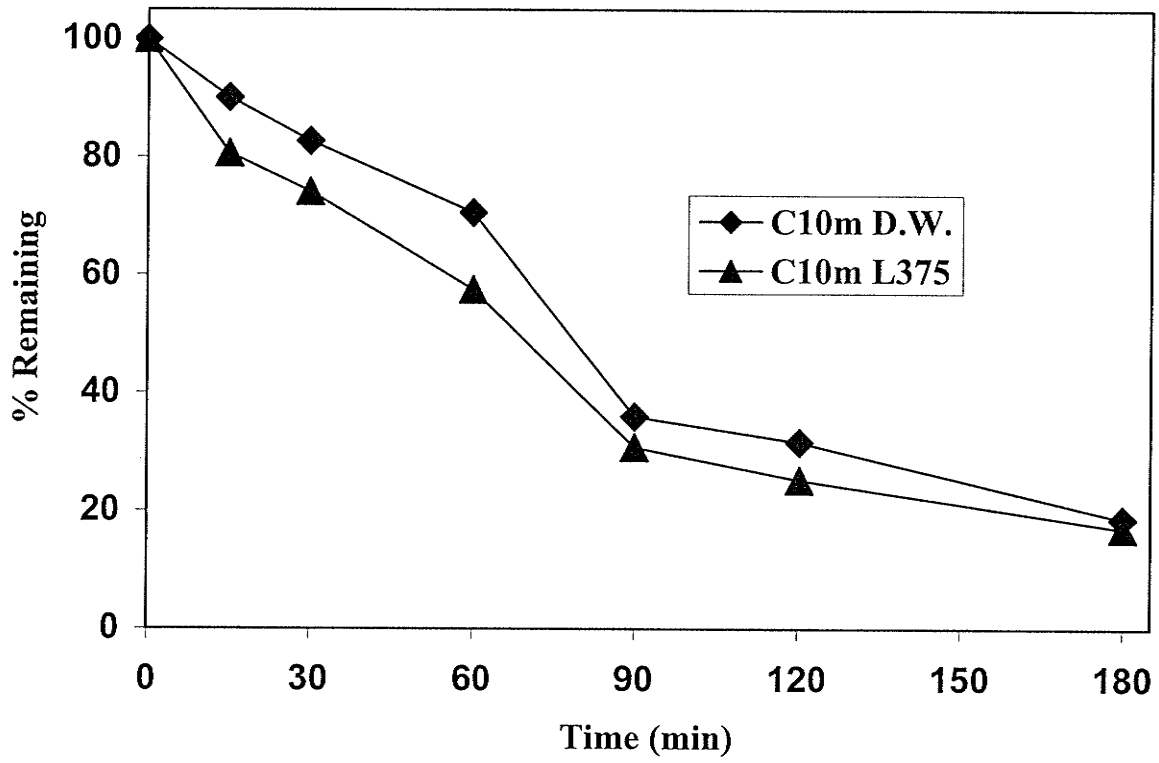

Figure 4.44: Homogeneous photodegradation of the chlorinated decane (Σ $C_{10}Cl_{5\text{-}8}$) mixture in Lake 375 and Milli Q water in the presence of 2 x 10^{-2} M H_2O_2 in 0.1 m $NaClO_4$ using 300 nm light.

4.3.3.3. Photo-Fenton Conditions in Pure Water

As discussed previously, modified photo-Fenton conditions often accelerate the decomposition of organic chemicals in water. In the presence of $1x10^{-3}$ M Fe^{+3} and 0.02 M H_2O_2 at pH 2.8, the photodegradation of all of the PCA mixtures are shown in Figures 4.45 to 4.48. Similar to results in H_2O_2 alone, there is a weak inverse correlation between reactivity and degree of chlorination. No clear correlation was observed between reactivity and carbon chain length as illustrated in Figure 4.49.

4.3.3.4. Photo-Fenton Conditions in Lake Water

PCA mixtures were irradiated in Lake 375 water using the same photo-Fenton conditions as for Milli Q water (Figures 4.50 to 4.53). It was noted that increased chlorine number again had a moderate effect on the degradation rate for C_{10} to C_{12} chain lengths. For the chlorinated tridecanes (C_{13}) all chlorine congener groups showed virtually the same degradation rate (Figure 4.53). Changes in carbon chain lengths did not have significant effects on reactivity as shown in Figure 4.54, since enhanced production of $^{\bullet}OH$ radicals by the photo-Fenton reaction decreased the competition between individual isomers of PCA for $^{\bullet}OH$. The results in Figure 4.55 indicate that transformation of PCA mixtures in Lake 375 water is moderately increased relative to Milli Q water. The decreased DOC in Lake 375 (compared to Lake Winnipeg) decreases the effects of light attenuation such that OH radical production is enhanced increasing photolytic degradation. Overall, the homogeneous photodegradation of PCA mixtures is enhanced significantly in the presence of modified photo-Fenton conditions due to enhanced production of OH radicals (Figure 4.56). PCAs do not degrade significantly

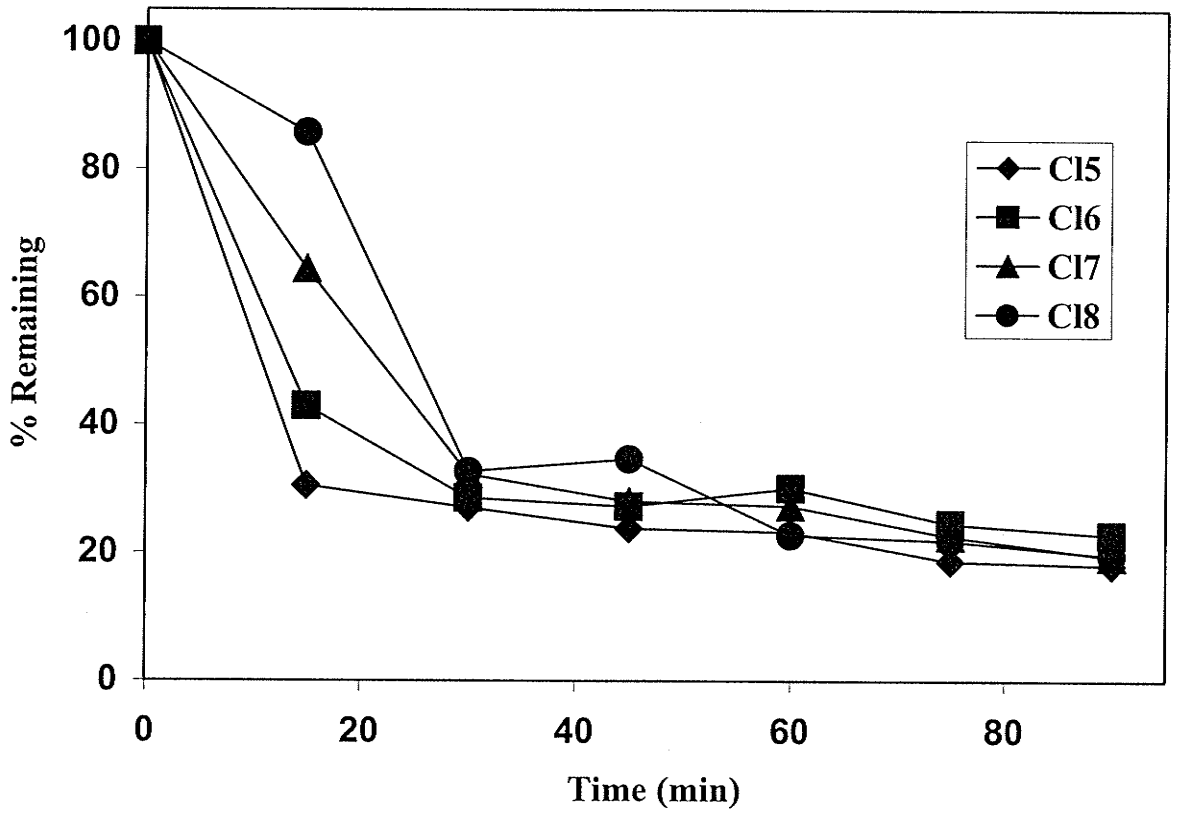

Figure 4.45: Homogeneous photodegradation of the chlorinated decane (Σ $C_{10}Cl_{5-8}$) (250 µg/L) mixture in Milli Q water under modified photo-Fenton (2 x 10^{-2} M H_2O_2/1x10^{-3} M Fe^{+3}) conditions in 0.1 M $NaClO_4$ and pH 2.8 using 300 nm UV light.

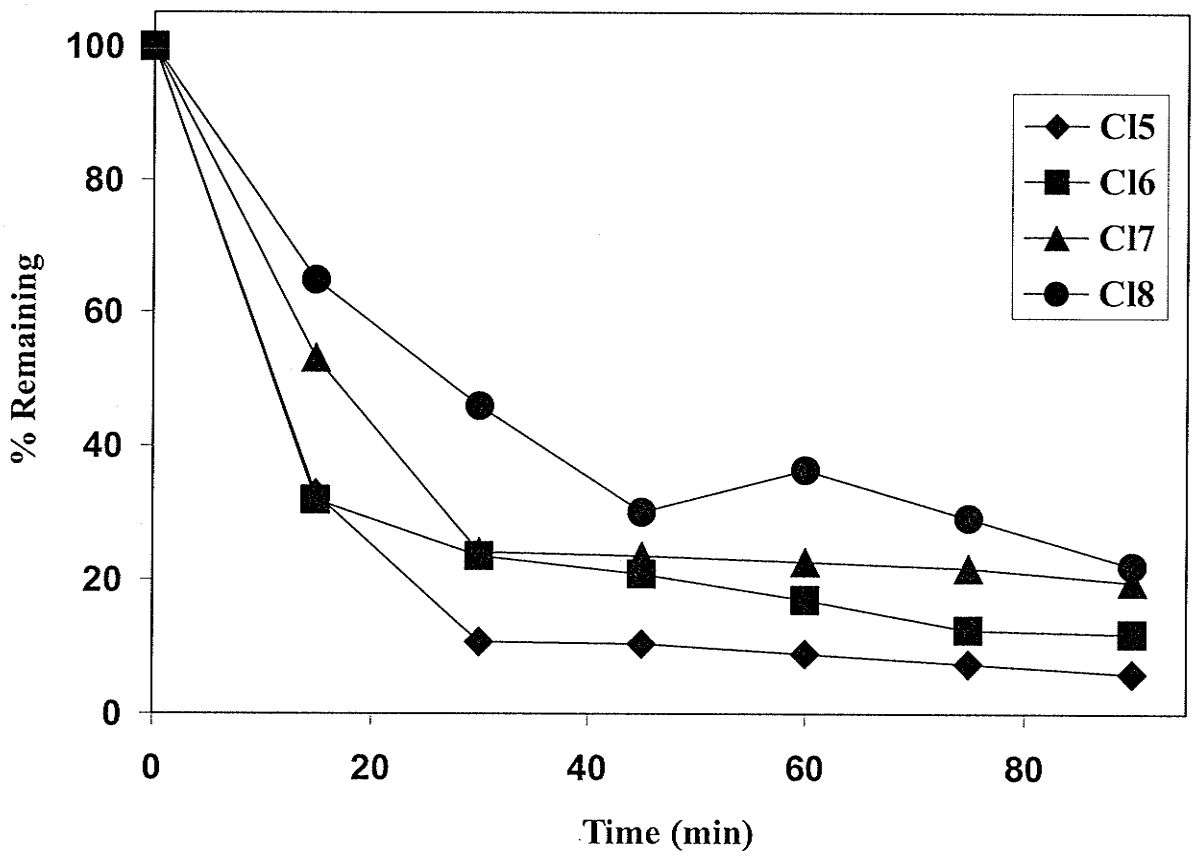

Figure 4.46: Homogeneous photodegradation of the chlorinated undecane (Σ $C_{11}Cl_{5\text{-}8}$) (250 μg/L) mixture in Milli Q water under modified photo-Fenton (2 x 10^{-2} M H_2O_2/1x10^{-3} M Fe^{+3}) conditions in 0.1 M $NaClO_4$ and pH 2.8 using 300 nm UV light.

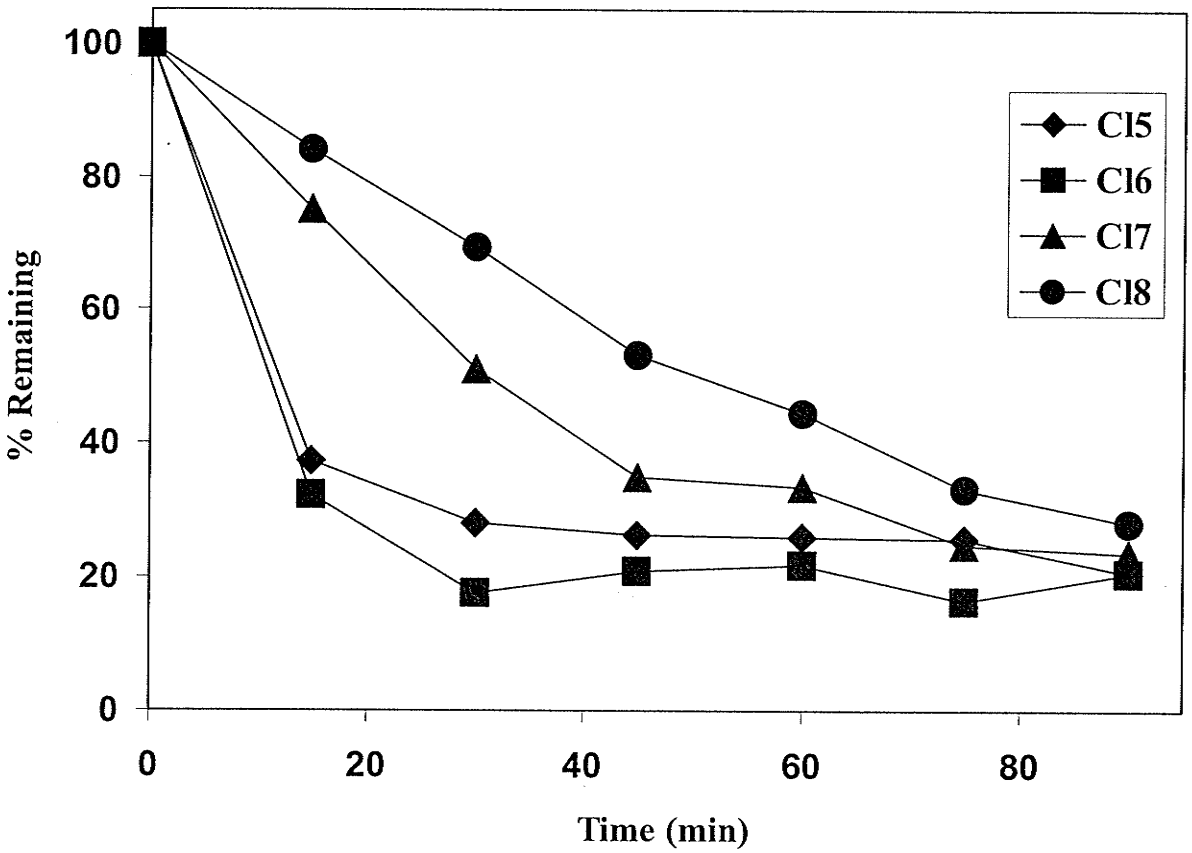

Figure 4.47: Homogeneous photodegradation of the chlorinated dodecane (Σ $C_{12}Cl_{5\text{-}8}$) (250 µg/L) mixture in Milli Q water under modified photo-Fenton (2×10^{-2} M H_2O_2/1×10^{-3} M Fe^{+3}) conditions in 0.1 M $NaClO_4$ and pH 2.8 using 300 nm UV light.

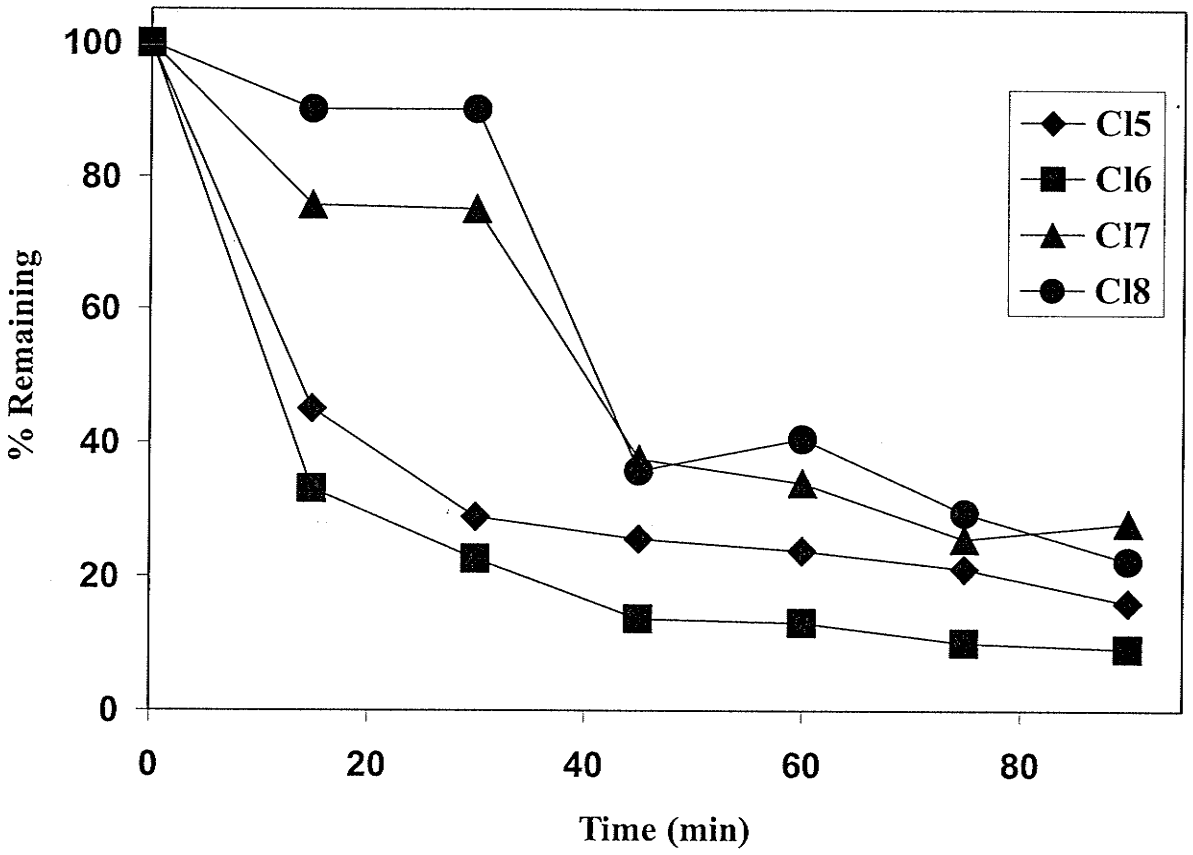

Figure 4.48: Homogeneous photodegradation of the chlorinated tridecane (Σ $C_{13}Cl_{5\text{-}8}$) (250 μg/L) mixture in Milli Q water under modified photo-Fenton (2 x 10^{-2} M H_2O_2/1x10^{-3} M Fe^{+3}) conditions in 0.1 M $NaClO_4$ and pH 2.8 using 300 nm UV light.

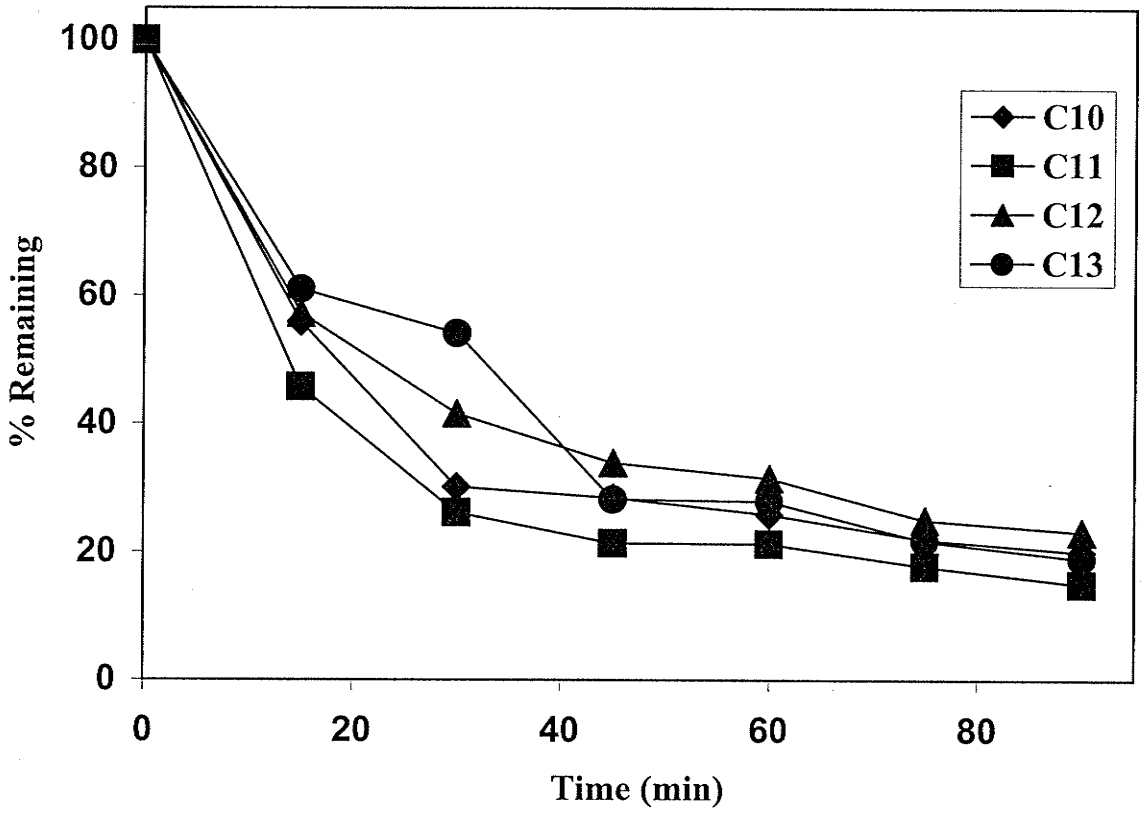

Figure 4.49: Homogeneous photodegradation of individual PCA mixtures (Σ $C_{10}Cl_{5\text{-}8}$ to Σ $C_{13}Cl_{5\text{-}8}$) (250 μg/L) in Milli Q water under modified photo-Fenton (2×10^{-2} M H_2O_2/1×10^{-3} M Fe^{+3}) conditions in 0.1 M $NaClO_4$ and pH 2.8 using 300 nm UV light.

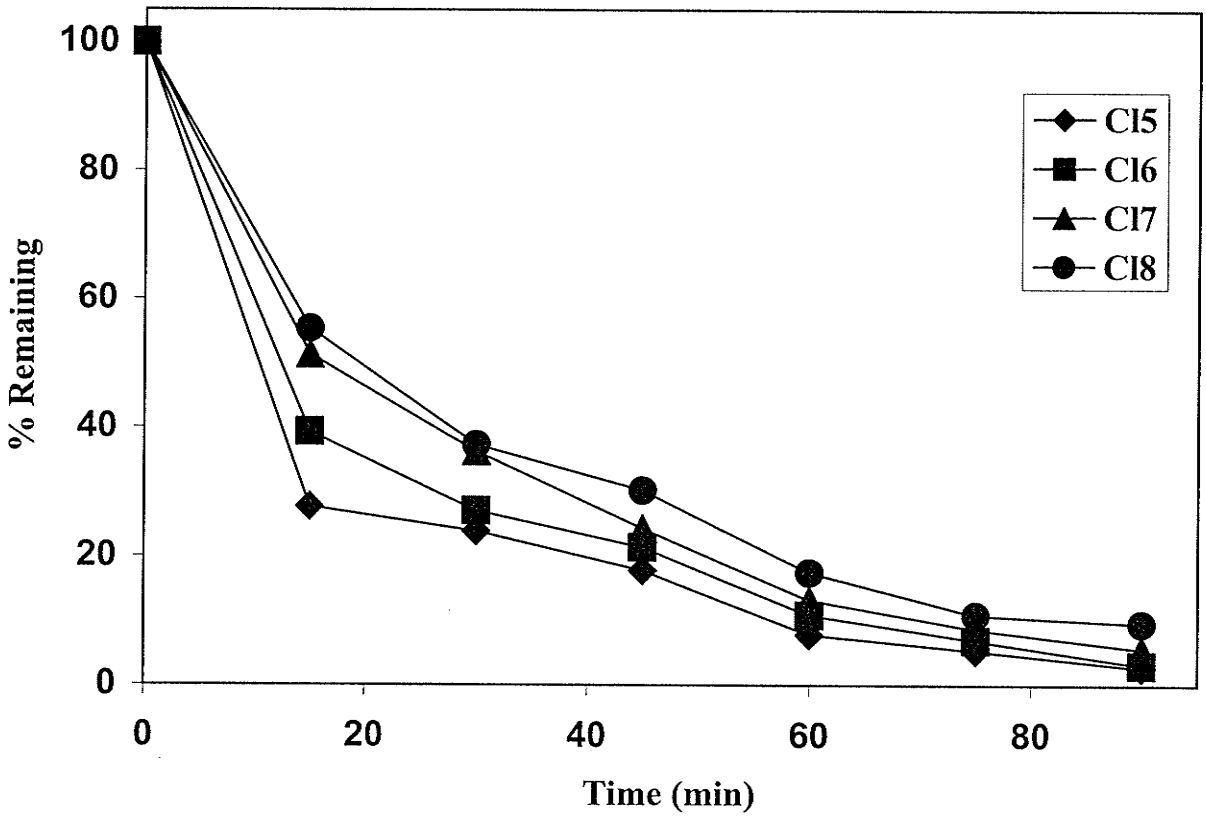

Figure 4.50: Homogeneous photodegradation of the chlorinated decane (Σ $C_{10}Cl_{5-8}$) (250 µg/L) mixture in Lake 375 water under modified photo-Fenton (2 x 10^{-2} M H_2O_2/1x10^{-3} M Fe^{+3}) conditions in 0.1 M $NaClO_4$ and pH 2.8 using 300 nm UV light.

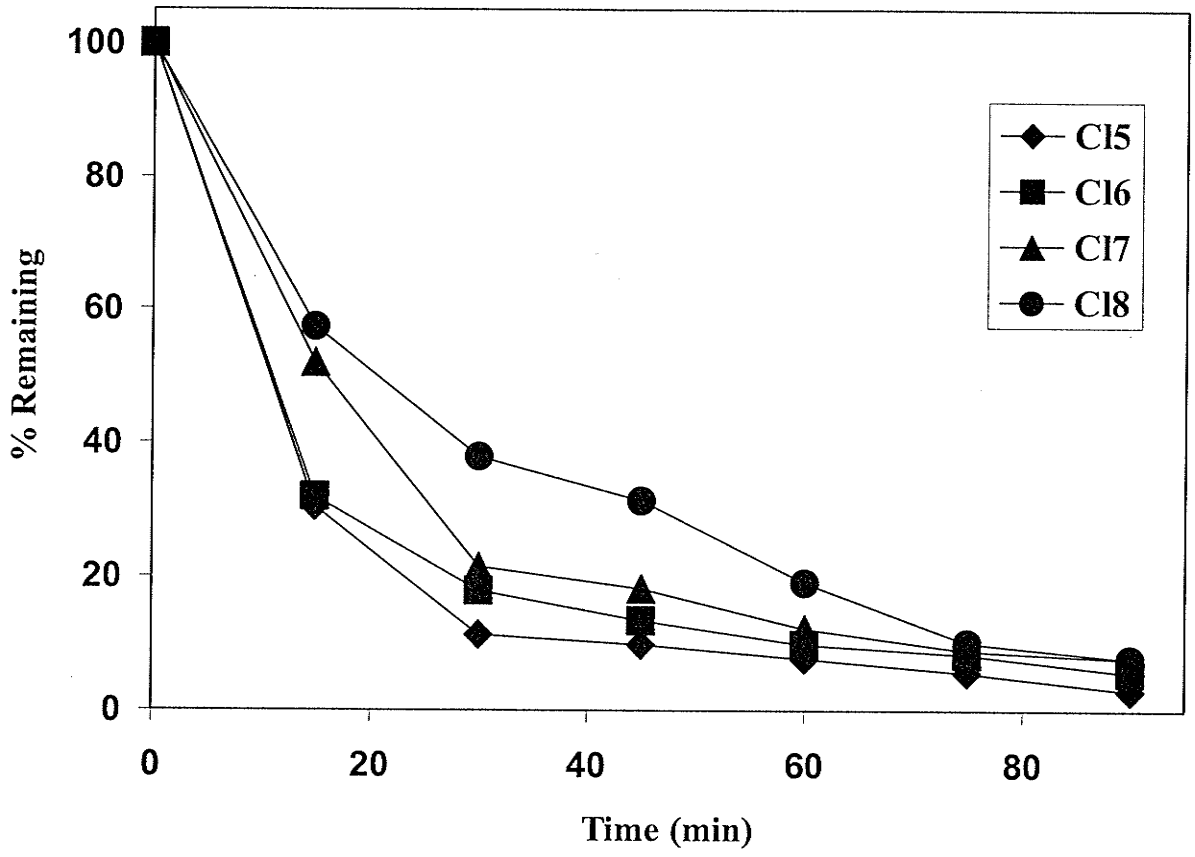

Figure 4.51: Homogeneous photodegradation of the chlorinated undecane (Σ $C_{11}Cl_{5\text{-}8}$) (250 μg/L) mixture in Lake 375 water under modified photo-Fenton (2 x 10^{-2} M H_2O_2/1x10^{-3} M Fe^{+3}) conditions in 0.1 M $NaClO_4$ and pH 2.8 using 300 nm UV light.

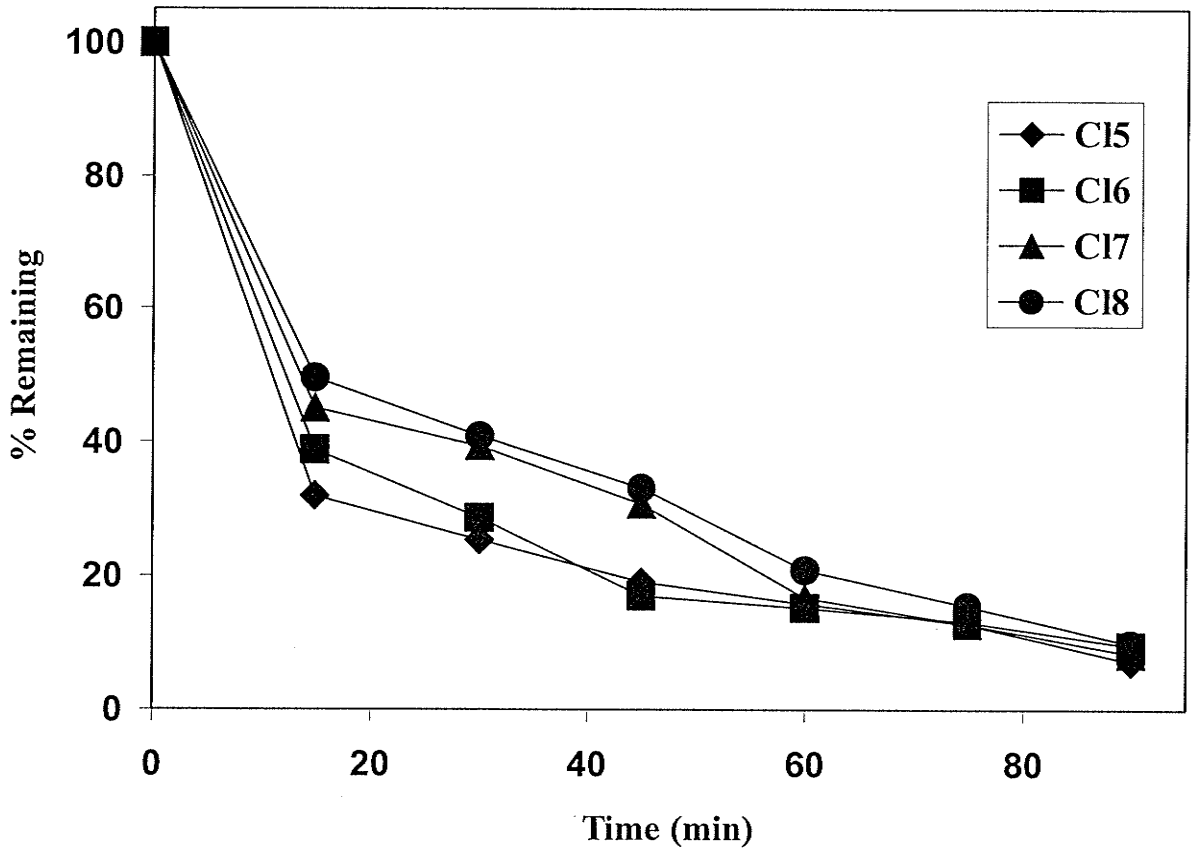

Figure 4.52: Homogeneous photodegradation of the chlorinated dodecane (Σ $C_{12}Cl_{5\text{-}8}$) (250 μg/L) mixture in Lake 375 water under modified photo-Fenton (2 x 10^{-2} M H_2O_2/1x10^{-3} M Fe^{+3}) conditions in 0.1 M $NaClO_4$ and pH 2.8 using 300 nm UV light.

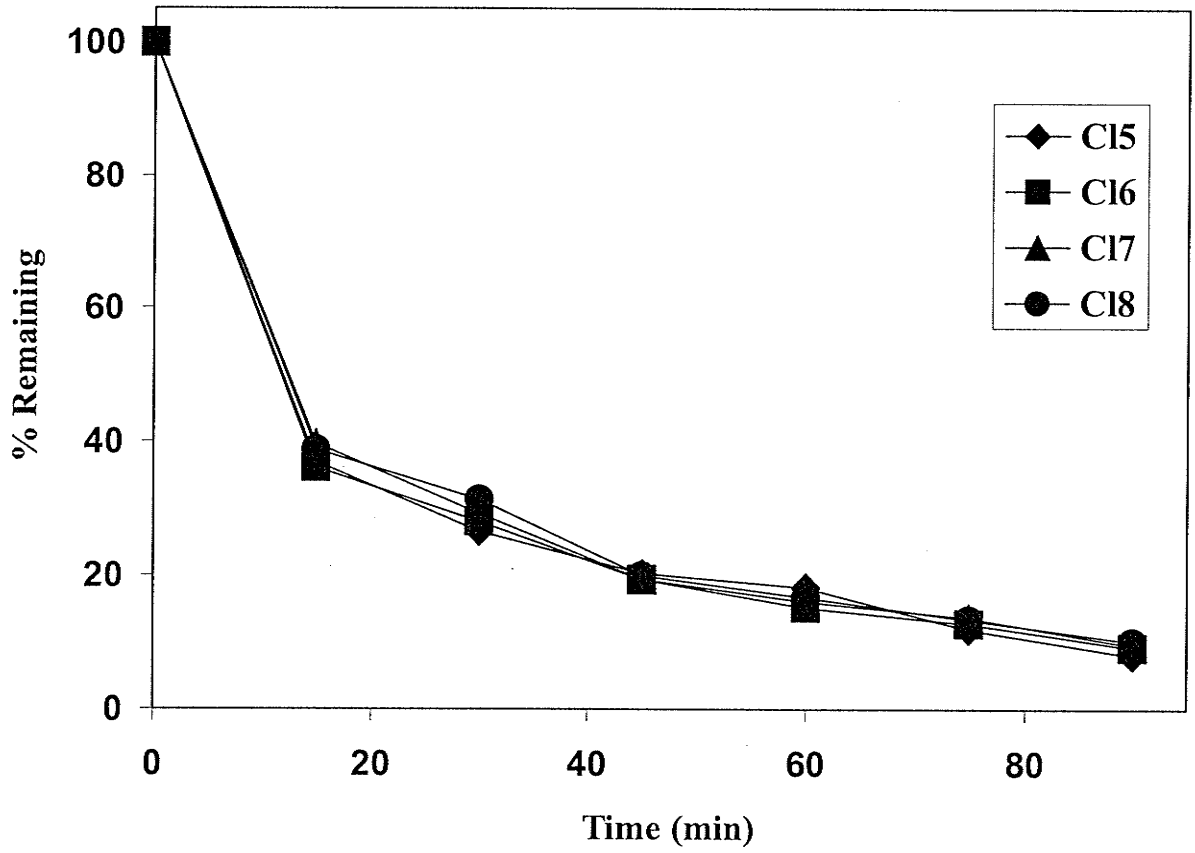

Figure 4.53: Homogeneous photodegradation of the chlorinated tridecane (Σ $C_{13}Cl_{5\text{-}8}$) (250 µg/L) mixture in Lake 375 water under modified photo-Fenton (2 x 10^{-2} M H_2O_2/1x10^{-3} M Fe^{+3}) conditions in 0.1 M $NaClO_4$ and pH 2.8 using 300 nm UV light.

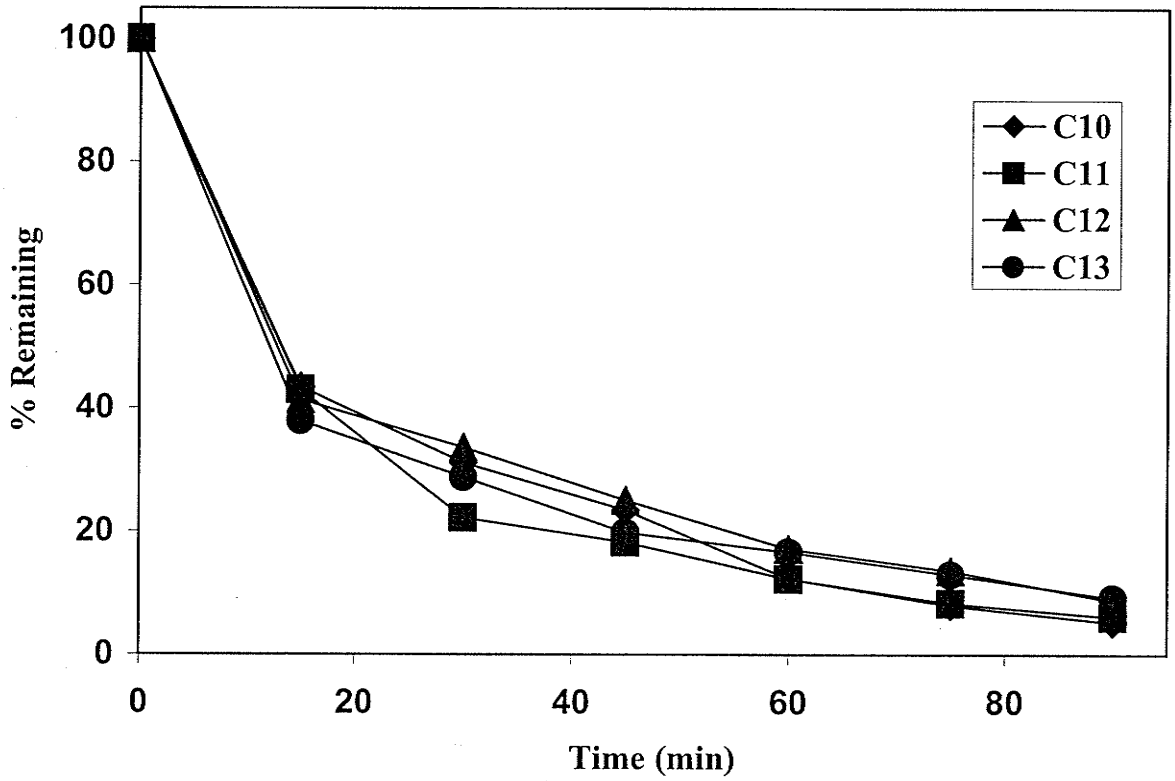

Figure 4.54: Homogeneous photodegradation of individual PCA mixtures ((Σ $C_{10}Cl_{5\text{-}8}$ to Σ $C_{13}Cl_{5\text{-}8}$) (250 μg/L) mixture in Lake 375 water under modified photo-Fenton (2 x 10^{-2} M H_2O_2/1x10^{-3} M Fe^{+3}) conditions in 0.1 M $NaClO_4$ and pH 2.8 using 300 nm UV light.

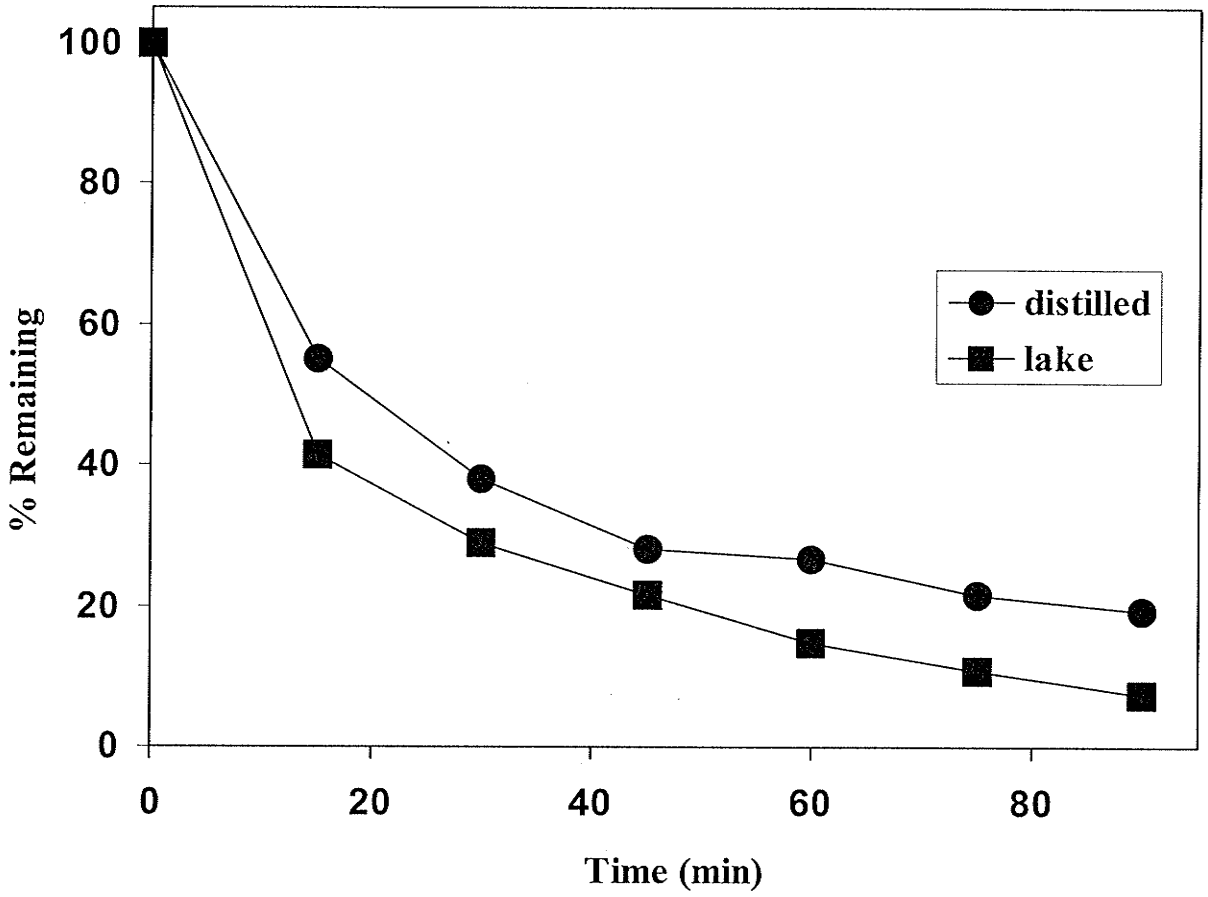

Figure 4.55: Degradation of the composite PCA (Σ $C_{10}Cl_{5\text{-}8}$ to Σ $C_{13}Cl_{5\text{-}8}$) (250 μg/L) mixture in Milli Q and Lake 375 water under modified photo-Fenton (2×10^{-2} M H_2O_2/1×10^{-3} M Fe^{+3}) conditions in 0.1 M $NaClO_4$ and pH 2.8 using 300 nm UV light.

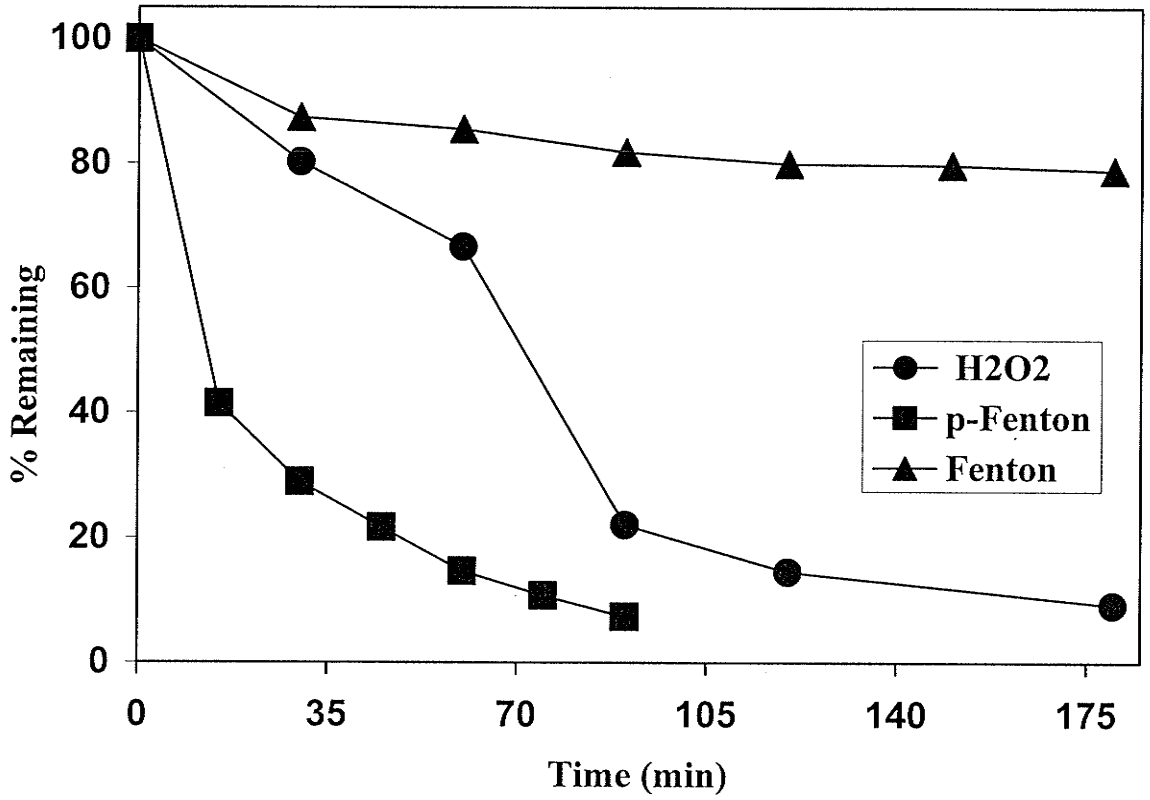

Figure 4.56: Homogeneous photodegradation of the composite PCA (Σ $C_{10}Cl_{5\text{-}8}$ to Σ $C_{13}Cl_{5\text{-}8}$) mixture (250 μg/L) in Lake 375 water in (H_2O_2/UV), Fenton (H_2O_2/Fe^{+3}) and modified photo-Fenton (H_2O_2/UV/Fe^{+3}) conditions in 0.1 M $NaClO_4$ and pH 2.8 using 300 nm UV light.

under Fenton conditions (H_2O_2/Fe^{+3}). Although PCAs are degraded in H_2O_2/UV, the reaction is much more effective under photo-Fenton conditions for these complex mixtures

4.3.10. By-Products of PCA Photooxidation with H_2O_2/UV

Although degradation products were not the emphasis of this study, the extent of dechlorination of PCAs and the total organic carbon were determined during the photodegradation reaction of T_4C_{10} and of a composite mixture of PCAs. Studies were carried out to determine if mineralization of PCAs occurred in the presence of H_2O_2/UV at pH 2.8.

For 1,2,9,10-tetrachlorodecane (T_4C_{10}) a near stoichiometric release of Cl^-, was observed with the ratio of $[Cl^-]/[T_4C_{10}]_o$ approaching 4 after 80 min of irradiation (Figure 4.57). The rate of Cl^- release was slower than the rate of degradation of T_4C_{10} as was evident with the $[Cl^-]/[T_4C_{10}]_o$ ratio which approached 2 within the time required for the T_4C_{10} to reach nondectable levels. The $[Cl^-]/[T_4C_{10}]_o$ ratio reached 4 approximately 30 min after complete disappearance of T_4C_{10}. The results are consistent with a pathway which includes formation of chlorinated organic intermediates which degrade more slowly than the parent tetrachlorodecane. Further Cl^- release, with the $[Cl^-]/[T_4C_{10}]_o$ reaching 4, is observed after longer irradiation times (80 min) as the intermediates are degraded.

Mineralization of PCA mixtures in Lake 375 water was studied by determining total organic carbon and chloride ion in the presence of 0.02 M H_2O_2 during the course of the reaction. Changes in total organic carbon during the photodegradation of PCA mixtures are shown in Figure 4.58. The results indicate that the photolysis of the PCA mixture results in more than 50% of the parent compound transformed in the first 60 min with 60% disappearance of total organic carbon. Furthermore, approximately 95% of

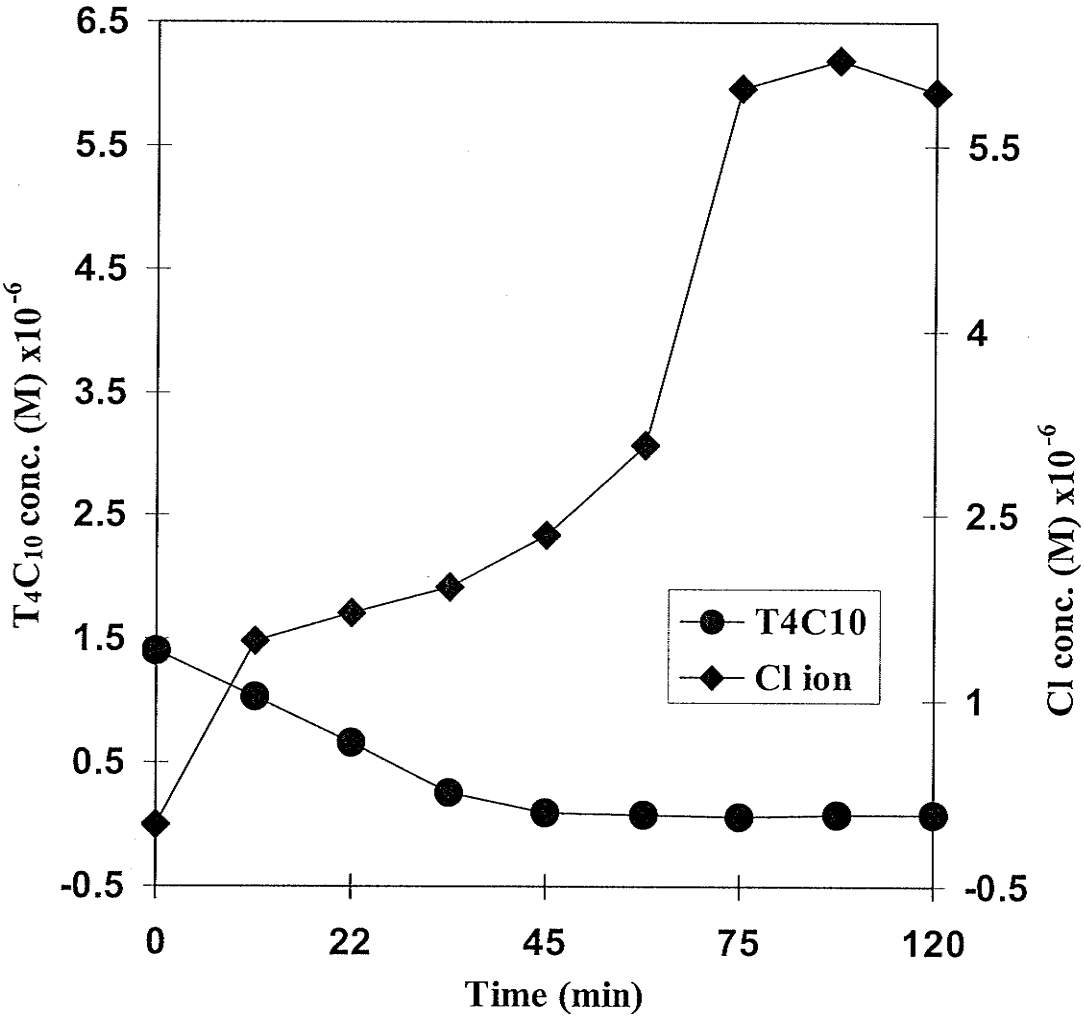

Figure 4.57: Dechlorination of 1,2,9,10-tetrachlorodecane during photolysis using 300 nm UV light in aqueous H_2O_2 solution ($1x10^{-2}$ M) containing 0.1M $NaClO_4$ at pH of 2.8.

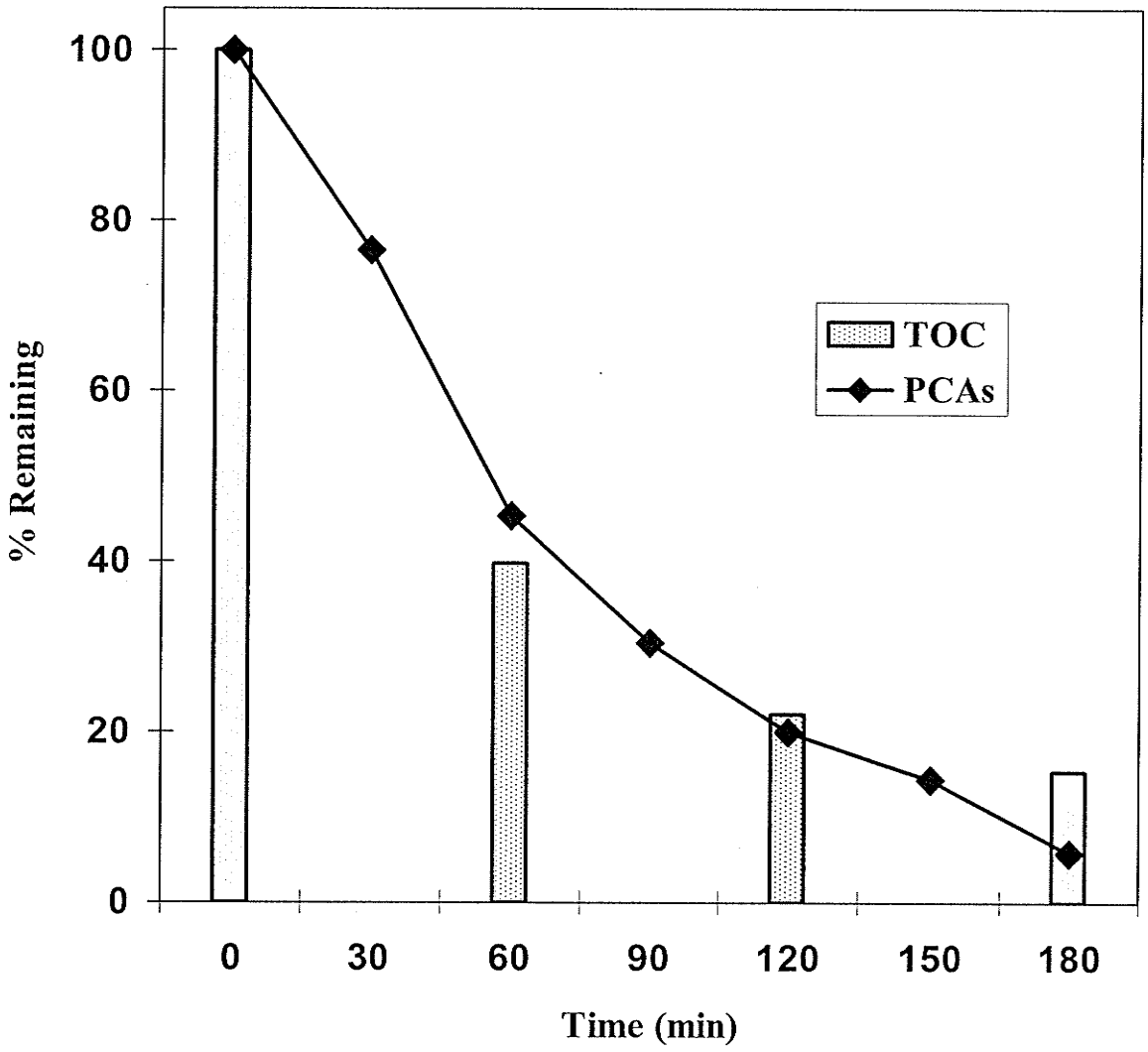

Figure 4.58: Changes in total organic carbon and parent PCA ($\Sigma C_{10}Cl_{5\text{-}8}$ to $\Sigma C_{13}Cl_{5\text{-}8}$) concentrations during photodegradation of PCA mixtures (250 μg/L) using 300 nm UV light in aqueous H_2O_2 solution ($2x10^{-2}$ M) in Lake 375 water at the natural pH of 6.8.

PCA mixture degraded in 3 h with approximately 85% of total organic carbon mineralized in the same time. This suggests the formation of degradation products which are more difficult to degrade than the parent PCAs. Selected ion monitoring (SIM) profiles (Figure 4.59) show the disappearance of the PCA mixture in lake water in the presence of 0.02 M H_2O_2 at different irradiation times.

Increased release of chloride ion and decreased total organic carbon during the reaction (Figure 4.60) provide additional evidence that the homogeneous photodegradation of PCA mixtures in aqueous solutions of H_2O_2/UV light results in near mineralization.

4.4. Conclusions

PCA isomers photooxidize rapidly in pure water using H_2O_2/UV with half-lives ranging from 9 to 24 min. Photolysis rates decreased with increasing dissolved organic carbon with half-lives up to 31 min in lake water (Lake Winnipeg) and 65 min in bog water. Modified photo-Fenton conditions (Fe^{3+}/H_2O_2/UV) proved to be the most effective method for the photodegradation of PCA isomers. For example, 79% disappearance of T_4C_{10} occurred in 20 min of irradiation in pure water; the rate increased slightly to 90% disappearance in lake water in the same irradiation period.

Although homogeneous photodegradation was effective for PCA mixtures, the degradation rates were observed to be slower compared to PCA isomers. For example, in pure water 80% disappearance of a composite mixture of PCAs occurred in 3 h in the presence of H_2O_2/UV. Photodegradation was again significantly enhanced using the modified photo-Fenton system (Fe^{3+}/H_2O_2/UV), with 75% disappearance of a composite mixture of PCAs in 1 h of irradiation. In lake water (Lake 375), the photodegradation of PCA mixtures was slightly enhanced in both H_2O_2/UV and Fe^{3+}/H_2O_2/UV systems. The

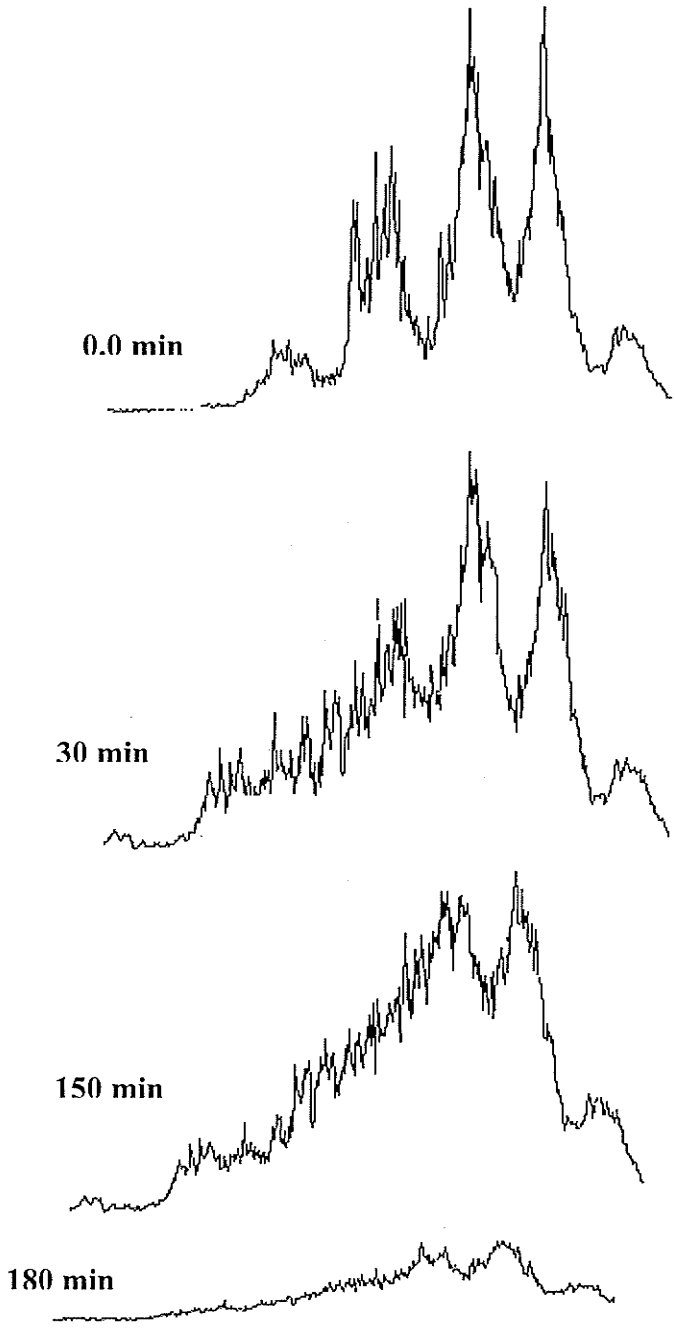

Figure 4.59: Photodegradation of the composite PCA mixture (Σ $C_{10}Cl_{5\text{-}8}$ to Σ $C_{13}Cl_{5\text{-}8}$) in Lake 375 water in the presence of ($2x10^{-2}$ M) H_2O_2 using 300 nm UV light.

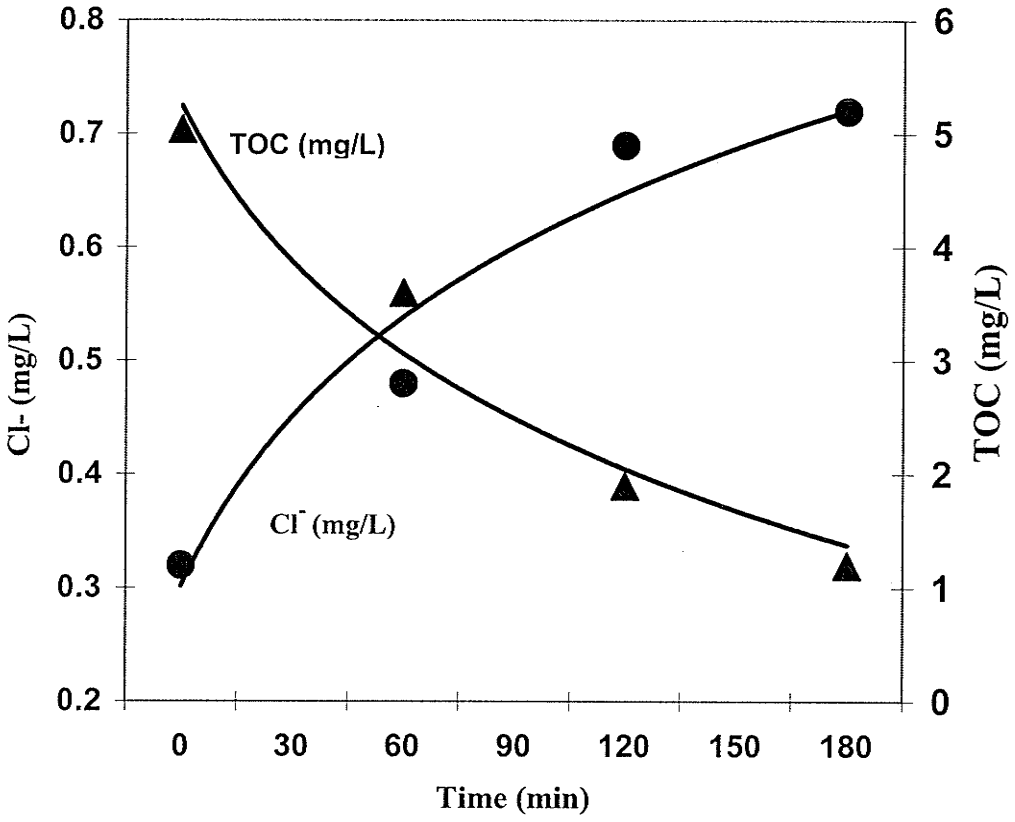

Figure 4.60: Release of chloride ion and disappearance of total organic carbon (TOC) during the photodegradation of the composite PCA mixture (Σ $C_{10}Cl_{5\text{-}8}$ to Σ $C_{13}Cl_{5\text{-}8}$) in Lake 375 water in the presence of ($2x10^{-2}$ M) H_2O_2 using 300 nm UV light.

dissolved organic and inorganic carbon levels in Lake 375 were less than in Lake Winnipeg, hence the effect of hydroxyl radical scavenging is decreased. The observed increased degradation rates may be due to the presence of natural sensitizers in the lake water.

Analysis of the extent of mineralization of the T_4C_{10} isomer indicated quantitative dechlorination in 80 min of irradiation in the H_2O_2/UV system. The slower rate of Cl^- release compared to the rate of degradation of T_4C_{10} suggested that the reaction involved formation of chlorinated organic intermediates which degraded more slowly than the parent tetrachlorodecane. For the composite PCA mixture the degradation of TOC was slightly slower than the disappearance of the parent PCAs. In 3 h of irradiation 93% chloride ion release and 85% TOC degradation suggested that PCA degradation is approaching complete mineralization.

Chapter 5

Heterogeneous Photocatalytic Degradation of Polychlorinated *n*-Alkanes using TiO_2 as a Photocatalyst

5.0. Introduction

Heterogeneous photocatalytic oxidation, in which a metal oxide semiconductor is activated by irradiation with near-UV and visible light, is another advanced oxidation process [269]. The light energy excites an electron from a bonding into an anti-bonding orbital in the solid, creating a hole in the valence band and an electron in the conduction band. The subsequent electron-hole pair, which is formed on the surface of the semiconductor, can degrade the contaminants by direct or indirect interaction [270-271]. The hydroxyl radical which is generated *in situ* at the surface of TiO_2 is the most important oxidizing agent in water due to its high reactivity. The hydroxyl radical reacts with organic chemicals either by addition (for aromatic and olefinic compounds), or by hydrogen abstraction (for saturated organics) producing a radical cation. The resulting radical can react with dissolved oxygen and begin a series of oxidative reactions. Chlorine and other halogens present in the organic chemicals are converted into inorganic halide ions [272].

5.1. Experimental Methods

5.1.1 Chemicals And Reagents

PCA isomers and mixtures were used as described in Chapter 2. Anatase TiO_2 (99.9%) and tetranitromethane were purchased from Aldrich Chemical Co. (Milwaukee,

WI USA). Silver nitrate, ferric nitrate, (supplied by BDH, Toronto, Canada) and copper nitrate (100%) (supplied by J.T. Baker, Phillipsburg, N.J USA) were used as received. Potassium iodide (99.0%) supplied by BDH and methanol (HPLC grade, 99.97%) supplied by EM Science (Gibbstown, NJ USA) were used as electron scavengers. Hydrogen peroxide (30%) was purchased from Mallinckrodt (Paris, KY USA). Oxygen, nitrogen and helium gases were supplied by BOC gases (Mississauga ON, Canada). All organic solvents used in the sample work-up and analysis were HPLC and/or spectrophotometric grade.

5.1.2. Preparation of Stock Solutions

A stock solutions of commercial (D_2C_{10} and D_2C_{12}) or synthesized isomers (T_4C_{10}, H_6C_{10} and T_4C_{11}) were prepared in 1:1 (v/v) Milli-Q water and acetonitrile as described in Chapter 2. While solutions of synthesized mixtures of PCAs (decanes, undecanes, dodecanes and tridecanes) were prepared in acetone. Aqueous solutions used for photocatalysis by TiO_2 were prepared by diluting microliter volumes of the stock solutions into water (containing 0.00015 (v/v) CH_3CN), with a final concentration of 240 μg/L for most isomers and mixtures. D_2C_{12} was prepared at a concentration of 20 μg/L due to its low water solubility [15]. All concentrations were below water solubility limits.

5.1.3. Photocatalysis in Pure Water

TiO_2 (150 mg/L) was suspended in the aqueous solution of the PCAs and pre-equilibrated for 15-20 min with stirring prior to photolysis. Under these conditions, solution pH was determined to be 5.4. To determine whether PCAs degraded by direct photolysis, corresponding experiments were conducted without the photocatalyst. Also, dark control experiments in the presence of TiO_2 were performed to check for thermal degradation. Photocatalysis experiments were carried out in 50 mL Pyrex centrifuge

tubes with a Rayonet Photochemical Reactor equipped with a carousel and 16 RPR 300 nm lamps [273]. Emission intensities of 3.6×10^{-5} Ein $\bullet L^{-1}$ min^{-1} were established by ferrioxalate actinometry. In both direct UV photolysis (without TiO_2) and photocatalysis (with TiO_2 and UV) experiments, the photolysis tubes were filled with 40 mL aliquots of the samples and irradiated. Samples were typically removed after irradiation times of 0, 10, 20, 30, 40, 50, 60, 90, 120 and 180 min. For most solutions, control experiments were performed to determine the extent of thermal degradation.

After irradiating for a specified time, samples were removed and solutions transferred to separatory funnels and extracted once with 60 mL of hexane. The extraction efficiencies are summarized in Table 3.1 for all isomers. After extraction, samples were rotoevaporated to 10 mL and transferred to 15 mL centrifuge tubes. Lindane was added as an internal standard (15 ng/μL) and the solutions were concentrated to 150 μL under nitrogen gas for analysis by GC/MS.

5.1.4. Addition of Modifiers

In experiments with modifiers or scavengers such as silver nitrate, methanol, and tetranitromethane, the procedure was altered slightly. These modifiers or scavengers were added to water prior to introduction of PCAs or TiO_2. Once the modifier was added, procedures followed that outlined above. When gases were used, the solutions were purged with the selected gas for 30 to 50 min prior to addition of any other substances. The photolysis and analysis procedures were then identical to those described in previous Chapter. In experiments with acetonitrile as solvent, a 20 min sonication period was required to form the necessary TiO_2 suspension. Once sonication was complete, D_2C_{10}

was added, and photolysis and analysis proceeded as above. Most experiments were run in duplicate unless otherwise reported.

5.1.5. Adsorption

Adsorption studies were performed by allowing PCAs to equilibrate in aqueous suspensions of TiO_2 with stirring for specified periods of time under dark conditions. Once the appropriate time had elapsed, two 40 mL aliquots were centrifuged (2000 rpm for 40 min) in 50 mL Pyrex centrifuge tubes. The clear supernatant was removed by pipet and extracted with 50 mL of hexane as described above. The mass of PCAs sorbed to TiO_2 was generally determined by mass balance. However, for several solutions the solid was analyzed directly to confirm sorption of PCAs to TiO_2. In these cases TiO_2 was resuspended in clean Milli-Q water after withdrawing the original supernatant. The suspensions were filtered through 0.22 μm Millipore filters, and the filters were Soxhlet extracted with 180 mL of hexane for approximately 4 h. Lindane was added and the solutions were concentrated and transferred to glass inserts for analysis as described above.

5.1.6. Photolysis of Adsorbed PCAs

To investigate the effect of adsorption on photolysis, solutions were equilibrated in aqueous suspensions of TiO_2 with stirring under dark conditions. After sorption times of (7.3, 19, 69, 158 and 186 h), samples (40 mL) were irradiated in the Photoreactor. Duplicate samples (40 mL) were removed periodically (0, 10, 20, 30, 40, 50 and 60 min) to follow the course of photodegradation.

5.1.7. Photolyses in Natural Water

Natural waters (Lake Winnipeg and bog water) were filtered through glass fiber filters (as described previously) to remove suspended particles. All photocatalysis experiments in natural water were conducted at the natural pH of 8.3 (lake water) and 8.6 (bog water). The effect of pH was determined by also performing experiments at pH 5.4, the pH of suspended TiO_2 in pure water.

5.2. Analyses

A Hewlett-Packard (HP) 5890 series II gas chromatograph, fitted with a 30 m x 0.25 mm x 0.25 μm high resolution column (Supelco), equipped with a HP 5989A Mass Selective Detector was for analysis. PCA isomers were analyzed using EI- MS, while PCA mixtures were characterized in NCI mode. The column temperature program and the total time were described in Chapter 2.

Oxygen: Determination of the concentration of dissolved oxygen (ppm) in the aqueous solutions utilized a YSI Model 57 Oxygen meter, equipped with an oxygen electrode. The meter was calibrated using air saturated water at room temperature.

5.3. Results and Discussion

5.3.1. Determination of the Optimal Conditions for D_2C_{10} in Pure Water

5.3.1.1. Optimum Photocatalyst Concentration

The photocatalytic degradation of D_2C_{10} (240 μg/L) with varying concentration of TiO_2 (37.5 mg/L, 100 mg/L, 150 mg/L, and 300 mg/L) are summarized in Table 5.1. Photolysis rates reached a maximum at a TiO_2 concentration of 150 mg/L. The increase in the degradation rate with increases in TiO_2 concentrations up to 150 mg/L is attributed

Table 5.1: Photocatalytic degradation rate constants (k) for D_2C_{10} (240 μg/L) with different concentrations of TiO_2 at pH 5.4 using 300 nm UV light

TiO_2 (mg/L)	k (min^{-1})
37.5	0.026 ± 0.002
100	0.029 ± 0.003
150	0.042 ± 0.002
300	0.033 ± 0.002

to the increasing supply of redox species, e^-_{cb} and h^+_{vb} which are available active sites at which D_2C_{10} degradation occurs [274]. As the concentration of TiO_2 increased to 300 mg/L the solutions became more opaque, and the total light penetration decreased. These light attenuation effects [275-276] reduced the formation of active sites [216], leading to decreased rates of degradation of D_2C_{10}. On the other hand decreasing the amount of TiO_2 to 37.5 mg/L lowered the total number of active sites provided by the photocatalyst, thereby slowing the degradation rate. Hence in subsequent experiments the optimum concentration (150 mg/L) was used.

5.3.1.2. Optimum Substrate Concentration

At a constant concentration (150 mg/L) of TiO_2, the effect of D_2C_{10} concentration was investigated by photolyzing solutions with D_2C_{10} concentration of 120 μg/L, 150 μg/L, 180 μg/L and 240 μg/L. Photodegradation rates increased as the initial concentration of D_2C_{10} increased as shown in Table 5.2. Increasing the concentration of the substrate in the solution increased its amount on the surface of the photocatalyst. Thus, the active sites are degrading more substrate through increased contact with the photocatalyst [277]. The concentration of D_2C_{10} was not increased past 240 μg/L due to its water solubility limit of 257 μg/L [278]. Therefore, in all subsequent experiments the TiO_2 concentration was maintained at 150 mg/L and the initial concentration of the substrates (PCA isomers and mixtures) were from 240 to 250 μg/L.

3.3.2. Photocatalysis of PCA Isomers

The photocatalytic degradation of 240 μg/L of D_2C_{10} with 150 mg/L of TiO_2 was relatively rapid with 62% disappearance in 15 min of irradiation as shown in Figure 5.1. A dark control showed no significant change in concentration over the photoperiod

Table 5.2: Photocatalytic degradation rate constants (k) for different concentrations of D_2C_{10} with 150 mg/L TiO_2 at pH 5.4 using 300 nm UV light

D_2C_{10} (μg/L)	k (min^{-1})
120	0.032 ± 0.002
150	0.034 ± 0.005
180	0.036 ± 0.003
240	0.042 ± 0.002

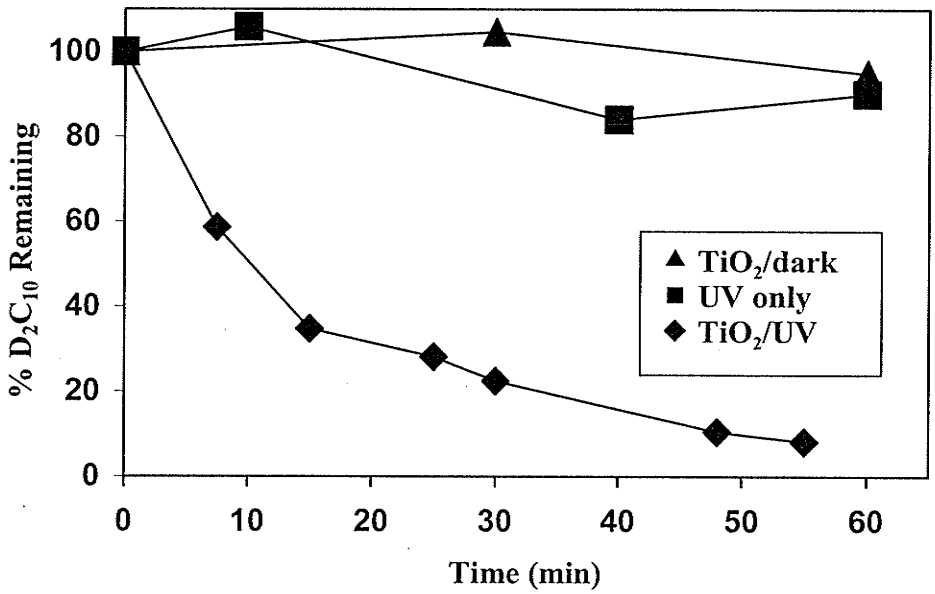

Figure 5.1: Degradation of 1,10-dichlorodecane (240 μg/L) in a dark control, in a solution without TiO_2 and in the presence of 150 mg/L of TiO_2 in Milli-Q water at pH 5.4 using 300 nm light.

indicating that thermal reactions were negligible. Reaction of D_2C_{10} in the absence of TiO_2 was indistinguishable from the dark control, indicating that direct photolysis was not contributing significantly to the measured rates of photolysis of D_2C_{10} with TiO_2. Chloride ion may inhibit the degradation of PCA isomers with high chlorine number by scavenging of $^{\bullet}OH$ (equation 4-14) as discussed in Chapter 4. The rate of photodegradation of chlorinated decanes decreased with increasing chlorine number from Cl_2 to Cl_6 as shown in Figure 5.2. The results showed 68.3% disappearance of H_6C_{10} compared to 33.8% for T_4C_{10} in the first 30 min. Also, increasing carbon chain length decreased the degradation rate of PCA isomers. This is illustrated in Figure 5.3 for isomers with chlorine number 4 and in Figure 5.4 for isomers with chlorine number 2.

5.3.3. Identification of The Reactive Species

In photocatalytic processes involving TiO_2 and substrate the reactions may proceed through reduction by conduction band electrons (e^-_{cb}) [279] or oxidation by valence band hole species, (h^+_{vb}) [280] or by trapped hole species (h^+_{vb}/ $^{\bullet}OH$) [209] as summarized in equations (5-1 to 5-3).

$$\text{Substrate} + e^-_{cb} \longrightarrow \text{Substrate}^{\bullet} \qquad (5\text{-}1)$$

$$\text{Substrate} + h^+_{vb} \longrightarrow [\text{Substrate}]^+ \qquad (5\text{-}2)$$

$$\text{Substrate} + h^+_{VB}/\ ^{\bullet}OH \longrightarrow [\text{Substrate}]^+ \qquad (5\text{-}3)$$

Information regarding the type of photocatalytic reaction may be provided by determining the influence of different hole and electron scavengers on the rate of degradation of PCAs. Scavengers were added to the reaction medium to remove either the h^+_{vb} (both forms) or the e^-_{cb}. As will be discussed later, the degradation of the substrate may occur on the surface of the photocatalyst (TiO_2) or in the bulk solution.

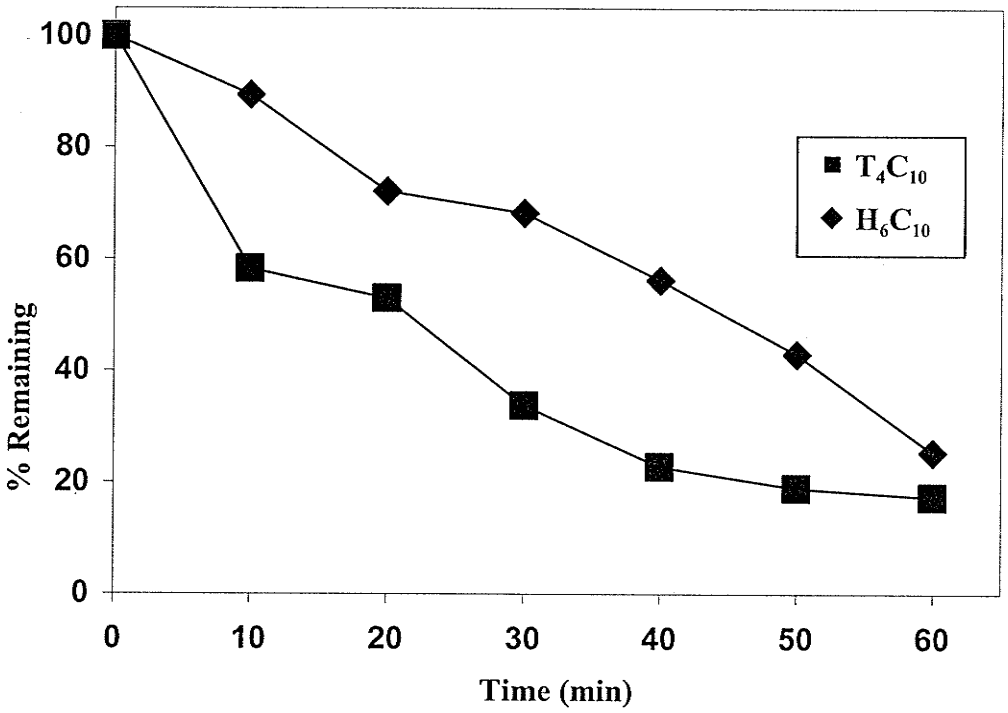

Figure 5.2: Degradation of 1,2,9,10-tetrachlorodecane and 1,2,5,6,9,10-hexachlorodecane (250 μg/L) in Milli-Q water with 150 mg/L of TiO_2 at pH 5.4 using 300 nm light.

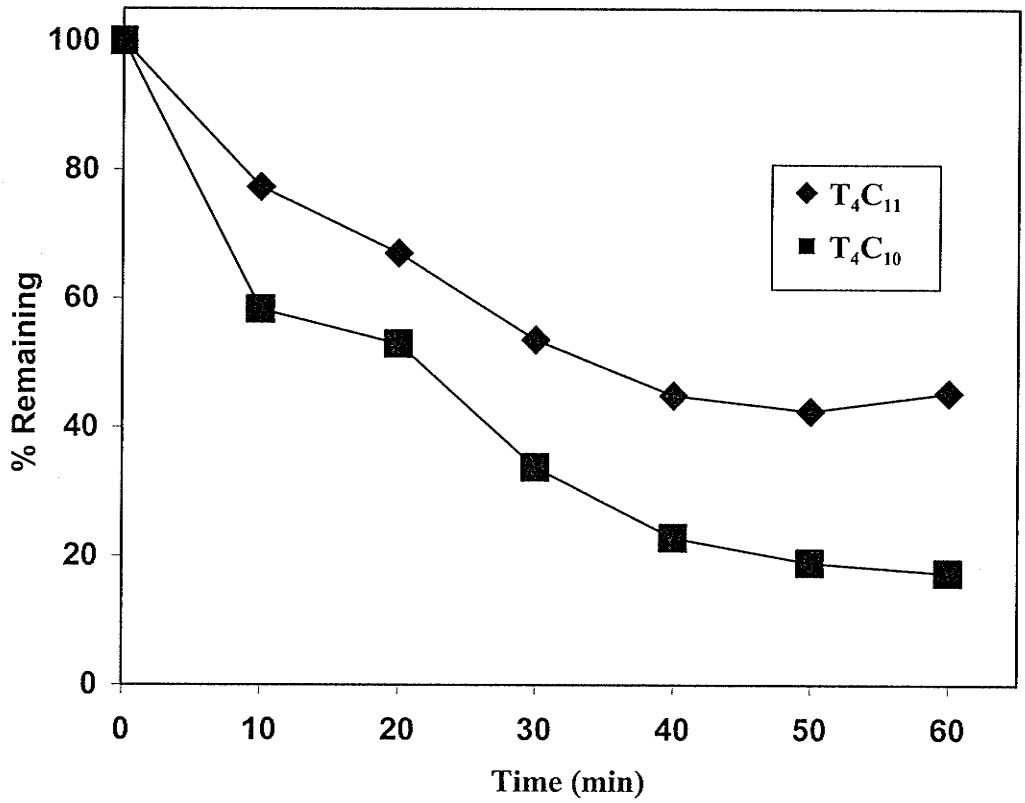

Figure 5.3: Degradation of 1,2,9,10-tetrachlorodecane and 1,2,10,11-tetrachloroundecane (250 μg/L) in Milli-Q water with 150 mg/L of TiO_2 at pH 5.4 using 300 nm light.

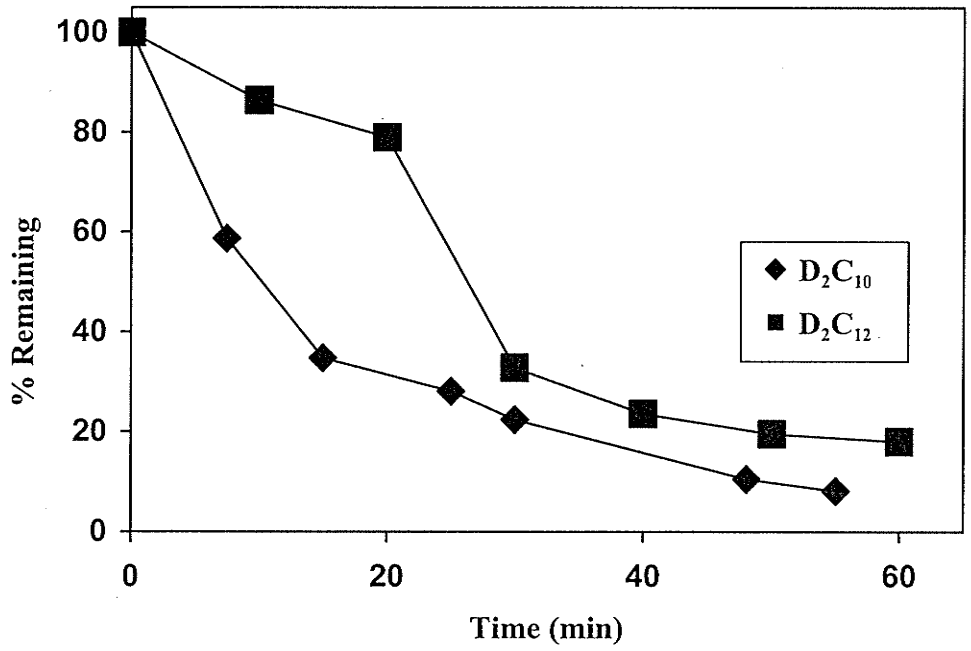

Figure 5.4: Degradation of 1,10-dichlorodecane and 1,12-dichlorododecane (250 μg/L) in Milli-Q water with 150 mg/L of TiO_2 at pH 5.4 using 300 nm light.

Removing one of these reactive species may inhibit the degradation rate (on the surface of the photocatalyst or in the bulk solution) by producing a competition for the active site of interest, or it may enhance degradation by preventing charge recombination.

Methanol and iodide ion were added as hole scavengers, while molecular oxygen and transition metals such as Ag^{+}, Cu^{+2} and Fe^{+3} were added as electron scavengers. The effect of the scavengers was followed by observing changes in the degradation rate of D_2C_{10} relative to its degradation rate in the absence of the scavenger.

5.3.3.1. The Effect of Hole Scavengers

Methanol: Methanol was added in three different concentrations; 1 mM, 10 mM and 100 mM, at pH 2.8. Methanol is known as an efficient scavenger of h^{+}_{vb}/ $^{\bullet}OH$ free in the bulk solution, or adsorbed to the surface of TiO_2 [281]. Since the redox potential of the h^{+}_{vb}/ $^{\bullet}OH$ is thermodynamically favorable for oxidation of methanol [282], methanol may associate with the h^{+}_{vb} on the TiO_2 surface and/or react with hydroxyl radicals to create the hydroxymethyl radical, $^{\bullet}CH_2OH$ [283]:

$$CH_3OH + {}^{\bullet}OH \longrightarrow {}^{\bullet}CH_2OH + H_2O \qquad (5\text{-}4)$$

The hydroxymethyl radical will then undergo a reaction with oxygen to produce formaldehyde, which will yield formic acid and finally carbon dioxide, upon further oxidation [283]. The rate of degradation of D_2C_{10} (Figure 5.5) was strongly inhibited with increasing methanol concentration due to increased competition for the oxidizing species. This result suggested that D_2C_{10} was being photooxidized by direct interaction with the valence-band hole or by reaction with $^{\bullet}OH$ radicals.

Iodide Ion (I^{-}): To confirm that the degradation is a photooxidation process the experiment was repeated with addition of KI, another known h^{+}_{vb}/ $^{\bullet}OH$ scavenger. The

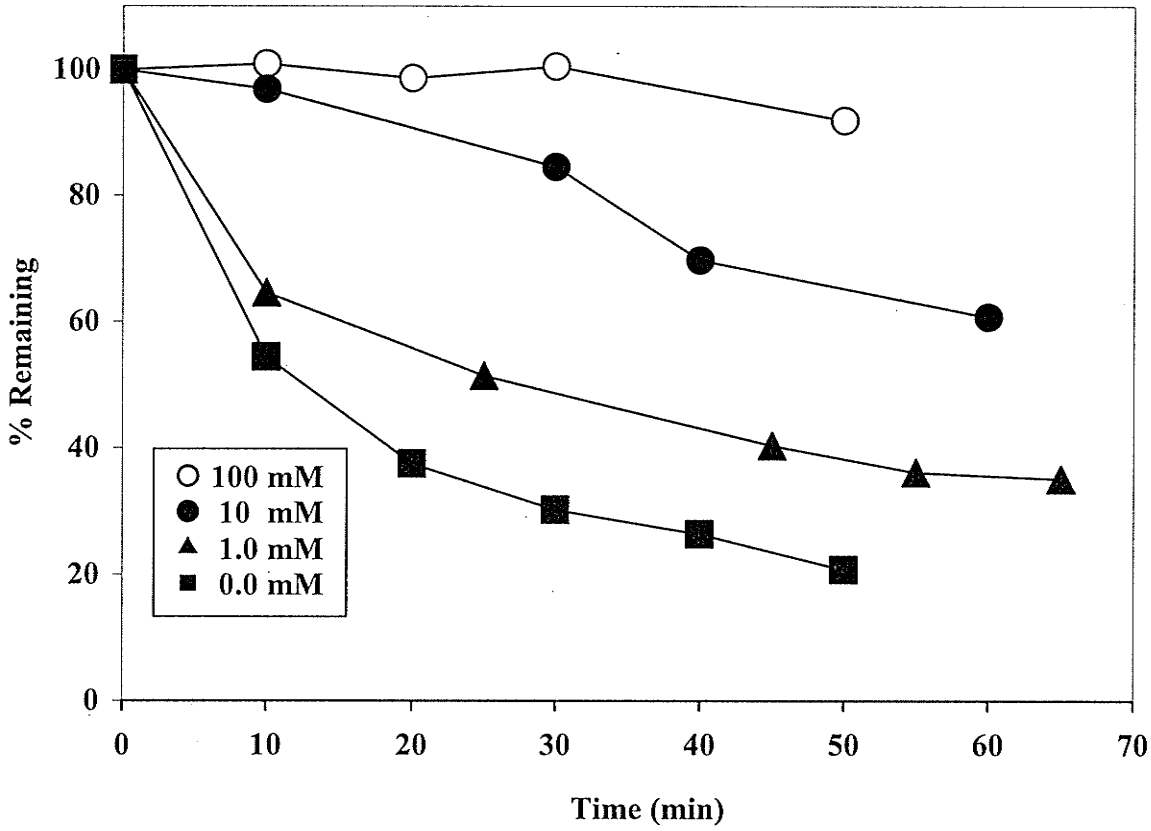

Figure 5.5: Effect of the hole scavenger, methanol, on the photo-degradation of 1,10-dichlorodecane (240 μg/L) in Milli-Q water with 150 mg/L of TiO_2 at pH 2.8 using 300 nm light.

photocatalytic degradation of D_2C_{10} was also inhibited by iodide ion (I^-) as shown in Figure 5.6, lending further support for an oxidative degradation of D_2C_{10}. Iodide ion reacts with h^+_{vb}, (equations 5-5 to 5-8) as a primary electron donor [284-286]. Iodide also reacts with adsorbed $^\bullet OH$ radicals [287] (equations 5-9 to 5-10) producing iodine radicals ($I^\bullet$ and $I_2^{\bullet -}$) that reducesing the number of oxidizing species available on the TiO_2 surface for reaction with D_2C_{10}.

$$I^- + \text{hole} \longrightarrow I^\bullet \qquad (5\text{-}5)$$

$$I^\bullet + I^- \longrightarrow I_2^{\bullet -} \qquad (5\text{-}6)$$

$$\text{Substrate} + h^+_{VB}/\ ^\bullet OH \longrightarrow [\text{Substrate}]^+ \qquad (5\text{-}7)$$

$$I_2^{\bullet -} \longrightarrow I_2 + e^- \qquad (5\text{-}8)$$

$$I^- + OH^\bullet_{ads} \longrightarrow I^\bullet + OH^-_{ads} \qquad (5\text{-}9)$$

$$\text{or } I_2 + OH^\bullet_{ads} \longrightarrow HOI + I^\bullet \qquad (5\text{-}10)$$

Addition of 10^{-5} M Cu^{+2} (Figure 5.7) to the reaction medium minimized the effects of I^-. By effectively scavenging conduction band electrons (e^-_{cb}), Cu^{+2} is reduced to unstable Cu^+ which may remove I^- from the solution as CuI [288-290]:

$$Cu^{+2} + e^-_{cb} \longrightarrow Cu^+ \qquad (5\text{-}11)$$

$$Cu^+ + I^- \longrightarrow CuI \qquad (5\text{-}12)$$

5.3.3.2. The Effect of Electron Scavengers

Electron scavengers were useful in confirming that the photocatalytic degradation of D_2C_{10} was an oxidative process. If the substrate was being reduced by reaction with conduction band electrons, then e^-_{cb} scavengers would inhibit its rate of degradation. If the substrate was being oxidized then the presence of electron scavengers could enhance

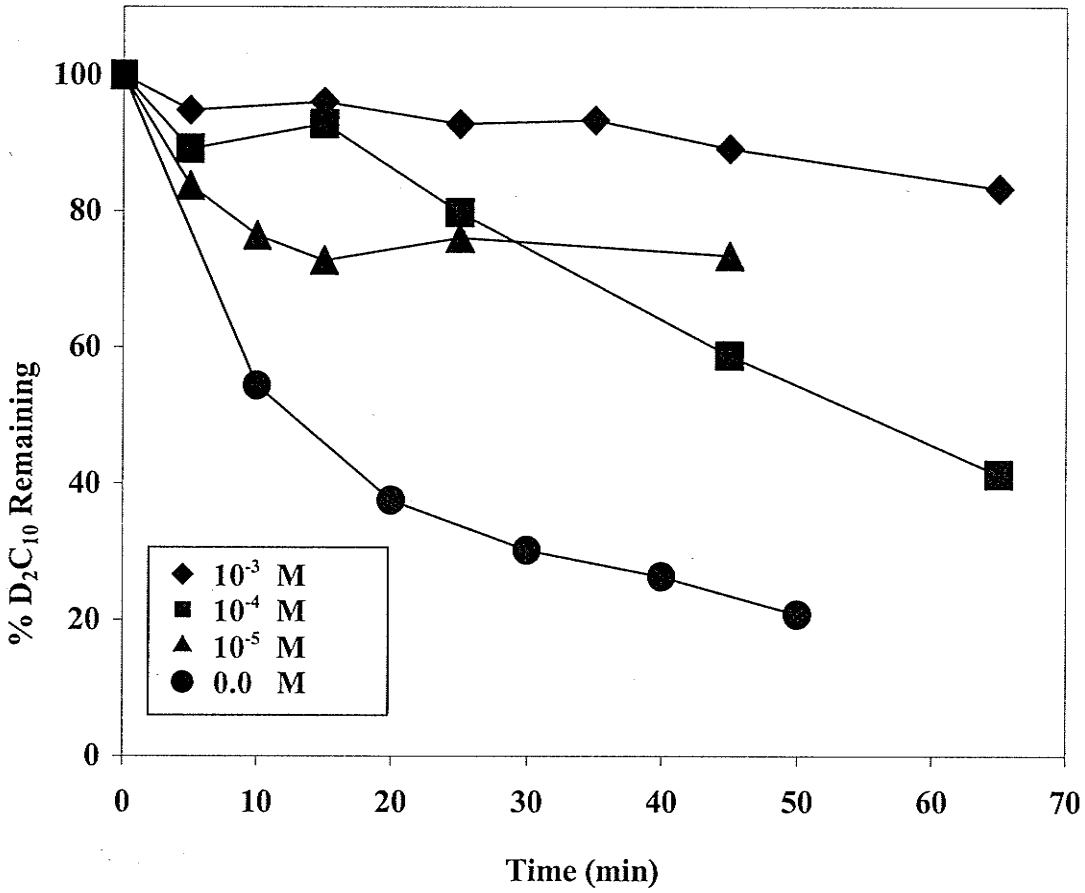

Figure 5.6: Effect of the hole scavenger, iodide ion (I^-), on the photocatalytic degradation of 1,10-dichlorodecane (240 μg/L) in Milli-Q water with 150 mg/L of TiO_2 at pH 5.4 using 300 nm light.

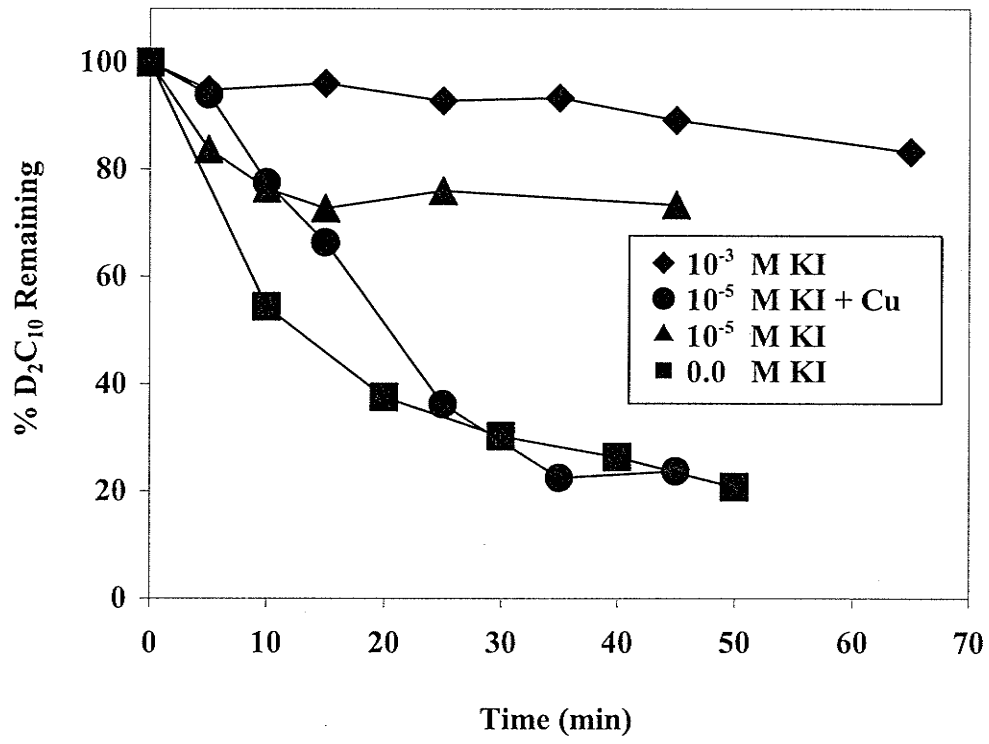

Figure 5.7: Effect of Cu^{+2} on the effect of iodide ion (I^-) in the photocatalytic degradation of 1,10-dichlorodecane (240 μg/L) in Milli-Q water with 150 mg/L of TiO_2 at pH 5.4 using 300 nm light.

its rate of photocatalytic degradation by minimizing the rate of recombination of e^-_{cb} and h^+_{vb} [291].

Molecular Oxygen: Molecular oxygen is a well-known e^-_{cb} scavenger, being converted to the superoxide anion radical [106], $O_2^{\bullet-}$, which eventually regenerates adsorbed oxygen, $O_{2\,ads}$:

$$O_{2\,ads} + e^-_{cb} \longrightarrow O_2^{\bullet-} \qquad (5.13)$$

$$O_2^{\bullet-} + e^-_{cb} \longrightarrow O^{2-}_2 \qquad (5.14)$$

$$O_2^{\bullet-}{}_{ads} \longrightarrow O_{2\,ads} + O^{2-}_{2\,ads} \qquad (5.15)$$

The photocatalytic degradation of D_2C_{10} was rapid with dissolved oxygen levels of 0.5 mM and was not affected significantly by N_2 purging which reduced O_2 levels to 0.03 to 0.06 mM as seen in Figure 5.8. It appears that large concentrations of oxygen are not required for this photooxidation, perhaps because of the cyclic nature of the process.

Silver and Copper Ions: Silver ion, another effective electron scavenger, is reduced by e^-_{cb} to metallic Ag:

$$Ag^+ + e^-_{cb} \longrightarrow Ag_{(s)} \qquad (5.16)$$

[293-297], increasing the availability of h^+_{vb} or $^\bullet OH$ for reaction with D_2C_{10}. A slight increase in the rate of reaction of D_2C_{10} in the presence of Ag^+, particularly at low oxygen concentrations (Figure 5.9) is attributed to a decrease in the degree of electron-hole recombination [298]. Addition of 1.5 mM Cu^{+2} to a solution containing 1.0 mM Ag^+ inhibited the degradation of D_2C_{10} (Figure 5.9) since Cu^+ is formed [299], which competes with D_2C_{10} for the oxidants, h^+_{vb} or $^\bullet OH$.

$$Cu^+ + h^+_{vb}/\ OH^\bullet \longrightarrow Cu^{+2} \qquad (5\text{-}17)$$

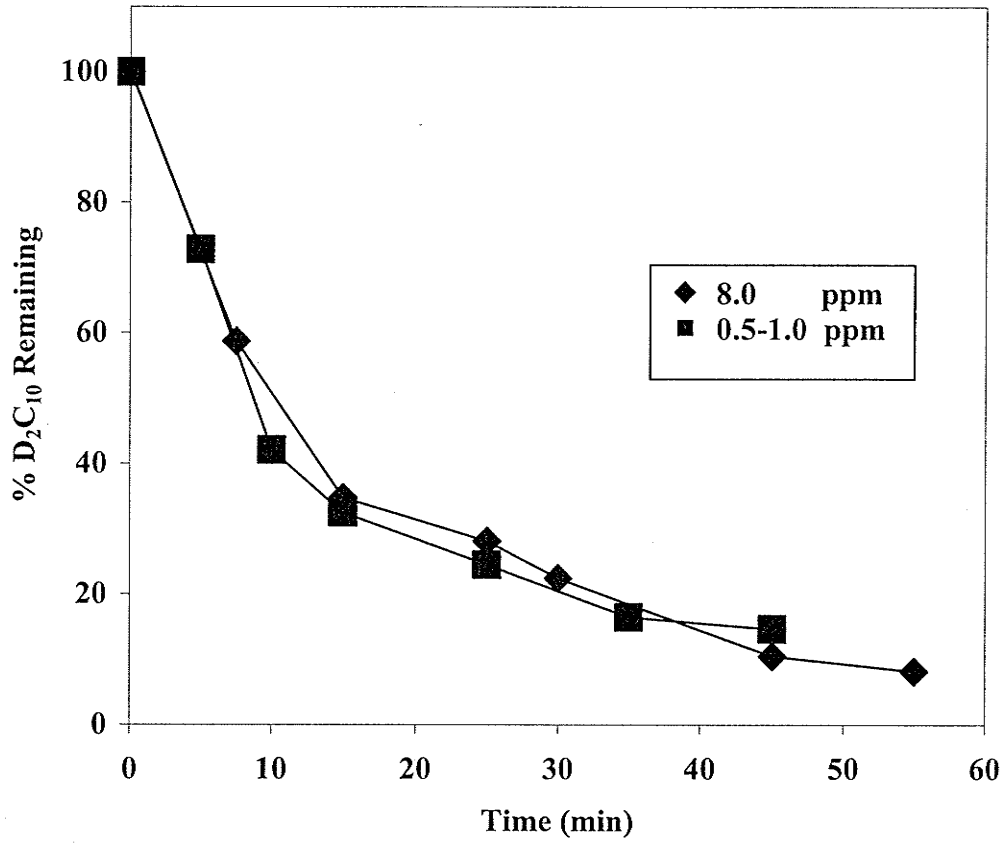

Figure 5.8: Effect of molecular oxygen levels on the photocatalytic degradation of 1,10-dichlorodecane (240 μg/L) in Milli-Q water with 150 mg/L of TiO_2 at pH 5.4 using 300 nm light.

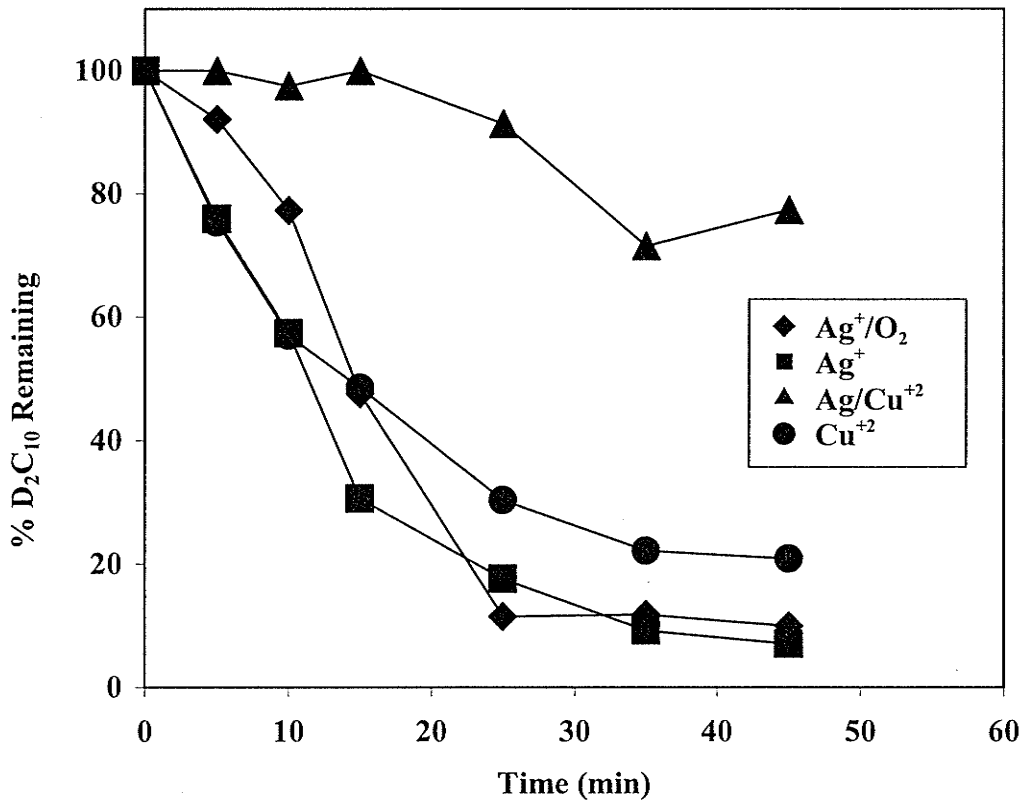

Figure 5.9: Effect of the electron scavenger, 1.0 mM Ag^+, on the photocatalytic degradation of 1,10-dichlorodecane (240 μg/L) in Milli-Q water with 150 mg/L of TiO_2 in presence of molecular oxygen and 1.5 mM Cu^{+2} at pH 5.4 using 300 nm light.

Iron: The presence of Fe^{+3} had little effect on the degradation rate. A rapid initial rate of reaction suggested a relatively rapid reduction of ferric to ferrous ion, a fact which was confirmed by the disappearance of the yellow color of the solution. This initial reduction prevents electron-hole recombination [293,297] and enhances the degradation of D_2C_{10}, but will not continue to do so after the majority of Fe^{+3} has been transformed to Fe^{+2}:

$$Fe^{+3} + e^-_{cb} \longrightarrow Fe^{+2} \qquad (5\text{-}18)$$

The slow degradation of D_2C_{10}after consumption of Fe^{+3} is attributed to the removal of active centers from the reaction medium [112]. As illustrated in Figure 5.10, Ag^+ is the most efficient e^-_{cb} scavenger, since the product Ag (s) precipitates out of the solution. On the other hand, the tendency of Cu^{+2} to adsorb to the surface of TiO_2 [299], and the creation of the unstable Cu^+ ion [293], account for the slower degradation rates observed in the presence of Cu^{+2}. Thus the degradation rate of D_2C_{10} is slow in solutions containing copper with or without another electron scavenger present.

Hydrogen Peroxide: Addition of 10 mM H_2O_2 to solutions containing either natural or reduced levels of oxygen caused a slight reduction in the rate of photocatalytic degradation of D_2C_{10} (Figure 5.11). H_2O_2 is capable of reacting with h^+_{vb} and $OH^\bullet$ [294], in addition to scavenging conduction band electrons:

$$H_2O_2 + h^+_{vb}/OH^\bullet \longrightarrow HO_2^\bullet + H_2O/H^+ \qquad (5\text{-}19)$$

$$H_2O_2 + 2\,e^-_{cb} + 2H^+ \longrightarrow 2\,H_2O \qquad (5\text{-}20)$$

$$H_2O_2 + e^-_{cb} \longrightarrow OH^\bullet + OH^- \qquad (5\text{-}21)$$

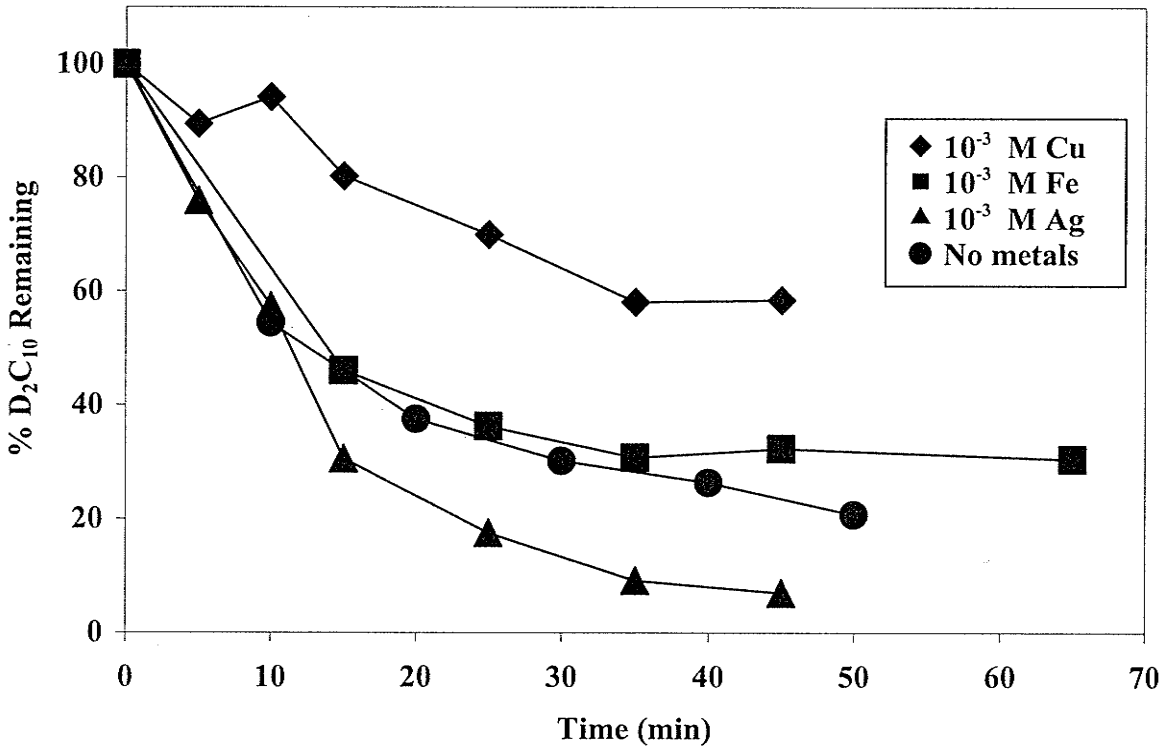

Figure 5.10: The effect of electron scavengers (10^{-3} M Cu^{+2}, 10^{-3} M Fe^{+3} and 10^{-3} M Ag^{+}) on the photocatalytic degradation of D_2C_{10} (240 μg/L) in Milli-Q water with 150 mg/L of TiO_2 at pH 5.4 using 300 nm light.

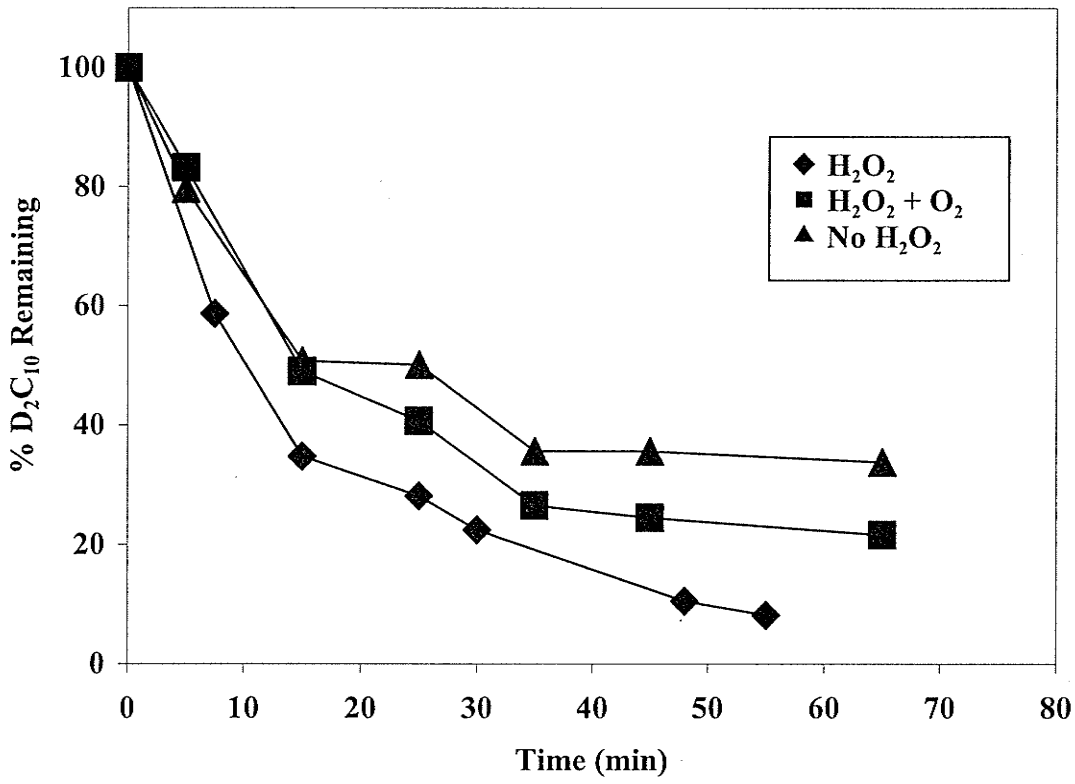

Figure 5.11: The effect of 10^{-2} M hydrogen peroxide on the photocatalytic degradation of D_2C_{10} (240 μg/L) in solutions with oxygen concentrations of 0.045 ± 0.015 mM by 150 mg/L of TiO_2 at pH 5.4 using 300 nm light.

The electron scavenging ability of H_2O_2 is therefore offset by the formation of a less reactive oxidant the perhydroxyl radical ($HO_2^{\bullet}$), which blocks the oxidation sites [292-293] leading to decreased reaction rates.

5.3.4. The Site of The Reaction

Experiments were carried out to determine whether the photooxidation of D_2C_{10} was direct photooxidation by reaction with h^+_{vb} or indirect photooxidation via reaction with $^{\bullet}OH$ radicals. Both oxidizing species h^+_{vb} and $^{\bullet}OH$ are capable of initiating an oxidation independent of the other:

$$D_2C_{10} + h^+_{vb} \longrightarrow D_2C_{10}^+ \quad (5\text{-}22)$$

or

$$h^+_{vb} + H_2O \longrightarrow h^+_{vb}/\,^{\bullet}OH \quad (5\text{-}23)$$

$$D_2C_{10} + h^+_{vb}/\,^{\bullet}OH \longrightarrow D_2C_{10}^+ + H_2O \quad (5\text{-}24)$$

Certain reports indicate oxidation by $^{\bullet}OH$ [182], others have found oxidation primarily by h^+_{vb} [278], and yet others hold that the two are indistinguishable [301]. In order to differentiate between the two possible reactions acetonitrile was used to minimize the formation of $^{\bullet}OH$ radicals. In order to prepare TiO_2 suspensions in acetonitrile, the solvent was purged with oxygen followed by sonication and addition of substrate. Any oxidation observed in this system is ascribed to the valence band hole [302] since $^{\bullet}OH$ radicals cannot form in acetonitrile. Although other studies have found partial oxidations occurring in acetonitrile, and thus have attributed this partial degradation to oxidation by h^+_{vb} [302-304], Figure 5.12 illustrates the complete lack of transformation of D_2C_{10} in acetonitrile. Saturating acetonitrile with oxygen, solubility 2.42 ± 0.15 m*M* [305], did not promote the degradation of D_2C_{10}. Therefore, D_2C_{10} oxidation is proceeding by reaction with $^{\bullet}OH$ radicals [207,302].

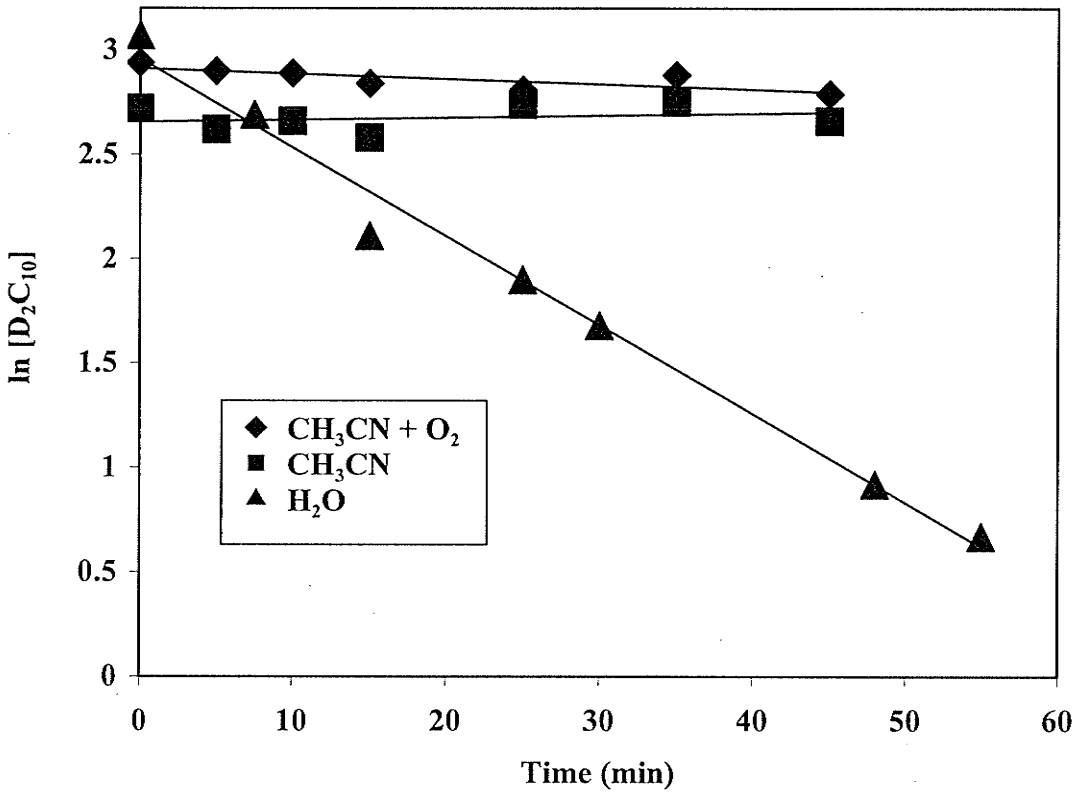

Figure 5.12: Effect of acetonitrile on the photocatalytic degradation of D_2C_{10} (240 μg/L) with 150 mg/L of TiO_2 using 300 nm light.

5.3.5. Heterogeneous vs Homogeneous Oxidation

Although a heterogeneous process appeared more plausible [207], several approaches were used to determine if the oxidation of D_2C_{10} by $^{\bullet}OH$ radicals was a heterogeneous reaction occurring on the TiO_2 surface or a homogeneous reaction in the bulk solution. The initial rates of photodegradation of D_2C_{10} followed the modified Langmuir-Hinshelwood (L-H) kinetic model [306], for solid-liquid interfaces as shown in Figure 5.13. As discussed in the introduction, degradation of solute on the surface of TiO_2 follows the modified L-H model:

$$\frac{1}{r} = \frac{1}{k} + \left(\frac{1}{kK}\right)\frac{1}{C} \qquad (5-25)$$

where the initial rate (r) is calculated as the product of the initial first-order rate constant (k_o, min^{-1}) and the initial D_2C_{10} concentration (C, μg/L) and K is the adsorption coefficient of the reactant onto TiO_2 [307]. Although the data fit a model of prior substrate adsorption followed by photodegradation up to D_2C_{10} concentrations of 240 μg/L, further experimental evidence is required for its substantiation [207]. As such, two independent experiments, a photolysis with tetranitromethane, and a dark adsorption study, were performed.

5.3.5.1. Photolysis with Tetranitromethane

Free $^{\bullet}OH$ radicals in the bulk solution may arise from adsorbed $^{\bullet}OH$ radicals which diffuse from the surface of the photocatalyst [207], or by reduction of hydrogen peroxide formed from a reaction involving the superoxide anion radical [258]:

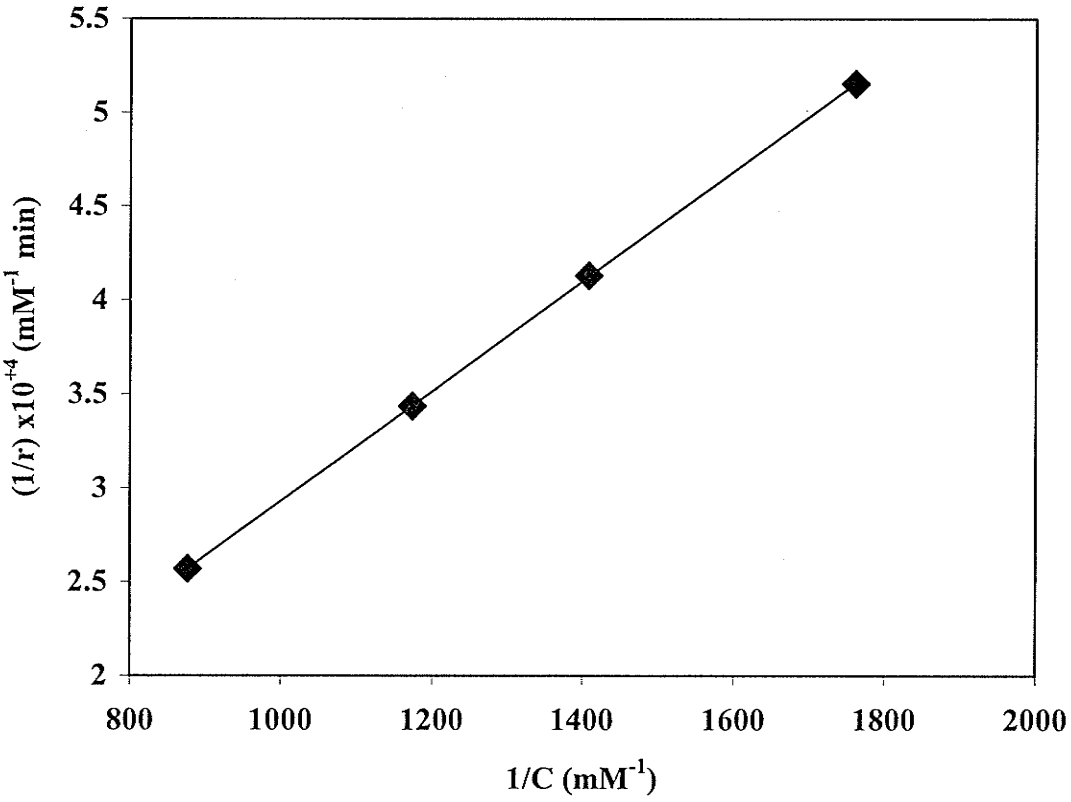

Figure 5.13: Fitting the kinetics of photocatalytic degradation of 1,10-dichlorodecane with TiO_2 to the Langmuir-Hinshelwood model ($r^2 = 0.99$), where C is the initial concentration of 1,10-dichlorodecane (mM) and r is the initial reaction rate (mM/min).

$$O_2^{\bullet -} + O_2^{\bullet -} + 2H^+ \longrightarrow H_2O_2 \quad (5\text{-}26)$$

$$H_2O_2 + O_2^{\bullet -} \longrightarrow {}^{\bullet}OH + OH^- + O_2 \quad (5\text{-}27)$$

$$H_2O_2 + e^-_{cb} \longrightarrow {}^{\bullet}OH + OH^- \quad (5\text{-}28)$$

$$H_2O_2 + Ti^{(III)} \longrightarrow {}^{\bullet}OH + OH^- + Ti^{(IV)} \quad (5\text{-}29)$$

There is evidence that diffusion of surface-bound $^{\bullet}OH$ radicals from the TiO_2 surface into the bulk solution is minimal [258, 207]. The powerful oxidizing agent tetranitromethane (TNM) was used to remove electrons and other reductants from solution [258], thus eliminating the species responsible for the formation of free $OH^{\bullet}$ radicals in solution:

$$C(NO_2)_4 + e^-_{cb}/O_2^{\bullet -}/Ti^{(III)} \longrightarrow C(NO_2)_4^- + NO_2 + O_2/Ti^{(IV)} \quad (5\text{-}30)$$

However TNM will not remove adsorbed $^{\bullet}OH$ radicals, since TNM is not strongly adsorbed to the surface of TiO_2 [258,308]. The photooxidation of D_2C_{10} was not affected by the presence of TNM (Figure 5.14), indicating that the photoxidation of D_2C_{10} involved surface bound rather than free $^{\bullet}OH$ radicals.

5.3.5.2. Adsorption Study

To further support the oxidation by surface bound $^{\bullet}OH$ radicals, a conclusion drawn from the Langmuir-Hinshelwood model and the TNM results, adsorption of D_2C_{10} onto the surface of TiO_2 was investigated. Adsorption of a substrate onto the TiO_2 surface [309], can either enhance the initial rate of degradation [187] or facilitate the adsorption of a second species which otherwise would not become greatly associated with the TiO_2

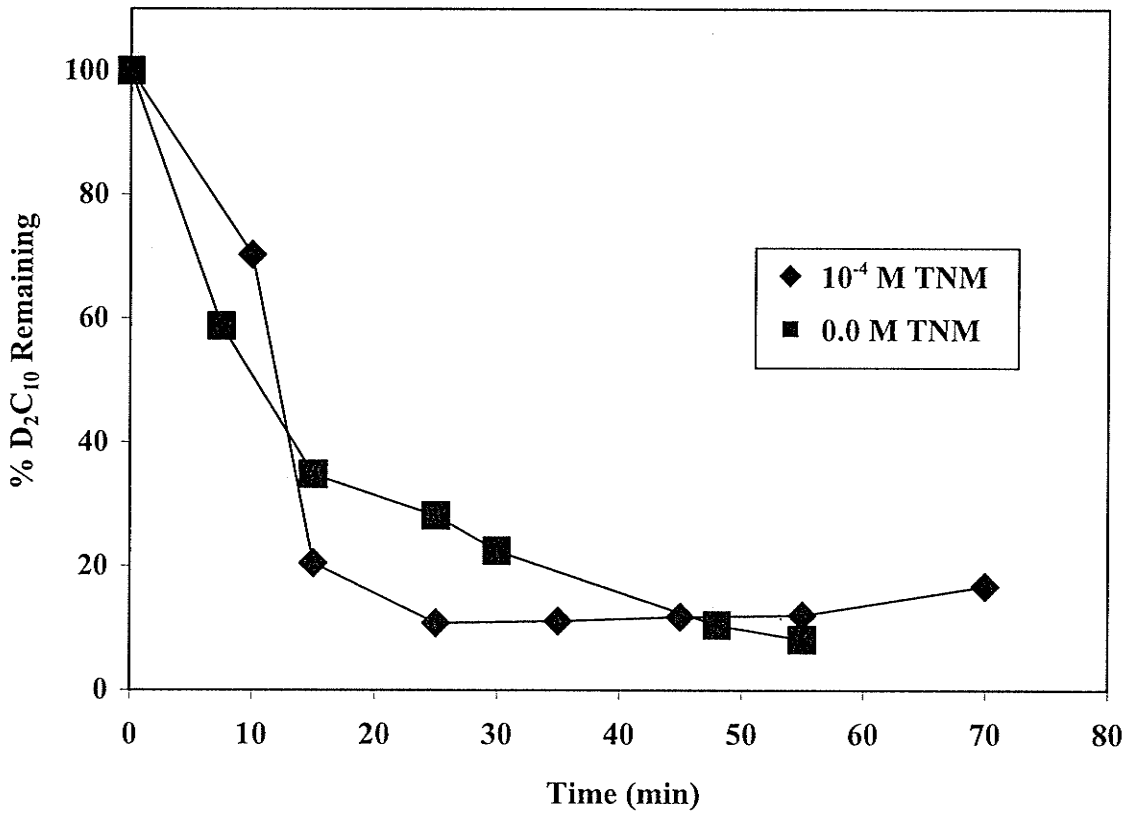

Figure 5.14: The effect of 10^{-4} M tetranitromethane on the photocatalytic degradation of 1,10-dichlorodecane in Milli Q water with 150 mg/L of TiO_2 at pH 5.4 using 300 nm light.

surface [310]. In this experiment the adsorption isotherm of D_2C_{10} onto TiO_2 was determined under dark conditions.The amount of D_2C_{10} associated with the solid phase was determined by mass balance after analysis of D_2C_{10} in the dissolve phase as a function of equilibration time. The results demonstrated that D_2C_{10} reached sorptive equilibrium with TiO_2 in approximately 70 hours (see Figure 5.15). The process appears to be biphasic, with a large initial rate of sorption within the first 20 min, followed by a slower sorption rate. Since all photolytic experiments were carried out after a 15 to 20 min equilibration period following solution preparation, D_2C_{10} was at least 75% sorbed prior to photolysis. Therefore, it appears that adsorbed D_2C_{10} was being oxidized by adsorbed $^{\bullet}OH$ radicals. This is further supported by the fact that the photodegradation rate correlated fairly closely with the degree of adsorption as shown in Figure 5.16. The degradation rate increased nearly twofold as the degree of adsorption of D_2C_{10} onto the TiO_2 surface increased with longer equilibration times. This result supports the common assumption that the substrate is always in contact with the semiconductor surface [203, 309, 311]. Therefore, D_2C_{10} is effectively photooxidized in aqueous suspensions of TiO_2, reacting with adsorbed $^{\bullet}OH$ radicals produced.

5.3.6. Photocatalytic Degradation of PCA Isomers in Lake Winnipeg Water

Photocatalytic degradation of D_2C_{10} was very effective in the presence of 150 mg/L TiO_2 in Lake Winnipeg water Figure 5.17 with 81% disappearance in the first 50 min. Increasing chlorine content from Cl_2 to Cl_6 again decreased the degradation of chlorinated decanes, with 60 and 47% disappearance of T_4C_{10} and H_6C_{10}, respectively, in the same irradiation time (Figure 5.17).

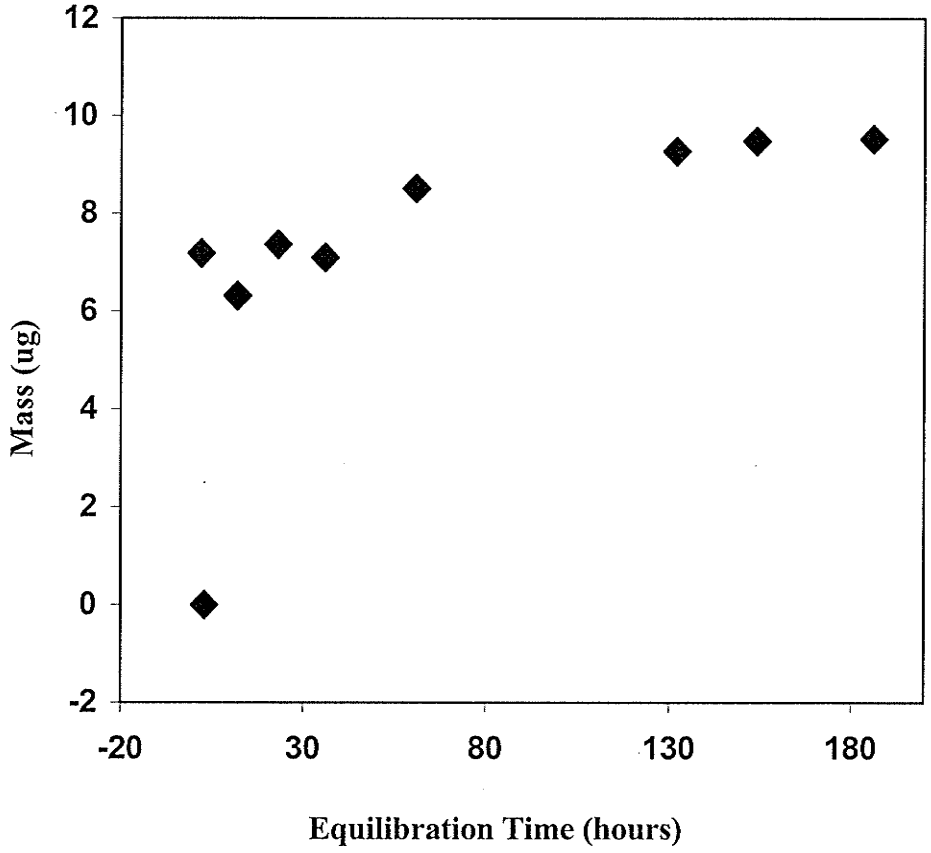

Figure 5.15: The rate of adsorption of 1,10-dichlorodecane to TiO_2, showing the mass of solute sorbed to the photocatalyst as a function of the equilibration time.

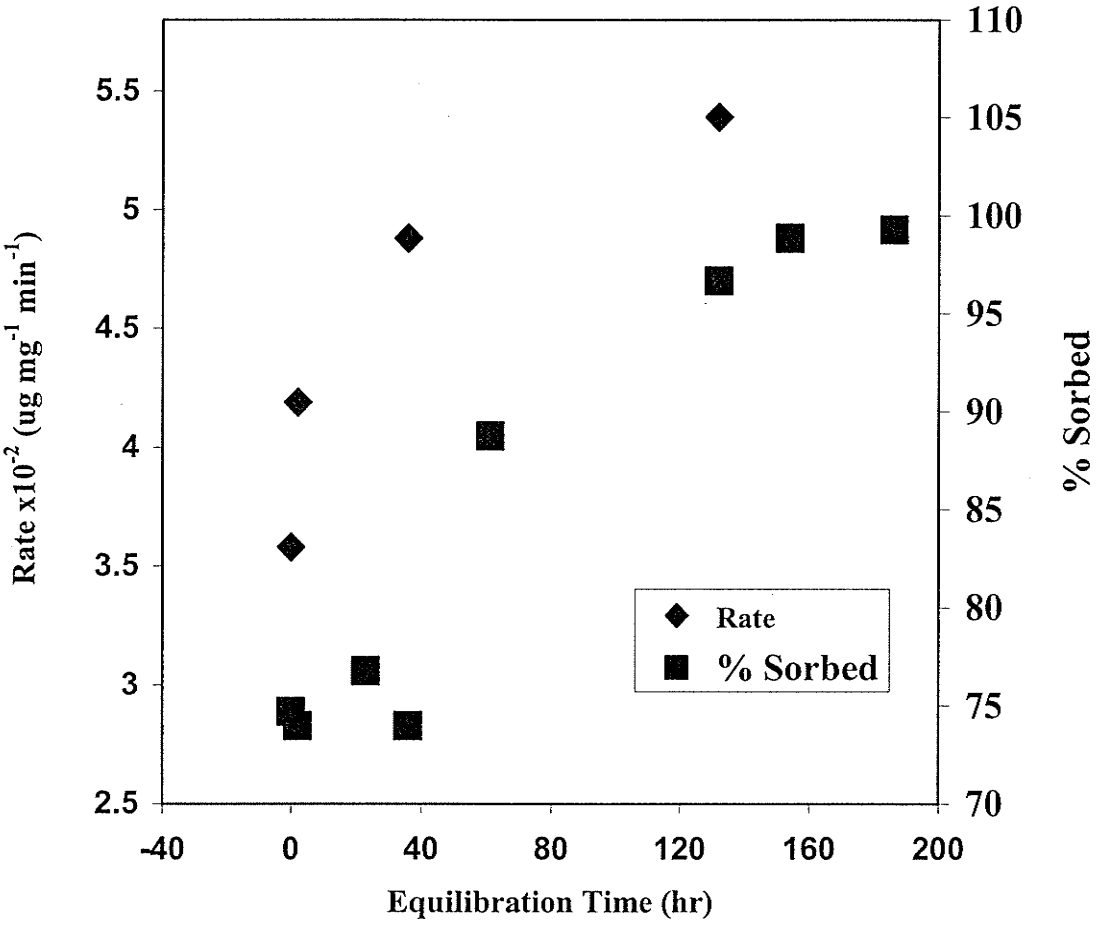

Figure 5.16: Plots showing the correlation between the degree of adsorption of 1,10-dichlorodecane to TiO_2 and the rate of its photodegradation.

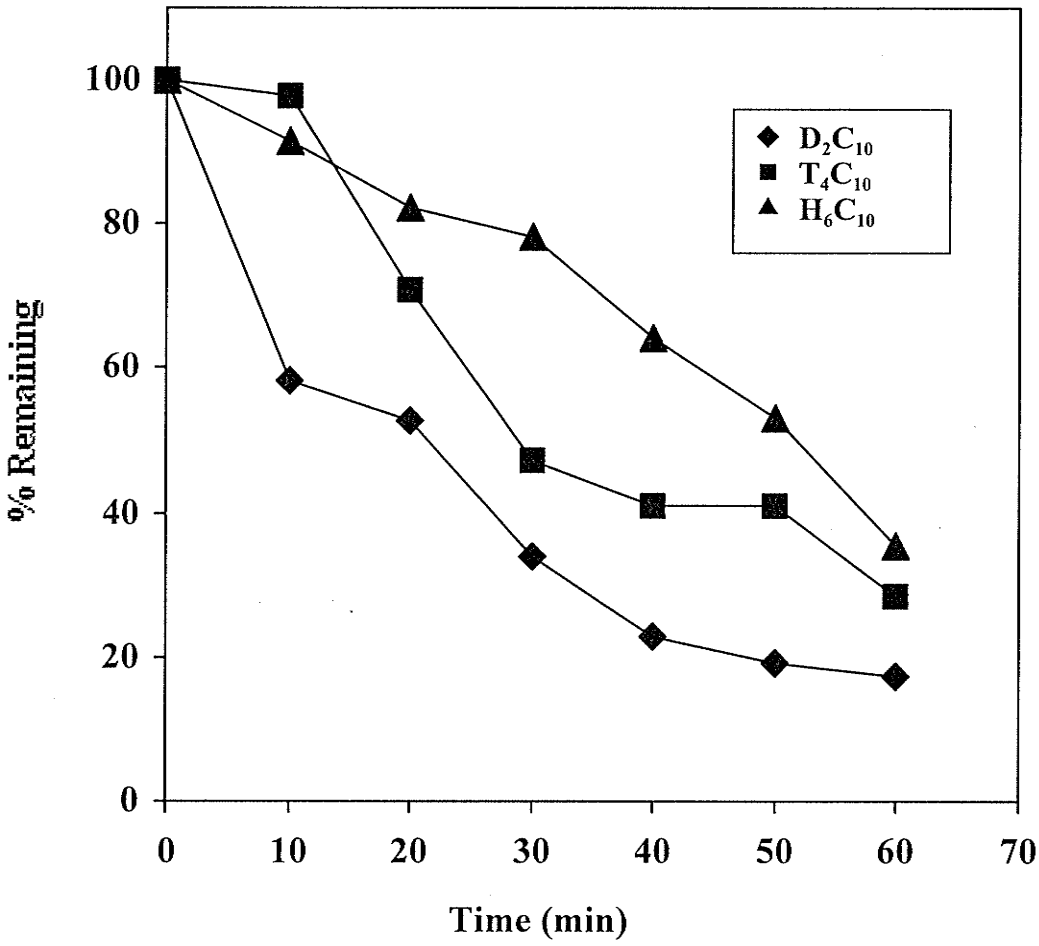

Figure 5.17: Effect of chlorine number on the photocatalytic degradation of chlorinated decanes in lake water in the presence of 150 mg/L TiO_2 at pH 8.6 using 300 nm light.

Increasing carbon chain length also resulted in decreased degradation rates of PCA isomers as summarized in Figures 5.18 and 5.19.

The degradation of D_2C_{10} was significantly reduced in lake water relative to pure water as shown in Figure 5.20. Lake Winnipeg water samples with a pH of 8.6, contained 2.35 mg/L dissolved inorganic carbon (DIC) and 0.99 mg/L dissolved organic carbon (DOC) (Table 3.1). Dissolved organic matter may reduce degradation by light attenuation. However, at this pH the presence of inorganic salts such as bicarbonate (HCO_3^-) may lead to scavenging of hydroxyl radicals which would also inhibit degradation of the substrate [312]:

$$HCO_3^- \rightleftharpoons H^+ + CO_3^{2-} \qquad (5\text{-}30)$$

$$CO_3^{2-} + {}^{\bullet}OH \longrightarrow OH^- \; CO_3^- \qquad (5\text{-}31)$$

Decreasing the pH of the solution from 8.6 to 5.4 (pH of suspended TiO_2 in distilled water) increased the rate of degradation of D_2C_{10} (Figure 5.21). The increased acidity shifts the carbonate equilibrium toward bicarbonate reducing $^{\bullet}OH$ radical scavenging.

5.3.7. Photodegradation of PCA Isomers in Bog Water

The degradation of D_2C_{10} was slower in lake water than in pure water; however, the degradation was even slower in bog water (Figure 5.22). The decreased rate in bog water may be due to light attenuation caused by the nearly 3-fold increase in the levels of dissolved organic carbon in bog water (2.90 mg/L) relative to lake water [313-314]. Although the bog water contains only one-half the level of dissolved inorganic carbon present in the lake water, scavenging of $^{\bullet}OH$ radicals by carbonate ion could also decrease the degradation rate.

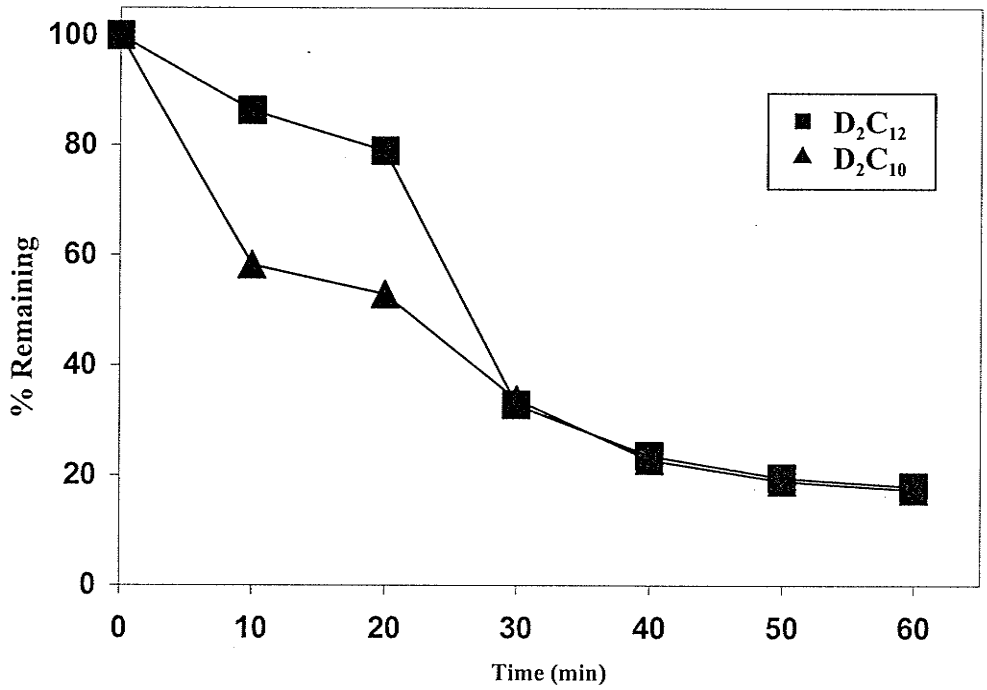

Figure 5.18: Photocatalytic degradation of 1,10-dichlorodecane and 1,12-dichlorododecane in lake water in the presence of 150 mg/L TiO_2 at pH 8.6 using 300 nm light.

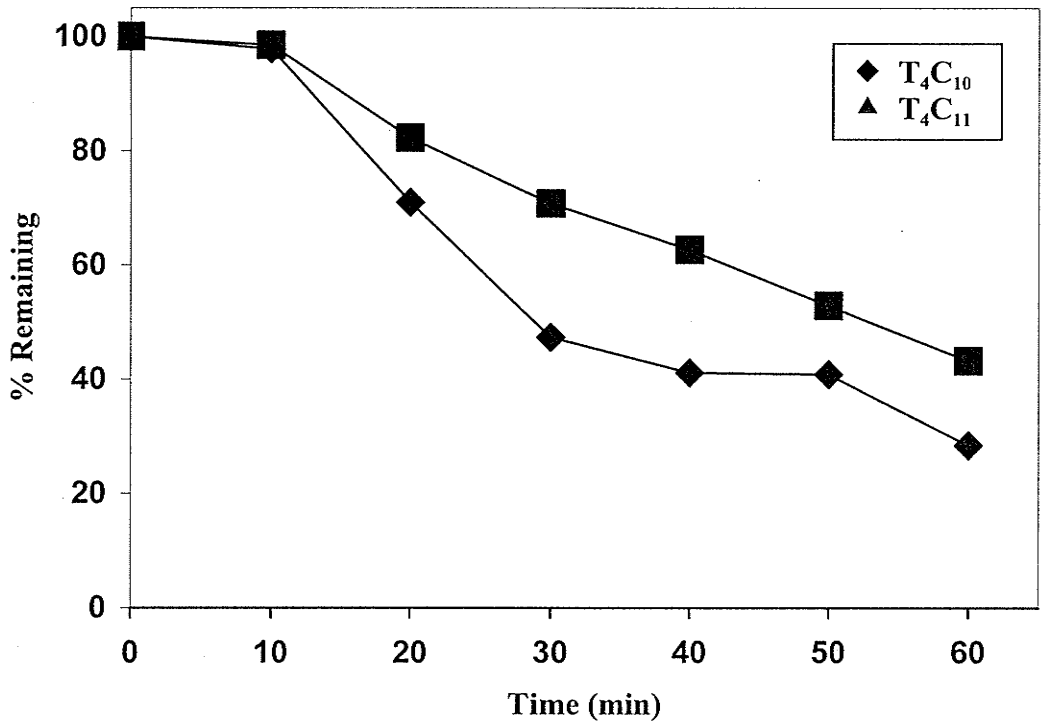

Figure 5.19: Photocatalytic degradation of 1,2,9,10-tetrachlorodecane and 1,2,10,11-tetrachloroundecane in Lake Winnipeg water in the presence of 150 mg/L TiO_2 at pH 8.6 using 300 nm light.

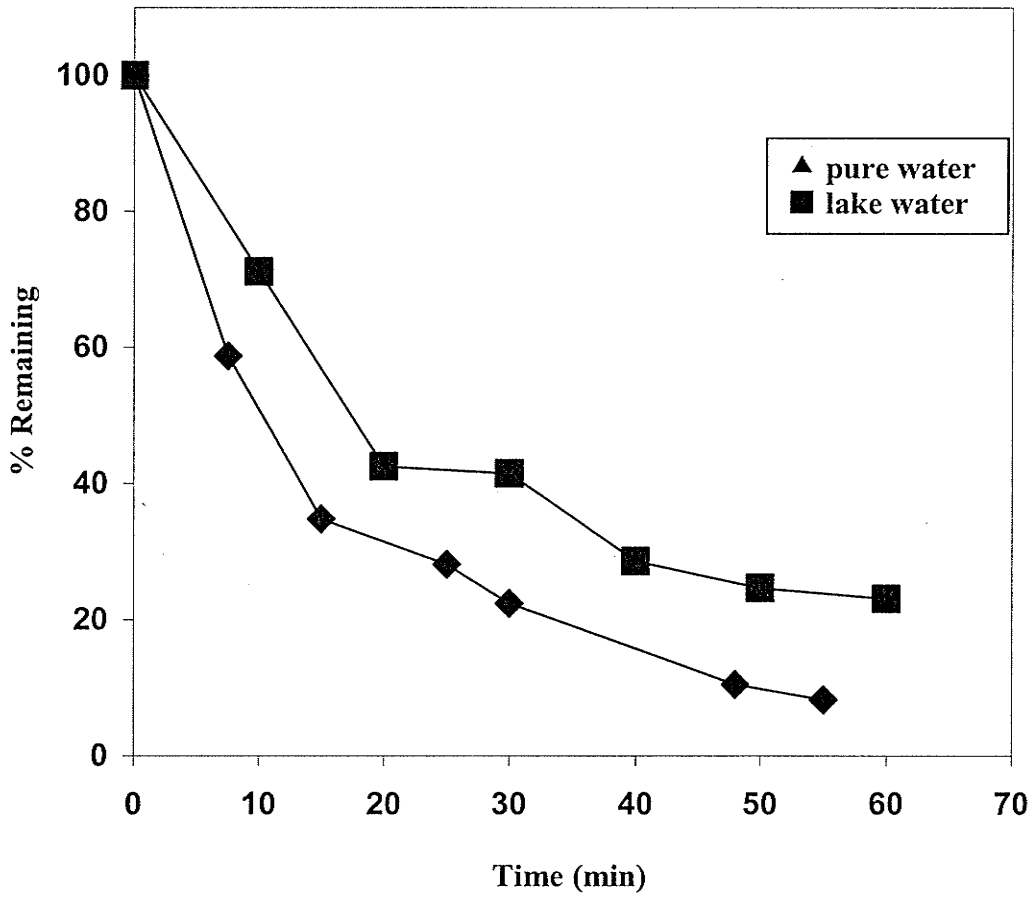

Figure 5.20: Effect of dissolved organic matter on photocatalytic degradation of 1,10-dichlorodecane in Lake Winnipeg water in the presence of 150 mg/L TiO_2 at pH 8.6 using 300 nm light.

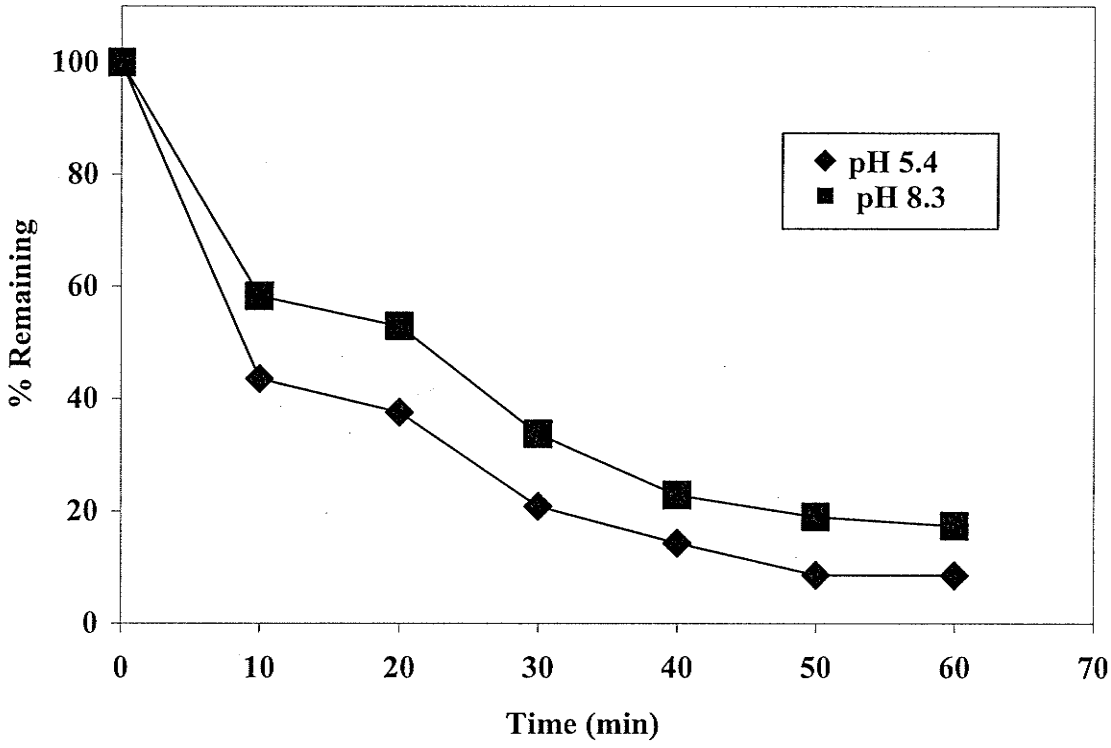

Figure 5.21: Effect of pH on the photocatalytic degradation of 1,10-dichlorodecane in Lake Winnipeg water in the presence of 150 mg/L TiO_2 using 300 nm light.

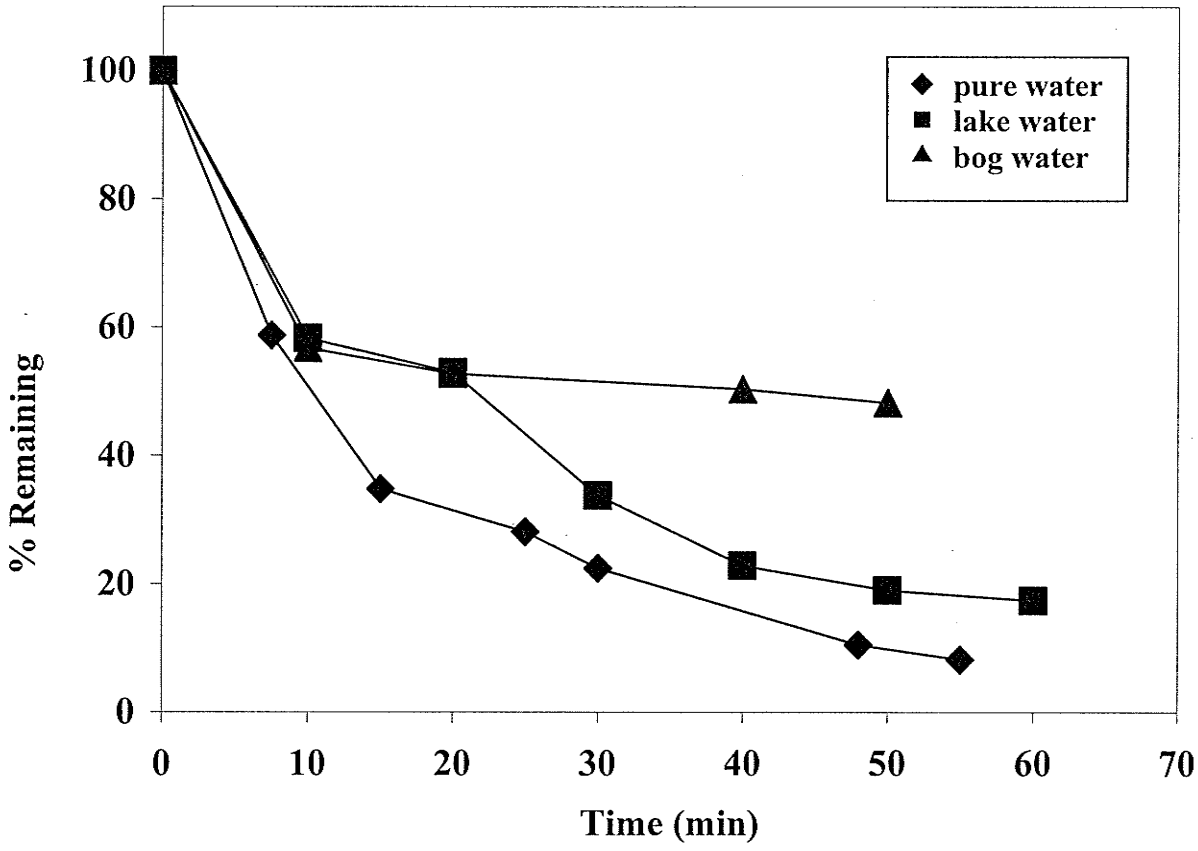

Figure 5.22: Photocatalytic degradation Of 1,10-dichlorodecane in pure, lake and bog water in the presence of 150 mg/L TiO_2 using 300 nm light.

The degradation rates of chlorinated decanes again decreased with increased chlorine number as shown in figure 5.23. This is due to the competition of released Cl^- ions for the $^{\bullet}OH$ radicals. Also, increasing carbon chain length resulted in the expected decrease in the degradation rate (Figures 5.24).

5.3.8. Photocatalytic Degradation of PCA Mixtures in Lake 375 Water

The photocatalytic degradation of PCA mixtures in an aqueous suspension of 200 mg/L TiO_2 in Lake 375 water was very effective, as illustrated in Figures 5.25 to 5.28 for the chlorinated decane (C_{10}), undecane (C11), dodecane (C_{12}) and tridecane (C_{13}) mixtures. Although not a dramatic effect, there is a noted decrease in degradation rate at high chlorine numbers. However, no clear trend between reactivity and carbon chain length was observed (Figure 5.29).

The photooxidation of the composite PCA mixture by three different photocatalytic techniques, TiO_2/UV, H_2O_2/UV and Fe^{+3}/H_2O_2/UV, are compared in Figure 5.30. Although all three processes were effective in degrading PCAs, the photo-Fenton system (Fe^{3+}/H_2O_2/ UV) is the most efficient. For example 85% disappearance of total PCAs was observed in 60 min of irradiation compared to 50 and 33% disappearance in the TiO_2/UV and H_2O_2/UV systems, respectively. As discussed in Chapter 4, the photolysis of H_2O_2 in the absence of Fe^{3+} is very slow with the 300 nm light source used, due to the recombination of $^{\bullet}OH$ radicals. The presence of Fe^{3+} has a dramatic effect on the decomposition of H_2O_2 to produce $^{\bullet}OH$ radicals. The higher efficiency of the photo-Fenton system for the degradation of PCAs can be explained by the contribution of multiple reactions which generate $^{\bullet}OH$ radicals including photolysis of H_2O_2, photolysis

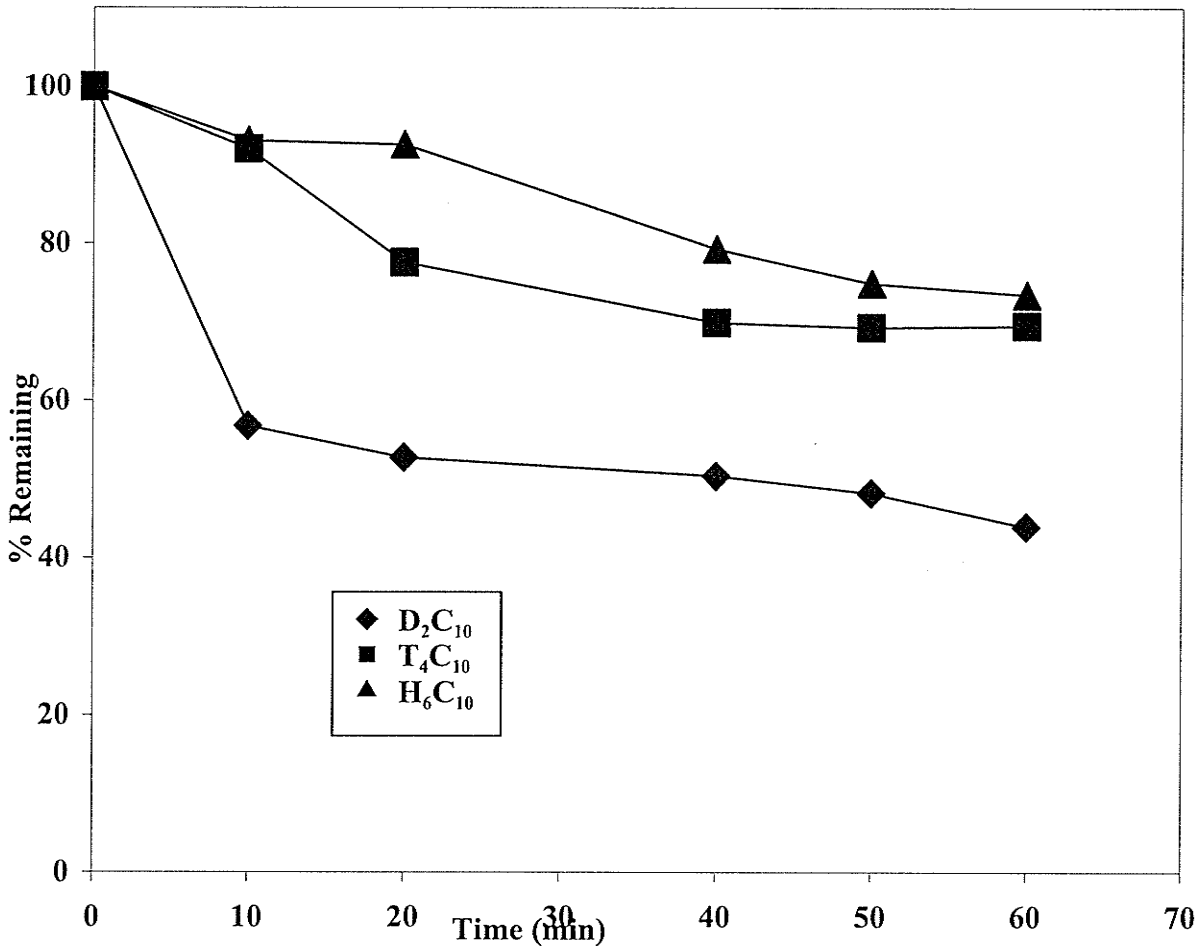

Figure 5.23: Effect of chlorine number on the photocatalytic degradation of chlorinated decanes in bog water in the presence of 150 mg/L TiO_2 using 300 nm light.

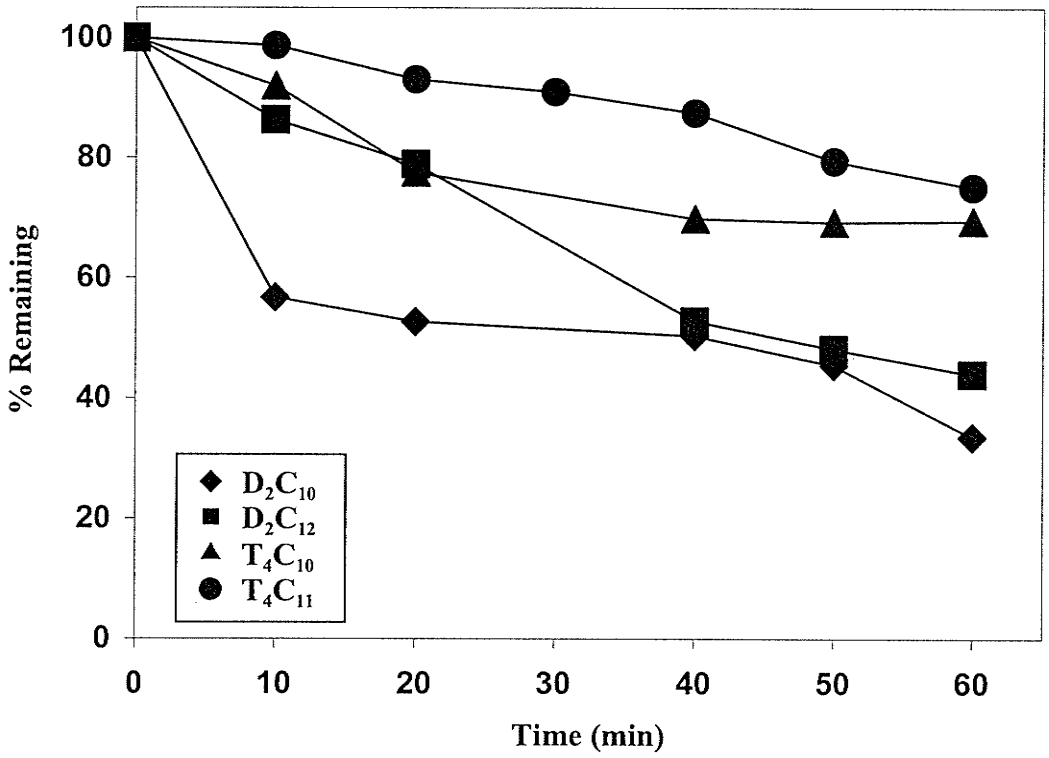

Figure 5.24: Photocatalytic degradation of PCA isomers in bog water in the presence of 150 mg/L TiO_2 using 300 nm light.

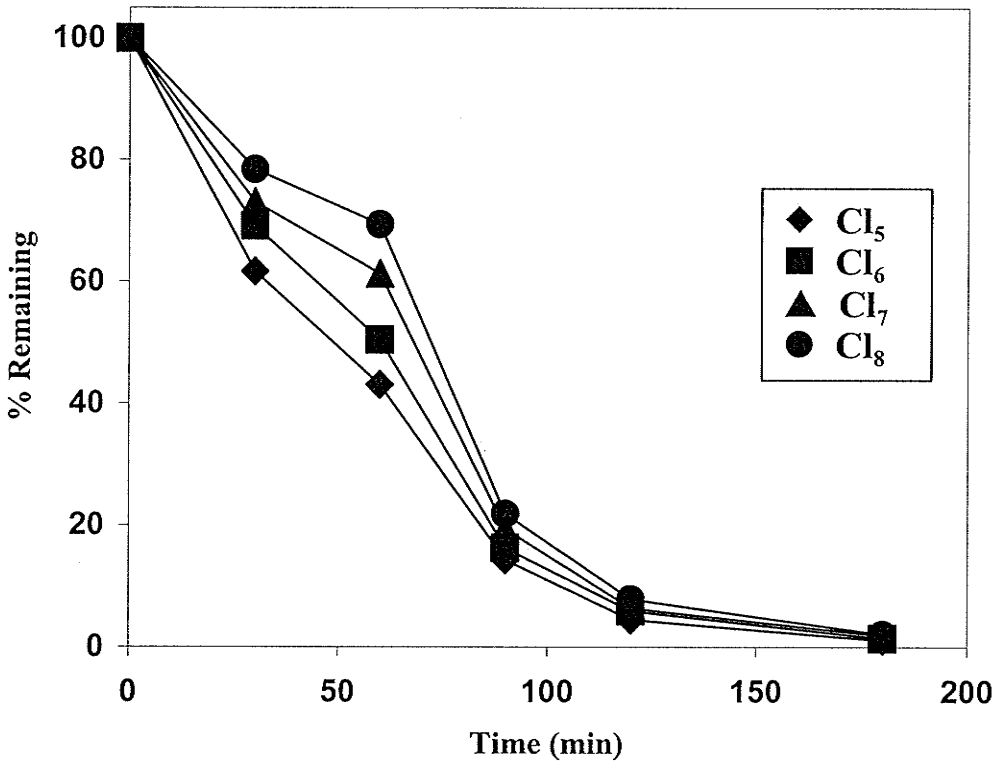

Figure 5.25: Photocatalytic degradation of the chlorinated decane ($\Sigma C_{10}Cl_{5\text{-}8}$) mixture (250 μg/L) in Lake 375 water in the presence of 200 mg/L TiO_2 in 0.1M $NaClO_4$ and pH 6.8 using 300 nm UV light.

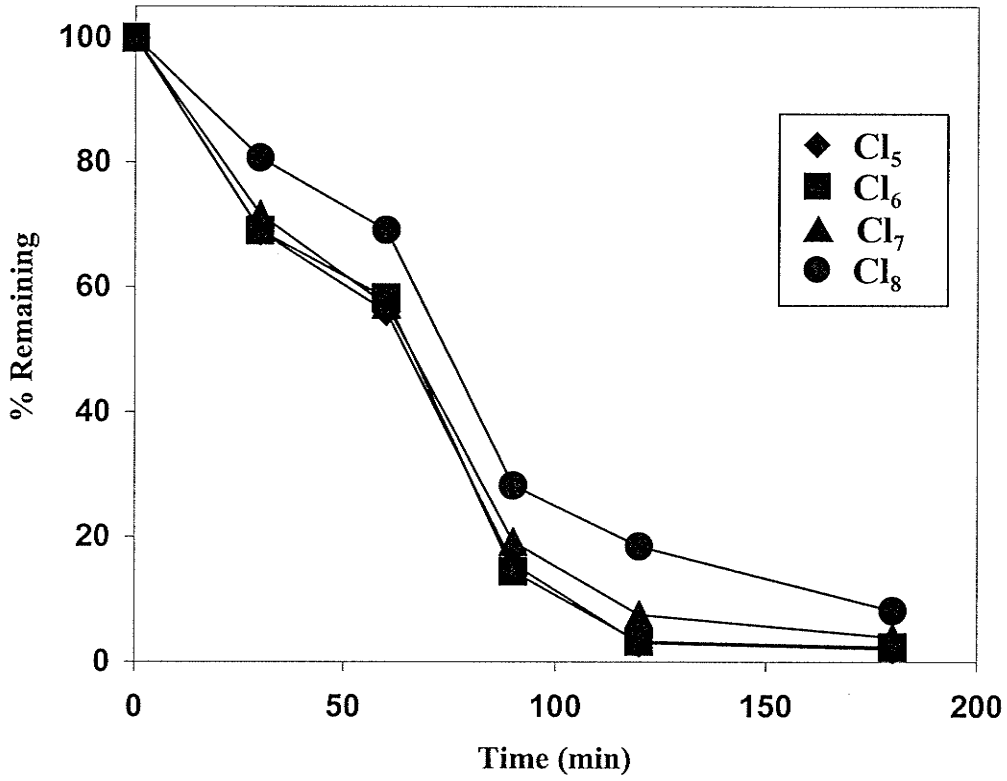

Figure 5.26: Photocatalytic degradation of the chlorinated undecane ($\Sigma C_{11}Cl_{5\text{-}8}$) mixture (250 μg/L) in Lake 375 water in the presence of 200 mg/L TiO_2 in 0.1M $NaClO_4$ and pH 6.8 using 300 nm UV light.

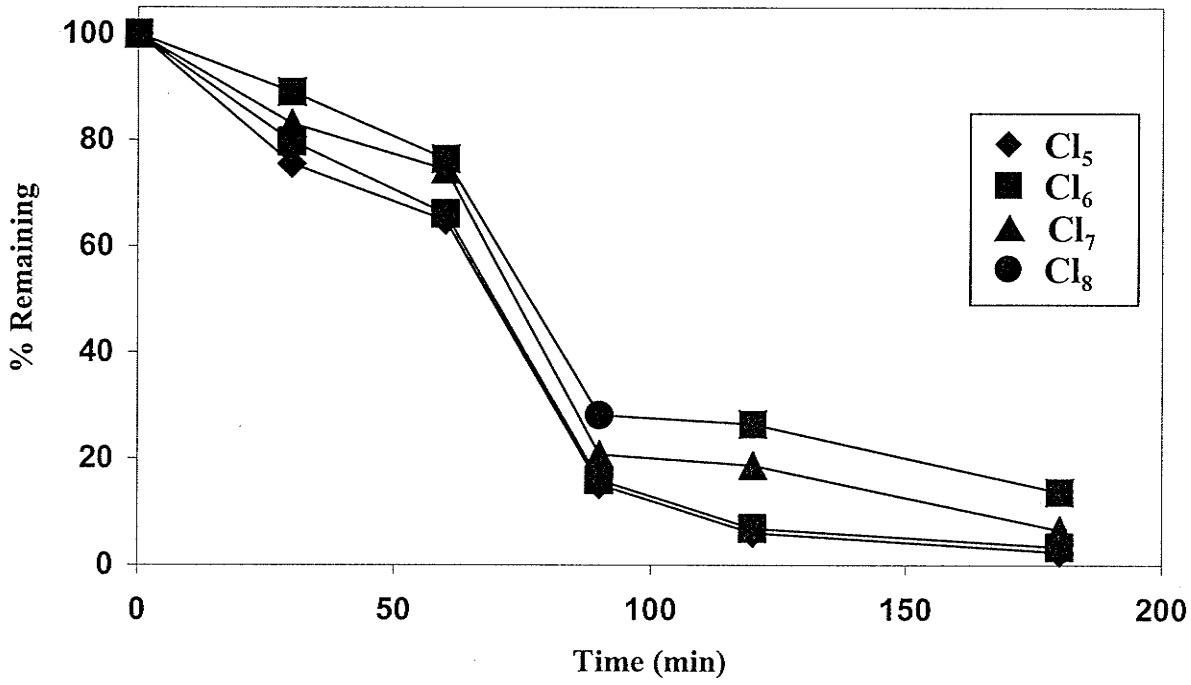

Figure 5.27: Photocatalytic degradation of the chlorinated dodecane ($\Sigma C_{12}Cl_{5\text{-}8}$) mixture (250 μg/L) in Lake 375 water in the presence of 200 mg/L TiO_2 in 0.1M $NaClO_4$ and pH 6.8 using 300 nm UV light.

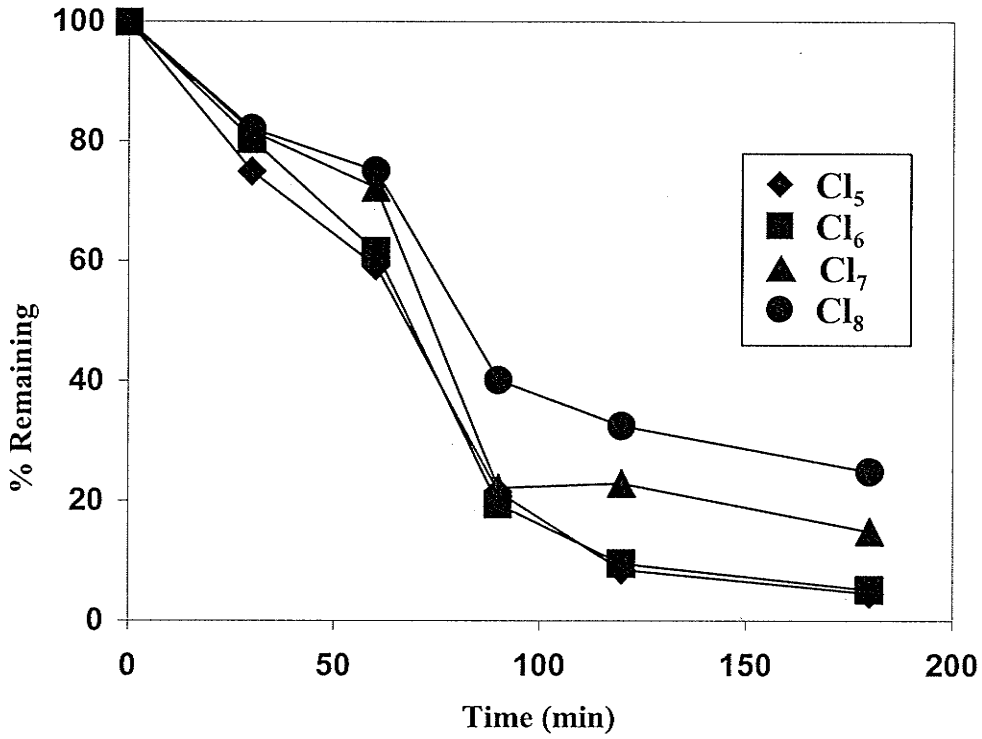

Figure 5.28: Photocatalytic degradation of the chlorinated tridecane ($\Sigma C_{13}Cl_{5\text{-}8}$) mixture (250 μg/L) in Lake 375 water in the presence of 200 mg/L TiO_2 in 0.1M $NaClO_4$ and pH 6.8 using 300 nm UV light.

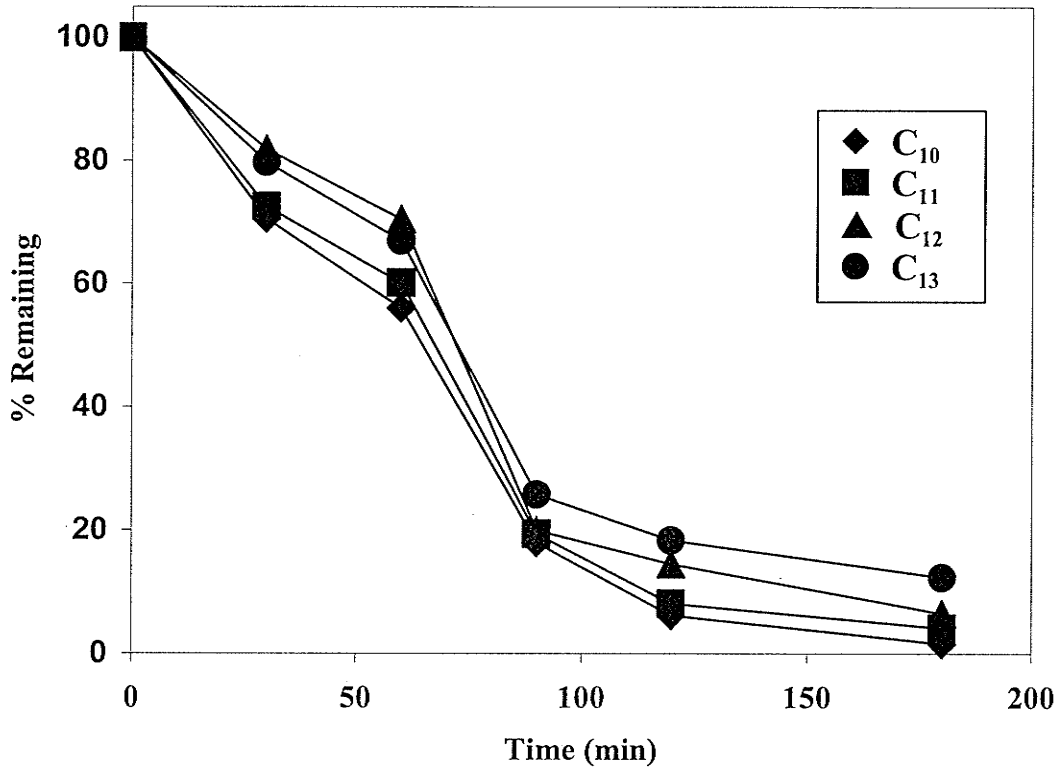

Figure 5.29: Photodegradation of individual PCA mixtures (Σ $C_{10}Cl_{5\text{-}8}$ to Σ $C_{13}Cl_{5\text{-}8}$) (250 μg/L) in Lake 375 water with 200 mg/L TiO_2 in 0.1 M $NaClO_4$ and pH 6.8 using 300 nm UV light.

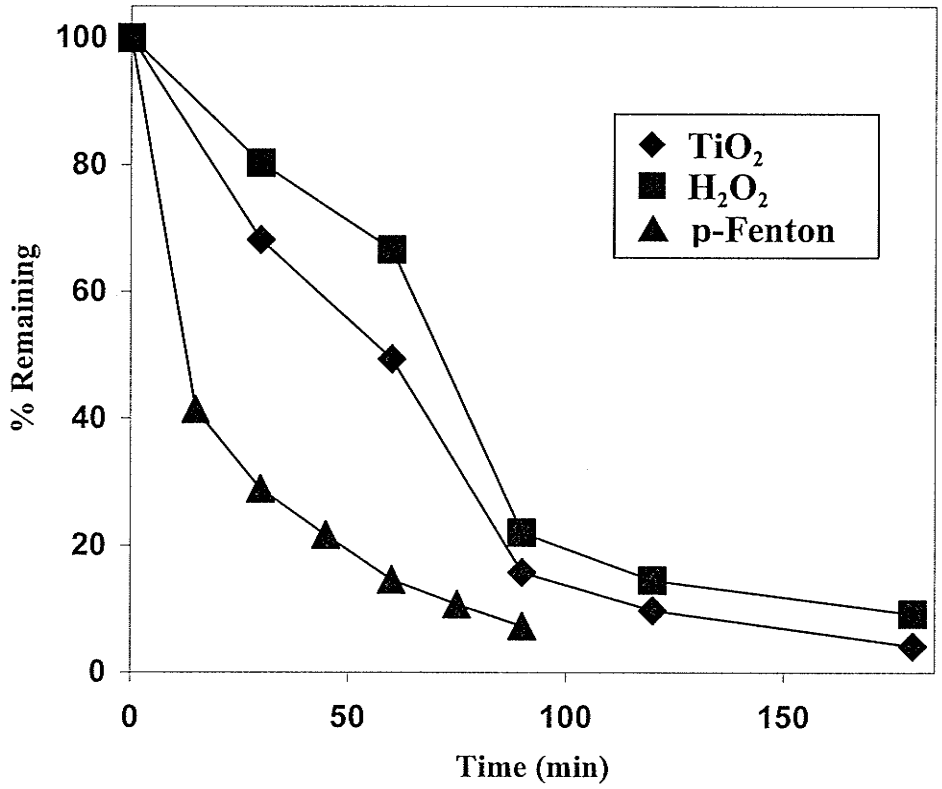

Figure 5.30: Photodegradation of the composite PCA mixture (Σ $C_{10}Cl_{5\text{-}8}$ to Σ $C_{13}Cl_{5\text{-}8}$) (250 μg/L) in Lake 375 water in the presence of 200 mg/L TiO_2, 1 x10^{-2} M H_2O_2 and photo-Fenton conditions (1 x 10^{-3} M Fe^{+3}/1 x 10^{-2} M H_2O_2) in 0.1 M $NaClO_4$ using 300 nm UV light.

of Fe^{+3} and reaction of H_2O_2 with Fe^{+2} (produced *in situ* in the modified Fenton reaction) which also leads to a recycling of Fe^{+3} [315]. These results are consistent with the increased rate of photodegradation of acetone (1.0 mM) in $Fe^{+3}/H_2O_2/UV$ compared to H_2O_2/UV [315] at pH 3. De Laat et al [315] observed 85% mineralization of acetone in 120 min in the $Fe^{+3}/H_2O_2/UV$ system compared to 51% under the H_2O_2/UV process. Ghaly et al [316] also reported the enhancement of the photochemical oxidation of *p*-chlorophenol (100 mg/L) under modified photo-Fenton conditions with a 5-9 fold increase in the oxidation rate relative to H_2O_2/UV.

5.4. Conclusion

Short chain PCAs were effectively photodegraded in aqueous suspensions of TiO_2 using 300 nm UV light. The kinetics of this photocatalytic degradation followed the Langmuir-Hinshelwood model suggesting that the reaction occurred on the surface of the photocatalyst. Inhibition of the degradation reaction in the presence of h^+_{vb}/$^\bullet$OH radical scavengers, including methanol and iodide, supported a photooxidation reaction. The lack of transformation of PCAs in acetonitrile as solvent indicated that the major oxidants were $^\bullet$OH radicals. The presence of tetranitromethane, effectively eliminating the formation of free $^\bullet$OH radicals, did not affect the degradation rates significantly. This result, combined with the observed increases in photolysis rates with the degree of adsorption of PCAs onto the surface of the photocatalyst, confirmed that the reaction involved adsorbed PCAs and surface bound $^\bullet$OH radicals. The slower photooxidation of PCAs in natural water compared to pure water may be due to light attenuation by dissolved organic carbon [313-314] and/or scavenging of $^\bullet$OH radicals by carbonate ion in natural water. Overall the photooxidation of the composite PCA mixture with TiO_2/UV was efficient with 50% disappearance of total PCAs in 1 h of irradiation.

5.5. Future Studies

1. Detailed studies of the hydrolysis of PCAs at different pH especially in acidic medium to clarify the role of both neutral and basic hydrolysis.
2. Study the photolysis of PCAs in different natural waters and at lower temperatures and compare photolysis rates in sunlight with rates determined using a xenon light source.
3. Determine the optimum Fe to H_2O_2 ratio in photo-Fenton systems, and follow the degradation by monitoring TOC, Cl^- ion and potential organic intermediates to determine the extent of mineralization.
4. Use LC/MS to determine the degradation products since some of the products may be too polar for GC analysis.
5. Investigate the zero-point charge of TiO_2 for the removal of the photocatalyst from the solution to facilitate extraction and analysis of TOC, Cl^- ion and degradation intermediates.

5.6. Overall conclusions:

The relatively slow rates of hydrolysis and photolysis determined in this study suggest that short chain PCAs are relatively persistent, accounting for their occurrence in remote locations in the environment. Efficient treatment of water contaminated with polychlorinated *n*-alkanes (PCAs) is one of the key issues in the protection of the environment. Homogeneous photodegradation including H_2O_2/UV and the photo-Fenton system, and heterogeneous photocatalysis using TiO_2/UV processes tested in this study were very effective in the degradation of short chain PCAs. Hydrogen peroxide is commonly used in the treatment of contaminated water because it is readily available, easy to handle, thermally stable and dissolves in water over a wide range of

concentrations. Furthermore H_2O_2 produces no air emissions, which is the problem with ozone treatment. The H_2O_2/UV process also produces $^{\bullet}OH$ with a high efficiency (quantum yields typically around 0.5) [82] and is more efficient than the O_3/UV process for the degradation of chlorinated hydrocarbons such as tetrachloroethylene [118]. The disadvantage of using hydrogen peroxide is its low molar absorptivity (ε_λ) in the ultraviolet region, ranging from 18 to190 M^{-1} cm^{-1} at 254 and 200 nm, respectively [130]. Thus, a high concentration of hydrogen peroxide relative to that of pollutant is necessary in order for significant degradation to occur. The use of solar energy with the H_2O_2/UV process remains under investigation [130]. Our results have shown that photodegradation of PCAs is significantly enhanced in the photo-Fenton system (H_2O_2/Fe/UV) due to the multiple production of $^{\bullet}OH$ radicals. Irradiation of Fenton-type systems with UV or UV/visible light in aqueous solution at lower pH can greatly enhance its oxidizing power [147-150]. The photo-Fenton method is one of the AOPs which utilizes visible light (wavelengths < 580 nm) for the generation of hydroxyl radicals. Thus 2 $^{\bullet}OH$ are generated per photocatalyzed cycle of the ferric/ferrous system. Applying the photo-Fenton system at the pilot plant scale will however, require removal of iron salts at the end of the process.

Our results have shown that the degradation of PCAs in the presence of TiO_2/UV was very effective, the reaction proceeding *via* oxidative (electrophilic) attack by adsorbed $^{\bullet}OH$ radicals. TiO_2 has been favored in wastewater treatment because of its ability to mineralize toxic/recalcitrant organic pollutants or to modify their structure. At the same time, TiO_2 is abundant, inexpensive, reusable, and resists photo-corrosion. Compared to the other AOPs, the TiO_2/UV process is used in wastewater treatment without addition of chemicals and is applied over a wide range of pH values. Although

using the powder form of TiO_2 will increase the surface area and the adsorption of the substrate hence enhancing the degradation process, this will require filtration of TiO_2 from the solution as a last step. Our study indicated that the modified photo-Fenton system was the most efficient process for the degradation of PCAs. It may be beneficial if both TiO_2/UV and photo-Fenton systems are combined as a degradation method for water contaminated with PCAs. As is evident from a recent study [317] addition of H_2O_2 to TiO_2/UV enhanced the degradation of alachlor 3.3 times at 300 nm. We postulate that addition of iron in the method (the photo-Fenton system) would further assist degradation and also extend the process for use in the visible region of the spectrum.

References

1. Environmental Canada, Priority Substances Program, CEPA Assessment report, Chlorinated paraffins. Commercial Chemicals Branch, (1993), Hull Quebec.
2. Zitko, V. In Handbook of Environmental Chemistry, Springer-Verlag, New York, (1980), Vol. **3A**, pp 149-156.
3. Chambers, G. Ubbelohde, A.R., The effect of molecular structure of paraffins on relative chlorination rates, *J. Chem.Soc.* (1955), 285-295.
4. Colebourne, N. Stem, E.S., The chlorination of some *n*-alkanes and alkyl chlorides, *J.Chem.Soc.* (1965), 3599-3605.
5. Mukherjee, A.B., The use of chlorinated paraffins and their possible effects in the environment. National Board of Waters and the Environment, *Helsinki, Finland, Ser.* **A 66** (1990).
6. Kirk-Othmer Chlorinated Paraffins. Kirk-Othmer Encyclopedia of chemical technology, (1980), **3rd** Eds. Wiley, New York.
7. Mackay, D. Shiu, W.Y. Ma, K.C., Illustrated handbook of physical and chemical properties and environmental fates for organic chemicals, (1992), Vol.**1**.Monoaromatic hydrocarbons, chlorobenzenes, and PCBs. Lewis, Chelsea, MI..
8. Mackay, D. Shiu, W.Y. Ma, K.C., Illustrated handbook of physical and chemical properties and environmental fates for organic chemicals, (1997), Vol. **5**. Chlorinated pesticides. Lewis, Chelsea, MI.
9. Muir, D.C.G. Stern, G. A Tomy, G.T., Chlorinated paraffins. The handbook of environmental chemistry. (2000), Vol. **3.** Part K, New types of persistent halogenated compounds, Chp. **8**. Springer-Verlag Berlin Heidelberg.
10. Tomy, G.T. Fisk, A.T. Westmore, J.B., Environmental chemistry and toxicology of polychlorinated *n*-alkanes, *Rev. Environ.Contam. Toxicol.* (1998), **158**, 53-128.
11. Tomy, G.T. Muir, G.C.D. Stern, G.A. Westmore, J.B. Levels of C_{10}-C_{13} polychloro-*n*-alkanes in marine mammals from the arctic and the St. Lawrence River estuary, *Environ.Sci. Technol.* (2000), **34**, 1615- 1619.
12. Environment Canada Priority Substances List Assessment Report: Chlorinated paraffins. (1993), En 40 215/17E. Health and Welfare Canada, Ottawa, Ontario.

13. Windrath, O.M. Stevenson, D.R., Chlorination and bromochlorination paraffins as flame retardants. In: Plastics Compounding, (1985), Vol. **1,** pp 38-52.

14. Morrison, R.T. Boyd, R.N., *Organic Chemistry*, (1983), 4th Eds. Allyn and Bacon, Newton, MA.

15. Drouillard, K.G. Tomy, G.T. Muir, D.C.G. Friesen, K. J., Volatility of chlorinated *n*-alkanes (C_{10}-C_{12}): Vapor pressures and Henry's Law constants. *Environ Toxicol Chem.* (1998), **17**, 1252-1260.

16. K.G. Drouillard, T. Hiebert, P.Tran, G.T. Tomy, D.C.G. Muir, K.J. Friesen, Estimating the aqueous solubilities of individual chlorinated n-alkanes (C_{10}-C_{12}) from measurements of chlorinated alkane mixtures. *Environ Toxicol Chem.* (1998), **17**, 1261-1267.

17. Tomy, G.T. Billeck, B. Stern, G.A., Synthesis, isolation and purification of C_{10}-C_{13} polychloro-*n*- alkanes for use as standards in environmental analysis, *Chemosphere*, (2000), **40**, 679-683.

18. Drouillard, K.G., Physico-chemical property determination on chlorinated *n*-alkanes (C_{10}-C_{12}). parameters for estimation of the environmental fate of chlorinated *n*-paraffins. MSc, (1996), University of Manitoba, Winnipeg, Canada.

19. Bidleman, T.F., Estimation of vapor pressure for nonpolar organic compounds by capillary gas chromatography, *Anal. Chem.* (1984), **56**, 2490-2496.

20. Lyman, W.J. Reehl, W.F. Rosenblatt, D.H., Handbook of chemical property estimation methods: Environmental behavior of organic compounds. (1990), Am.Chem.Soc, Washington, DC.

21. Sijm, D.T.H.M. Sinnige, T.L., Experimental octanol/ water partition coefficients of chlorinated paraffins. *Chemosphere*, (1995), **31**: 4427-4435.

22. De Bruijn, J.F. Busser, F. Seinen, W. Hermens, J., Determination of octanol/water partion coefficients with the slow-stirring method. *Environ Toxicol Chem.* (1989), **8**, 499- 512.

23. Bergman, A. Leonardsson, I. Wachtmeister, C.A. , Synthesis of polychlorinated [^{14}C] alkanes (PCAs) of high specific activity. *Chemosphere* (1981), **10**, 857-863.

24. Fisk, A.T. Wiens, S.C. Webster, G.R.B. Bergman, Å. Muir, D.G.C., Accumulation

and depuration of sediment sorbed C_{12}- and C_{16}-polychlorinated alkanes by oligochoates lumbriculus variegatus. *Environ Toxicol. Chem.*, (1998), **17**,2019-2026.

25. Karickhoff, S.W., Semi-empiricalestimation of sorption of hydrophobic pollutants on normal sediments and soils. *Chemosphere*, (1981), **10**, 833-846.
26. Friedman, D. Lombardo, P., Photochemical technique for the elimination of chlorinated aromatic interference in the gas-liquid chromatographic analysis for chlorinated paraffins. *J. Assoc.of anal. Chem.* (1975), **58**, 703-706
27. Sadek, S.A. Ebraheem, S, El-Morsi, T.M., Friesen, K. J. and Abd-El-Aziz, A. S. Photodegradation of 1,12-dichlorododecane in aquatic media with a Xenon light source, *International Journal of Scince & Technology,* (2002), **13**, 45-50.
28. Atkinson, R., Kinetics and mechanisms of gas phase reactions of the hydroxyl radical with organic compounds under atmospheric conditions. *Chem. Rev.* (1986), **86**, 69- 201.
29. Willis, B. Crookes, J M. Diment, J. Dobson, S.D., Environmental hazard assessment: chlorinated paraffins. Toxic Substances Division. Dept. of Environment. London, UK, (1994).
30. Reiger, R. Ballschmiter, K., Semivolatile organic compounds as markers in sewer films. *Fresenius J Anal Chem* (1995), **352,** 715-724.
31. Lahaniatis, E.S. Paralar, H. Klein, W. Korte, F., Analysis and photochemistry of high boiling polychlorinated paraffin mixtures. *Chemosphere*, (1975), **4**, 83-88.
32. Mukherjee, A.B., The use of chlorinated paraffins and their possible effects in the environment. *National Board of Waters and the Environment*, Helsinki, Finland, (1990), Ser. **A 66**.
33. D.W.F. Hardie, Chlorinated paraffins. Kirk-Othmer Encyl Chem Technol, (1964), 2nd Eds, Vol. **5**.
34. Environment Canada, Priority substances program, CEPA, Assessment report: Chlorinated paraffins. Commercial chemicals branch, (1993), Hull, Quebec.
35. Environment Canada, A technical & Socio-Economic Comparison of Options Ch.**15**-Chlorinated flame-retardants (1998).
36. Environmental Protection Agency, Office of Toxic Substances. Rm1 decision Package, Chlorinated paraffins. Environmental risk, EPA, Washington DC (1991).

37. Campbell, I. McConnell, G., Chlorinated paraffins and the environment. 1: Environmental occurrence. *Environ. Sci. Technol.* (1980), **14,** 1209-1214.
38. Metcalfe-Smith, J.L. Maguire, R.J. Batchelor, S.P. Bennie, D.T., Occurrence of chlorinated paraffins in the St. Lawrence River near a manufacturing plant in Cornwall, ON. Aquatic ecosystem protection branch. National Water Research Institute. Burlington, Ontario (1995).
39. Swedish National Chemicals Inspectorate Rm1 decision package. Chlorinated paraffins. Environmental risk assessment. KEMI Rep.1. Environmental Protection Agency, Office of Toxic Substances, Washington, DC (1991).
40. World Health Organization, Environmental health criteria 181: chlorinated paraffins, (1996), WHO, Geneva, Switzerland
41. Birtley RDN, Conning DM, Daniel JW, Ferguson DM, Longstaff E. Swan AAB The toxicological effects of chlorinated paraffins in mammals. *Toxicol. Appl. Pharmacol.* (1980), **54,** 514-525.
42. Thompson, R.S. Madeley, J.R., The acute and chronic toxicity of chlorinated paraffin to the mysid shrimp mysidopsis bahia. Brixham Rep. BL/B/2373. Imperial Chemical Industries PLC, Devon, UK (1983).
43. Madeley, J.R. E. Gillings, The determination of the solubility of four chlorinated paraffins in water. ICI Confidential Rep. BL/B/2301. Imperial Chemical Industries PLC, Devon, UK (1983).
44. Thompson, R.S. Madeley, J.R., Toxicity of a chlorinated paraffin to the green alga Selenastrum capricornutum, Brixham Rep. BL/B/2321. Imperial Chemical Industries, PLC, Devon, UK (1983).
45. Madeley, J.R. Maddock, B.G., The bioconcentration of a chlorinated paraffin in the tissues and organs of rainbow trout Salmon gairdneri. Brixham Rep. BL/B/2310. Imperial Chemical Industries PLC, Devon, UK (1983).
46. Madeley, J.R. Birtley, R., Chlorinated paraffins and the environment. 2. Aquatic and avian toxicology. *Environ Sci Technol.* (1980), **14,** 1215-1221
47. Nilsen, O.G. Toftgard, R. Glaumann, H., Effects of chlorinated paraffins on rat liver microsomal activities and morphology. *Arch Toxicol.* (1981), **49,** 1-13.
48. Wyatt, I. Coutts, C.T. Elcombe, C.R., The effect of chlorinated paraffins on hepatic

enzymes and thyroid hormones. *Toxicology*, (1993), **77,** 81-90.

49. World Health Organization, Environmental health criteria 181: Chlorinated paraffins. WHO, Geneva, Switzerland (1996).

50. C.R. Elcombe, S.C. Watson, I. Wyatt, J.R. Foster, Chlorinated paraffins (CP): mechanisms of carcinogens. *Toxicologist*, (1994), **14**, 276.

51. Bucher, J.R. Alison, R.H. Montgomery, C.A. Huff, J. Haseman, J.K. Farnell, D. Thompson, R. Prejean, J.D., Comparative toxicity and carcinogenicity of two chlorinated paraffins in F344/N rats and B6C3F1 mice. *Fundam Appl Toxicol.* (1987), **9**,454-468.

52 Frroescheis, O. and Ballschmiter, K., Electron capture negative ion (ECNI) mass spectrometry of complex mixtures of chlorinated decanes and dodecanes: An approach to ECNI mass spectra of chlorinated paraffins in technical mixtures. *Fresenius J. Anal Chem* (1998), **361**, 784-790.

53 Tomy G.T., Stern G.A., Muir D.C.G., Fisk A.T., Cymbalisty C.D., Westmore J.B., Quantifying C_{10}-C_{13} polychloroalkanes in environmental samples by high-resolution gas chromatography electron capture negative ion high resolution mass spectrometry. *Anal Chem* (1997), **69**, 2762-2771.

54 Gjos N, Gustavsen KO, *Anal Chem,* (1982), **54**, 1316-1318.

55. Vialaton, D. and Richard,C, Phototransformation of aromatic pollutants in solar light: photolysis versus photosensitized reactions under natural water conditions, *Aquat. Sci*, (2002),**64**, 207–215.

56. Boethling R.S., Mackay D. Hand book of property Estimation methods for chemicals, environmental and helth sciences. Lewis Publishers, New York, CRC Press LLC (2002).

56a. Visualizing redox chemistry: propping environmental oxidation-reduction reactions with indicators dyes, *The Chemical Educator*, (2001), **6**,1-11.

56b Pedersen,E. J. and Marinas, B.J., The hydroxide assisted hydrolysis of cyanogens chloride in aqueous solution, *Wat. Res.* (2001), **35**, 643-648.

56c Strek, H.J. Fate of chlorsulfuron in the environment. 1.Laboratory evaluations, *Pestic. Sci.,* (1998), **53**, 29-51.

57. Wolfe, N.L. and Macalady, D.L. New perspectives in aquatic redox chemistry:

Abiotic transformations of pollutants in groundwater and sediments. *J. Contam. Hydrol.* (1992), **9**, 17-34.

58. Macalady, D.L. P.G. Tratnyek, and T.J. grrundl., abiotic reduction reactions of anthropogenic organic chemicals in anaerobic systems. *J.Contam. Hydrol.*(1986),**1**, 1-28.

59 Mabey, W.R. and Mill, T., Critical review of hydrolysis of organic compounds in water under environmental conditions*J. Phys. Chem. Ref. Data.* (1978), **7**, 383-415.

60. Leifer A., The kinetics of environmental aquatic photochemistry, American Chemical Society, Washington, D.C. (1988).

61. Miyamoto, J., Environmental and health issues, *Pure& Appl. Chem.*(1996), **68**, 1737-1748.

62. Draper, W.M. and Crosby D.G. Hydrogen peroxide and hydroxyl radical: Intermediates in indirect photolysis reactions in water. *Journal of Agricultural and Food Chemistry* (1981), **29**, 699.

63. Draper, W.M. and Crosby D.G. Solar photooxidation of pesticides in dilute hydrogen peroxide. *Journal of Agricultural and Food Chemistry,* (1984), **32**, 231.

64. Zepp, R.G. and Cline D.M. Rates of direct photolysis in aquatic environments. *Environmental Science and Technology* (1977), **11**, 359.

65. Zepp, R.G. et al. Singlet oxygen in natural waters. *Nature* (1977), **267,** 421.

66. Zepp, R.G. et al. Comparison of photochemical behavior of various humic substances in water: I. Sunlight induced reactions of aquatic pollutants photosensitized by humic substances. *Chemosphere* (1981),**10,**109.

67. Zepp, R.G. et al. Comparison of photochemical behavior of various humic substances in water: II. Photosensitized oxygenations. *Chemosphere* (1981), **10,** 119.

68. Wolff, C.J.M. et al. The formation of singlet oxygen in surface waters. *Chemosphere* (1981), **10,** 59.

69. Haag, H.R. et al. Singlet oxygen in surface waters, Part I; Furfuryl alcohol as a trapping agent. *Chemosphere* (1984), **13**, 631.

70. Haag, W.R. et al. Singlet oxygen in surface waters, Part II: Quantum yields of its production by some natural humic materials as a function of wavelength.

Chemosphere(1984), **13**, 641.

71. Cooper W.J. and Zika R.G. Photochemical formation of hydrogen peroxide in surface and ground waters exposed to sunlight. *Science* (1983), **220,** 711.
72. Draper W.M. and Crosby D.G. The photochemical generation of hydrogen peroxide in natural waters. *Archives of Environmental Contami-nation and Toxicology* (1983),**12**, 121.
73. Zepp, R.G. et al. Photosensitized transformations involving elec-tronic energy transfer in natural waters: role of humic substances. *Environ-mental Science and Technology* (1985), **19,** 74.
74. Atkinson, R. A structure activity relationship for the estimation of the rate constants for the gas-phase reactions of OH radicals with organic compounds. *Int. J. Chem. Kinetics*, (1987), **19**,799-828.
75. Westrick, J.J. Mello, W. Thomas, R.F., *J. Am Water Works Assoc*, (1984), **76,** 52-59.
76. Lykins, B.W. et al., Granular activated carbon for removing nitrohalomethane organics from drinking water, Water Engineering Research Laboratory, USEPA PB85-120970; EPA, (1984), **600/S2**, 84-165
77. Clark, R.M. Fronk, C.A. Lykins Jr, B.W., Removing organic contaminants from Groundwater, *Envron. Sci Technol*, (1988), **22**, 1126-1129.
78. Marye Anne Fox and Maria T. Dulay Heterogeneous Photocatalysis. *Chem. Rev.* (1993), **93**,341-357
79. Prashant V. Kamat, Photochemistry on Nonreactive and Reactive (Semiconductor) Surfaces, *Chem. Rev.* (1993), **93**, 267-300.
80. Legrini, O. Oliveros, E. and Braun, M.A., Photochemical Processes for Water Treatment, *Chem. Rev.* (1993), **93**, 671-698.
81. Pelizzetti, E., Photocatalytic processes for destruction of organic water contaminants, in: Chemical Reactor Technology for environmental Safe Reactors and products, H.I. De Lasa, et al. Eds, Kluwer Academic Publishers, (1993), pp.577-608.
82. James, R. Bolton and Stephen, R. Cater, in *Aquatic and Surface Photochemistry*, (1994), p 467-488.
83. Mihaela, I. Stefan and James R. Bolton, Mechanism of the degradation of 1,4-Dioxane in dilute Aqueous solution using the UV/hydrogen peroxide process,

Environ. Sci. Technol. (1998), **32**,1588-1595.

84. Huang, C.-R. Shu, H.-Y. The reaction-kinetics, decomposition pathways and intermediate formation of phenol in ozonation, UV/O3 and UV/H2O2 processes, *J. Hazard. Mater.* (1995), **41**, 47-64.
85. Shen, Y.-S. Ku, Y. Lee, K.-C. The effect of light absorbancy on the decomposition of chlorophenols by ultraviolet-radiation and UV/H2O2 processes, *Water Res.* (1995), **29**, 907-914.
86. Scheck, C. K. Frimmel, F.H. Degradation of phenol and salicyliacid by ultraviolet radiation hydrogen-peroxide oxygen, *Water Res.* (1995), **29**, 2346-2352.
87. Guittonneau, S.De Laat, J. Duguet, J. P. Bonnel, C. Dore, M. Oxidation of parachloronitrobenzene in dilute aqueous-solution by O_3 + UV and H_2O_2 + UV a comparative- study, *Ozone Sci. Eng.* (1990), **12**,73-94.
88. Benitez, F.J. Beltran-Heredia, J. Acero, J.L. Gonzalez, T. Degradation of protocatechuic acid by two advanced oxidation processes:ozone/UV radiation and H2O2/UV radiation, *Water Res.* (1996), **30**,1597-1604.
89. Stefan, M. I. Hoy, A.R. Bolton, J.R. Kinetics and mechanism of the degradation and mineralization of acetone in dilute aqueous solution sentitized by the UV photolysis of hydrogen peroxide, *Environ. Sci. Technol.* (1996), **30**, 2382-2390.
90. Sundstrom, D. W. Klei, H.E. Nalette, T.A. Reidy, D.J. Weir, B.A. *Hazard. Waste Hazard. Mater.* (1986), **3**,101.
91. Hirvonen, A. Tuhkanen, T. Kalliokoski, P. *Environ. Technol.* (1996), **17**, 263.
92. Hirvonen, A. Tuhkanen, T. Kalliokoski, P. *Water Sci. Technol.* (1996), **33**, 67.
93. Yue, P.L. Legrini, O. *Water Poll. Res. J. Canada* (1992), **27**, 123.
94. Hoigne,J.and Bader, H. Ozonation of water: role of hydroxyl radicals as oxidizing intermediates, *Science,* (1975),**190**,782.
95. Beltran, F.J. Ovejero, G. Encinar, J. M. Rivas, J. Oxidation of polynuclear aromatic hydrocarbons in water, 1.Ozonation, *Ind. Eng. Chem. Res.* (1995), **34**, 1596.
96. Beltran, F.J. Ovejero, G. Garcia-Araya, J.F. Rivas, J. Oxidation of polynuclear aromatic hydrocarbons in water, 2.UV radiation and ozonation in the presence of UV radiation, *Ind. Eng. Chem. Res.* (1995), **34**, 1607.
97. Beltran, F.J. Ovejero, G. Rivas, J. Oxidation of polynuclear aromatic hydrocarbons in

water, 4.Ozone combined with hydrogen peroxide, *Ind. Eng. Chem. Res.* (1996), **35**, 891.

98. Beltran, F.J. Encinar,J.M. Alonso, M.A.. Nitroaromatic hydrocarbon ozonation in water, 1.Single ozonation, *Ind. Eng. Chem. Res.* (1998), **37**, 25.
99. Beltran, F.J. Encinar,J.M. Alonso, M.A.. Nitroaromatic hydrocarbon ozonation in water, 2.combined ozonation with hydrogen peroxide or UV radiation, *Ind. Eng. Chem. Res.* (1998), **37**, 32.
100. Glaze, W.H. Kang, J.-W. Chapin, D.H. The chemistry of water-treatment processes involving ozone, hydrogen- peroxide and ultraviolet-radiation, *Ozone Sci. Eng.* (1987), 9, 335-352.
101. Peyton, G.R. Glaze, W.H. Destruction of pollutantants in water with ozone in combination with ultraviolet-radiatio.3. photolysis of aqueous ozone, *Environ. Sci. Technol.* (1988), **22**, 761-767.
102. Staehelin, J. and Hoigne, J. Decomposition of ozone in water: rate of initiation by hydroxide ions and hydrogen peroxide. *Environ. Sci. Technol.* (1982), **16**, 676-681.
103. Staehelin, J. and Hoigne, J. Decomposition of ozone in water in the presence of organic solutes acting as promoters and inhibitors of radical chain reactions, *Environ. Sci. Technol.* (1985), **19**, 1206-1213.
104. Rate constants of reactions of ozone with organic and inorganic-compounds in water .3. Inorganic-compounds and radicals, Hoigne J. Bader, H. Haag, W.R., Staehelin, J., *Water Res.* (1985),**19**, 993-1004.
105. Gunz D.W., Hoffmann M.R.Atmospheric chemistry of peroxides - A review *Atmospheric Environment part A-General Topics*, (1990), **24,** 1601-1633.
106. Glaze, W.H. Kang, J.W. Advanced oxidation processes-description of a kinetic-model for the oxidation of hazardous materials in aqueous –media with ozone and hydrogen-peroxide in a semibatch reactor, *Ind. Eng. Chem. Res.* (1989), **28**, 1573-1580.
107. Glaze, W.H. and Kang, J.W. Advanced oxidation processes *for treating groundwater contaminated with TCE and PCE-laboratory studies, Journal AWWA* (1988), **80**, 57-63.
108. Wallace, J.L. Vahadi, B. Fernandes, J.B. Boyden, B.H. The combination of ozone

hydrogen-peroxide and ozone UV-radiation for reduction of trihalomethane formation potential in surface-water, *Ozon Sci. Eng.* (1988), **10**, 103-112.

109. Lewis, N. Topudurti, K. Welshans, G. Foster, R. A field demonstration of the UV oxidation technology to treat ground-water contaminated with VOCS *J. Air Waste Manag. Assoc.*(1990), **40**, 540-547.
110. Khan, S.R. Huang, C.R. Bozelli, *J.W. Environ. Prog.* (1985), **4**, 229-238.
111. Omura, K. Matsuura, T. *Tetrahedron* (1968), **24**, 3475.
112. Mill, T. Gould, C.W. Environ. Sci. Technol. (1975), 13, 205.
113. Baxendale, J.H. and Wilson J.A. The photolysis of Hydrogen peroxide at high light intensities, *Trans. Faraday Soc.* (1957), **53**, 344.
114. Lunak, S. and Sedlak, P. Photoinitiated reactions of hydrogen preoxide in the liquid phase. *J.photochem. photobiol.* (1992), **68**, 1-33.
115. Weeks, J.L. and Matheson, M.S., The primary quantium yield of hydrogen peroxide decomposition, *J. Am. Soc.* (1956), **78**, 1273.
116. Volman, D.H. and Chen, J.C. *J. Am. Chem. Soc.* (1959), **81**, 4141-4144.
117. Mills, A. Davies, R.H. and Worsley, D., Water purification by semiconductor photocatalysis, *Chem. Soc. Rev.* (1993), **22**, 417-425.
118. Guittonneau, S., Glaze, W.H. Duguet, J.P. Wable, O. Mallevialle, J., Characterization of natural-water for potential to oxidize organic pollutants with ozone. *Ozone-Science & Engineering,* (1992), **14**, 185-196.
119. Holman, Martin M. Photodegradation of water pollutants, , CRC Press, Inc. New York. (1996).
120. Kawaguchi, H., Photooxidation of formic acid in aqueous solution in the presence of hydrogen peroxide, *Chemosphere* (1993), **26**, 1965-1970.
121. Kawaguchi, H., Photooxidation of propanol in aqueous solution in the presence of hydrogen peroxide, *Chemosphere* (1993), **27**, 577-584.
122. Kawaguchi, H., Photooxidation of phenol in aqueous solution in the presence of hydrogen peroxide, *Chemosphere* (1993), **24**, 1707-1712.
123. Kawaguchi, H., Oxidation efficiency of hydroxyl radical in the photooxidation of 2-chlorophenol using ultraviolet radiation and hydrogen peroxide, *Environ. Sci. Technol.* (1993), **14**, 289-293.

124. Lipczynska-kochany, E. and Bolton J.R. Flash photolysis/HPLC applications.2. Direct photolysis vs. hydrogen peroxide mediated photodegradation of 4-chlorophenol as studied by a flash photolysis/HPLC technique, *Environ. Sci. Technol.* (1992), **26**, 259-262.

125. Hessler, D.P. Gorenflo, V. and Frimmel, F.H. Degradation of aqueous atrazine and metazachlor solutions by UV and UV/H2O2- influence of pH and herbicide concentration, *Acta Hydrochim. Hydrobiol.* (1993), **21**, 209-214.

126. Beltran, F.J. Ovejero, G. and Acedo, B. Oxidation of atrazine in water by ultraviolet radiation combined with hydrogen peroxide, *Water Res.* (1993), **27**, 1013-1021.

127. Ho, P.C., Photooxidation of 2,4-dinitrotoluene in aqueous solution in the presence of hydrogen peroxide, *Environ. Sci. Technol.* (1986), **20**, 260-267.

128. Lipczynska-Kochany, E., Degradation of nitrobenzene and nitrophenols by means of advanced oxidation processes in a homogeneous phase. Photolysis in the presence of hydrogen peroxide versus the Fenton reaction, *Chemosphere* (1992), **24**, 1369-1380.

129. Glaze W.H. Lay, Y. Kang, J.W. Advanced oxidation processes - a kinetic-model for the oxidation of 1,2-dibromo-3-chloropropane in water by the combination of hydrogen peroxide and UV-radiation, *Industrial & Engineering Chemistry Research*, (1995), **34**, 2314-2323.

130. Julian Blanco Glavez et al. Solar detoxification (2001), ww.unesco.org/science/wsp/puplications/solar.htm.

131. Walling C. Fenton's reagent revisited, *Acc. Chem. Res.*(1975), **8**,125-131.

132. David L. Sedlak and Anders W. Andren, Oxidation of chlorobenzene with Fenton's reagent, , *Environ. Sci. Technol.* (1991), **25**, 777-782.

133. Murphy, A. P. Boegli, W.J. Price, M.K. and Moody, C.D., A Fenton-like reaction to neutralize formaldehyde waste solutios, *Environ. Sci. Technol.* (1989), **23**, 166-169.

134. De Laat, J. and Gallard, H. Catalytic decomposition of hydrogen peroxide by Fe (III) in homogeneous aqueous solution: mechanism and kinetic modeling, *Environ Sci Technol* (1999), **33**, 2726-2732.

135. Pignatello, J.J. Dark and photoassisted Fe^{3+} catalyzed degradation of chlorophenoxy herbicides by hydrogen peroxide, *Environ. Sci. Technol.* (1992), **26**, 944-951.

136. Helz, G. Zepp, R. Crosby, D. Aquatic and surface chemistry, (1995), Lewis

publishing Co. Boca Raton, FL.

137. Nadtochenko, V. Kiwi, J. Primary photochemical reactions in the photo-Fenton system with ferric chloride. 1. A case study of xylidine oxidation as a model compound, *Environ. Sci. Technol.* (1998), **32**, 3273-3281.
138. Sawyer, D. Sobkowiak, A. Matsushita, T. *Acc. Chem. Res.* (1996), **29**, 409-.
139. Ruppert, G. Bauer, R. Heisher, G. *J. Photochem. Photobiol. A* (1993), **73**, 75-
140. Plimmer, J.R. Kearney, P.C. Klingebil,U.I. J.Agric. Food Chem. (1971),**19**, 572-573.
141. Sedlak, D.L. Andren, A.W. *Environ. Sci. Technol.* (1991), **25**, 777-782.
142. Sudoh, M. Kodera, T. Sakai, K. Zhang, J. Q. Koide, K. *J. Chem. Eng. Jpn.* (1986), **19**, 513-518.
143. Watts, R.J. Udell, M.D. Rauch, P.A. Leung, S.W. *Hazard. Waste Hazard Mater.* (1990), **7**, 335-345.
144. Barbeni, M. Minero, C. Pelizzetti, E. Borgarello, E. Serpone, N. Chemical degradation of chlorophenols with Fenton's reagent (Fe^{2+} + H_2O_2), *Chemosphere,* (1987), **16**, 2225-2237
145. Bowers, A.R. Gaddipati, P. Eckenfelder, W.W. Jr. Monesn, R.M. Water Sci. Technol. (1989), **21**, 477.
146. Carberry, J.B. Benzing, T.M. *Water Sci. Technol.* (1991), **23**, 367.
147. Kuo, W.G. *Water Res.* (1992), **26**, 881.
148. Margaret, A. E. Pignatello, J. J. Grasso, D., Degradation and detoxification of the wood preservatives creosote and pentachlorophenol in water by the photo-Fenton reaction, *Wat. Res.* (1999), **33**, 1151-1158.
149. Haag, W.R. Yao, C.C.D. *Environ. Sci. Technol.* (1992), **26**, 1005-1013.
150. Sedlak, P.Lunak, S. Lederer, P. *Collect. Czech. Chem. Commun.* (1987), **52**, 2451-2456.
151. Zepp, R.G., Faust, B.C., Hoigne, J., Hydroxyl radical formation in aqueous reactions (pH 3-8) of iron (II) with hydrogen peroxide: the photo-Fenton reaction. *Environ. Sci. Technol.* (1993), **26**, 313-319.
152. Kiwi, J. Pulgarin, C.Peringer, P. Appl. Catal. B. (1994), **3**, 335.
153. Sun Y. Pignatello J. J., Photochemical reactions involved in the total mineralization of 2,4-D by $Fe^{3+}/H_2O_2/UV$, *Environ. Sci. Technol.* (1993), **27**, 304-310.

154. Nadtochenko, V. Kiwi, J. Photochemical mineralization of xylidine by the Fenton reagent.2. implications of the precursors formed in the dark, *Environ. Sci. Technol.* (1998), **32**, 3282-3285.

155. Safarzadeh-Amiri, A. Bolton J.R. Cater, S.R. J. Adv. Oxid.Technol. (1996), **1**, 18-26.

156. Pignatello, J. Huang, L.Q. *Water Res.* (1993), **27**,1731-1736.

157. Merzellier, P. Jirkovsky, J. Bolte, M. *Pestic. Sci.* (1997), **49**, 259-267.

158. Korman, C. Bahnemann, D.W. Hoffman, M.R., (1991) *Environ.Sci,.Technol,* **25**, 494-500.

159. Davis, A. P. Huang, C. P. *Wat. Res.,* (1990), **24**, 543-550.

160. Darwent, J. R. Lepre, A. *J. Chem. Soc. Faraday Trans 2,* (1986), **82**, 1457 - 1468

161. Brandi, R. J. Alfano, O. M. and Cassano A. E., Evaluation of Radiation Absorption in Slurry Photocatalytic Reactions 1. Assessment of Methods in Use and New Proposal, *Environ. Sci. Technol.,* (2000), **34**, 2623-2630.

162. Palizzetti, E., Minero, C., and Maurino, V., The Role of Colloidal Particles in the Photodegradation of Organic Compounds of Environmental Concern in Aqauatic Systems. Advances in Colloid Interface, *Science*, (1990), **32**, 271-316.

163 Daintith, J., A dictionary of chemistry, 4th edition, Oxford University press Inc., New York, (2000), p.489.

164. Cotton F. Albert, Wilkinson G., Murillo Carlos A., Bochmann M.; Advanced Inorganic Chemistry, John Wiley & Sons, Inc., New York, (1999), p 43-45.

165. Kisch, H., 'What is the Photocatalysis'. *Photocatalysis: Fundamentals and Applications* Eds N. Serpone and E. Pelizzetti, John Wiley & Sons Inc.,New York (1989).

166. Stumm, Werner and Morgan, J. James Aquatic Chemistry Chemical Equilibrium and Rates in Natural Water , 3rd edition, John Wiley & Sons, Inc. (1996), p 755.

167. Kano Kanaan, Physical And Solid State Electronics ,Addison-Welsely Publishing comp.Inc.Ontario, , (1972), p 104.

168. Adrine W.Bott, Electrochemistry of semiconductors, *Current Separations* (1998), **17**, 3.

169. Fox, M. A. 'Mechanistic Photocatalysis in Organic Synthesis.' *Photocatalysis:*

Fundamentals and Applications Eds. N. Serpone and E. Pelizzetti, John Wiley & Sons Inc. New York, (1989), p 422-455.

170. Raquel F.P. Nogueira and Willson F. Jardim., J. of Chemical Education, (1993), **70**, 861-862.

171. Waite,T. D. 'Photoredox Chemistry of Collidal Metal Oxides. In Geochemical Processes at Mineral Surfaces'. J. A. Davis and K. F. Hayes, Eds. ACS Symp. Ser. No. 323, American Chemical Society, Washington, DC (1986).

172. Spada, L.T.and Foote, C.S. *J.Am.Chem.Soc,* (1980), **102**, 391.

173. Erkisen, J.and Foote, C.S., *J.Am.Chem.Soc*, (1983), **102**, 6083.

174. Evans, T.R.. Wake, R.W and Sifain, M.M. *Tetrahedron Lett,* (1973), 701.

175. .Mizuno, K, Ueda, H.and Otsujj, Y. Chem. Lett., (1981), 1237.

176. Barb, R.A, de Mayo, P. P.and Okada, K., *J. Chem. Soc., Chem.Commun*, 1982.1073.

177. Mizuno, K. Ishii M.and Otsujj, Y., *J.Am.Chem.Soc,* (1983), **103**, 5570.

178. Amalric, L., C. Guillard, and P. Pichat. 'Use of Catalase and Superoxide Dismutase to Assess the role of hydrogen peroxide and superoxide in the TiO_2 or ZnO Photocatalytic Dustrauction of 1.2-Dimethoxybenzene in water'. *Res Chem. Intermed.* (1994), **20**, 579-94.

179. Anpo, Masakuzu, Katsuichi Chiba, Masanori, Tomonari, Savatore, Coluccia, Michael Che, and Marye Anne Fox., Photocatalysis On Native and Platinum-loaded TiO_2 and ZnO Catalysts – Origines of Defferent Reactivities on Wet and dray Metal Oxides, *Bull. Chem.Soc. Jpn.* (1991), **64** , 543-51.

180. Bedja, Idriss, and Prashant V. Kamat. 'Capped Semiconductor Colloides. Synthesis and Photoelectrochemical Behavior of TiO_2 Capped SnO_2 Nanocrystallines.' J. Phys. Chem. (1995), **99**, 9182-8.

181. Casado, Juan, Jean Mari Herrmann, and pierre Pichat. Phototransformation of o-Xylene Over Atmospheric Solid Aerosols in the Presence of Molecular Oxygen and Water. Phys. Chem. Behav. Atoms. Pollut. [Proc.Eur. Symp.], (1990), '5^{th}, 283-8.

182. Courbon, Heenri, Jean Marie Herrmann, and Pierre Pichat., Effect of Platinum Deposits on Oxygen Adsorption and Oxygen Isotope Exchage Ovber Variously Pretreated, Ultraviolet-Illuminated Power Titanum Dioxide, *J. Phys. Chem.* (1984), **88**, 5210-14.

183. Fox Marye Anne, and Raul Cardona, and Elizabeth Gaillard. **1987.** 'Photoactivation of Metal Oxide Surfaces: Photocatalyzed Oxidation of Alcohols by Heteropolytungetates, *J. Am. Chem. Soc.* 109,6347-6354.

184. Fox, M. A., Haruo Ogawa, and Pierre Pichat. ' Regioselectivity in the Semiconductor- Mediated Photooxidation of 1,4 Pentadiol'. J. Org. Chem. (1989), **54**, 3847-3852.

185. Guillard, C. Hoang-Van, C. Pierre P., and Frederique M., 'Laboratory Study of the Respective Roles of Ferric Oxide and Release or Added Ferric Ions in the Photodegradation of Oxalic Acid in Aerated Liquid Water'. *J. Photochem. Photobiol., A* (1995), **89**, 221-227.

186. Herrmann, J. M., Jean, D., and Pierre Pichat. 'Photoassisted Platinum Deposition On Tio2 Powder Using Various Platinum Complexes, *J. Phys. Chem* (1986), 90, 6028-34.

187. Herrmann, J. MMARIE N. M. and Pierre P., Oxidation of Oxalic Acid in Aqueous Suspensions of Semiconductors Illuminated with UV or Visible Light, *J. Photochem.* (1983), **22**, 333-334.

188. Krishnan, M., James R. w. Marye, A.F., and Allen J. Bard. ' Integrated Chemical System: Photocatalytsis at Semiconductors Incorporated into Polyme (Nafion/ Mediator Systems.' J. Am. Chem. Soc. (1983), **105**, 7002-7003.

189. Gerisher, H. *J. Electroanal.Chem,* (1975), **68**, 263.

190. Gerisher, H.and Willing, F. *Top. Curr.Chem.,* (1976), **61**, 33.

191. Wrighton, M.S. *Acc.Chem. Res.,* (1979), **12**, 303.

192. Barad, M.S. *J. Photoichem,* (1979), **10**, 50.

193. Barad, A.J. *Science,* (1980), **207**, 139.

194. Barad, A.J.. J. Phys. Chem., (1982), **86**,172.

195. Rothenberger, G. Moser, J. Gratzel, M. Serpone, N. and Sharma, D.K. *J.Am.Chem.Soc,* (1985), **107**, 8054.

196. Kolle, U. Moser, J. and Grozel, M., *Inorg. Chem.,* (1985), **24**, 2253.

197. Kalanasundarm, K. Valchopoulos, N. Krishnan, V. Monnier, A. and Gratzel, M., J. Phys. Chem., (1987), **91**, 2342.

198. Uczynski Moser J. K and Thomas, J.K. *Chem.Phys. Lett.,* (1982), **88**, 4445.

199. Boehm, H.P. *Discuss. Faraday Soc.,* (1971), **52**, 264.

200. Nakato, V., Tsumura, A., Tsubomura, H., "Photo-and-Electroluminescence spectra from an n-TiO2 semiconductor Electrode As Related to the Intermediates of the Photooxidation Reaction of Water, *J. Phys. Chem,* (1983), **87**, 2402-2405.

201. Yesodharan, E. Yesodharan, S. and Gratzel, M. *Sol. Energy Mater,* (1984), **10,** 287.

202. Abdullah, M., Low , G., Matthews, R., *J. Phys. Chem.,* (1990), **94**, 6820-6825.

203. Pichat, J., D'Oliveria, C., Maffre, F., Mas, D., *Photocatalytic purification and* treatment of water and air, Eds. Ollis, D., Al-Ekabi, H., Elsevier Science: NewYork, (1993), p. 683-688.

204. Butler, E., Davis, A., Photocatalytic oxidation in aqueous titanium dioxide suspensions: the influence of dissolved transition metals, *J. Photochem. Photobiol. A: Chem*, (1993), 273-283.

205. Turchi, C., Ollis, D., Photocatalytic degradation of organic water contaminants: mechanisms involving hydroxyl radical attack, *J. of Catalysis,* (1990), **122**, 178-192.

206. Sun. Y., Pignatello, J., "Evidence for a surface Dual Hole-Radical Mechanism in the TiO_2 photocatalytic oxidation of 2,4-Dichlorophenoxyacetic acid, *Environ. Sci. Technol.,* (1995), **29**, 2065-2072.

207. Serpone, N., Pelizzetti, E., Hidaka, H., "Identifying primary events and the nature of intermediates formed during the photocatalyzed oxidation of organics mediated by irradiated semiconductors" Photocatalytic Purification and Treatment of water and ari, Eds. Ollis, D., Al Ekabi, H., Elsevier Science: New York (1993), p.225-250.

208. Al-Ekabi, H., Serpone, N., J. Phys.Chem, (1988), **92**, 5726-573.

209. Mao, Y., Schonetich, C., Asmus, K., Indentifacation of organic acids and other intermediates in oxidative degradation of chlorinated ethanes on TiO_2 surface route to mineralization; A combined photocatalytic and radiation chemistry study, *J. Phys. Chem,* (1991), **95**, 10080-10089.

210. Fox, M., Dulay, M., Chem. Rev. (1993), **93**, 341-357.

211. Pelizzetti, E., Minero, C., Maurino, V., Hidaka, H., Serpone, N., Terzian, R., 'Photocatalytic Degradation of Dodecane and of Some Dodecyl Derivatives, *Annali, dichimca, by Societa chimica Italiana,* (1990), **80**, 81-87.

212. Minero, C., Maurino, V., Pelizzetti, E., Marine Chemistry, (1997), **58**, 361-372.

213. Nussbaum, M., Nekimken, L., Nieman, T., *Anal. Chem.,* (1987), **59,** 211-212.

214. Calabrese, G., Christian-Maillet, L., *Anal.* Chem, (1992), **64**, 120-123

215. Hermann, J., Guillard, C., Pichat, P., "Heterogeneous photocatalysis: an emerging technology for water treatment, *Catalysis Today*, (1993), **17**, 7-20.

216. Matthews, R.,W 'Purification of Water with Near-UVIlluminated Suspensions of Titanum Dioxide, *Wat. Res.,* (1990), **24**, 653-660.

217. Fox, M. in Photocatalytic Purification and Treatment of Water and Air. eds Ollis,D., Al-Ekabi, H. Elsevier Science Publishers,New York (1993), pp 163-167.

218. Hoffmann, M., Martin, S., Choi, W.,Bahnemann, D., Environmental Applications of Semiconductor Photocatalysis, *Chem. Rev,* (1995), **95**, 69-96.

219. Pelizzetti, E., Minero, C., Mechanism of the photo-oxidative Degradation of organic pollutants over TiO_2 particles, *Electrochemica Acta,* (1993), **38**, 47-55.

220. Yamazaki-Nishida, S., Nagano, K., Phillips, L., Cervera Mareh, S., Anderson, M., *J Photochem. Photobiol. A; Chem.,* (1993), **70**, 95-99.

221. Teruaki, H., Harada, K., and Tanaka, K., 'Photocatalytic Degradation of Organochlorine Compounds in Suspended TiO_2'. *J. Photochem. And Photobiol., A Chem.* (1990), 54, 113-18.

222. Sclafani,Antonino, Leonardo Palmisano, and Mario Schiavello. 'Phenol; and Nitrophenol Photodegradation Using Aqueous TiO_2 Dispersions'. *Aquat. Surf. Photochem.*, eds. George R. Helz, Richald G. Zepp, and Donald G. Crosby, Boca Raton, Fla,: Lewis, (1994), 419-25.

223. Kesselman, N. S. L. and Michael R. H., Photoelectrochemical degradation of 4-chlorocatechol at TiO_2 electrodes: comparison between sorption and photoreaction, *Environ. Sci. Technol,* (1997), **31**, 2298-2302.

224. Vinodgopal, K. Ulick Stafford, Kimberly A. Gray and Prashant V. Kamat, 'Electrochemically Assisted Photocatalysis . 2. 'The Role of Oxygen and Reaction Intermediates in the Degradation of 4- Chlorophenol on Immobilized TiO_2 Particulate Films'. *J. Phys. Chem.* (1994), **98**, 6797-6803.

225. Hoang-Van, C., Pichat, P., and Mozzanega, M.N., 'Room Temperature Hydrogen Transfer From Liquid Methanol or 2-Propanol to Diphenylacetylene over Group VIII Metal/TiO_2 Photocatalysts, *J. Mol. Catal.* (1994), **92**, 187-99.

226. Zhao, J., Wu, T., Wu., K., Oikawa, K., Hidaka, H., Serpone, N., 'Photoassisted Degradation of Dye Pollutants. 3. Degradation of the Cationic Dye Rhodamine B in Aqueous Anionic Surfactant/TiO2 Dispersions under Visible Light Irradiation : Evedence for the Need of Substrate Adsorption on TiO_2 Particles'. *Environ. Sci. Technol.,* (1998), **32,** 2394-2400.

227. Hilgendorff, M., Marcus Hilgendorff, and Bahnemann, D. W., 'Mechanism of Photocatalysis: Thr Reductive Degradation of Tetrachloromethan in Aqueous Titanum Dioxide Suspensions, *J. Adv. Oxid.,* (1996), **1**, 35-43.

228. Jacoby, W., Maness, P. Wolfrum, E., Blake, D., Fennel, J., *Environ. Sci. Technol.* (1998), **17**, 2650-2653.

229. Noguchi, T., Fujishima, A., Sawunyama, P., Hashimoto, K., *Environ. Sci. Technol*, (1998), **32**, 3831-3833.

230. Ollis, D., Pelizzetti, E., Serpone, N., *Environ. Sci. Technol.,* (1991), **25**, 1523-1529.

231. Saquib, M. Muneer, M.TiO_2-mediated photocatalytic degradation of a triphenylmethane dye (gentian violet), in aqueous suspensions, *Dyes and Pigments* (2003), **56,** 37–49.

232. Wen, S. Zhao, J. Sheng, G. Fu, J. Peng, P., Photocatalytic reactions of pyrene at TiO2/water interfaces, *Chemosphere* (2003) **50**,111–119.

233 Bhatkhande, D.S. Pangarkara,V.G. Anthony. A. C.Beenackers, M., Photocatalytic degradation of nitrobenzene using titanium dioxide and concentrated solar radiation: chemical effects and scale up, *Water Res.* (2003), **37**, in press.

234. Ksibi, M. Ben Amor, S. Cherif, S. Elaloui, E. Houas, A. Elaloui, M., Photodegradation of lignin from black liquor using a UV/TiO2 system, *J.Photochem and Photobiol.A:Chem.* (2003), **154**, 211–218.

235. Formenti, M. Juillet, F. Meriaudeau, P. and Teichner, S.J., *Chem. Technol.,* (1971), **1**, 680,

236. Gravelle, P. Juillet, F. Meriaudeau P. and Teichner, S.J., *Discuss. Faraday Soc,* (1971)**, 52**, 140

237. Humphrys, W.R. Veerkamp, R.F. and Leland, T.W. *J. Catal,* (1976), **43**, 304.

238. Frank, S.W. and Bard, A.J. *J.Am.Chem. Soc.,* (1977), **99**, 303.

239. Frank S.W. and Bard, A.J. *J. Phy. Chem.* (1977), **81**, 1848.

240. Karutler, B. and Bard, A. J., *J.Am Chem. Soc,* (1978), **100,** 2239.

241. Karutler, B. and Bard, A. J. *J.Am Chem. Soc.,* (1978), **100**, 5985.

242. Formenti, M. Juillet, F.and Teichner, S.J. Bull.Soc. Chim. Fr., (1976), **9-10,** 1315.

243. Carey, J.H. Lawrence, J.and Tosine, H.M., Bull. Environ. Contam. Toxicol., (1976), **16**, 697.

244. Ausloos, P. Rebbert R.F. and Glasgow, L. J. Res. Natl. Bur. Stand., (1979), **82**, 1.

245. Oliver, B.G. Cosgrove, E.G.and Carey, J.H. *Environ. Sci. Technol.,* (1979), **13**, 1075.

246 Mills, A. Le Hunte, S., An overview of semiconductor photocatalysis, *J.Photochem and Photobiol.A:Chem*, (1997), **108** ,1-35.

247. Tomy, G.T. The mass spectrometric characterization of polychlorinated *n*-alkane and the methodology for their analysis in the environment. Ph.D. Thesis (1998), University of Manitoba, Winnipeg, MB, Canada

248. March, J., Advanced Organic Chemistry, 3rd Ed., John Wiley&Sons.Toronto (1985).

249. Marie-Louise Nilsson, Monica Waldeback, Gustay Liljegren, Henrik Kylin, Karin E. Markides, Pressurized-fluid extraction (PFE) of chlorinated paraffins from the biodegradable fraction of source-separated household waste, *Fresenius J. Anal. Chem.* (2001), **370**, 913-918.

250. Mehmet Coelhan, Determination of short-chain polychlorinated paraffins in Fish samples by short-column GC/ECNI-MS, *Anal. Chem.* (1999), **71**, 4498-4505.

251. Preze-Bendito, D. Rubio, S., Practical aspects of environmental sampling, *Environmental Analytical Chemistry*, Wilson & Wilson's Elsevier, **XXXII** (1999).

252. Jeffers, P.M. Ward, L.M. Woytowitch, L.M. Wolfe, N.L., Homogeneous hydrolysis rate constants for selected chlorinated methanes; ethans,ethenes and propanes, *Environ Sci Technol*, (1989), **23**, 965-969.

253. Lion, L.W. Stuffer, T.B. MacIntyre, W.G., *J Contam Hydrol* (1990), **5**, 215-234.

254. Organization for Economic Co-operation and Development (OECD), Guidelines for testing chemicals: Hydrolysis, (1981), **111**, 1-23.

255. Dudakawski, W.R., Azo dye incorporating cyclopentadienyliron moieties synthesis, polymerization and decomplexation studies, MSc Thesis, (2002), University of Manitoba, Winnipeg, MB, Canada

256. Comparison of Dioxane

257. Hatchard, C.G. Parker,C.A., A new sensitive chemical actinometer II.Potassium ferrioxalate as a standard chemical actinometer, *Proc.R.Soc.London Ser.A.* (1956) **235**, 518-536.

258. Kosaka, K., Yamada, H., Matsui, S., Echigo, S., Shishida, K., Comparison among the methods for hydrogen peroxide measurements to evaluate advanced oxidation processes: application of a spectrophotometric method using copper (II) ion and 2,9-dimethyl-1,10-phenanthroline. *Environ. Sci. Technol.* (1998), 32, 3821-3824.

259. Kang, J.-W., Hung,H.-M., Lin, A., Hoffmann, M.R., *Environ. Sci. Technol,* (1999), 33, 3199-3205.

260. Walling, C.H., *Acc. Chem. Res.* (1975), **8**, 125-131.

261. Bossmann, S. H., Oliveros, E., Göb, S., Siegwart, S., Dahlen, E.P., Payawan, L., Straub, M., Wörner, M., Braun, A.M., *J. Phys. Chem. A.* (1998), **102,** 5542–5550.

262. Rabani, J., Yamashita, K., Ushida, K., Stark, J., Kira, A., *J. Phys. Chem. B.* (1998), 102, 1689-1695.

263. Ruppert, G., Bauer, R., Heisler, G., *Chemosphere,* (1994), **28**, 1447-1454.

264. Hislop, K.A., Bolton, J.R., Environ. Sci. Technol. (1999), **33**, 3119–3126.

265. Buxton, G.V., Greenstock, C.L., Helman, W.P., Ross, A.B., *J. Phys. Chem. Ref. Data* (1988), *17*, 513-886.

266. Pignatello, J. J., *Environ. Sci. Technol.* (1992), **26**, 944-951.

267. De Laat, J., Gallard, H.,. Environ. Sci. Technol. (1999), **33**, 2726-2732.

268. Pichat, P. Mozzanega, M.N. Courbon, H., Investigation of the mechanism of photocatalytic alcohol dehydrogenation over Pt/TiO_2 using poisons and labeled ethanol, *J. Chem Soc Faraday Trans,* (1987), 83:697.

269. Vinodgopal, K. Kamat, P.V., Photochemistry on surfaces. Photodegradation of 1,3- diphenylisobenzofuran over metal oxide particles. *J Phys Chem* (1992), **96**,5053.

270. Baird, C.N., Free radical reactions in aqueous solutions: examples from advanced oxidation processes for wastewater and from the chemistry in airborne water droplets, *J. Chem Edu,* **74**, 817-823.

271. Choudhary, G.G.; Webster, G.R.B. *Chemosphere* (1985), *14*, 9-26.

272. Hermann, J., Guillard, C., Pichat, P., *Catalysis Today*, (1993), **17**, 7-20.

273. Martin, S.T.; Lee, A.T.; Hoffmann, M.R. *Environ. Sci. Technol.* (1995), ***29***, 2567-2573

274. Matthews, R. *Wat. Res.* (1990), **24**, 653-660.

275. Fox, M., Dulay, M., *Chem. Rev.*, (1993), **93**, 341-357.

276. Drouillard, K.G. Hiebert, T. Tran, P.Tomy, G.T.Muir, D.C.G. Friesen, K.J., Estimating the aqueous solubilities of individual chlorinated n-alkanes (C_{10}-C_{12}) from measurements of chlorinated alkane mixtures *Environmental Toxicology and Chemistry*, (1998), **17**, 1261-1267.

277. Calze, P.; Minero, C.; Pelizzetti, E. *Environ. Sci. Technol.* (1997), **31**, 2198-2203.

278. Carraway, E.R.; Hoffman, A.J.; Hoffmann, M.R. *Environ. Sci. Technol.* (1994), **28**, 786-793.

279. Sun. Y.; Pignatello, J.J. *Environ. Sci. Technol.* (1995), **29**, 2065-2072.

280. Pelizzetti, E., Minero, C., *Electrochemica Acta*, (1993), **38**, 47-55.

281. Pichat, J., D'Oliveria, C., Maffre, F., Mas, D., in "Photocatalytic purification and treatment of water and air." Ollis, D., Al-Ekabi, H., Eds. (Elsevier Science: New York), 1993, p. 683-688.

283. Anpo, M., Shina, T., Kubokawa, Y., *Chem Lett.* (1985), 1799.

284. Krautler, B., Bard, A., *J. Am. Chem. Soc.* (1978), **100**, 4317 4318.

285. Al-Sayyed, G., D'oliveira, J., Pichat, P., *J. Photochem. Photobiol. A: Chem.* (1991), **58**, 99-114.

286. Rabani, J.; Yamashita, K.; Ushida, K.; Stark, J.; Kira, A. *J. Phys. Chem. B.* (1998), **102,** 1689-1695.

288. Skoog, D., West, D., Holler, J., Analytical Chemistry, (Saunders College: New York) (1988), p. 819-820.

289. Goldstein, S., Czapski, G., Rabani, J., *J. Phys. Chem.* (1994), **98**, 6586-6591.

290. Buxton, J., Greenstock, C., Helman, W., Ross, A., *J. Phys. Chem. Ref. Data,* (1988), 17,513.

291. Halmann, M.M., Photodegradation of Water Pollutants, CRC Press, New York, NY (1996), p.7-17.

292. Turchi, C.S.; Ollis, D.F. *J. Catal.* (1990), **122,** 178-192.

293. Sakata, T, Kawai, T.; Hashimoto, K. *J. Phys. Chem.* (1984), **88**, 2344-2350.

294. Schiavello, M., Some working principles of heterogeneous photocatalysis by semiconductor, *Electrochim. Acta.* (1993), **38**, 11-14.
295. Nishimoto, S., Ohtani, B., Kajiwana, H., Kagiya, T., *J. Chem. Soc., Faraday Trans.* (1983), **79**, 2685 2694.
296. Ohtani, B., Okugawa, Y., Nishimoto, S., Kagiya, T., *J. Phys. Chem.* (1987), **91**, 3550-3555.
297. Butler, E., Davis, A., *J. Photochem. Photobiol. A: Chem.* (1993), 273-283.
298. Palmisano, L.; Schiavello, M.; Sclafani,. A.; Martin, C.; Martin, I.; Rives, V. *Catal. Lett.* (1994), **24,** 303-315.
299. Zang, L. Liu, C-Y. Ren, X-M. *J. Chem. Soc. Chem. Commun.* (1994), 1865-1866.
300. Draper, R., Fox, M., *J. Phys. Chem.* (1990), **94**, 4628-4634.
301. Lawless, D., Serpone, N., Meisel, D., *J. Phys. Chem.* (1991), **95**, 5166-5170.
302. O'Shea, K., Conde, A., in "Photocatalytic Purifacation and Treatment of water and air, Ollis, D., Al-Ekabi, H., Eds. (1993), p.707-712.
303. Fox, M., in "Photocatalysis-Fundamentals and Applications." Serpone, N., Pelizzetti, E., Eds., Wiley Interscience: New York, (1989), 421-455.
304. Peral, J., Casado, J., Domenech, J., *J. Photochem. Photobiol. A: Chem.* (1988), **44**, 209.
305. Franco, C. and Olmsted, J. Photochemical determination of the solubility of oxygen in various media, *Talanta*, (1990), **37**, 905-909.
306. D'Oliveira, J-C.; Al-Sayyed, G.; Pichat, P. *Environ. Sci. Technol.* (1990), **24,** 990-996.
307. Glaze, W.H.; Kenneke, J.F.; Ferry, J.L. *Environ. Sci. Technol.* (1993), **27,** 177-184.
308. Ferry, J.L.; Glaze, W.H. *J. Phys. Chem. B* (1998), **102,** 2239-2244.
309. Cunningham, J., Al-Sayyed, G., *J. Chem Soc. Faraday Trans.* (1990), **86**, 3935-3941.
310. Zhao, J., Wu, T., Wu., K., Oikawa, K., Hidaka, H., Serpone, N., *Environ. Sci. Technol.* (1998), **32**, 2394-2400.
311. Kesselman, J.M.; Lewis, N.S.; Hoffmann, M.R. *Environ. Sci. Technol.* (1997), **31,** 2298-2302.
312. Yii-Shyan Lay, Ph.D. Thesis (1989), University of California, Los Angeles,
313. Hussain Al-Ekabi, Nicke Serpone, Ezio Pelizzetti, Claudio Minero, Marye Anne Fox

and R.Barton Draper; Kinetic Studies in Heterogeneous Photocatalysis.2 TiO2-Mediated Degradatio of 4-Chlorophenol Alone and in a Three-Component Mixture of 4-Chlorophenol, 2,4,-Dichlorophenol, and 2,4,5-Trichlorophenol in Air-Equilibrated Aqueous Media, *Langmuir,* (1989), **5**, 250-255.

314. Morel, FMM., Hering, JG. Principales and Applications of Aquatic Chemistry.Photochemical Reactions, Wiley Interscience, New York (1993), p 477-479.
315. De Laat, J. Gallard, H., Ancelin S. and Legube B., Comparitive study of the oxidation of atrazine and acetone by H_2O_2/UV, Fe (III)/UV, Fe (III)/H_2O_2/UV and Fe (II) or Fe(III)/ H_2O_2, *Chemosphere,* (1999), **39**, 2693-2706.
316. Ghaly, M., Hartel, G., Mayer, R., Haseneder, R. Photochemical oxidation of p-chlorophenol by UV/H_2O_2 and photo-Fenton process. A comparative study, *Waste Management,* (2001), **21**, 41-47.
317. Wong, C.C. and Chu, W., The hydrogen peroxide-assisted photocatalytic degradation of alachlor in TiO2 suspensions, *Environ. Sci. Technol.* (2003), **37,** 2310-2316.